Phytochemical and Antimicrobial Studies on Selected Kuwaiti Flora

Thesis submitted by

MICHAEL STAVRI

for the degree of

DOCTOR OF PHILOSOPHY

University of London

School of Pharmacy

Centre for Pharmacognosy and Phytotherapy,

The School of Pharmacy,

University of London,

29-39 Brunswick Square,

London WC1N 1AX, UK.

September 2004

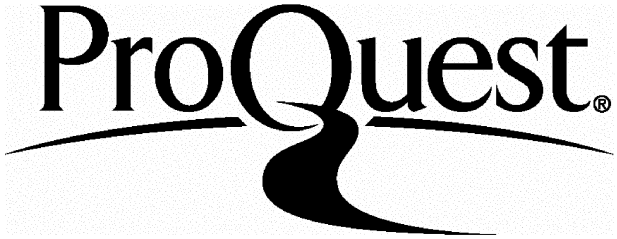

This thesis is dedicated to my family
for their love, support and belief in me.

Acknowledgements

There are a number of people I would like to thank for their expert advice, time, help and encouragement during the course of this PhD research.

Firstly, I would like to thank my supervisor Dr Simon Gibbons for the expert advice and passion for the field of Natural Products Chemistry and also encouragement when things did not always go according to plan. I also thank my second supervisor Dr Joanne Barnes for help and support during my PhD. I would also like to thank my undergraduate supervisor Dr Colin T. Bedford, whose passion for Natural Products Chemistry inspired me to progress further in this field. I thank Dr Mire Zloh for all the help given in the field of NMR spectroscopy. I would also like to thank Professor Franz Bucar for performing numerous analyses and assays of my compounds. Dr R. Thomas Williamson for the absolute stereochemical determinations performed. Dr Trevor Gibson for recording mass spectrometry for this research and Professor Christopher Ford for the cytotoxicity study carried out. I thank Mr Gus Ronngren for technical assistance throughout this PhD research. I also thank all of my friends and colleagues in the department and the School of Pharmacy for making this research an enjoyable experience.

I would also like to thank my family for all their love, support, encouragement and patience during this PhD research.

Finally, I would like to thank the University of London School of Pharmacy for the award of a studentship.

Abstract

This thesis describes the phytochemical and antimicrobial studies of six Kuwaiti plants. The plants investigated belong to four families, Apiaceae (*Anethum graveolens* and *Ducrosia anethifolia*), Asteraceae (*Artemisia monosperma* and *Pulicaria crispa*), Convolvulaceae (*Ipomoea pes-caprae*) and Scrophulariaceae (*Scrophularia deserti*).

A study of the aerial plant parts of *Artemisia monosperma* yielded a total of 12 compounds. Six of the compounds isolated were new including a C_{10} polyacetylene 1,3*R*,8*R*-trihydroxydec-9-en-4,6-yne and the glucoside 3(ζ),8(ζ)-dihydroxydec-9-en-4,6-yne-1-*O*-β-D-glucopyranoside. A new eudesmane sesquiterpene *rel*-1β,3α,6β-trihydroxyeudesm-4-ene was also isolated from this plant as well as the first report of the 3*R*,8*R* stereoisomer of 16,17-dehydrofalcarindiol.

Ducrosia anethifolia yielded only two compounds, the monoterpene glucoside 8-debenzoylpaeoniflorin and the prenylated furocoumarin pangelin. Pangelin demonstrated moderate activity against a panel of rapidly growing mycobacteria.

An investigation of the aerial plant parts of *Ipomoea pes-caprae* led to the isolation of the common triterpenes lupeol and α-amyrin as well as the sterol β-sitosterol. The known flavonol quercetin-3-*O*-β-D-glucopyranoside was also isolated from this species and demonstrated activity against a multidrug resistant (MDR) strain of *Staphylococcus aureus*.

Bioassay-guided fractionation of the whole herb *Anethum graveolens* led to the isolation of falcarindiol. This polyacetylenic natural product exhibited both antimycobacterial and anti-staphylococcal activity, including a MDR strain of *Staphylococcus aureus*. A further 6 compounds were isolated from this species including three prenylated furocoumarins.

A phytochemical study of the whole herb of *Pulicaria crispa* yielded 12 compounds including a sesquiterpene with a novel skeleton, 2α,6α-dimethyltetracyclo-decal-3-en-2,12-diol-8α,13-olide (pulicrispiolide), isolated from the hexane extract. Four guaianolides, three of which are new, were also purified from the hexane extract of this species. The new epimer 5,10-*epi*-2,3-dihydroaromatin also demonstrated weak anti-staphylococcal activity.

A study of *Scrophularia deserti* resulted in the isolation of 10 compounds, including seven iridoid glycosides. A new C_{18} fatty acid 3(ζ)-hydroxy-octadeca-

4(*E*),6(*Z*)-dienoic acid was isolated from this species and possessed moderate antimicrobial activity.

Contents

1.0 Introduction

1.1 Objectives of Thesis

This thesis describes the phytochemical studies of six plants collected from Kuwait. The plants fall within four families, including the Apiaceae (*Anethum graveolens* and *Ducrosia anethifolia*), Asteraceae (*Artemisia monosperma* and *Pulicaria crispa*), Convolvulaceae (*Ipomoea pes-caprae*) and Scrophulariaceae (*Scrophularia deserti*).

The plants evaluated ranged from the poorly studied, such as *D. anethifolia*, but also included well known plants such as *A. graveolens*, better known as the common herb dill, used widely as a medicinal herb and in cookery. The diverse nature of the plants studied in this thesis enabled a wide range of plant natural products to be characterised, including iridoids, polyacetylenes, furocoumarins and flavonoids.

The natural products isolated from each of the six plants investigated also underwent antibacterial characterisation. This included multidrug resistant (MDR) and methicillin-resistant (MRSA) strains of *Staphylococcus aureus* as well as a panel of rapidly growing mycobacteria, including *Mycobacterium fortuitum*, *Mycobacterium aurum*, *Mycobacterium phlei*, *Mycobacterium smegmatis* and *Mycobacterium abscessus*. *M. fortuitum* was initially used to screen Kuwaiti plant extracts prior to deciding on which plant should be investigated further. Antibacterial characterisation yielded activity from both known and new compounds and the activity recorded ranged from weak to strongly active.

1.2 Kuwait: climate and landscape

Kuwait is located at the north-west corner of the Gulf and is characterised by having very hot, dry summers and mild rainy winters (Daoud 1985b). Temperatures regularly exceed 50°C in the summer but fall to below freezing in the winter. The rainfall can be both erratic and inconsistent and shows great temporal and seasonal fluctuations (Daoud 1985b). Therefore it is crucial that plants growing in this environment are capable of coping with the harsh and extreme weather conditions to survive and grow.

The general landscape of Kuwait is flat to gently undulating (Daoud 1985b). The land of Kuwait is mainly one of desert. However, this landscape is broken up by five main geomorphologic features: elevations, wadis (drainage lines), depressions, sand dunes and salt marshes (Daoud 1985b). This facilitates a great diversity of plants to grow in a relatively small region because of the nature of the land and the climate.

Figure 1.2A Wadi Al-Batin

Figure 1.2B Kuwait Institute for Scientific Research (KISR)

1.3 Description of the families and species investigated in this thesis

1.3.1 Apiaceae

The Apiaceae (Umbelliferae) family is also known as the parsley family. It is comprised of approximately 3000 species belonging to about 280 genera that are mainly found growing in temperate regions of the northern hemisphere (Heinrich *et al.*, 2004). The plants are annual, biennial or perennial and mostly herbaceous (Daoud 1985b). They have a characteristic inflorescence often as a compound umbel (clusters of flowers in an umbrella-like formation). This family is important for its medicinal uses for example, *Carum carvi* (caraway), *Coriandrum sativum* (coriander) and *Foeniculum vulgare* (fennel) are used as carminatives, whilst *Levisticum officinale* (lovage) possesses antidyspeptic activity (Heinrich *et al.*, 2004). *Pimpinella anisum* (anise-fruit) is another useful member of the Apiaceae family that is used as an expectorant, spasmolytic and carminative (Heinrich *et al.*, 2004). However, it is also a rich source of food which includes vegetables such as carrots, parsnips and turnips as well as herbs and spices like dill, cumin, chervil, coriander and parsley. Characteristic chemical classes produced by members of this family range from coumarins including furocoumarins to polyacetylenes and flavonoids. Members of this family are also a rich source of essential oils, which are of pharmaceutical importance (Heinrich *et al.*, 2004).

1.3.1.1 *Anethum graveolens* L.

Anethum graveolens is a member of the Apiaceae family. This aromatic herb grows to 50-150 cm in height and produces yellow flowers that form umbrella-like clusters which are typical of plants belonging to the Apiaceae family. It is commonly known as dill and has been cultivated in Europe since antiquity for use as an aromatic herb and spice (Ishikawa *et al.*, 2002) and has even been mentioned in the Holy Bible as well as Sanskrit (Jirovetz *et al.*, 2003).

The fruit of *A. graveolens* has been used for medicinal purposes to relieve digestive problems and also to stimulate milk for nursing mothers (Ishikawa *et al.*, 2002). Previous phytochemical studies have identified the monoterpene carvone to be the main constituent (50-60%) of the essential oil (Ishikawa *et al.*, 2002). This monoterpene has a calming effect; hence it's use in gripe water preparations (Heinrich *et al.*, 2004).

The major odourants of *A. graveolens* have been elucidated over the past 25 years. These include the benzofuran dill ether, (+)-4*S*-α-phellandrene, myristicin, and (*Z*)-3-hexenol (Blank *et al.*, 1992; Blank and Grosch 1991; Charles *et al.*, 1995). This is important economically as the essential oil of *A. graveolens* is used in the food industry to flavour food products (Jirovetz *et al.*, 2003). Other natural product classes isolated from this species include flavonoid glycosides, coumarins, sterols, monoterpene glycosides, aromatic compound glycosides and alkyl glycosides (Ishikawa *et al.*, 2002; Rizk 1986).

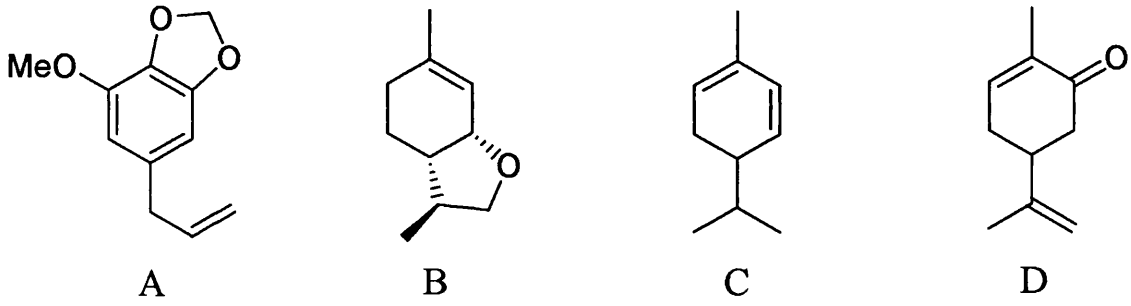

Figure 1.3.1.1 Structures of myristicin (A), dill ether (B), α-phellandrene (C) and carvone (D)

1.3.1.2 *Ducrosia anethifolia* (DC.) Boiss.

Ducrosia anethifolia is a member of the Apiaceae family and is an annual herb. The genus is composed of 5-6 species which are found growing in Afghanistan, Middle East and Pakistan (Ashraf *et al.*, 1979). This species was first found growing in Kuwait in the 1990's in the Khiran area (Shuaib 1995). It has soft grey-green leaves that are indented and when the plant is small, the leaves look very blue against its acid yellow flowers (Shuaib 1995). When it grows into a large thick-stemmed plant the foliage fades to grey (Shuaib 1995). The most distinctive feature of *D. anethifolia*, and the Apiaceae family in general, is the inflorescence. The flower heads are small and clustered together like an umbrella.

The plant is used locally as fodder for sheep and camels (Ashraf *et al.*, 1979). However, in Iran it is used in traditional medicine to treat catarrh, headache and backache as well as improving the smell of food and drink; in Karoon an infusion of the seeds is given to children to treat colic (Janssen *et al.*, 1984). Phytochemical work

on this plant has been limited to date. Janssen *et al.* (1984) investigated the antimicrobial activity of the essential oils in the herb and fruit oils. The herb oil was described as showing 'remarkable activity against some fungi that are known to cause skin infections in humans' (Janssen *et al.*, 1984). The fungi susceptible to the herb oil were *Trichophyton mentagrophytes*, *T. rubrum* and *Epidermophyton floccosum*.

1.3.2 Asteraceae

The Asteraceae (Compositae) family is also referred to as the daisy or sunflower family. It is the largest family of flowering plants being comprised of approximately 1500 genera and around 23000 species (Ghafoor 2002). They are annual, biennial or perennial herbs, shrubs and rarely trees (Ghafoor 2002). The inflorescence of all species within this family is called a capitulum or head (Chaudhary and Al-Jowaid 1999). This is when flowers are composed of many small florets. This family is important both for economical and medical purposes. Some of these plants are used for food, for example, *Helianthus annuus* (the common sunflower) used for production of margarine and also sunflower oil, *Lactuca sativa* (lettuce) and *Cynara scolymus* (artichoke). Medicinal uses of this family include *Arnica montana* (used topically, especially for bruises), *Artemisia annua* (used to treat malaria) and *Echinacea purpurea* (used commonly as an immunostimulant) (Heinrich *et al.*, 2004). Chemically, this family produces a wide range of compounds including sesquiterpene lactones such as guaianolides, xantholides and germacranolides, di- and triterpenes, polyfructanes (e.g. inulin), flavonoids, polyacetylenes and alkaloids (Heinrich *et al.*, 2004; Rizk 1986).

1.3.2.1 *Artemisia monosperma* Del.

Artemisia monosperma is a perennial fragrant herb belonging to the Asteraceae family. This species grows along the northwestern border with Iraq, and its distribution in Kuwait is restricted to the sandy gullies of Wadi Al-Batin (Stavri *et al.*, 2004a). It has paniculately arranged floral heads but this herb is rarely grazed due to its bitter taste (Chaudhary and Al-Jowaid 1999). The genus *Artemisia* is one of the largest within the Asteraceae with some 400 species, distributed mainly in the northern temperate region (Tan *et al.*, 1998; Wright 2002).

Figure 1.3.2.1A *Artemisia monosperma* Del.

This species has been used in folk medicine for its antispasmodic and antihelmintic activity and also for the treatment of hypertension (Abu-Niaaj *et al.,* 1993). Phytochemical studies of *A. monosperma* yielded the flavanone, 7-*O*-methyleriodictyol and the flavone eupatilin. These were subsequently found to exert a relaxant effect on isolated smooth muscle preparations and also to inhibit contractions caused by spasmogens like acetylcholine and oxytocin (Abu-Niaaj *et al.,* 1993; Abu-Niaaj *et al.,* 1996). This finding corroborates the use of this plant, in folk medicine, for its antispasmodic effect. Further phytochemical studies on this herb have resulted in a wide range of natural products being isolated. This includes an aromatic diacetylene, 3-methyl-3-phenyl-1,4-pentadiyne, possessing insecticidal activity (Saleh 1984) as well as monoterpenes, sesquiterpenes, triterpenes, coumarins and acetophenones (Elgamal *et al.,* 1997; Saleh 1985).

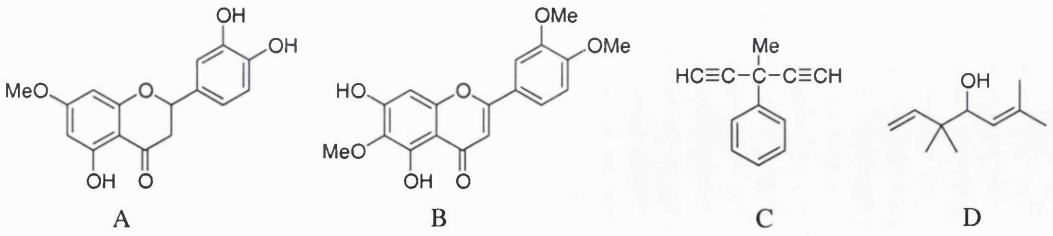

Figure 1.3.2.1B Structures of 7-*O*-methyleriodictyol (A), eupatilin (B), 3-methyl-3-phenyl-1,4-pentadiyne (C) and Artemisia alcohol (D)

1.3.2.2 *Pulicaria crispa* Sch. Pip.

Figure 1.3.2.2A *Pulicaria crispa* Sch. Pip.

Pulicaria crispa (syn. *Francoeuria crispa*) belongs to the Asteraceae family. It is an annual herb that produces small bright yellow flowers. This herb can be found growing in dry, sandy soil and is prevalent in countries such as Saudi Arabia, Kuwait, Iran, Iraq and Egypt (Daoud 1985a).

Figure 1.3.2.2B *Pulicaria crispa* flower

P. crispa is a medicinal plant used by people of southern Egypt and Saudi Arabia to treat inflammation and also as an insect repellent (Ross *et al.,* 1997). This species, like many within the genus, has been well studied phytochemically. It is a rich source of sesquiterpene lactones including guaianolides, xantholides and eudesmanolides as well as kaurane diterpenes.

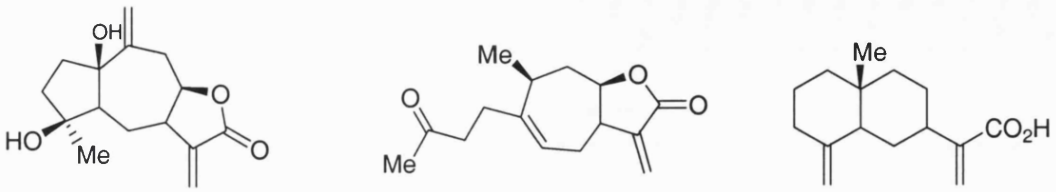

A B C

Figure 1.3.2.2C Structures of commonly found sesquiterpenes from *P. crispa*, including guaianolides (A), xantholides (B) and eudesmanolides (C)

1.3.3 Convolvulaceae

The Convolvulaceae family is comprised of around 1650 species belonging to some 55 genera that are mainly found growing in tropical and subtropical regions (Chaudhary and Al-Jowaid 1999). They are generally perennial herbs, shrubs and rarely trees (Chaudhary and Al-Jowaid 1999). This family is known to produce compounds such as alkaloids, flavonoids and kauranols (Rizk 1986).

1.3.3.1 *Ipomoea pes-caprae* (L.) R. Br.

Figure 1.3.3.1A *Ipomoea pes-caprae* (L.) R. Br.

Ipomoea pes-caprae, also known as 'salsa-da-praia' or 'batateira-da-praia' in Brazil, belongs to the family Convolvulaceae. The genus *Ipomoea* is composed of more than 200 species which are widely distributed in tropical and sub-tropical countries (Souza *et al.*, 2000). This plant is an evergreen perennial that flourishes along sandy dunes and beaches. It is tolerant to both heat and saline conditions, being able to grow even in soil temperatures of 40°C and not being affected by the salinity of the sea water (Chaudhary and Al-Jowaid 1999). The flowers produced are pink to lavender purple funnels that are no more than a few centimetres off the ground.

I. pes-caprae is a traditional medicinal plant that has been used in a large number of tropical countries, including Thailand, as an anti-inflammatory (Pongprayoon *et al.*, 1991; Pongprayoon *et al.*, 1992). This includes an efficacy to treat patients in a clinical study with jellyfish sting dermatitis (Pongprayoon *et al.*, 1991). The most potent inhibitors of the inflammatory process were from phenolic compounds and arachidonic acid analogues. These compounds, which include (-)-mellein, eugenol and 4-vinylguaiacol **(Figure 1.3.3.1A)**, inhibited the enzymes cyclooxygenase and 5-lipoxygenase (Pongprayoon *et al.*, 1991), which are involved in the synthesis of prostaglandins and leukotrienes respectively. This plant has also demonstrated antispasmodic activity in the lipophilic extract. The active components were identified as the isoprenoids β-damascenone and *E*-phytol **(Figure 1.3.3.1B)**, which showed comparable inhibitory effects to the alkaloid papaverine, a general spasmolytic agent (Pongprayoon *et al.*, 1992).

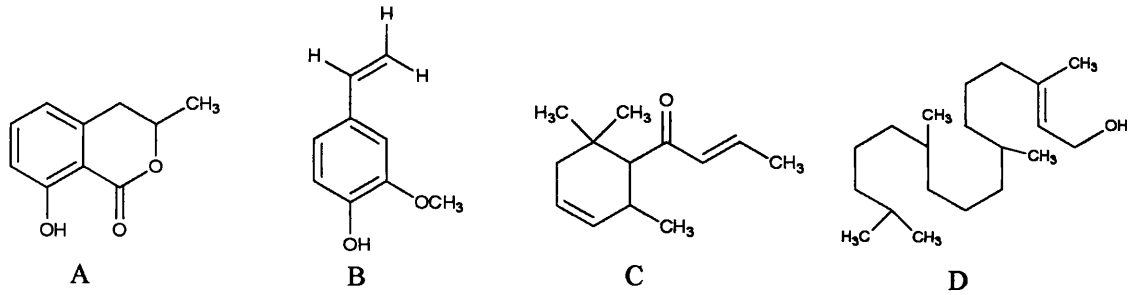

Figure 1.3.3.1B Structures of (-)-mellein (A), 4-vinylguaiacol (B), β-damascenone (C) and *E*-phytol (D)

1.3.4 Scrophulariaceae

The Scrophulariaceae family, also known as the figwort family, is comprised of approximately 3000 species belonging to around 210 genera (Daoud 1985b). Members of this family may be annual or perennial herbs, shrubs and rarely trees (Chaudhary and Al-Jowaid 1999). Species within this family are greatly used around the world as ornamentals for example, *Antirrhinum*, *Linaria*, *Mimulus* and *Verbascum* (Chaudhary and Al-Jowaid 1999). However, there are some species that are of medicinal importance such as *Digitalis*, a producer of cardiac glycosides (Chaudhary and Al-Jowaid 1999). From a phytochemical perspective, this family is a rich source of iridoid glycosides especially the genera *Buddleja*, *Scrophularia* and *Verbascum* (Ahmed *et al.*, 2003; Miyase *et al.*, 1991; Seifert *et al.*, 1989). The isolation of alkaloids, flavonoids and tannins from species within this family has also been reported (Rizk 1986).

1.3.4.1 *Scrophularia deserti* Del.

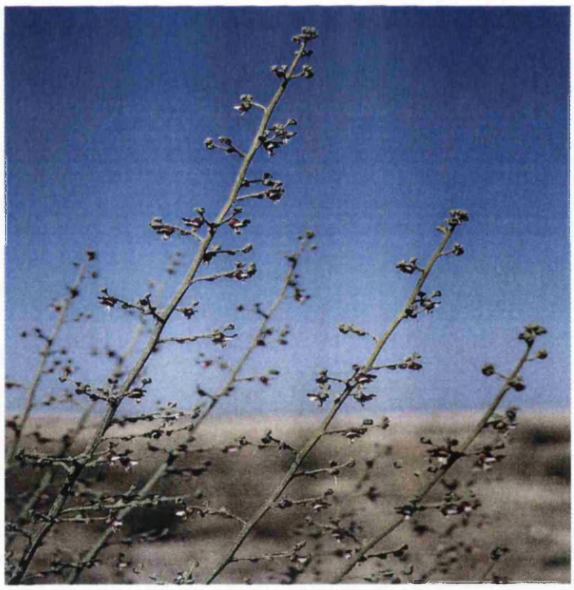

Figure 1.3.4.1A *Scrophularia deserti* Del.

Scrophularia deserti is the most common figwort found in Kuwait and is fairly abundant in areas where limestone underlies the sand (Shuaib 1995). Its basic leaves spring from old roots from which sprays of flowers grow out from the stems (Shuaib 1995). It produces a small deep red flower that is almost bell-shaped

with two lips; the bottom lip is white with a tongue like fringe of yellow stamens (Shuaib 1995). *S. deserti* can mainly be found growing in the Middle East, including Egypt, Palestine, Jordan, Syria, Iraq and Iran as well as Kuwait (Daoud 1985b).

S. deserti is used as an antipyretic, a remedy for kidney diseases, cardiotonic, hypoglycaemic, and diuretic in typhoid fever, inflammation of mouth, lungs, large intestine, bladder and heart and as a remedy for tumours and cancer of the lung (Ahmed *et al.*, 2003). To date, *S. deserti* has been poorly studied phytochemically. A total of five iridoid glycosides have been isolated from this particular species including two new compounds, scropolioside-D_2 and harpagoside-B (Ahmed *et al.*, 2003). This natural product class is a common feature of the genus (Fernandez *et al.*, 1995).

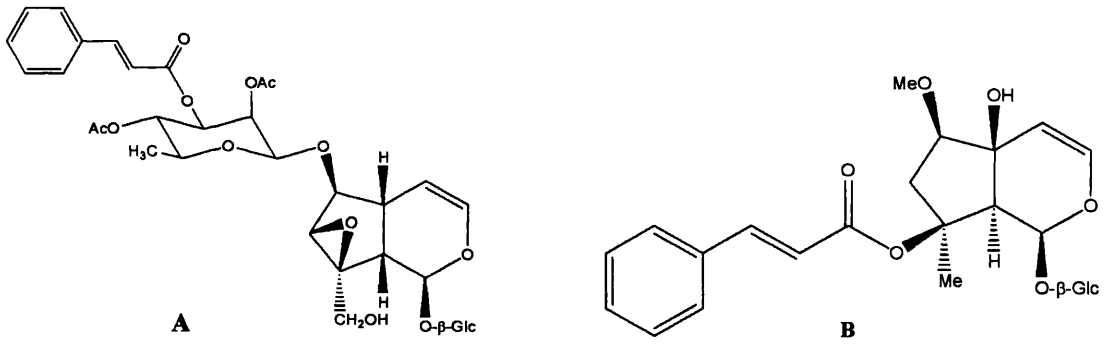

Figure 1.3.4.1B Structure of scropolioside-D_2 (A) and harpagoside-B (B)

1.4 Drug Resistance

1.4.1 Biochemical Basis of Resistance

Bacterial resistance has been a problem for scientists as far back as the penicillin era of drug discovery. Chain and Abraham found bacteria to be either unsusceptible to penicillin or had mechanisms to deactivate the antibacterial formulations as early as 1940 (Mann and Crabbe 1996). The challenge of keeping one step ahead in the fight against bacterial infectious disease is greater now than at any previous point in time. This is due to the speed at which bacteria are evolving and developing resistance even to the most recently introduced drugs.

There are 5 principal mechanisms of resistance employed by bacteria. They are:

1. destruction or inactivation of the antibiotic.
2. alteration of the drug target site to reduce or prevent binding of the antibiotic to the target.
3. loss of cell permeability to an antibiotic.
4. synthesis of a new antibiotic-insensitive target enzyme
5. production of an increased concentration of a metabolite that antagonises the antibiotic.

Table 1.4.1 Resistance mechanisms for the major groups of antibiotics

Inactivation or modification	Altered target site	Reduced permeability or access	Metabolic by-pass
β-Lactam antibiotics	β-Lactam antibiotics	β-Lactam antibiotics	Trimethoprim
Chloramphenicol	Streptomycin	Tetracyclines[c]	Sulphonamides
Aminoglycosides[a]	Chloramphenicol	Chloramphenicol	
	Erythromycin[b]	Quinolones[c]	
	Fusidic acid	Aminoglycosides	
	Quinolones		
	Rifampicin		
	Glycopeptides[b]		

[a] Resulting in reduced drug uptake.

[b] Resulting from enzymatic modification.

[c] Resulting from an increased efflux

Reprint from Towner (2001)

1.4.1.1 Antibiotic inactivation or destruction

The inactivation or destruction of an antibiotic is a mechanism that bacteria use to confer resistance to a particular compound or class of compound. An example of this mechanism would be the inactivation of β-lactam antibiotics by β-lactamase enzymes. This is achieved by β-lactamase reacting with penicillin, for example, to form a penicilloyl-enzyme complex, which results in the cleavage of the β-lactam ring.

Chloramphenicol resistance has been achieved in both Gram-positive and Gram-negative bacteria by the enzyme chloramphenicol acetyl-transferase, which converts the drug to either the mono- or diacetate (**Figure 1.4.1.1**) (Towner 2001).

Similarly, aminoglycosides can be inactivated by either phosphorylation or adenylation of the hydroxyl groups or acetylation of the amino groups present in the molecule (Williams *et al.*, 1996).

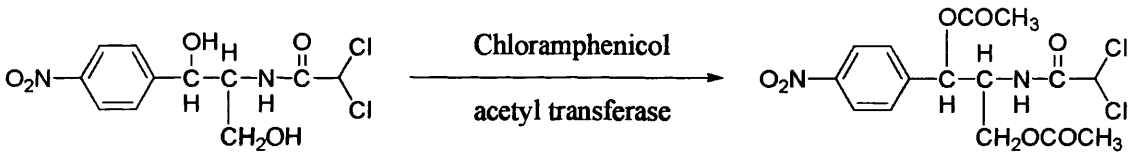

Figure 1.4.1.1 Inactivation of chloramphenicol by chloramphenicol acetyl-transferase

1.4.1.2 Target site modification

The modification of a target site can result in resistance being achieved towards an antibiotic. For example, *Streptococcus pneumoniae* produce a methylase enzyme that methylates an adenine residue of the 23S rRNA, which prevents macrolide antibiotics such as erythromycin A to bind and exert their effect (Mann and Crabbe 1996).

Penicillin binding protein (PBP) mutations that result in a lowering of affinity towards β-lactam antibiotics but still retain affinity for its natural substrate are how methicillin-resistant *Staphylococcus aureus* (MRSA) is able to confer resistance to virtually all drugs within this chemical class. A mutation leading to the production of the low-affinity PBP2A rather than PBP2 enables MRSA to achieve resistance to β-lactam antibiotics (Poole 2002).

Resistance to fluoroquinolones has been gained by mutation within the genes encoding for DNA gyrase (*gyrA*) and topoisomerase (*parC*) (Poole 2002).

1.4.1.3 Reduced cell permeability to an antibiotic

Changes in the structure of the outer membrane can prevent the passage of an antibiotic from reaching its target. The intrinsic resistance of Gram-negative bacteria towards macrolide antibiotics like erythromycin can partly be attributed to the difficulty of passing through the outer membrane (Poole 2002). A reduction in the number of porins in the outer membrane can limit the passage of antibiotics passing into the cytosol where other mechanisms of resistance can be employed such as active efflux or antibiotic inactivation.

1.4.1.4 Duplication of a new antibiotic-insensitive target enzyme

Resistance towards trimethoprim by Gram-negative bacilli has been achieved by a plasmid-borne gene encoding for dihydrofolate reductase. The affinity for trimethoprim is approximately 20,000 fold lower than the chromosomally encoded enzyme.

1.4.1.5 Interference in metabolic pathways

Sulphonamides, such as sulfamethoxazole, act as competitive inhibitors of the enzyme dihydropteroate synthetase while trimethoprim selectively inhibits bacterial, rather than eukaryotic, dihydrofolate reductase (Mann and Crabbe 1996). Incorporation of *p*-aminobenzoic acid (PABA) into folic acid is inhibited by sulphonamides while trimethoprim prevents the reduction of dihydrofolate to tetrahydrofolate (Mann and Crabbe 1996). Resistance towards sulphonamides has been achieved by bacteria increasing the production of PABA to compete with the sulphonamides for the active site of the enzyme dihydropteroate synthetase.

1.4.2 Genetic Basis of Resistance

Bacteria can also confer resistance to antibiotics *via* genetic modification. They can achieve this in one of two ways, either by acquiring DNA encoding resistance determinants in the form of plasmids or transposons, or by mutation(s) within their chromosomal DNA. Plasmids are capable of replicating within a bacterial cell and may have high copy numbers, which can then be passed onto other bacterial cells by cell-to-cell contact in a process known as conjugation. This mechanism can therefore transfer resistant determinants to previously susceptible

bacterial cells. The process of acquiring chromosomal and plasmid DNA can be achieved by transduction or transformation.

1.4.3 Microbial Multidrug Efflux

Microbial multidrug efflux was first reported in the early 1980's for tetracycline by Ball *et al.*, (1980) and McMurry *et al.*, (1980). Resistance by efflux was identified to be encoded by *tet* (tetracycline) determinants, which can either be plasmid or transposon encoded (Poole 2001). The transfer of this DNA can be readily achieved from organism to organism enabling previously susceptible bacteria to become resistant to this class of compound. Since the initial discovery of the tetracycline efflux pump, further efflux systems have been identified in Gram-positive and Gram-negative bacteria as well as mycobacteria. The efflux systems can be divided into 5 main families and have the capability of extruding chemically diverse drugs. This relatively new mode of drug resistance is therefore a great challenge to the clinician and also for drug discovery. The classification of efflux pumps into one of the five families is based on their supramolecular assembly, mechanism and amino acid sequence homology (**Table 1.4.3**) (Nikaido 1994). The extrusion of drugs by these efflux pumps is achieved either by a uniport mechanism coupled to ATP hydrolysis or, more commonly, by an antiport mechanism in which the drug efflux is coupled to proton influx i.e. driven by the proton motive force (pmf) (Marshall and Piddock 1997). Efflux of drugs from the cytoplasm of a Gram-positive bacterium is mediated by a single cytoplasmic membrane-located transporter of the SMR (small multidrug resistance), MFS (major facilitator superfamily) or ABC (ATP binding cassette) families (Marshall and Piddock 1997). The efflux mechanism in Gram-negative organisms is more complex due to the presence of an outer membrane. They form a tripartite protein channel, which requires a protein situated in the periplasm known as the membrane fusion protein (MFP) and an outer membrane efflux protein (OEP) along with the cytoplasmic membrane-located transporter. It is not uncommon for an organism to code for more than one efflux pump, which may either be expressed constitutively or in direct response to the presence of a substrate. *Pseudomonas aeruginosa* constitutively expresses the MexAB-OprM multidrug efflux pump, which is the main member of the RND (resistance-nodulation division) family in *P. aeruginosa* (Li *et al.*, 2003). However, this organism also codes for the MexXY-OprM pump which can be induced in the presence of one of the substrates

for this pump. Multidrug efflux pumps therefore contribute to the intrinsic resistance of *P. aeruginosa* and bacteria which code for such efflux pumps (Li *et al.*, 2003). The identification of these efflux pumps opens up the possibility of another target that can be used in the fight against problematic infectious diseases such as methicillin-resistant *Staphylococcus aureus* (MRSA) and *P. aeruginosa*.

A genetic approach to determine the consequences of inhibiting the efflux pumps in *P. aeruginosa* was undertaken by Lomovskaya *et al.*, (1999). Inhibition of efflux pumps was found to:

- significantly decrease the level of intrinsic resistance
- reverse acquired resistance
- result in a decreased frequency of emergence of *P. aeruginosa* in strains highly resistant to fluoroquinolones in clinical settings

Therefore identifying efflux pump inhibitors to be used in conjunction with current drugs that are pump substrates can recover clinically relevant activity of those compounds and thus may reduce the need for discovery and development of new antimicrobial agents that are not pump substrates (Kaatz 2002).

Table 1.4.3 Bacterial drug transporters

Family	Translocation energy source	Examples	Antibacterial agent substrates	Example hosts (genera)
ABC	Drug extrusion coupled to ATP hydrolysis	LmrA, MsrA	Macrolides, TCNs, Chloramphenicol	*Lactococcus*, *Staphylococcus*
MATE	Drug: Na^+ or H^+ exchange	NorM	Aminoglycosides, Monocationic dyes, FQs	*Bacteroides*, *Vibrio*
MFS	Drug: H^+ exchange	NorA, TetK	TCNs, FQs, Chloramphenicol, Monocationic disinfectants and dyes	*Bacillus*, *Escherichia*, *Lactococcus*, *Staphylococcus*
RND	Drug: H^+ exchange	AcrA, MexB	Aminoglycosides, FQs, TCNs, Chloramphenicol, Macrolides	*Escherichia*, *Haemophilus*, *Neisseria*, *Pseudomonas*
SMR	Drug: H^+ exchange	EmrE, QacD	Macrolides, TCNs, Monocationic disinfectants and dyes	*Escherichia*, *Staphylococcus*

ABC: ATP binding cassette; MATE: Multiple antibiotic and toxin extrusion; MFS: Major facilitator superfamily; RND: Resistance-nodulation division; SMR: Small multi-drug resistance; FQ: Fluoroquinolone; TCN: Tetracycline (Kaatz 2002)

1.4.4 Mycobacteria and efflux mechanisms

Whilst the identification of efflux pumps in both Gram-positive and Gram-negative bacteria has been known for 25 years, it has only been in the last decade that mycobacteria have been shown to actually possess such pumps. The first efflux pump was found in the rapidly growing mycobacterium *Mycobacterium smegmatis*. The efflux pump LfrA, belonging to the proton antiporter MFS family, was shown to

confer low-level fluoroquinolone resistance (Takiff *et al.*, 1996). The gene *lfrA*, encoding the efflux pump appears to recognise hydrophilic fluoroquinolones, ethidium bromide, acridine and some quaternary ammonium compounds and has been found to be a homologue to *qacA* from *S. aureus* and *emrB* of *E. coli* (Takiff *et al.*, 1996; Viveiros *et al.*, 2003). Another multidrug efflux pump characterised in both *Mycobacterium fortuitum* and *Mycobacterium tuberculosis* is known as Tap. The sequences of the putative Tap proteins showed 20 to 30% amino acid identity to membrane efflux pumps of the MFS family (Ainsa *et al.*, 1998). The Tap proteins confer low-level resistance to aminoglycosides and tetracycline. Another gene, *P55*, located in both *Mycobacterium bovis* and *M. tuberculosis* conferred resistance to both aminoglycosides and tetracycline when transformed into *M. smegmatis* (Silva *et al.*, 2001). Other efflux pumps isolated from mycobacteria include the *tet(V)* gene which uses the pmf for the extrusion of tetracycline from *M. smegmatis* (Viveiros *et al.*, 2003), Mmr (SMR family) and DrrAB (ABC family) were reported in *M. tuberculosis* and found to mediate low-level resistance against certain antimicrobial agents (Li *et al.*, 2004). Whist the number of efflux pumps identified in mycobacteria is relatively small, in comparison to Gram-positive and Gram-negative bacteria, it is clearly only a matter of time before more are identified and shown to be a major factor in the intrinsic resistance of these organisms.

1.4.5 Resurgence of Tuberculosis

Over the past 15-20 years there has been a worldwide resurgence of tuberculosis (TB). *M. tuberculosis* is the major cause of this disease, although *M. bovis* and *Mycobacterium africanum* are also listed within the *M. tuberculosis* complex (Newton *et al.*, 2000; Wolinsky 1992). Each year approximately 8 million people are infected with the tubercle bacilli, which causes around 3 million deaths, more than any other single bacterial infectious disease. The World Health Organisation has estimated that between 2000 and 2020 nearly one billion people will be newly infected, 200 million will develop TB and 35 million will die from the disease (WHO 2000). It has been described as 'Ebola with wings' by the head of TB control for the WHO (Ainsworth and Mackenzie 2001). The problem lies in the fact that scientists believed that TB was eradicated from developed countries in the 1970's. Since this period of time there have been no new antimycobacterial drugs with new modes of action. Over such a lengthy period without any new drugs to

combat TB, even the slow growing *M. tuberculosis* has been able to gain resistance to those currently used in the clinic. Chromosomal gene mutation has been the single explanation for genetically based resistance in *M. tuberculosis* and the sequential accumulation of these mutations lead to a multidrug resistant (MDR) phenotype (Viveiros *et al.*, 2003). However, the efflux mechanisms identified in mycobacteria, acquiring of DNA, drug inactivating enzymes, the permeability barrier and reduction in the number of porins in the outer membrane all play a role in the emergence of MDR strains of *M. tuberculosis*. MDR strains are defined as those resistant to at least isoniazid and rifampicin (Silva *et al.*, 2001). The emergence of MDR strains of *M. tuberculosis* and the global human immunodeficiency virus (HIV) pandemic have greatly amplified the incidence of TB, reaffirming this disease as a primary public health threat (Xu *et al.*, 2004). Countries such as Kazakhstan, Uzbekistan, Estonia, Latvia, Lithuania and Russia have the highest incidence of MDR-TB, with around 14% of new cases being of the MDR type. With the ease that humans can travel today, the problem of MDR-TB is not just restricted to these countries but is a global problem. The cost of treating a patient with a non-resistant strain can take 6 to 9 months and costs around US$10 per day whilst treating an MDR strain can mean 2 years of daily injections and hospital care costing £100,000 (Ainsworth and Mackenzie 2001). Ensuring that patients see out the entire drug regimen is also a further problem to fight against the rise of MDR-TB, as once patients feel better they can forget or deliberately stop taking their treatment as prescribed.

There is therefore a great need to find new antimycobacterial drugs to combat the rapidly emerging MDR strains causing TB, as this problem will only deteriorate with time. The number of lives at risk and the crippling cost of treating MDR-TB must make finding new drugs a priority.

1.4.6 Anti-TB drugs used in the clinic

The current first line drugs used to treat TB include isoniazid, rifampicin, ethambutol and pyrazinamide (**Figure 1.4.6**). A combination of 2 to 4 of these drugs may be used for 6 to 9 months to treat a non-resistant strain of TB in the absence of infection with HIV (Viveiros *et al.*, 2003). The most widely accepted regimen is the combination of isoniazid, rifampicin, ethambutol and pyrazinamide daily for 2 months (early bactericidal activity phase), followed by isoniazid and rifampicin daily for an additional 4 months (sterilising activity phase) (Viveiros *et al.*, 2003). The treatment

for MDR-TB normally involves the use of second line drugs such as capreomycin, kanamycin, cycloserine, ethionamide and fluoroquinolones which are often more toxic and can take up to 2 years to treat, including self-injection (Newton *et al.*, 2000).

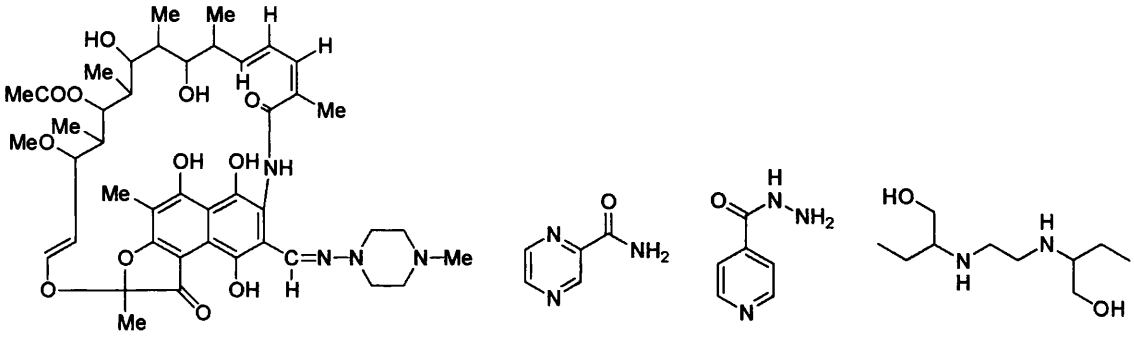

A B C D

Figure 1.4.6 Structure of rifampicin (A), pyrazinamide (B), isoniazid (C) and ethambutol (D)

1.4.7 Cell Surface Permeability Barriers

Mycobacteria are capable of surviving in the presence of many antibiotics. They can achieve this by combining two modes of resistance. They produce effective permeability barriers, comprising the outer membrane and the mycolate-containing cell wall, on the cell surface (Nikaido 2001). If an antibiotic does penetrate this hydrophobic barrier then there are efflux pumps which can actively extrude this back into the external environment thus subjecting the cell to a subcidal dose of the antibiotic.

The outer membrane is composed of very long chain fatty acids known as mycolic acids, which can contain 70-90 carbons (Lambert 2002). The outer surface also contains other complex lipids and waxes including lipopolysaccharides, glycopeptidolipids and phenolic glycolipids (Lambert 2002). The inner region of the outer membrane contains arabinogalactan which is linked to peptidoglycan of the cell wall (Lambert 2002). Mycobacteria, like Gram-negative bacteria, possess porins that span the outer membrane and facilitate the passage of low molecular weight hydrophilic nutrients. Relatively hydrophobic antimicrobials such as fluoroquinolones and rifampicin may penetrate the outer membrane and cell wall slowly by diffusion. These compounds can then be extruded by one of the efflux mechanisms if they are able to reach the cytoplasm of the cell. The uptake of nutrients and small hydrophilic

antimicrobials, such as isoniazid, *via* the porins is slow and could also be subject to one of the efflux pumps. However, mycobacteria can also combat the passage of these compounds by reducing the number of porins in the outer membrane and therefore further decrease the concentration of antimicrobial passing through in this way.

1.4.8 *Staphylococcus aureus* NorA

NorA is a pmf dependent multidrug efflux pump in *S. aureus* that provides intrinsic resistance to fluoroquinolones and other chemically diverse substrates (Price *et al.*, 2002). It is a chromosomally encoded efflux system belonging to the MFS family. A mutation in the *norA* gene was originally thought to be the cause of reduced susceptibility of *S. aureus* to hydrophilic fluoroquinolones and was originally thought to be an allele of *gyrA* (Marshall and Piddock 1997). However it was later identified that NorA was a protein involved in active efflux of drugs that shares 44% amino acid homology with Bmr from *Bacillus subtilis* (Marshall and Piddock 1997).

1.4.9 Methicillin-resistant *Staphylococcus aureus*

Over the past 20 years there has been a rapid rise in multidrug resistant pathogens such as methicillin-resistant *S. aureus* (MRSA) and vancomycin-resistant enterococci (VRE) (Baysallar *et al.*, 2004). As Gram-positive bacteria are more permeable to antibacterial compounds, than Gram-negative bacteria and mycobacteria, they must have efficient mechanisms to prevent these compounds from exerting their bacteriostatic or bactericidal effects. Methicillin resistance in staphylococci is due to the expression of the *mecA* gene which encodes for a PBP2A that has a reduced affinity for β-lactams and therefore conferring resistance to this chemical class of drugs (Ang *et al.*, 2004). Vancomycin, a glycopeptide, has been the first-line drug used to treat infections caused by MRSA and has been effective since its introduction in 1985 in Europe and USA and in the Far East since 1991 (Gemmell 2004). However, recent reports of infections due to vancomycin-resistant *S. aureus* (VRSA) have grave implications regarding the future treatment of such infections (Cha *et al.*, 2003). Linezolid, the first drug of a new chemical class known as oxazolidinones, has recently been approved for use by the FDA to treat infections caused by MRSA (Bozdogan and Appelbaum 2004). The mode of action of oxazolidinones has not been completely delineated although it has been shown that they bind to the 50S subunit of ribosomes, preventing formation of the 70S ribosome

complex. Resistance to linezolid by two strains of MRSA has already been reported in Turkey prior to clinical use (Baysallar *et al.*, 2004). The only reported mechanism of resistance towards linezolid has been by target modification, thus decreasing linezolid binding to the 23S rRNA ribosome subunit (Bozdogan and Appelbaum 2004). Daptomycin, a novel cyclic lipopeptide antibiotic, and quinupristin/dalfopristin (Synercid), a mixture of two streptogramins, have recently been approved for clinical use against Gram-positive infections including MRSA and vancomycin-resistant enterococci (VRE).

These new drugs have shown good activity against these difficult-to-treat Gram-positive strains. Further work on identifying new antibiotics with novel mechanisms of action is urgently required to combat the rapid rise in multidrug resistant strains of Gram-positive bacteria.

1.5 Nuclear Magnetic Resonance Spectroscopy

Nuclear magnetic resonance (NMR) spectroscopy has proved to be an invaluable tool for natural product chemists ever since this phenomenon was first observed in 1946 (Williams and Fleming 1995). It is a technique of primary importance for the elucidation of natural product compounds. NMR spectroscopy can also be applied to crude extracts and fractions to ascertain the presence of various chemical classes within a complex mixture. Improvements to this technique by way of increased magnetic field strengths (up to 900 MHz ^{1}H frequency), being commercially available, have resulted in greater resolution of ^{1}H spectra. This has facilitated the use of this powerful tool across a wide range of scientific disciplines.

1.5.1 ^{1}H NMR Spectroscopy

^{1}H NMR spectroscopy was the first experiment to be recorded for a purified compound. Spectra were either recorded on a 400 or 500 MHz spectrometer. The information provided by this experiment alone can be sufficient to elucidate the structure of a compound. The ^{1}H NMR spectrum provides information as to the chemical shift (δ), expressed in parts per million (ppm), of the protons within a molecule relative to the solvent used. Signals appearing downfield (left-hand side) in the ^{1}H spectrum require an higher frequency to bring these protons into resonance than signals appearing upfield (right-hand side). The protons appearing downfield are in an environment with a low electron density and are said to be deshielded. Whereas protons appearing upfield are in an environment of high electron density and are said to be shielded. Signal multiplicity provides further information about adjacent protons to that being split as it is a result of spin-spin coupling. Therefore it is influenced by the environment of the proton being split. The splitting pattern is governed by the multiplicity rule ($2nI + 1$), where n is the number of equivalent protons and I is the nuclear spin quantum number. Hence if a proton is next to n equivalent protons, the signal will be split in to $2nI + 1$ peaks. The coupling constant (J) in Hz can be measured as the difference in frequency between two multiplet lines. Coupling can occur through two bonds (*geminal* coupling, ^{2}J), three bonds (*vicinal* coupling, ^{3}J) or four or five bonds (long-range couplings, ^{4}J and ^{5}J) (Breitmaier 1999). It can provide information as to whether neighbouring protons are *cis* or *trans* with respect to one another. Integration of all signals within a spectrum enables the number of protons in each signal to be established and therefore the number of protons within the molecule.

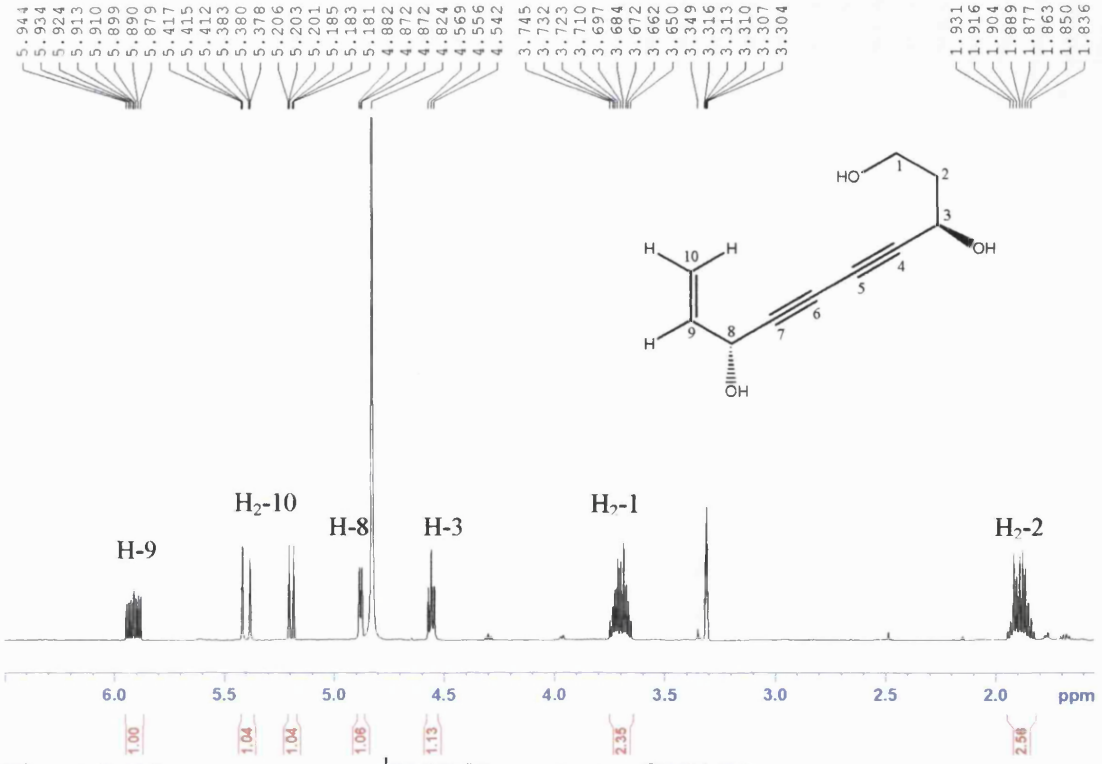

Figure 1.5.1 ^{1}H NMR spectrum of **MS-26**

The ^{1}H NMR spectrum of **MS-26** highlights the chemical shift and splitting pattern of this C_{10} polyacetylene natural product. The oxymethine proton, H-3, is adjacent to two equivalent protons (H_2-2), therefore using the multiplicity rule 2nI + 1 the resonance of this proton is split into a triplet. This can also be seen with H-8 which is next to one proton (H-9) and is split into a doublet. The splitting pattern of H-9 differs from H-3 and H-8 as the adjacent protons are all chemically non-equivalent. This gives rise to a doublet of doublet of doublets. The coupling constant of H-10a (δ_H 5.19) was measured as 10.1 Hz whilst the second, more downfield proton of H-10b (δ_H 5.40) was measured as 17.0 Hz. The coupling constants from the ^{1}H NMR spectrum therefore allow the more downfield proton of H-10 to be assigned as *trans* with respect to H-9, whilst the more upfield proton of H-10 can be placed in a *cis* position with respect to H-9. The chemical shift can also provide information as to the nature of the protons, for example, olefinic protons are normally detected between 4.5 - 6.0 ppm. Oxymethine protons tend to resonate between 3.8 – 5.2 ppm, whilst oxymethylene protons are normally found in the region 3.5 – 4.5 ppm.

1.5.2 ^{13}C NMR Spectroscopy

^{13}C NMR spectroscopy is a 1D experiment of great importance. ^{12}C nuclei are NMR inactive, however ^{13}C nuclei, with an odd number of protons is NMR sensitive. ^{13}C has a natural abundance of 1.1% and so it is highly unlikely that two adjacent carbon atoms will be able to split each others signal. Due to the small natural abundance of ^{13}C, it makes this 1D NMR experiment far less sensitive than ^{1}H NMR spectroscopy. An external magnetic field strength of 125 MHz was mainly used to record ^{13}C NMR spectra. A helpful feature of ^{13}C spectra is that each carbon within a molecule appears as a singlet as there is no carbon-carbon coupling and ^{1}H-^{13}C coupling is removed by broad band decoupling. This enables the number of carbons in a molecule to be quickly calculated by counting all the singlet peaks appearing in the spectrum. As the ^{13}C NMR spectrum is far wider in terms of coming into resonance, overlap of signals is not commonly observed unlike ^{1}H NMR spectra. Another aspect of ^{13}C spectra as compared to ^{1}H spectra is no integration is required to be performed. However, occasionally a single peak in the ^{13}C spectrum will be due to two or more carbons coming into resonance at exactly the same position. This phenomenon can normally be detected by the height of a peak as compared to the remainder of signals present in the spectrum. Due to the wider range that carbon signals can come into resonance, it is possible to identify carbon-containing functional groups by the characteristic shift values in the ^{13}C NMR spectra (Breitmaier 1999). For example, ketonic carbonyl carbons tend to appear between 190-220 ppm, whilst acetylenic carbons are characteristically detected between 65-85 ppm. The appearance of carbon functionalities may be slightly altered if they are attached to electronegative atoms such as oxygen or are in a highly strained ring system. This would have the effect of shifting carbon signals further downfield than would normally be expected. ^{13}C NMR spectra are of great use as they can be used not only to determine the number of carbons present in a molecule but also the nature of the carbons and hence give an indication of the class of compound present.

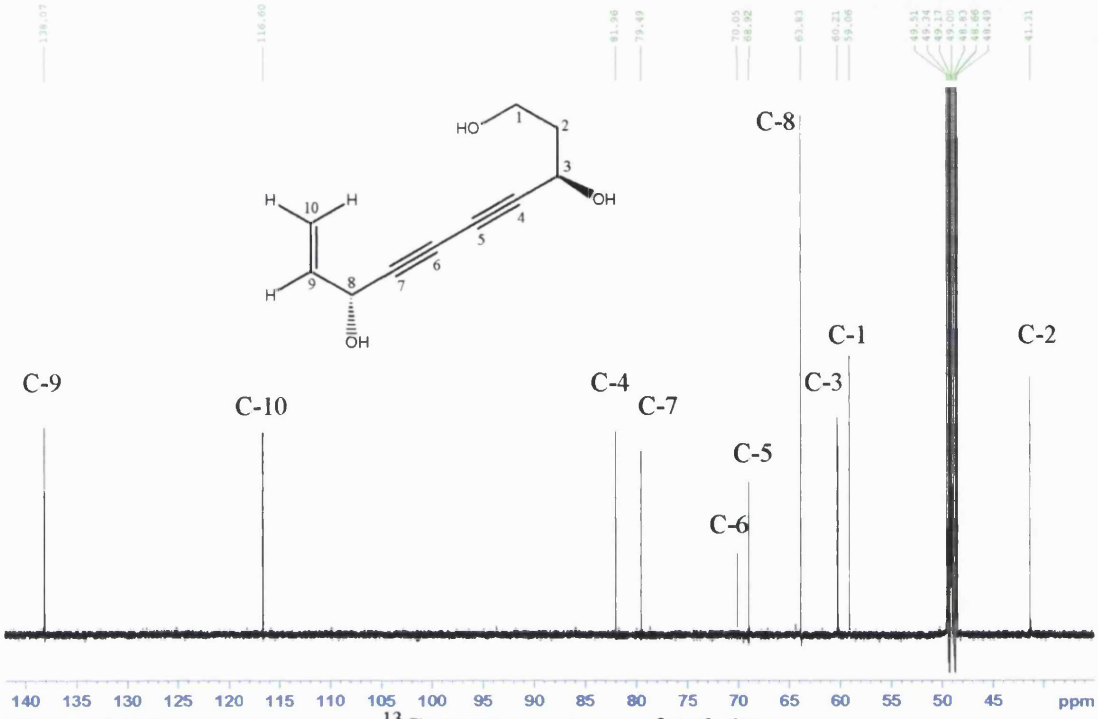

Figure 1.5.2 ^{13}C NMR spectrum of **MS-26**

The ^{13}C NMR spectrum details the number of carbons in **MS-26** along with the solvent peak, in this case deuterated methanol. The chemical shift values of the resonances can also provide valuable information as to the nature of the carbons. From **Figure 1.5.2**, a terminal olefinic methylene (δ_C 100 – 120) and olefinic (δ_C 115 – 145) carbons can be identified. The presence of four carbons in the region 65 – 85 ppm is also very characteristic of conjugated acetylenic carbons as is the presence of two oxymethine carbons between 60 - 80 ppm.

1.5.3 Distortionless Enhanced Polarisation Transfer

Distortionless enhanced polarisation transfer (DEPT) is the third 1D NMR technique used in this thesis. DEPT experiments were mainly recorded at 125 MHz. This technique provides an even simpler method for detecting the types of carbons present in a molecule, allowing methyl, methylene, methine and quaternary carbons to be distinguished from each other. The DEPT 135° experiment was exclusively used throughout this thesis. The number 135° describes the angle of the final ^{1}H decoupler pulse. This experiment is used to detect carbons directly attached to protons (^{1}H-^{13}C). Hence a DEPT 135° spectrum will show methyl, methylene and methine carbons whilst quaternary carbons are not present. Methyl and methine bearing carbons appear

above the baseline (positive) whilst methylene carbons appear below the baseline (negative) (**Figure 1.5.3**). Comparison of a DEPT 135° spectrum with the corresponding ^{13}C NMR spectrum facilitates the detection of quaternary carbons within the molecule.

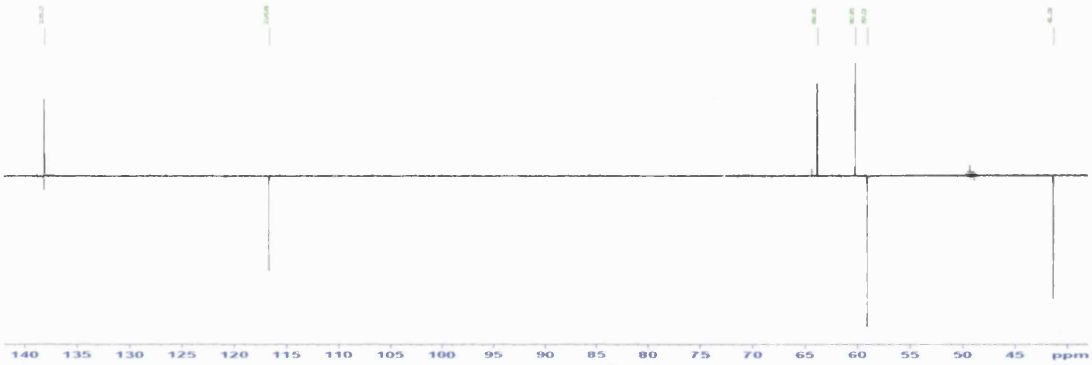

Figure 1.5.3 DEPT spectrum of **MS-26**

1.5.4 Heteronuclear Multiple Quantum Coherence

Heteronuclear multiple quantum coherence (HMQC) is a 2D NMR experiment that provides one bond ^{1}H-^{13}C connectivities. The HMQC spectrum correlates the ^{1}H spectrum with the ^{13}C spectrum of a compound. A signal from one carbon can be correlated to the corresponding proton signal. Therefore all proton signals must be accounted for in the HMQC and facilitate the structure elucidation of the compound.

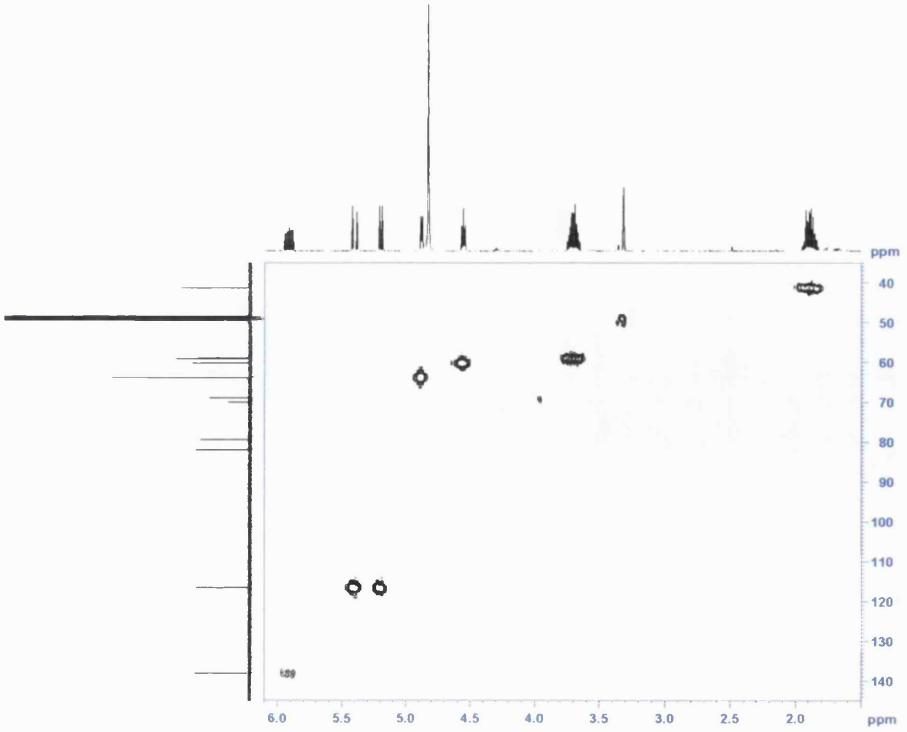

Figure 1.5.4 HMQC spectrum of **MS-26**

1.5.5 Heteronuclear Multiple Bond Connectivity

Heteronuclear multiple bond connectivity (HMBC) is a 2D NMR experiment similar to HMQC. The difference being it detects two- and three-bond connectivities rather than one-bond in the HMQC. Occasionally, four-bond connectivities are also detected. This experiment is vital to the unambiguous assignment of a compound. In this experiment a time delay in the pulse sequence is set to correspond to $^1/_{2J}$ where J is approximately 7 Hz, i.e. a delay of about 70 ms (Williams and Fleming 1995).

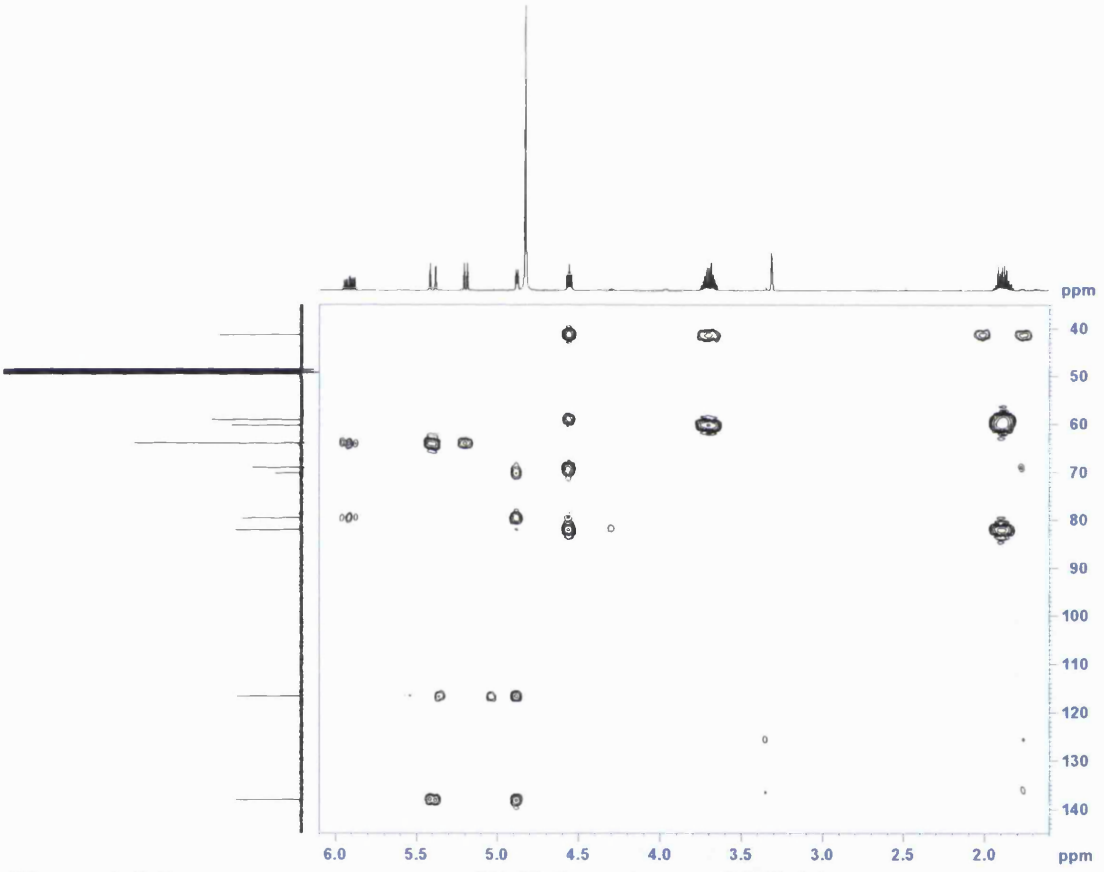

Figure 1.5.5 HMBC spectrum of **MS-26**

1.5.6 Correlation Spectroscopy

Correlation spectroscopy (COSY) is a technique that is used in addition to HMBC experiments to elucidate the structure of a compound. The COSY spectrum differs from HMQC and HMBC spectra in that it correlates the ^{1}H spectra on both frequency axes. This results in a spectrum with square symmetry. All peaks that are mutually spin-spin coupled are shown by cross-peaks that are symmetrically placed about the diagonal (Breitmaier 1999). This technique provides ^{1}H-^{1}H connectivities

for protons that are two- and three-bonds apart and occasionally for W-relationships (**Figure 1.5.6**).

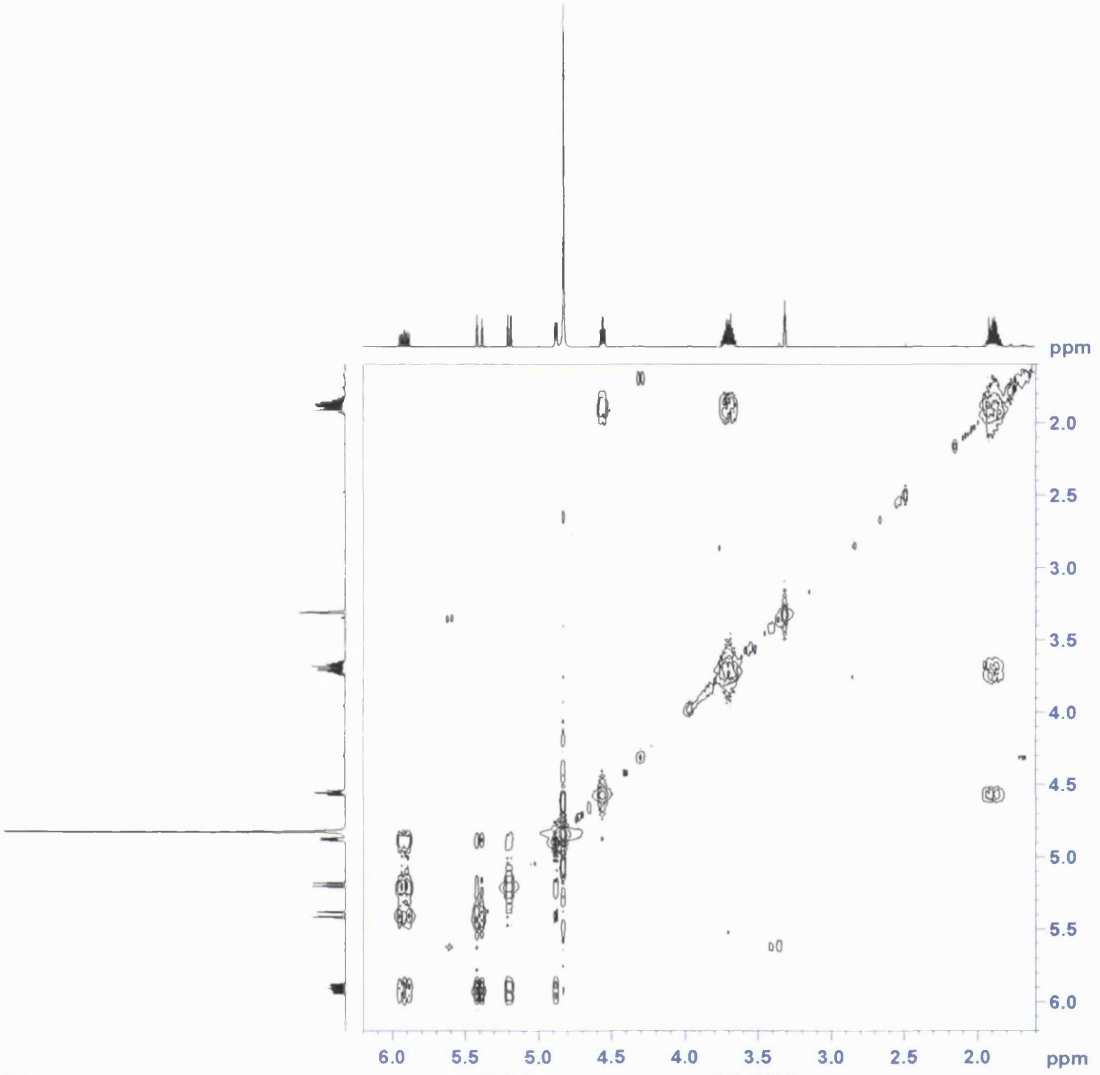

Figure 1.5.6 COSY spectrum of **MS-26**

1.5.7 Nuclear Overhauser Effect Spectroscopy

The nuclear Overhauser effect spectroscopy (NOESY) spectrum is similar to the COSY spectrum in that it correlates the ^{1}H spectra on both frequency axes. However, it differs by detecting through space interactions between protons. The interaction may appear as a more intense or weaker signal than normal and this is called the nuclear Overhauser effect (NOE) (Williams and Fleming 1995). NOE's can only be detected over short distances in the region 2-5 Å. This experiment is important to the determination of the relative stereochemistry of a compound.

2.0 Materials and Methods

2.1 Spectroscopic Techniques

UV spectra were recorded on a Perkin-Elma Lambda 15 spectrophotometer. Chloroform and methanol were the solvents used to record spectra. IR spectra were recorded on a Nicolet 360 FT-IR spectrometer as a thin film. All specific rotations, $[\alpha]_D$, were recorded on a Bellingham and Stanley ADP 220 polarimeter.

NMR studies of purified compounds were performed on either a Bruker AVANCE 400 or Bruker AVANCE 500 spectrometer at 400 and 500 MHz respectively. Deuterated solvents used to record NMR spectra of samples included $CDCl_3$, CD_3OD, C_6D_6 and C_5D_5N. The ^{13}C NMR experiments performed in this PhD included standard ^{13}C spectra at 125 MHz and DEPT 135. These experiments along with the HMQC and ^1H NMR spectra enabled the assignment of all carbon signals as a CH_3, CH_2, CH or quaternary carbons. Chemical shift values are reported in parts per million (ppm) relative to the NMR solvent. Coupling constants (*J* values) are given in Hertz. The 2D NMR experiments performed to enable characterisation of all natural products were HMQC, HMBC, COSY 90 and NOESY. Unless otherwise stated, ^1H and ^{13}C NMR spectra were carried out at 500 MHz and 125 MHz respectively.

Fast atom bombardment (FAB) and electron impact (EI) mass spectra were recorded on a VG Analytical ZAB-SE instrument. Electrospray ionisation (ESI) was performed on a Finnigan Navigator instrument. Accurate mass determinations were recorded on a Finnigan MAT 95 high-resolution magnetic sector mass spectrometer. GC-MS experiments were performed on an HP 5890 Series II Plus gas chromatograph interfaced to an HP 5989A mass spectrometer.

Table 2.1 Chemical shift (δ_H and δ_C) values of NMR solvents

Deuterated Solvent	δ_H (ppm)	δ_C (ppm)
Chloroform ($CDCl_3$)	7.26	77.0
Methanol (CD_3OD)	3.31	49.0
Benzene (C_6D_6)	7.16	128.7
Pyridine (C_5D_5N)	7.21 (H-2), 7.57 (H-3), 8.72 (H-1)	123.5 (C-2), 135.5 (C-3), 149.5 (C-1)

2.2 Mosher's ester methodology

2.2.1 *tert*-butyl dimethylsilyl (TBDMS) protection of primary alcohols

Prior to the esterification of **MS-26** by methoxyphenylacetic acid (MPA) the primary alcohol was protected with TBDMS. This ensured that the primary alcohol was not esterified with (*R*)-(-)- and (*S*)-(+)-MPA (Sigma), which could then lead to an erroneous assignment of the absolute stereochemistry at C-3. This was due to the close proximity of the primary alcohol to C-3, which could have had a shielding or deshielding effect on the protons attached at both C-1 and C-2.

MS-26 (500 µg, 2.8 µmol) was dissolved in 750 µl of $CDCl_3$. 20 µl aliquots of a 2.5:1 mixture of imidazole and TBDMS-Cl (1 µmol/ml) were added. The reaction was monitored by NMR. When protection of the primary alcohol had been achieved, the mixture was applied directly to a preconditioned 3 ml silica gel solid-phase extraction cartridge (Bakerbond). The TBDMS-protected **MS-26** was eluted with 50% ethyl acetate-hexane before being evaporated to dryness.

2.2.2 Methoxyphenylacetic acid (MPA) esterification of compounds

The two compounds subjected to Mosher's ester methodology were **MS-24** and **MS-26**. Two portions of a compound were dissolved in dry dichloromethane (2 ml) that contained 2 mg of dimethylaminopyridine (Sigma). Eight equivalents of PS-carbodiimide resin (Argonaut Technologies Inc.) were added to each portion. Six equivalents of either (*R*)- or (*S*)-MPA were added to a portion of the test compound. This resulted in the formation of bis-(*R*)- and bis-(*S*)- Mosher's esters of the test compounds respectively. The reaction mixture was then stirred for 24 h before being filtered to remove the PS-carbodiimide resin followed by drying under nitrogen. The esterified compound was then dissolved in 750 µl $CDCl_3$ and loaded into NMR tubes. ^1H NMR spectra were recorded to detect differences in the chemical shifts of protons in close proximity to the chiral centres. Esterification with the two isomers of MPA resulted in a difference in the chemical shift of the protons in close proximity. This may result in a greater shielding or deshielding effect. The difference in chemical shift was calculated using $\Delta_\delta = \delta_R - \delta_S$ where δ_R and δ_S are shifts (in ppm). A positive Δ_δ for a group of diagnostic resonances indicates *R* stereochemistry at the chiral centre in question. Whilst a negative Δ_δ for a group of diagnostic resonances indicates *S* stereochemistry at the chiral centre in question. The positive and negative magnitudes of Δ_δ were interpreted using the model adapted by Kakisawa and collaborators (Ohtani *et al.*, 1991) (**Figure 2.2.2A**).

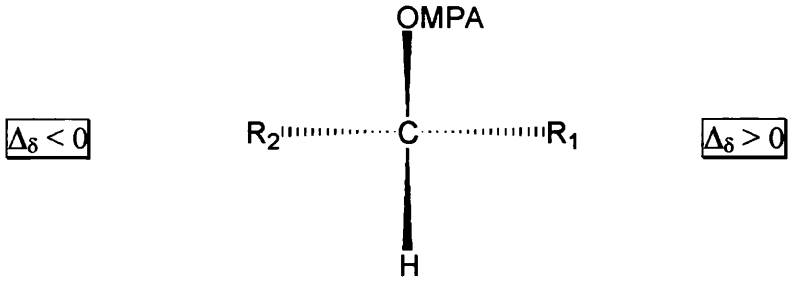

Figure 2.2.2A The Mosher's ester was (*R*)- or (*S*)-methoxyphenylacetic acid (MPA). When Δ_δ for a group of diagnostic resonances is positive then it is placed at R_1. When Δ_δ for a group of diagnostic resonances is negative then it is placed at R_2.

2.3 Extraction of Plant Material

Large-scale extractions of plant material were extracted in a Soxhlet extractor. The dry, powdered material was packed into a thimble and extracted sequentially with solvents (3 l each) of increasing polarity. Solvents used include hexane, chloroform, ethyl acetate and methanol. The extraction process lasted approximately 5 days for each solvent. The extracts were then dried on a rotary evaporator and stored in a freezer.

Small-scale extractions of plant material were performed to allow analytical TLC and bioactivity assays to be carried out. Approximately 5 g of material was extracted sequentially with ethyl acetate, methanol and water on a magnetic stirrer at room temperature.

2.4 Analytical and Bioactive Screening of Plant Extracts

A total of 30 plants were analysed by TLC on silica plates using standard solvent systems, which included ethyl acetate-hexane (60:40) and chloroform-methanol (60:40). Duplicate plates were developed which were first visualised at 254 nm (short wave) and then at 366 nm (long wave). Plates were then either sprayed with 4% vanillin sulphuric acid followed by heating or with Dragendorff's reagent.

Extracts were assayed for bioactivity using the standard MIC assay (section **2.6.2**) versus *M. fortuitum* ATCC 6841. The bioactivity of plant extracts was the principal determining factor as to which plant would be studied further. In the absence of any bioactivity the decision as to which plant would be studied was based on the results obtained by analytical TLC.

Table 2.2 Plant material and yield of extracts gained

Plant Species	Family	Date of Collection	Place of Collection	Plant Part Extracted	Material Extracted	Hexane Extract	Chloroform Extract	Methanol Extract
Anethum graveolens	Apiaceae	March 1999	Doha	Whole Herb	280 g	8.0 g	4.8 g	~70 g
Artemisia monosperma	Asteraceae	February 1999	Wadi Al-Batin	Aerial	285 g	10.0 g	15.5 g	43.5 g
Ducrosia anethifolia	Apiaceae	April 1999	Khiran Resort	Whole Herb	500 g	0.9 g	13.4 g	19.7 g
Ipomoea pes-caprae	Convolvulaceae	August 1999	Sheraton Hotel car park	Aerial	454 g	13.0 g	10.0 g	~60 g
Pulicaria crispa	Asteraceae	May 1999	Kuwait Institute of Scientific Research (KISR)	Whole Herb	186 g	6.7 g	5.9 g	22.0 g
Scrophularia deserti	Scrophulariaceae	February 1999	Wadi Al-Batin	Whole Herb	450 g	5.2 g	16.7 g	66.8 g

2.5 Chromatography Techniques

2.5.1 Vacuum Liquid Chromatography

This is a technique primarily used for the fractionation of plant extracts and complex mixtures. It is a quick and simple technique used to separate compounds of like polarity. The dimensions of the VLC column are 60 mm internal diameter and 130 mm height and it is fitted with a sintered glass frit at the base. The column was prepared using silica 60 $PF_{254+366}$ (Merck: 1.07748), which is preparative TLC grade silica. The column was packed to a height of 80 mm under vacuum. It is essential there are no cracks or pockets of air around the edges of the column to ensure good separation. The head of the column was evenly packed to ensure a good separation. Once this has been achieved the column can then be washed with hexane to remove any silica fines and to equilibrate the column.

Plant extracts were prepared by adsorbing them onto silica (1.5 times the weight of the extract) by making a solution with a minimal amount of solvent. This was then dried on a rotary evaporator and then applied to the head of the column and packed evenly. The extract was then fractioned using a step gradient system with 10% increments from 100% hexane to 100% ethyl acetate followed by a methanol wash. 200 ml fractions were collected of each solvent system. To ensure good separation and no compound bleeding, the column was allowed to go to dryness prior to addition of the next solvent system. For all non-polar plant extracts, a hexane-ethyl acetate step-gradient system was employed. However, for methanol extracts an ethyl acetate-methanol step-gradient system was necessary.

2.5.2 Flash Chromatography

This technique is ideally suitable for the further fractionation of a fraction rather than extract. The flash chromatography model used during this PhD was a Flash 40 model. Pre-packed silica columns (i.d 40 mm; 40M) allow for good reproducibility of chromatographic results. This method employs positive pressures, normally ~10 bar from a nitrogen cylinder, to pass the mobile phase through the column.

Fractions were prepared by adsorbing the material onto silica as described in section **2.5.1**. The adsorbed material was then packed evenly into a plastic column syringe body fitted with a frit. A second frit was applied to the head of the packed material. After column equilibration, the first solvent system was passed through the material and applied to the head of the column. Fractions were then collected and combined on the basis of analytical TLC results.

2.5.3 Solid Phase Extraction

This procedure can be applied to both crude extracts and simple fractions. It is a fast and efficient method that can be used to concentrate and purify compounds. Both normal phase (Strata Sl-1) and reverse phase (Strata C18-E) columns were employed with this technique. Pre-packed columns were mounted onto a manifold and equilibrated with starting mobile phase. The mobile phase was passed through the stationary phase under vacuum.

Samples were prepared by dissolving in not more than 1.5 ml of the starting mobile phase. Once the column was equilibrated the sample was applied to the head of the column. This was allowed to adsorb onto the top of the column prior to addition of the first mobile phase. In general, a step-gradient system was used with 50 ml fractions collected at a time. The column was not allowed to go to dryness, however, the column head frit was allowed to run dry before the tap was closed and the vacuum released.

2.5.4 Sephadex LH-20 Column Chromatography

Sephadex LH-20 chromatography is a technique used to separate compounds on the basis of their size and shape. Firstly, 120 g of Sephadex LH-20 was soaked in dichloromethane as a slurry and allowed to expand. After 1 h of soaking, the Sephadex LH-20 was poured into a column fitted with a sintered glass frit (40 mm internal diameter x 390 mm height) as a slurry in one continuous motion. The column was then allowed to settle before eluting the excess dichloromethane. Fractions were dissolved in a minimal amount of dichloromethane and applied to the column head. Dichloromethane fractions were then collected followed by a change in solvent to 100% methanol. Fractions were combined on the basis of analytical TLC results.

Sephadex LH-20 is a valuable technique for the fractionation of natural products with a molecular weight ranging from 100 – 4000. Larger compounds (MW>4000) are unretained and so are readily eluted. This technique can thus be used for the removal of ubiquitous, large MW compounds such as chlorophylls.

2.5.5 Preparative Thin Layer Chromatography

Samples were dissolved in a minimal volume of solvent before being applied as a band 2 cm from the bottom and 2 cm from the sides of the TLC plates. Plates were then allowed to dry prior to being placed in the solvent tank. Not more than 100 mg and 20 mg were applied to preparative and analytical plates respectively. Plates were removed from the solvent tanks once the solvent front reached the top of the plate.

Bands were scraped off and eluted on the basis of UV and/or vanillin-sulphuric acid spray followed by heating. Plates may also undergo multiple developments to enable resolution of compounds with similar R_f values.

TLC plates used include preparative (Silica 60 F_{254}; Merck: 1.05637) (2 mm plate thickness), analytical (Silica 60 F_{254}; Merck: 1.05554), alumina (aluminium oxide neutral 60 F254; Merck: 1.05550), reverse phase (RP-18 F_{254}; Merck: 1.05559). All TLC plates were aluminium backed except for the preparative plates which had a glass back.

2.5.6 High Performance Liquid Chromatography (HPLC)

This technique was used to isolate **MS-41** and also to separate the highly methoxylated flavones **MS-32** and **MS-33**. This was performed on a Waters 4000 HPLC system in the reverse phase mode. This utilised two octadecylsilyl radial compression modules (25 mm x 400 mm) in series with acetonitrile-acetic acid (99.5:0.5) as the solvent system. A flow rate of 50 ml/min was in operation and the UV detector was set at 254 nm. A total of 28 mg, containing **MS-32** and **MS-33**, was applied over the course of two HPLC runs (14 mg/run). This afforded 7.5 mg of **MS-32** (retention time = 15.5 min) and 11 mg of **MS-33** (retention time = 17.0 min).

MS-41 was isolated using a gradient system of acetonitrile-water. A total of 38 mg was applied to the head of the column using the same HPLC system, columns, flow rate and set wavelength as described above. **MS-41** was eluted after 10.1 min (69:31 water-acetonitrile solvent system) and afforded 2.3 mg. The mode of separation of these three compounds was by partition chromatography.

2.6 Bacterial Assays

2.6.1 Bacterial Strains

S. aureus strains were cultured on nutrient agar (Oxoid) whilst strains of mycobacteria were cultured on Columbia agar (Oxoid) supplemented with 5% defibrinated horse blood (Oxoid) and incubated for 24 h and 72 h respectively at 37°C prior to MIC determination.

Table 2.3 Bacterial strains used in this study

Bacterial Strain	Resistance Mechanism	Provided by:
Staphylococcus aureus SA 1199B	NorA	G. Kaatz, Division of Infectious Diseases, Department of Internal Medicine, School of Medicine, Wayne State University and John D. Dingell Department of Veterans Affairs Medical Centre, Detroit, Michigan.
Staphylococcus aureus EMRSA-15	MecA	P. Stapleton, Department of Microbiology, University of London School of Pharmacy, UK.
Staphylococcus aureus XU212	TetK and MecA	E. Udo, Department of Microbiology, Faculty of Medicine, Safat, Kuwait.
Staphylococcus aureus RN4220	MsrA	J. Cove, Department of Microbiology, University of Leeds, UK.
Staphylococcus aureus ATCC 25923	ATCC Strain	E. Udo, Department of Microbiology, Faculty of Medicine, Safat, Kuwait.
Mycobacterium fortuitum ATCC 6841	ATCC Strain	P. Lambert, Department of Microbiology Aston University, UK.
Mycobacterium aurum Pasteur Institute 104482	PI Strain	V. Seidel, Department of Microbiology, University of London School of Pharmacy, UK.
Mycobacterium phlei ATCC 11758	ATCC Strain	V. Seidel, Department of Microbiology, University of London School of Pharmacy, UK.
Mycobacterium smegmatis ATCC 14468	ATCC Strain	V. Seidel, Department of Microbiology, University of London School of Pharmacy, UK.
Mycobacterium abscessus ATCC 19977	ATCC Strain	V. Seidel, Department of Microbiology, University of London School of Pharmacy, UK.

2.6.2 Minimum Inhibitory Concentration Assay

The minimum inhibitory concentration (MIC) assay was used to determine the *in vitro* activity of compounds, fractions and plant extracts. The assay was performed in Mueller-Hinton broth (MHB; Oxoid) adjusted to contain 20 and 10 mg/l of Ca^{2+} and Mg^{2+} respectively. An inoculum density of 5 x 10^5 cfu/ml was prepared in saline solution (9 g/l). This was achieved using the McFarland standard to approximate the turbidity of a bacterial suspension. All assays were performed in 96-well microtitre plates (Nunc, 0.3 ml volume per well). Norfloxacin, isoniazid, ethambutol, (erythromycin and tetracycline) were obtained from Sigma Chemical Co. MHB (125 µl) was dispensed in wells 1-10 followed by addition of 125 µl of sample in the first well. Polar samples were dissolved directly in MHB, however, non-polar samples were first dissolved in DMSO to facilitate their solubilisation in MHB at the appropriate concentration. The DMSO concentration never exceeded a final concentration of 0.625%. After serial doubling dilution of the sample into each of the wells, 125 µl of the appropriate bacterial inoculum was added. Plates were incubated at 37°C for 72 h for mycobacteria strains (except *M. aurum* and *M. abscessus* which were incubated for 96 h and 120 h respectively). All other bacterial strains were incubated for 18 h. Positive and negative controls were carried out in all assays. The MIC was recorded as the lowest concentration at which no growth was observed and this was enhanced by the addition of 20 µg/ml methanolic solution of 3-[4,5-dimethylthiazol-2-yl]-2,5-diphenyltetrazolium bromide (MTT; Sigma) to each of the wells followed by incubation at 37°C for 20 min. A blue colouration indicated growth. No growth resulted in the well remaining yellow.

2.6.3 Microcytostasis assay

This assay was used to determine the chemosensitivity of dehydrofalcarindiol **(MS-24)** against 6 tumour cell lines. The 6 tumour cell lines studied included colorectal carcinomas LS174T, SKCO1, COLO320DM, WIDR and breast carcinomas MDA231 and MCF7. Dehydrofalcarindiol was tested at a concentration range of 500 – 1.95 µg/ml. DMSO controls from 1:10 – 1:2560 dilutions were performed, which would equate to the amount that would be present in the dehydrofalcarindiol dilutions. Initially the concentration of dehydrofalcarindiol used was 1000 µg/ml but this was lowered to conserve the compound. The MTT assay was used to determine the

chemosensitivity of the 6 tumour cell lines tested. The protocol for this assay was described by Ford *et al.*, (1989).

2.7 Isolation and Purification of Compounds

Details of the isolation and purification of compounds **MS-1** – **MS-46** are outlined in **Table 2.4**. Below is a list of abbreviations for **Table 2.4** on the isolation of compounds in this PhD thesis.

Compound

This indicates the code of the compound listed in the thesis.

Species

This identifies the plant species a compound has been isolated from. The following abbreviations are for the six plant species studied in this thesis:

Ag = *Anethum graveolens*

Am = *Artemisia monosperma*

Da = *Ducrosia anethifolia*

Ip = *Ipomoea pes-caprae*

Pc = *Pulicaria crispa*

Sd = *Scrophularia deserti*

Extract

This is the extract from which a compound has been isolated from, for example:

HX = Hexane

C = Chloroform

M = Methanol

Class

This is the chemical classification of the natural product isolated.

VLC Fraction

This identifies the VLC fraction from which a compound has been isolated. The mobile phase composition indicates the polarity at which a compound has been eluted.

Purification Procedure

This shows the number of steps required to isolate a natural product and also the techniques and solvents required to achieve purification.

FC = Flash Chromatography

SP = Sephadex

NP-SPE = Normal Phase Solid Phase Extraction

RP-SPE = Reverse Phase Solid Phase Extraction

RP = Reverse Phase

PTLC = Preparative Thin Layer Chromatography

MPTLC = Multiple Development Preparative Thin Layer Chromatography

HPLC = High Performance Liquid Chromatography

Solvents

A = Acetic Acid, ACN = Acetonitrile, C = Chloroform, DCM = Dichloromethane, DE = Diethyl ether, E = Ethyl Acetate, H = Water, HX = Hexane, M = Methanol, PE = Petroleum Ether, T = Toluene.

R_f

This indicates the migration of a compound on a particular stationary phase and mobile composition and is expressed as a ratio:

$$R_f = \frac{\text{Distance migrated by compound from the origin}}{\text{Solvent front distance from the origin}}$$

Weight

This indicates the amount of a pure compound that was isolated.

Table 2.4 Isolation of compounds **MS-1 – MS-46**

Compound	Species	Extract	Class	VLC Fraction	1	Purification 2	Procedure 3	4	R_f	Weight
MS-1	Ag, Ip	M	Hemiterpene	30% M-E	RP-SPE 100% H	-	-	-	0.50 7:3 E-M + A	18 mg
MS-2	Ag, Da	C	Monoterpene Glycoside	100% M	FC 1:1 C-M	MPTLC (2) 8:2 C-M + A	-	-	0.16 7:3 C-M + A	14 mg
MS-3	Pc	HX	Monoterpene	70% HX-E	NP-SPE 7:3 HX-DE	MPTLC (2) 7:3 HX-DE	MPTLC (RP) (2) 75:25 M-H + A	-	0.42 75:25 (RP) M-H + A	6.4 mg
MS-4	Am	M	Monoterpene glycoside	30% M-E	RP-SPE 7:3 H-M	PTLC (RP) 1:1 H-M	-	-	0.37 1:1 H-M (RP)	4.8 mg
MS-5	Sd	C	Iridoid Glycoside	100% M	SP 100% M	RP-SPE 7:3 H-M	PTLC 95:15 E-M + A	-	0.32 95:15 E-M + A	27 mg
MS-6	Sd	C	Iridoid Glycoside	100% M	SP 100% M	RP-SPE 1:1 H-M	MPTLC (3) Alumina 7:3 E-M + A	MPTLC (RP) (2) 6:4 M-H + A	0.49 6:4 (RP) (2) M-H + A	5.9 mg
MS-7	Sd	C	Iridoid Glycoside	100% M	SP 100% DCM	MPTLC (2) 95:10 E-M + A	PTLC (RP) 85-15 M-H	-	0.57 85:15 (RP) M-H	6.8 mg
MS-8	Sd	M	Iridoid Glycoside	30% M-E	SP 1:1 M-DCM	MPTLC (2) 5:80:2:18 TEA + M	-	-	0.30 5:80:2:18 TEA + M (2)	4.8 mg
MS-9	Sd	C	Iridoid Glycoside	100% M	SP 100% M	RP-SPE 6:4 M-H	MPTLC (3) Alumina 7:3 E-M + A	MPTLC (RP) (2) 6:4 M-H + A	0.46 6:4 (RP) (2) M-H +A	15 mg

Compound	Species	Extract	Class	VLC Fraction	1	Purification 2	Procedure 3	4	R_f	Weight
MS-10	Sd	C	Iridoid Glycoside	100% M	SP 100% M	RP-SPE 8:2 M-H	MPTLC (2) 95:10 E-M + A	-	0.44 95:15 E-M + A	10 mg
MS-11	Sd	C	Iridoid Glycoside	100% M	SP 100% M	RP-SPE 1:1 H-M	MPTLC (3) Alumina 7:3 E-M + A	MPTLC (RP) (2) 6:4 H-M	0.52 6:4 (RP) (2) M-H + A	4.7 mg
MS-12	Pc	HX	Sesquiterpene	50% HX-E	SP 100% DCM	NP-SPE 7:3 HX-E	MPTLC (2) 80:18:2 TEA	-	0.50 80:18:2 TEA (2)	7.5 mg
MS-13	Am	HX	Sesquiterpene	70% HX-E	FC 9:1 H-E	MPTLC (3) 9:1 HX-E	PTLC 80:18:2 TEA	-	0.54 90:9:1 TEA	14 mg
MS-14	Am	HX	Sesquiterpene	60% HX-E	FC 8:2 H-E	MPTLC (3) 75:25 HX-E	-	-	0.12 6:4 E-H	3.1 mg
MS-15	Pc	HX	Guaianolide Sesquiterpene	20% HX-E	SP 100% DCM	RP-SPE 6:4 M-H	-	-	0.46 75:25 (RP) M-H	12 mg
MS-16	Pc	HX	Guaianolide Sesquiterpene	20% HX-E	SP 100% M	MPTLC (RP) (2) 1:1 H-M	-	-	0.29 1:1 H-M (RP) (2)	7.6 mg
MS-17	Pc	HX	Guaianolide Sesquiterpene	40% HX-E	SP 100% DCM	MPTLC (2) 65:35 HX-E	-	-	0.31 6:4 H-E (2)	9.5 mg
MS-18	Pc	HX	Guaianolide Sesquiterpene	50% HX-E	SP 100% DCM	White ppt after addition of HX	-	-	0.35 80:18:2 TEA (2)	100 mg

Compound	Species	Extract	Class	VLC Fraction	1	Purification 2	Procedure 3	4	R_f	Weight
MS-19	Pc	M	Diterpene Glycoside	30% M-E	RP-SPE 1:1 H-M	MPTLC (2) 20:80:2:20 TEA + M	-	-	0.35 20:80:2:20 TEA + M	12 mg
MS-20	Ip	HX	Sterol	30% E-HX	NP-SPE 9:1 HX-E	MPTLC (3) 8:2 HX-E	-	-	0.42 75:25 H-E	13 mg
MS-21	Ip	HX	Triterpene	30% E-HX	SP 100% DCM	PTLC 9:1 T-E	PTLC (RP) 100% M	PTLC (RP) 100% M	0.30 100% M (RP) (2)	5.7 mg
MS-22	Ip	HX	Triterpene	30% E-HX	SP 100% DCM	PTLC 9:1 T-E	PTLC (RP) 100% M	-	0.26 100% M (RP) (2)	24 mg
MS-23	Ag	HX	Polyacetylene	40% E-HX	NP-SPE 9:1 PE-C	PTLC 75:25:2 TEA	-	-	0.47 75:25:2 TEA	8.8 mg
MS-24	Am	HX	Polyacetylene	40% E-HX	FC 8:2 HX-E	MPTLC (3) 75:25 HX-E	MPTLC (3) 80:20 HX-E	-	0.55 7:3 H-E + A	14 mg
MS-25	Am	C	Polyacetylene	30% E-HX	FC 7:3 HX-E	PTLC 75:25:2 TEA	-	-	0.47 80:18:2 TEA	2.1 mg
MS-26	Am	C	Polyacetylene	90% E-HX	SP 100% DCM	PTLC 30:68:2 TEA	-	-	0.39 30:68:2 TEA	9.8 mg
MS-27	Am	M	Polyacetylene	30% M-E	RP-SPE 8:2 H-M	PTLC (RP) 7:3 H-M	-	-	0.40 7:3 (RP) H-M	18 mg

Compound	Species	Extract	Class	VLC Fraction	1	Purification 2	Procedure 3	R_f	Weight
MS-28	Da	HX	Furocoumarin	60-100% E-HX	FC 6:4 HX-E	MPTLC (2) 1:1 HX-E	-	0.52 1:1 E-H (2)	25 mg
MS-29	Ag	C	Furocoumarin	50% E-HX	NP-SPE 8:2 HX-E	MPTLC (RP) (2) 7:3 M-H	MPTLC (RP) (3) 65:35 M-H	0.27 65:35 (RP) (3) M-H	6.3 mg
MS-30	Ag	HX	Furocoumarin	50% E-HX	NP-SPE 6:4 HX-E	MPTLC (2) 100% C	PTLC (RP) 100% M + A	0.68 100% (RP) M + A	35 mg
MS-31	Ag	C	Furocoumarin	70% E-HX	SP 100% DCM	MPTLC (2) 65:35:2 TEA	-	0.54 65:35:2 TEA (2)	8.1 mg
MS-32	Am	HX	Flavonoid	80% E-HX	MPTLC (2) 60:48:2 TEA	HPLC 100% ACN + A	-	0.52 75:25 (RP) ACN-H	11 mg
MS-33	Am	HX	Flavonoid	80% E-HX	MPTLC (2) 60:48:2 TEA	HPLC 100% ACN + A	-	0.35 75:25 (RP) ACN-H	6.9 mg
MS-34	Ip	M	Flavonoid	20% M-E	RP-SPE 100% H	PTLC (RP) 6:4 H-M	-	0.13 6:4 H-M (RP)	5.8 mg
MS-35	Am	C	Flavonoid	60% E-HX	SP 100% M	MPTLC (3) 80:18:2 TEA	-	0.53 70:28:2 TEA (2)	6.6 mg
MS-36	Am	C	Phenolic	100% E	SP 100% M	MPTLC (2) 30:68:2 TEA	-	0.59 30:68:2 TEA (2)	5.4 mg
MS-37	Am	M	Phenolic	70% M-E	RP-SPE 8:2 H-M	-	-	0.58 1:1 H-M (RP)	25 mg

Compound	Species	Extract	Class	VLC Fraction	Purification 1	Purification 2	Procedure 3	R_f	Weight
MS-38	Ag	C	Phenolic	90% E-HX	MPTLC (3) 50:50:2 TEA	-	-	0.26 40:60:2 TEA (2)	3.9 mg
MS-39	Pc	C	Phenolic	80% E-HX	SP 100% M	MPTLC (RP) (2) 1:1 M-H + A 75:25 M-H + A	-	0.44 65:35 M-H (RP) (2)	5.1 mg
MS-40	Ip	HX	Phenolic	30% E-HX	NP-SPE 9:1 HX-E	SP 100% M	PTLC 8:2 T-E	0.43 9:1 T-E	50 mg
MS-41	Pc	M	Aromatic Amino Acid	70% M-E	RP-SPE 20% M-H	HPLC 69:31 H-ACN	-	0.60 8:2 ACN-H (RP)	2.3 mg
MS-42	Sd	HX	Fat	100% M	SP 100% M	RP-SPE 75:25 M-H	MPTLC (RP) (2) 75:30 M-H + A	0.57 7:3 M-H + A (RP)	3.1 mg
MS-43	Sd	HX	Fatty Acid	60% E-HX	SP 100% M	MPTLC (RP) (2) 6:4 ACN-H + A	-	0.21 6:4 ACN-H + A (RP)	15 mg
MS-44	Sd	HX	Fatty Acid	60% E-HX	SP 100% M	MPTLC (RP) (2) 6:4 ACN-H + A	-	0.25 6:4 ACN-H + A (RP)	20 mg
MS-45	Pc	M	Fatty Acid	100% E	RP-SPE 10-30% M-H	PTLC 100% E +A	-	0.36 100% E + A	1.9 mg
MS-46	Ag	HX	Fatty Acid	30% E-HX	NP-SPE 10% E-HX	MPTLC (RP) (2) 100% M + A	-	0.61 100% M + A (RP) (2)	4.5 mg

3.0 Results and Discussion

3.1 Hemiterpene

3.1.1 Characterisation of MS-1 as 2*RS*,3*RS*-2-methyl-1,2,3,4-butanetetrol

MS-1 was isolated as a pale yellow oil from *A. graveolens* and *I. pes-caprae*. The ^{1}H and ^{13}C NMR spectra provided evidence for a small hydrophilic natural product. Five carbons were detected, which included an oxygen bearing quaternary carbon. A methyl, oxymethine and two oxymethylene groups made up the remainder of the molecule. This was confirmed by ESI-MS which provided the ion $[M+H]^{+}$ at *m/z* 136.8, indicating a molecular formula of $C_5H_{12}O_4$.

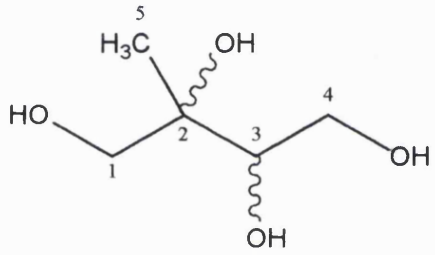

Figure 3.1.1A Structure of **MS-1**

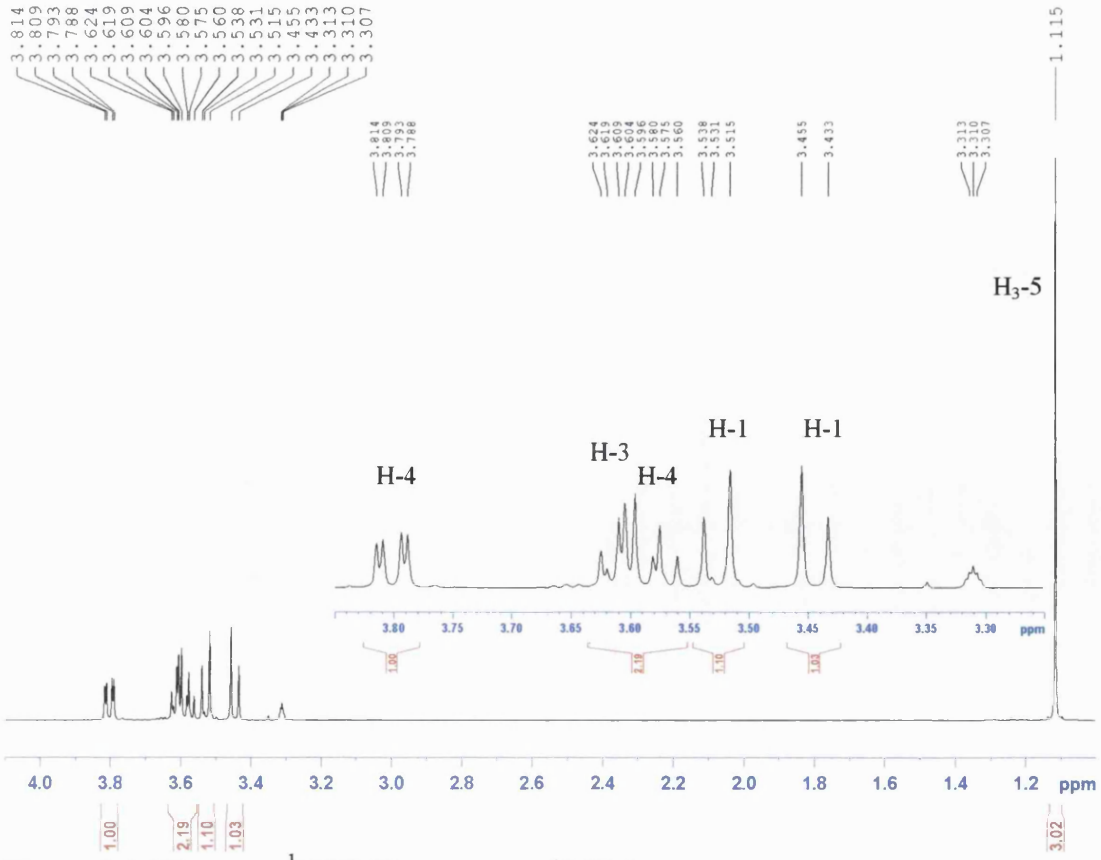

Figure 3.1.1B ^{1}H NMR spectrum of **MS-1**

The methyl group (δ_H 1.12, H_3-5) appeared as a singlet so was placed on the oxygen bearing quaternary carbon (δ_C 75.0, C-2). Two ^3J correlations from the methyl to oxymethine and oxymethylene protons placed these groups at C-3 (δ_H 3.61 m, δ_C 76.2) and C-1 (δ_H 3.46, 3.52 ABq, J = 11.0 Hz, δ_C 68.5), respectively. A COSY correlation between H-3 and the protons of the second oxymethylene (δ_H 3.58 m, δ_H 3.81 dd, J = 10.5, 2.5 Hz) placed this group at position 4. The downfield appearance of the groups at positions 1, 2, 3 and 4 suggested hydroxyl groups should be placed here, which was confirmed by ESI-MS. **MS-1** was isolated as a racemic mixture as no rotation of plane-polarised light was detected. This branched alditol was previously isolated as a racemate from *Convolvulus glomeratus* with ^1H and ^{13}C NMR data in D_2O (Anthonsen *et al.*, 1976; Shah *et al.*, 1976). **MS-1** was thus assigned as 2*RS*,3*RS*-2-methyl-1,2,3,4-butanetetrol.

Table 1 ^1H and ^{13}C NMR data and ^1H-^{13}C long-range correlations of **MS-1** recorded in CD_3OD

Position	^1H	^{13}C	^2J	^3J
1	3.46, 3.52 ABq (11.0)	68.5	C-2	C-3, C-5
2	-	75.0		
3	3.61 m	76.2	C-2	
4	3.58 m	63.8	C-3	C-2
	3.81 dd (10.0, 2.5)			
5	1.12 s	19.8	C-2	C-1, C-3

3.2 Monoterpenes

3.2.1 Characterisation of MS-2 as 8-debenzoylpaeoniflorin

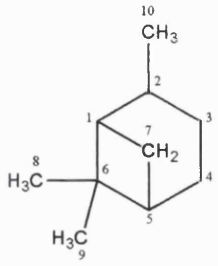

Figure 3.2.1A Pinane skeleton

MS-2 was isolated as a colourless amorphous solid from the chloroform extract of *D. anethifolia* and the methanol extract of *A. graveolens*. FABMS yielded a base ion of 399 $[M+Na]^+$. The ^1H and ^{13}C NMR spectra indicated the presence of a monoterpene glycoside with a molecular formula of $C_{16}H_{24}O_{10}$. The monoterpene was found to be made up of four quaternary carbons, three methylenes, two methines (one an acetal methine) and one methyl group.

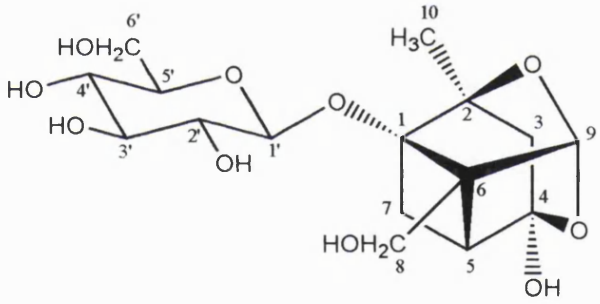

Figure 3.2.1B Structure of **MS-2**

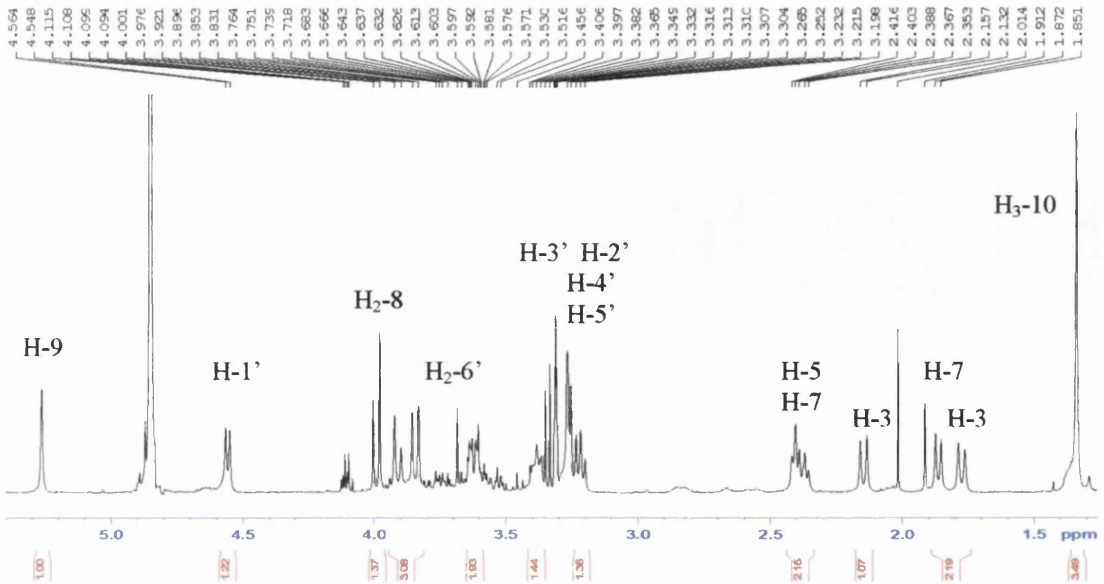

Figure 3.2.1C ^1H NMR spectrum of **MS-2**

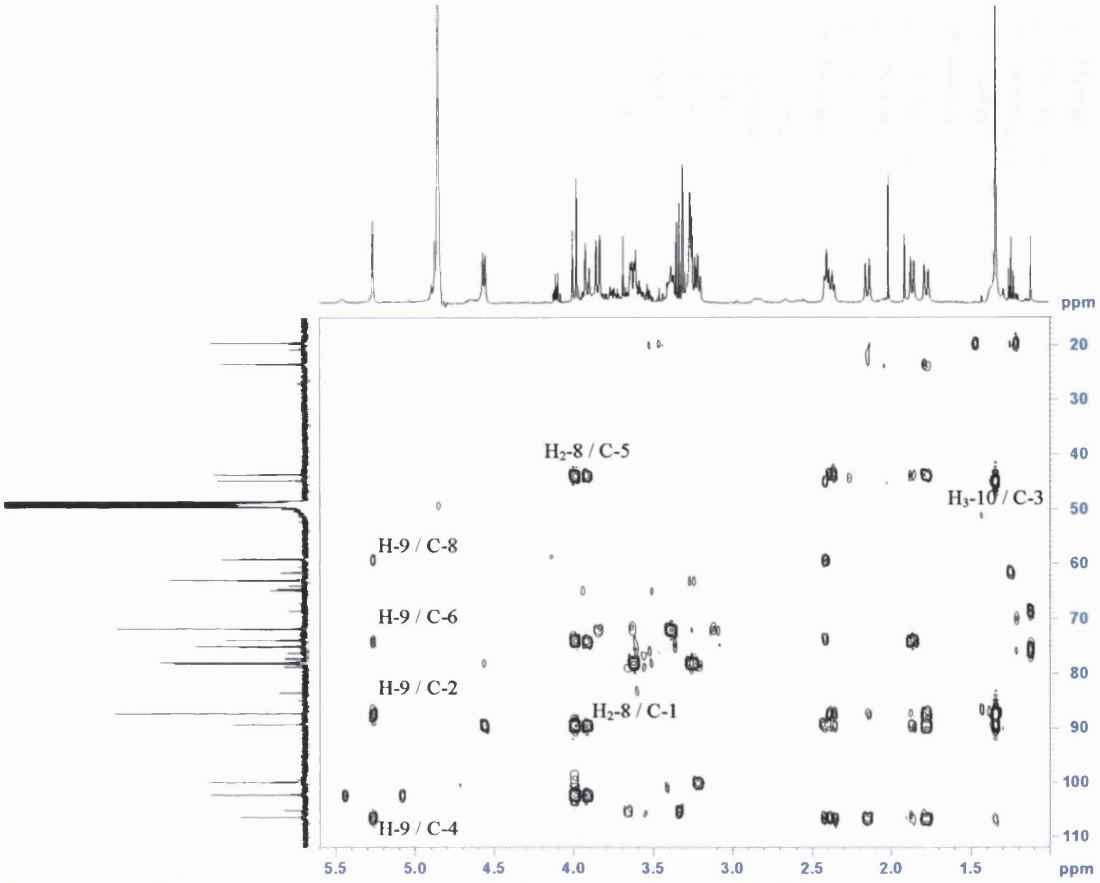

Figure 3.2.1D HMBC spectrum of **MS-2**

Assuming a basic pinane skeleton the structure of the monoterpene was elucidated by HMBC spectroscopy. Beginning with methyl-10 (δ_H 1.34 s), this gave a ^2J correlation towards an oxygen bearing quaternary carbon (δ_C 87.3, C-2) as well as ^3J correlations to a second oxygen bearing quaternary carbon C-1 (δ_C 89.4) and a methylene carbon C-3 (δ_C 44.7). H-3 exhibited ^2J correlations to C-2 and to a highly deshielded quaternary carbon (δ_C 106.4, C-4) along with ^3J signals to C-1 and a methine (C-5). This 6-membered ring was completed by a COSY correlation between H-5 and H_2-7, which also gave a ^2J signal to C-1. H-5 and H_2-7 showed ^2J and ^3J signals, respectively, to a quaternary carbon (δ_C 73.8, C-6). The protons of the oxymethylene (δ_H 3.91 and 4.00, H_2-8) exhibited strong signals to C-6, C-1 and C-5. This confirmed the position of the oxymethylene group at C-8 and also the point of attachment at C-6. H_2-8 also gave a ^3J signal to a highly deshielded acetal methine (C-9, δ_C 102.3, δ_H 5.25 s) and was placed adjacent to C-6. The methine proton (H-9) also showed correlations towards the quaternary carbons C-6, C-2 and C-4 and therefore completing this five ring system. Due to the deshielded nature of the quaternary carbon C-4 and molecular weight of this compound a hydroxyl must be placed here. These data were similar to those reported for pinane-type monoterpene glucosides

from *Paeonia albiflora* (Kaneda *et al.*, 1972; Yamasaki *et al.*, 1976). The anomeric proton of the hexose moiety showed a ^3J correlation to C-1 and so was placed here. COSY correlations from H-1' through to H_2-6' confirmed the presence of a hexose. The coupling measured between H-1' and H-2' was large (7.7 Hz) and as H-2' appeared as a triplet (J = 7.7 Hz) this indicated that these two protons and H-3' should have an axial configuration. The resonances for H-3', H-4' and H-5' were overlapping and so the remaining couplings could not be measured to determine whether the hexose should be designated as a glucose or galactose. **MS-2** (1 mg) was subjected to acid hydrolysis followed by GC-MS, the result being that the hexose sugar could be assigned as glucose.

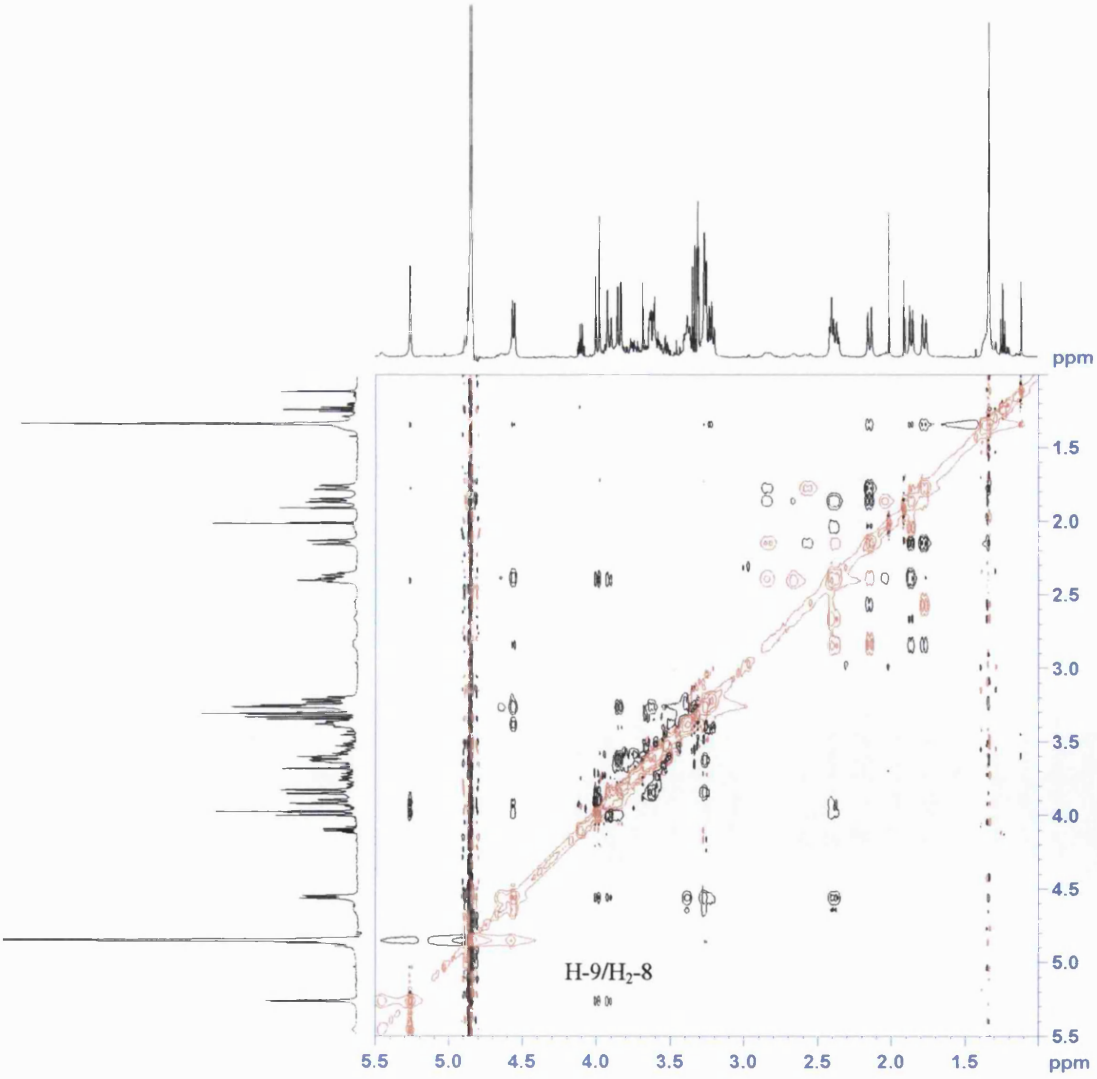

Figure 3.2.1E NOESY spectrum of **MS-2**

The NOESY spectrum showed a correlation between the highly deshielded acetal methine proton, H-9, and the oxymethylene protons H_2-8 indicating that they are on the same face of the molecule (Stavri *et al.*, 2003). **MS-2** is therefore assigned as the monoterpene glucoside 8-debenzoylpaeoniflorin. This compound has previously been cited as possessing antihyperglycaemic activity by Hsu *et al.*, (1997). However, no spectroscopic data has been recorded, despite this being alluded to by these authors as being present in cited references (Kaneda *et al.*, 1972; Yamasaki *et al.*, 1976). The full NMR data for **MS-2** has now been reported by Stavri *et al* (2003).

Table 2 ^{1}H and ^{13}C NMR data and ^{1}H-^{13}C long-range correlations of **MS-2** recorded in CD_3OD

Position	^{1}H	^{13}C	^{2}J	^{3}J
1	-	89.4		
2	-	87.3		
3	1.79 d (12.5)	44.7	C-2, C-4	C-1, C-5
	2.16 d (12.5)			
4	-	106.4		
5	2.40 m	43.7	C-4, C-6	C-1, C-8
6	-	73.8		
7	1.87 d (10.0)	23.4	C-1, C-5	C-2, C-4, C-6
	2.37 d (10.0)			
8	3.91 d (12.4)	59.1	C-6	C-1, C-5, C-9
	4.00 d (12.4)			
9	5.25 s	102.3	C-6	C-2, C-4, C-8
10	1.34 s	19.5	C-2	C-1, C-3
1'	4.56 d (7.7)	99.9		C-3', C-5', C-1
2'	3.24 t (7.7)	75.0		
3'	3.40 m	77.9		
4'	3.27 m	71.8		
5'	3.27 m	78.2		
6'	3.65 m	62.9	C-5'	
	3.85 m			

3.2.2 MS-3 tentatively assigned as methyl-1'-(2',3'α-epoxy-3'-methyl-5'-oxo-cyclopentyl)-propen-2-oate

MS-3 was isolated as a yellow amorphous solid from the hexane extract of *P. crispa*. The ^{1}H and ^{13}C NMR spectra showed the presence of two methyl groups, both as singlets, an *exo*-methylene group, two carbonyl carbons and an olefinic quaternary carbon.

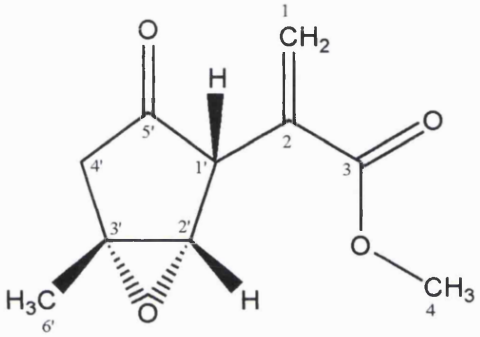

Figure 3.2.2A Proposed tentative structure of **MS-3**

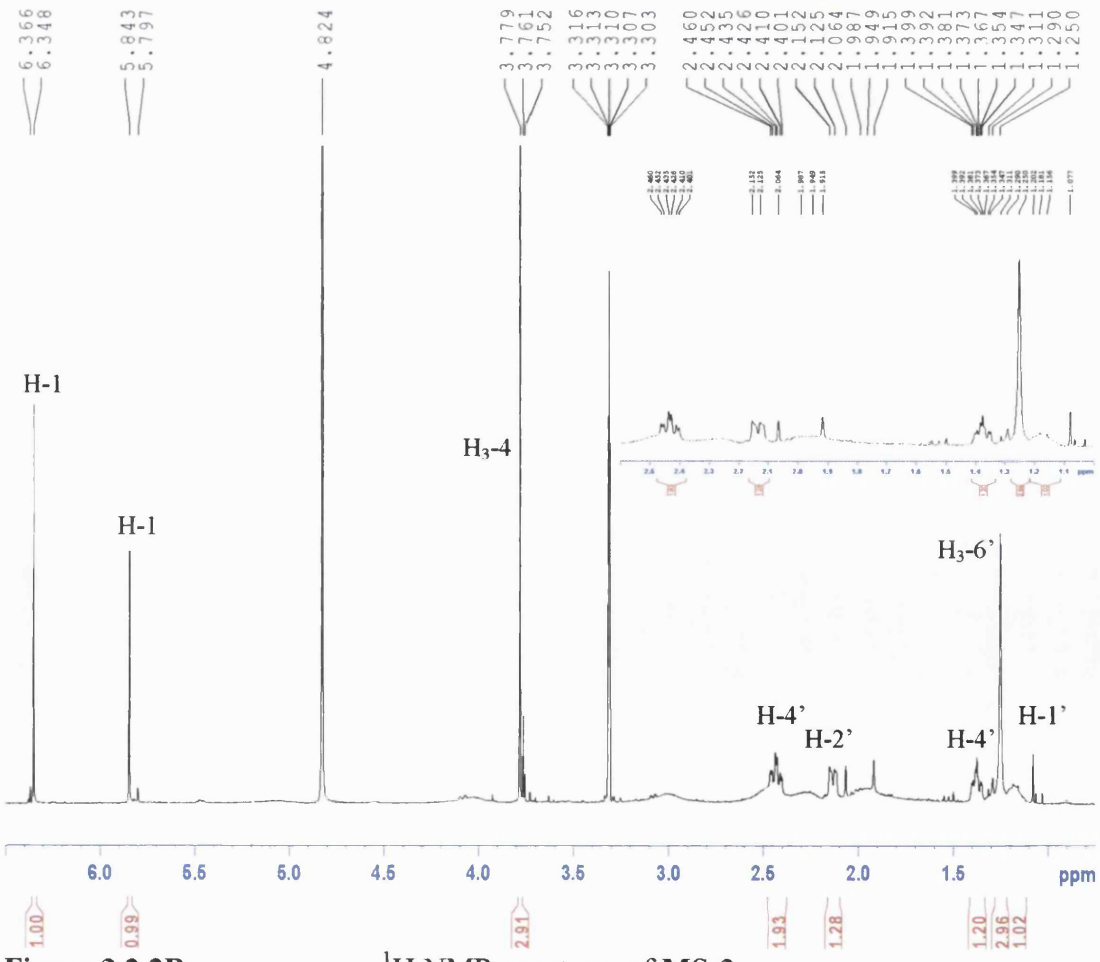

Figure 3.2.2B ^{1}H NMR spectrum of **MS-3**

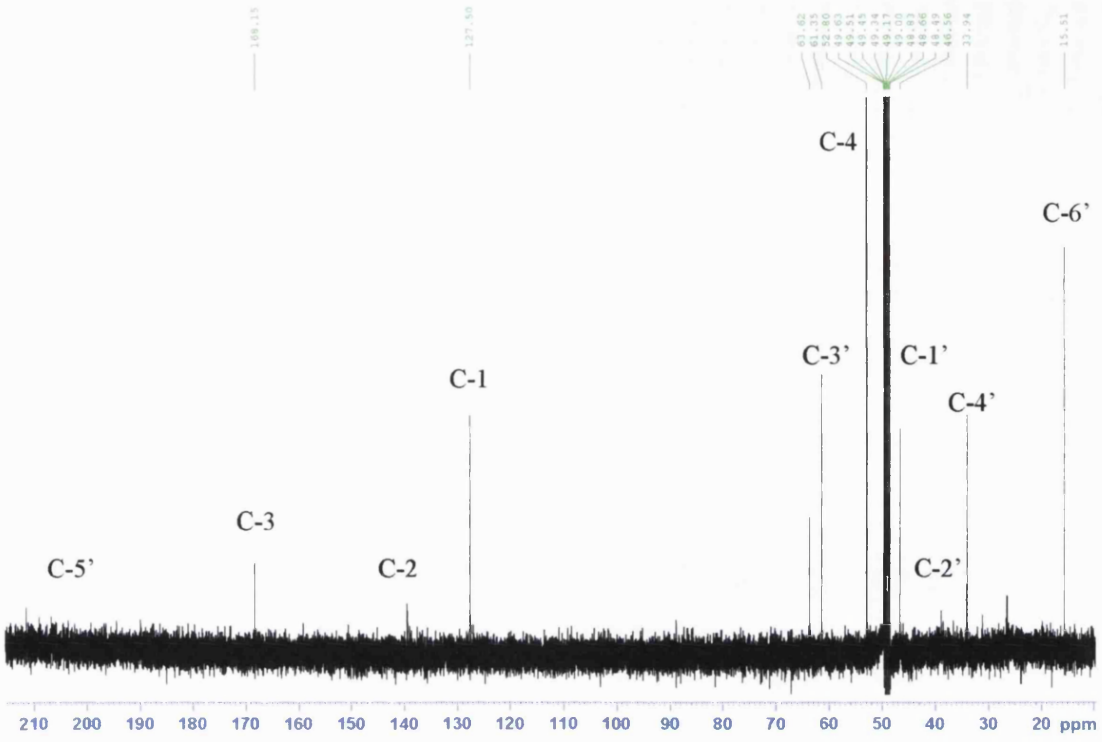

Figure 3.2.2C ^{13}C NMR spectrum of **MS-3**

From the HMBC spectrum, a ^{2}J correlation between the protons of the *exo*-methylene group (δ_H 5.84 s and 6.35 s, H_2-1) and the olefinic quaternary carbon (δ_C 139.4, C-2) placed this group here. A further two ^{3}J correlations in the HMBC spectrum from the *exo*-methylene protons to a shielded methine group (δ_H 1.18 bs, δ_C 46.6, C-1') and a carbonyl carbon (δ_C 168.2, C-3) placed these groups directly on the olefinic quaternary carbon (C-2). A ^{3}J signal between the downfield methoxyl singlet (δ_H 3.78, H_3-4) towards C-3 suggested this group should be attached to the carbonyl carbon *via* an ester linkage. The *exo*-methylene protons also gave a long-range (^{4}J) HMBC signal to a deshielded carbonyl carbon (δ_C 206.8, C-5'), placing this group next to the shielded methine group, C-1'. The downfield appearance of C-5' is indicative of a carbonyl group within a highly strained ring system. The shielded methine proton exhibited a COSY correlation to an oxymethine proton (δ_H 2.14 bdd, H-2'), which in turn showed a ^{2}J signal to an oxyquaternary carbon (δ_C 61.4, C-3'). The cyclopentane ring system was completed by placing a methylene group at C-4' (δ_H 1.37 and δ_H 2.44, H_2-4'). From the HMBC spectrum the methylene protons gave a ^{2}J correlation to C-3' and ^{3}J correlations to C-1' and C-2'. Therefore this group must be flanked by two quaternary carbons as no COSY signal was detected towards either

H-1' or H-2'. Two W-couplings between H_2-4' and H-2' (J = 3.5 Hz) and H_2-4' and H-1' (J = 3.5 Hz) further confirmed the arrangement of the five-membered ring. The second methyl group (δ_H 1.25 s, H_3-6') gave a ^2J correlation to C-3', placing this group here. The molecule was completed by the formation of an epoxide between C-2' and C-3'. The ^{13}C resonances for these two carbons were characteristic for an epoxide rather than for an hydroxyl attached at these groups.

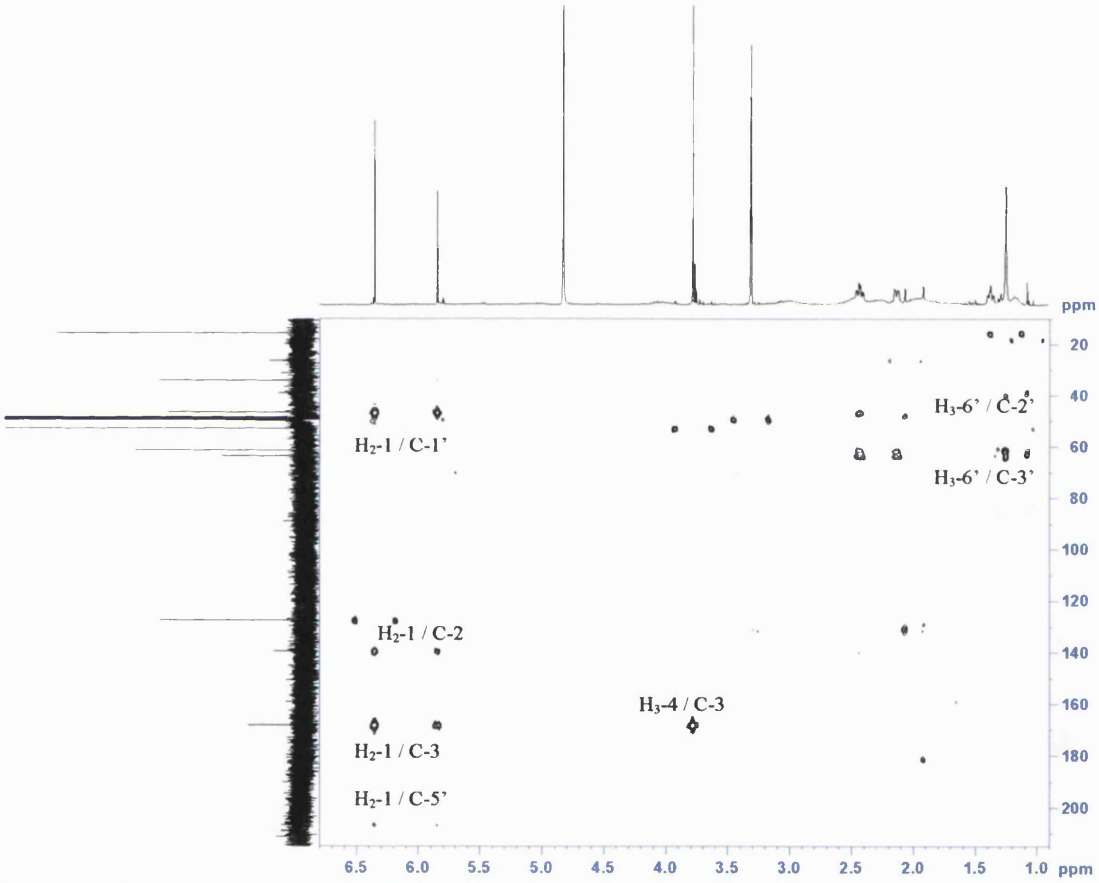

Figure 3.2.2D HMBC spectrum of **MS-3**

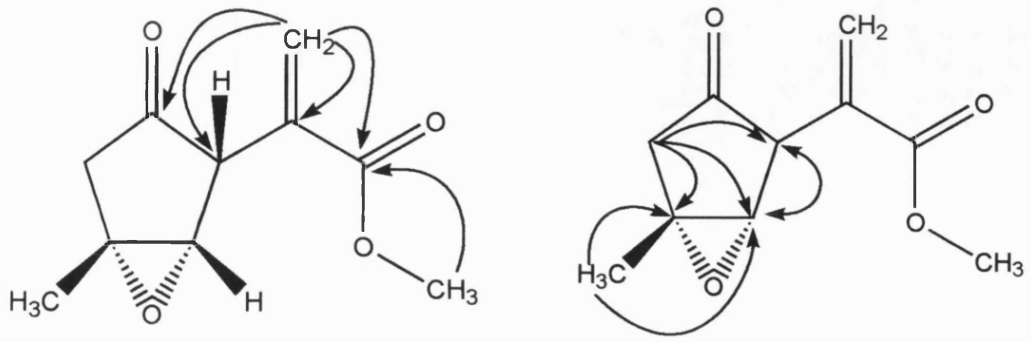

Figure 3.2.2E HMBC and COSY correlations for **MS-3**

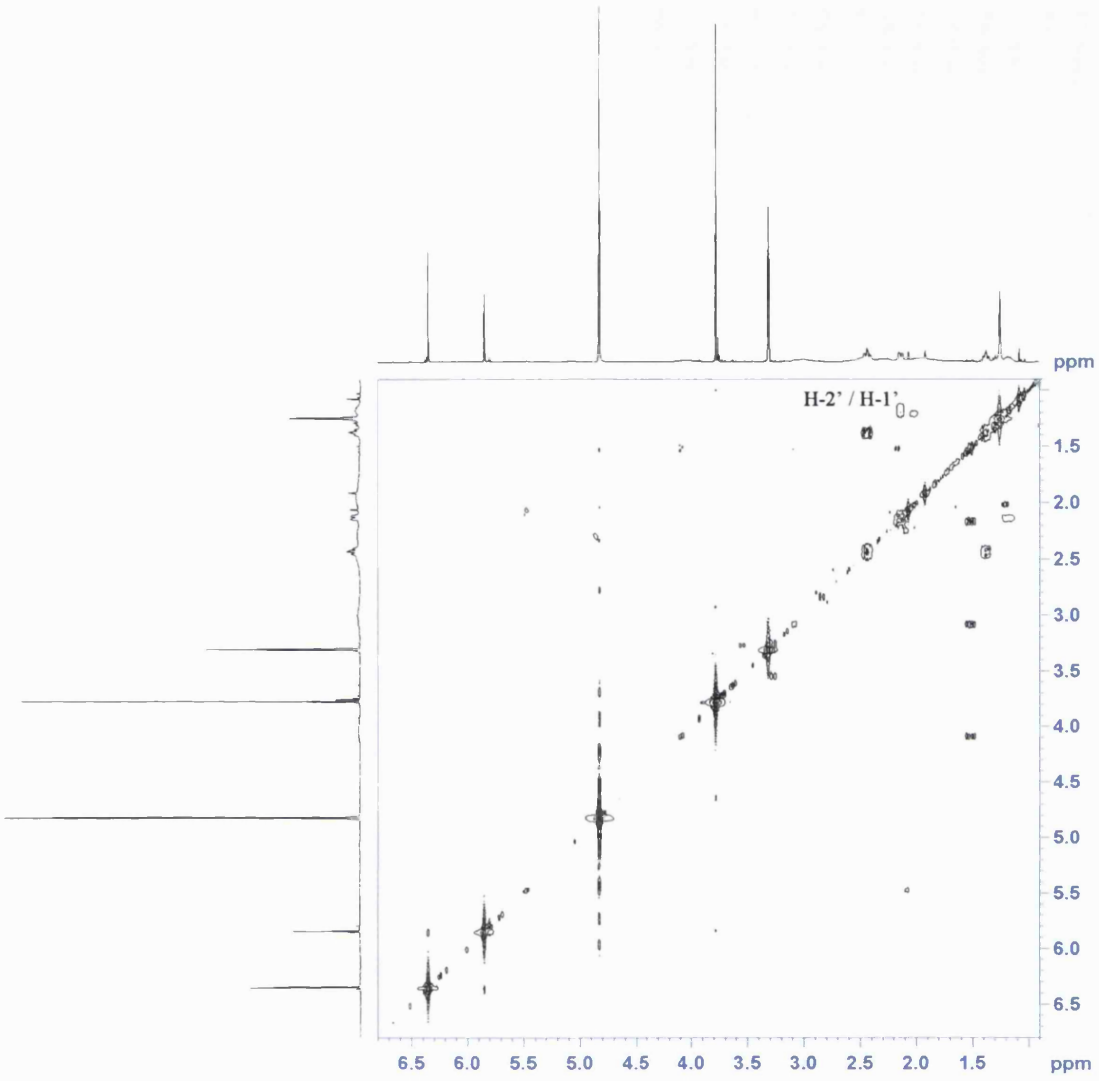

Figure 3.2.2F COSY spectrum of **MS-3**

The relative stereochemistry of **MS-3** was established from the NOESY spectrum. An NOE between H-2' and the methyl group, H_3-6', placed these protons on the same face of the molecule in a β-orientation. A further NOE between H-2' and H-1' also placed this proton on the same face of the molecule (β-oriented). A 1,3 interaction between H_2-4'β and H-1' placed this proton on the same face of the molecule as the methyl protons, H-1' and H-2'. This left the epoxide, which must therefore be α-orientated, on the opposite face of the molecule.

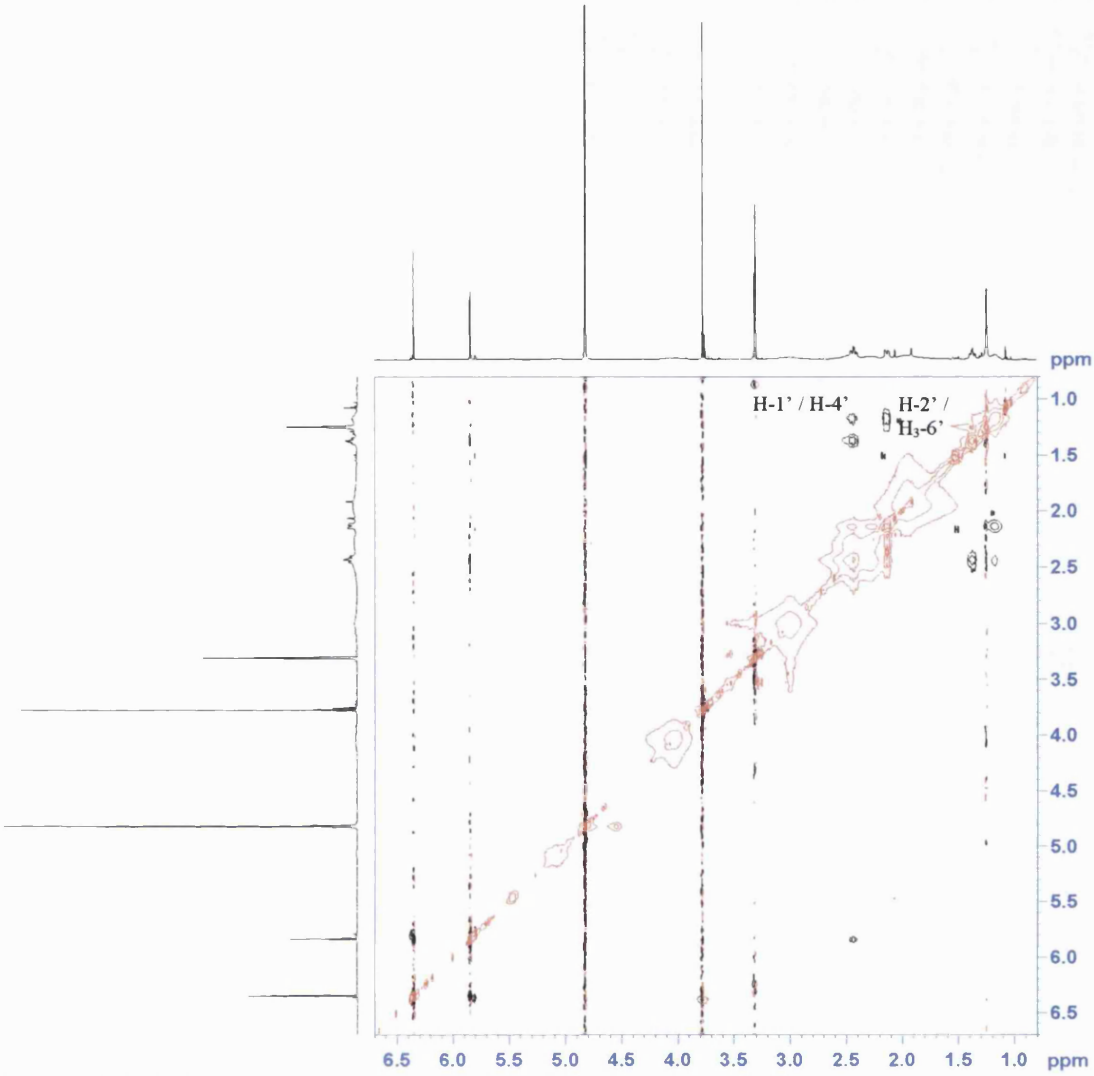

Figure 3.2.2G NOESY spectrum of **MS-3**

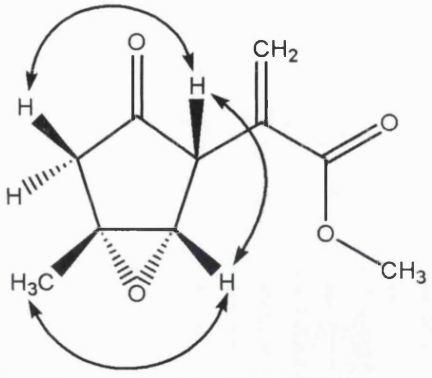

Figure 3.2.2H NOE correlations for **MS-3**

The structure of **MS-3** has tentatively been proposed as methyl-1'-(2',3'α-epoxy-3'-methyl-5'-oxo-cyclopentyl)-propen-2-oate, based on the 1D and 2D NMR experiments acquired. However, CI-MS of **MS-3** yielded the ions $[M+H]^+$ (279.1), $[M+NH_4]^+$ (296.2) along with the base ion $[M+H-H_2O]^+$ (261.1). This differs from the molecular weight of the proposed structure (MW = 196) by 82 daltons. The

acquisition of NMR data in deuterated benzene and deuterated pyridine failed to resolve the discrepancy between the molecular weight of the proposed structure to that determined by mass spectrometry. The accurate mass of **MS-3** yielded a molecular formula of $C_{16}H_{22}O_4$ ($[M]^+$ 278.1526, calculated for $C_{16}H_{22}O_4$: 278.1518), which is C_6H_{10} greater than that proposed for this compound. Due to the NMR data acquired, in various deuterated solvents, it was not possible to determine the precise molecular structure of **MS-3**. The part structure of **MS-3** is therefore tentatively assigned as methyl-1'-(2',3'α-epoxy-3'-methyl-5'-oxo-cyclopentyl)-propen-2-oate.

Table 3 ^1H and ^{13}C NMR data and ^1H-^{13}C long-range correlations of **MS-3** recorded in CD_3OD

Position	^1H	^{13}C	^2J	^3J
1	5.84 s	127.5	C-2	C-3, C-1', C-5'
	6.35 s			
2	-	139.4		
3	-	168.2		
4	3.78 s	52.8		C-3
1'	1.18 bs	46.6		
2'	2.14 bdd (13.0, 3.5)	38.8	C-3'	
3'	-	61.4		
4'	1.37 dt (13.0, 3.5)	33.9	C-3'	C-1', C-2'
	2.44 dt (12.5, 4.0)			
5'	-	206.8		
6'	1.25 s	15.5	C-3'	C-2'

3.2.3 Characterisation of MS-4 as 9-hydroxylinaloyl-3-*O*-β-D-glucopyranoside (racemate)

MS-4 was isolated from the methanol extract of *A. monosperma* as a yellow oil and a molecular formula $C_{16}H_{28}O_7$ was assigned by ESI-MS $[M+Na]^+$ (355.2) and $[2M+Na]^+$ (687.2). The ^1H and ^{13}C NMR gave signals indicating the presence of a monoterpene glycoside. An *exo*-methylene group (δ_H 5.17 and δ_H 5.22, H_2-1), two olefinic protons (δ_H 5.40, H-6 and δ_H 6.10, H-2), an oxymethylene group (δ_H 3.90, H_2-9), an olefinic quaternary carbon (δ_C 135.8, C-7) and an oxygen bearing quaternary carbon (δ_C 81.3, C-3) were detected. An anomeric proton (δ_H 4.33, H-1') together with signals for 4 oxymethines and an oxymethylene group was indicative of an hexose residue.

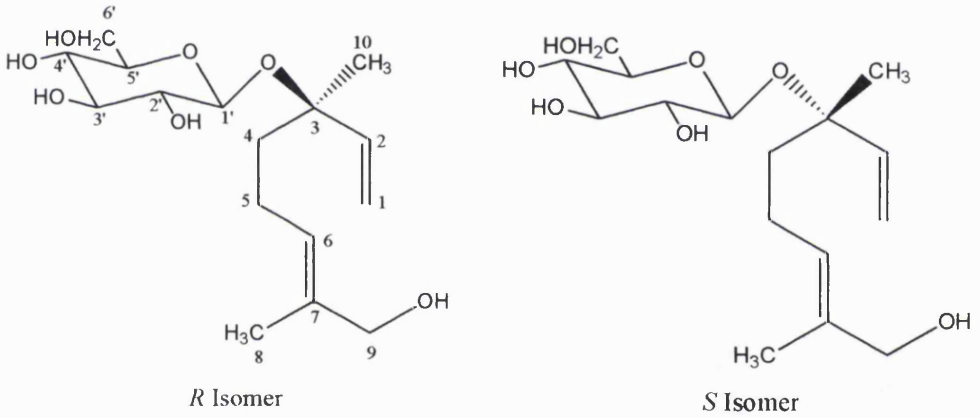

R Isomer *S* Isomer

Figure 3.2.3A Structure of the two enantiomers of **MS-4**

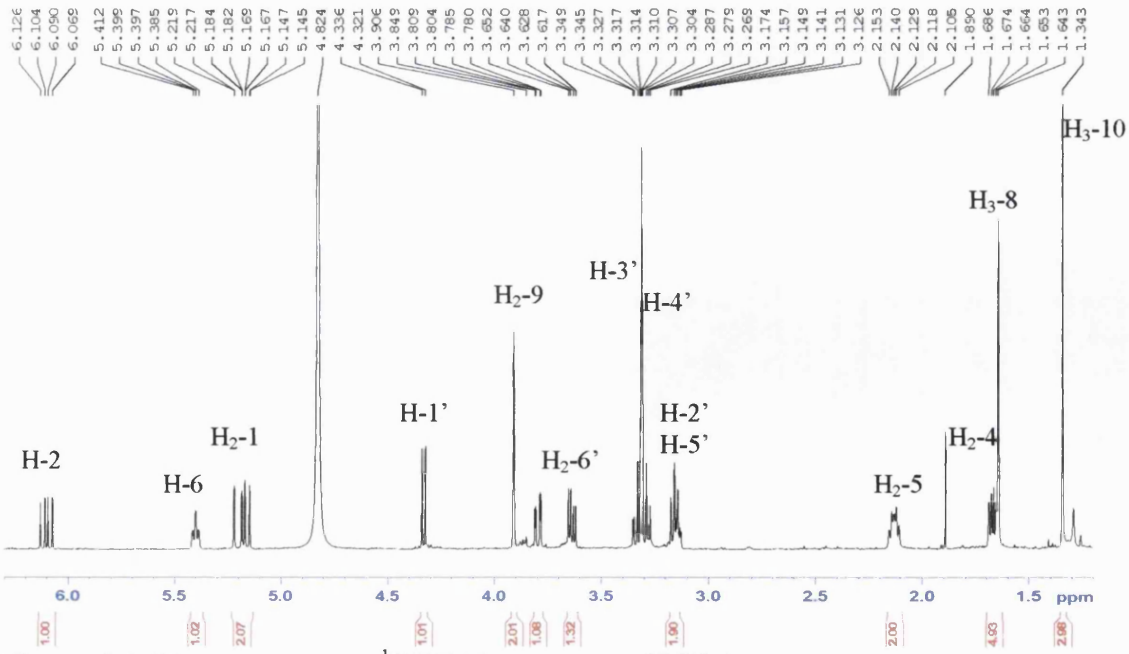

Figure 3.2.3B ^1H NMR spectrum of **MS-4**

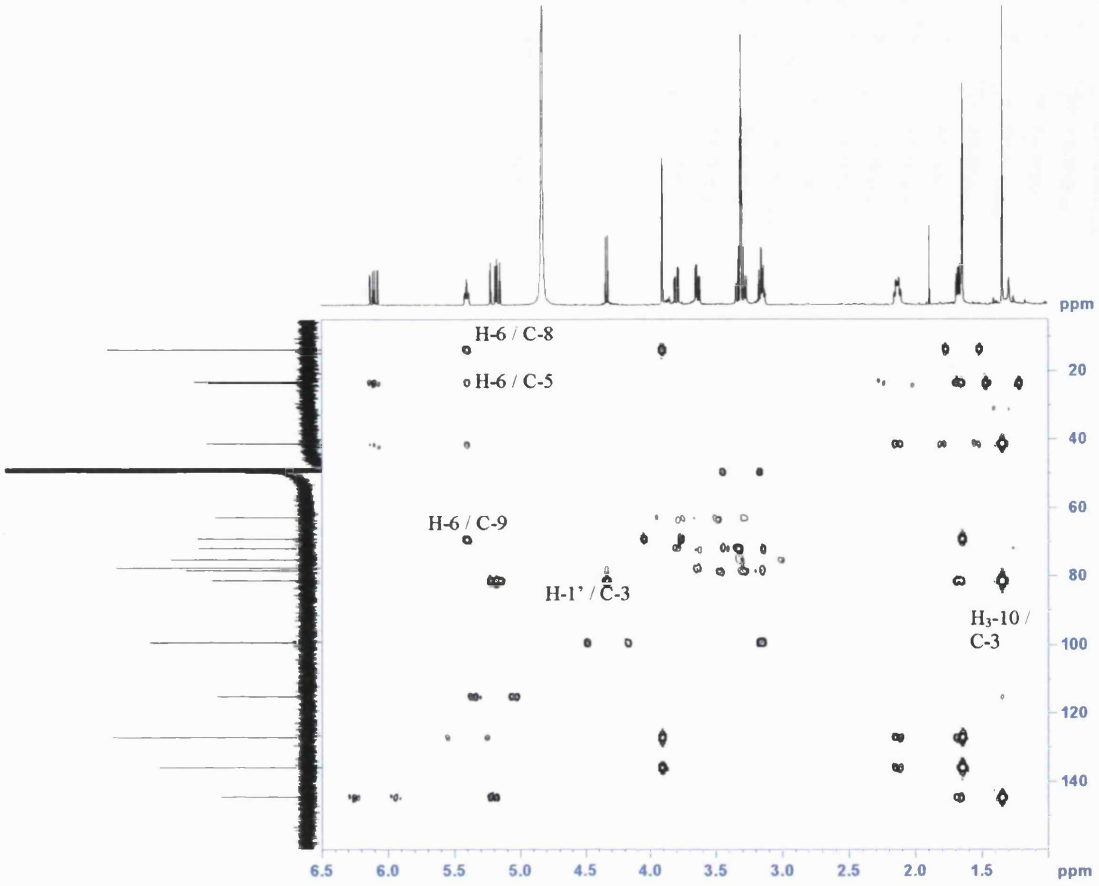

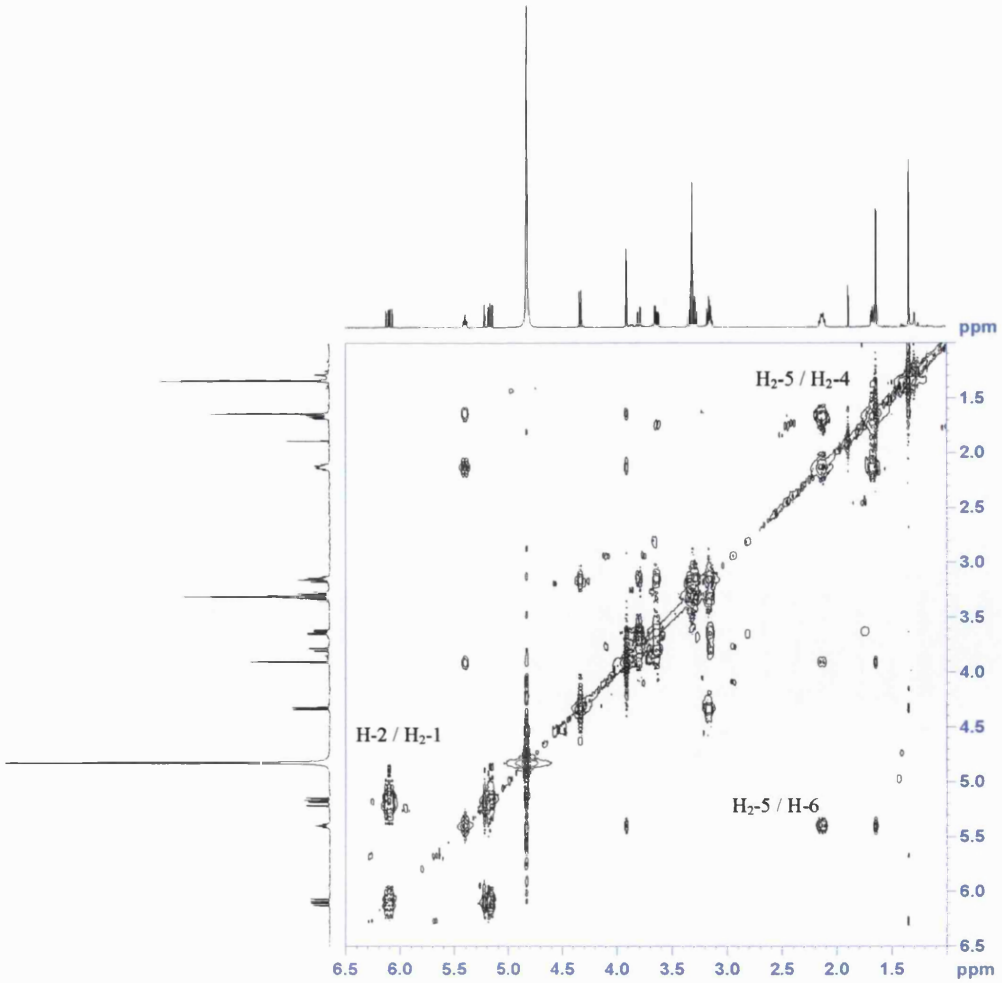

Figure 3.2.3C HMBC and COSY spectra of **MS-4**

The protons of the *exo*-methylene group (H_2-1) gave a COSY correlation to its olefinic partner (H-2) and a ^3J correlation in the HMBC spectrum to a downfield quaternary carbon (C-3). The olefinic proton gave two ^3J correlations to a methyl, appearing as a singlet, and a methylene group (δ_H 1.67 m, δ_C 41.3, C-4) and so both must be placed on C-3. A COSY correlation between H_2-4 and the protons of a second methylene group (δ_H 2.12 m, H_2-5) placed it here. This in turn coupled to a second olefinic proton (H-6) in the COSY spectrum. The olefinic quaternary carbon (C-7) detected in the ^{13}C NMR spectrum must be attached to this olefinic group. This was confirmed by ^3J correlations from H-6 to a methyl (C-8) and a downfield methylene (C-9) carbon, which both appeared as singlets and in turn gave ^2J correlations to the olefinic quaternary carbon. An hydroxyl group was attached at C-9 due to the downfield appearance of this methylene group. The remaining six carbons of the hexose residue were attached at the downfield quaternary carbon, C-3, due to a ^3J correlation from the anomeric proton towards this carbon. In the COSY spectrum the anomeric proton (H-1') coupled to H-2' (7.5 Hz), which in turn appeared as a triplet (δ_H 3.16, J = 8.5 Hz) with an HMBC correlation from H-3' (δ_H 3.32 m). The appearance of H-2' as a triplet with a large coupling constant indicated that H-1', H-2' and H-3' are in an axial configuration. H-3' gave a COSY correlation to H-4'. The hexose was completed by ^2J and ^3J correlations from H_2-6 to C-5' and C-4', respectively. The appearance of H-5' as a triplet with a large coupling constant (8.5 Hz) also indicated that H-4' and H-5' are in an axial configuration thus confirming the hexose residue as being glucose. The signals for H-3' and H-4' appear to be triplets with the wing peak of each being masked by the methanol peak. The coupling constant for each of the two peaks are also large further (H-3', J = 8.5 Hz and H-4', J = 9.0 Hz; data not shown in **Table 4**) confirming the presence of glucose. An NOE between H_2-9 and H-6 placed these protons on the same 'face' of the molecule. This was the only determination of the spatial arrangement for this molecule that could be made and this correlated well with the data published for this compound (Saracoglu *et al.*, 1995; Uchiyama *et al.*, 1989).

MS-4 was found to be a racemic mixture of the two enantiomers at position 3 of the molecule due to it being optically inactive. The NMR data was in close agreement with that of the literature published for this compound (Calis and Yuruker 1993). 9-hydroxylinaloyl-3-*O*-β-D-glucopyranoside has also been isolated from the

Lamiaceae plant *Phlomis armeniaca* (Saracoglu *et al.*, 1995), *Pluchea indica* (Asteraceae) (Uchiyama *et al.*, 1989) and *Cunila spicata* (Lamiaceae) (Manns 1995).

Table 4 ^{1}H and ^{13}C NMR data and ^{1}H-^{13}C long-range correlations of **MS-4** recorded in CD_3OD

Position	^{1}H	^{13}C	^{2}J	^{3}J
1	5.17 d (11.0)	115.0	C-2	C-3
	5.22 bd (18.0)			
2	6.10 dd (18.0, 11.0)	144.5		C-4, C-10
3	-	81.3		
4	1.67 m	41.3	C-3	C-2, C-6, C-10
5	2.12 m	23.3	C-4, C-6	C-7
6	5.40 t (7.0)	127.0	C-5	C-4, C-8, C-9
7	-	135.8		
8	1.64 s	13.7	C-7	C-6, C-9
9	3.90 s	69.0	C-7	C-6, C-8
10	1.34 s	23.6	C-3	C-2, C-4
1'	4.33 d (7.5)	99.3		C-3', C-3
2'	3.16 t (8.5)	75.1		
3'	3.32 m	78.3	C-2', C-4'	
4'	3.29 m	71.8	C-3'	C-6'
5'	3.16 t (8.5)	77.6	C-4'	
6'	3.64 dd (12.0, 6.0)	62.9	C-5'	C-4'
	3.80 dd (12.0, 2.5)			

3.2.4 Characterisation of iridoid glycosides from *Scrophularia deserti*

3.2.4.1 Characterisation of MS-5 as 6-*epi*-ajugoside

The compound **MS-5** was isolated as a colourless oil. It was elucidated as being the iridoid glycoside 6-*epi*-ajugoside and assigned the molecular formula $C_{17}H_{26}O_{10}$ by HRCIMS. Peaks due to $[M+H]^+$ (391.1613) and $[M+NH_4]^+$ (408.1865) were detected. The infrared spectrum showed signals that could be assigned to an acetoxy carbonyl (1707 cm^{-1}), a C=C group (1653 cm^{-1}) and hydroxyl groups (3383 cm^{-1}). The ^1H and ^{13}C NMR spectra showed the presence of 9 carbons indicative of an iridoid monoterpene. From the ^1H NMR spectrum signals for an acetal group (δ_H 5.85 s), two olefins (δ_H 6.21 dd, J = 6.5, 2.5, H-3 and δ_H 4.72 dd, J = 6.5, 1.0, H-4) an oxymethine (δ_H 4.01 d, J = 4.5 Hz, H-6) and a methyl group (δ_H 1.53 s, H-10) was indicative of an acetylated iridoid glycoside.

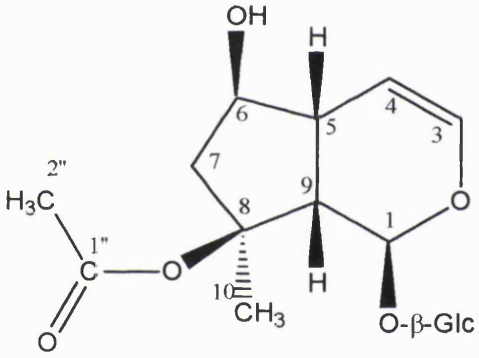

Figure 3.2.4.1A Structure of **MS-5**

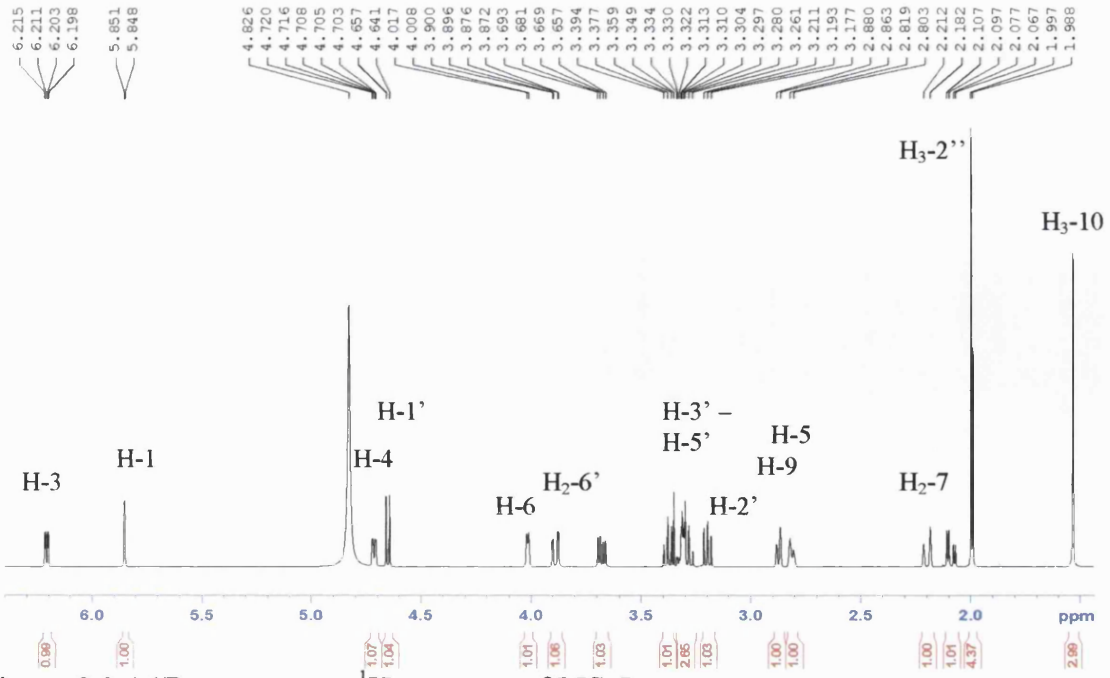

Figure 3.2.4.1B ^1H spectrum of **MS-5**

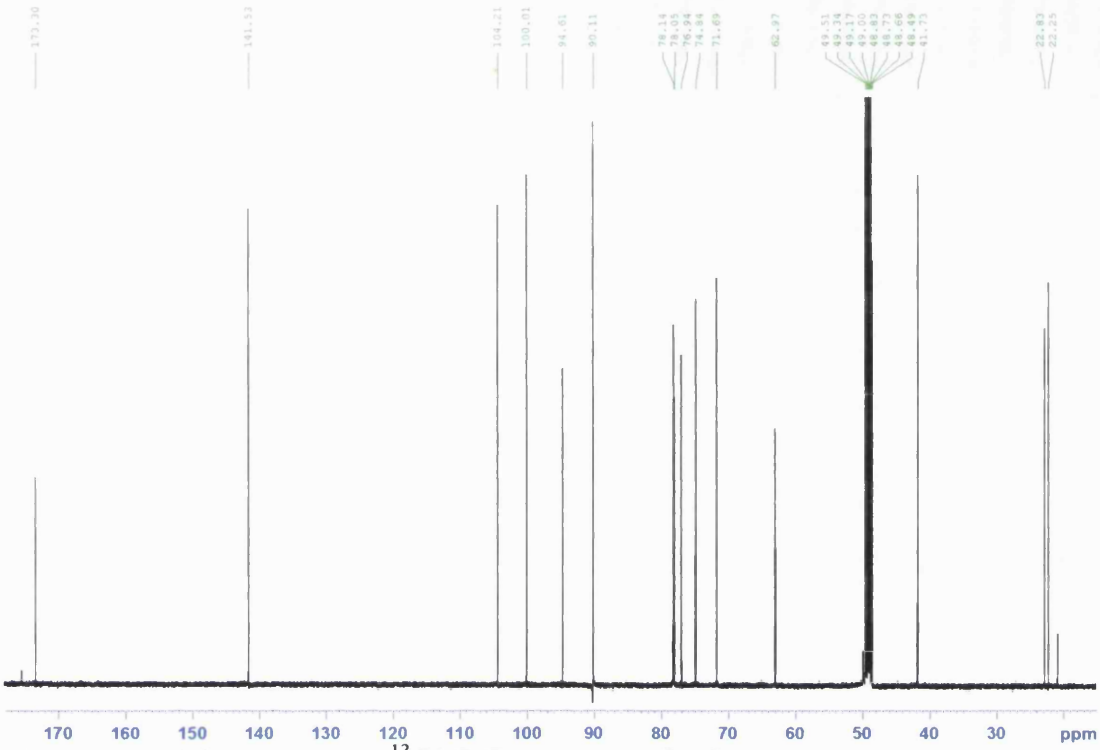

Figure 3.2.4.1C ^{13}C NMR spectrum of **MS-5**

HMBC and COSY spectra were used to elucidate the structure by identifying both long range correlations (two and three bond) and ^{1}H-^{1}H correlations. Assuming an iridoid structure for **MS-5**, methyl-10 showed a ^{2}J correlation to a quaternary carbon C-8 and ^{3}J correlations to C-7 and C-9 in the HMBC spectrum. H_2-7 exhibited a COSY coupling to a methine proton, H-6. Due to the downfield shift of this carbon (C-6) an hydroxyl group was placed here. COSY correlations between H-5 and H-6 and H-5 and H-9 confirmed the presence of a cyclopentane ring. This was further substantiated by HMBC correlations from H-6 to C-5, C-7, C-8 and C-9. An acetoxy group was placed at the quaternary carbon, C-8 (δ_C 90.1), rather than the oxymethine at C-6 (δ_C 76.9) due to the greater downfield shift of this carbon. This placement was supported by (Ahmed *et al.*, 2003) as an hydroxyl group positioned at C-8 would have caused an upfield shift (δ_C ~79 ppm). An ester, such as an acetoxy group, would have a deshielding effect on this quaternary carbon. This was further corroborated by the downfield shift of the methyl protons (δ_H 1.53, H_3-10), which would have been further upfield had an hydroxyl been attached at C-8 instead of an acetyl moiety (Ahmed *et al.*, 2003). The oxymethine proton, H-6, would have also been deshielded (δ_H ~5.0–5.5 ppm) further had an acetyl group been positioned here. A COSY coupling was detected between H-5 and an olefinic proton (δ_H 4.72) and so this was assigned as H-

4. This was confirmed by ^{3}J correlations from H-6 and H-9 to C-4. H-4 showed a COSY correlation to its olefinic partner (H-3, δ_H 6.20 dd, δ_C 141.5). Due to the downfield shift of C-3 in the ^{13}C NMR spectrum an oxygen atom must be directly attached here. A ^{3}J correlation between H-3 and a highly deshielded acetal methine carbon (C-1, δ_H 5.85 d, δ_C 94.6) enabled this to be positioned at C-1. This was confirmed by a COSY coupling between H-9 and H-1, therefore completing the B-ring. A glucose moiety was attached at this acetal group (C-1) due to a ^{3}J correlation observed in the HMBC spectrum between the anomeric carbon (C-1') and the acetal methine, H-1. The data is in agreement with that published for ajugoside (Guiso *et al.*, 1974). The hexose attached at C-1 was deduced as being β-D-glucose by inspection of the NOESY, ^{1}H spectra and relevant coupling constants. All the coupling constants measured were large (J = 8.0 Hz) which indicates the protons should be axial. Not all coupling constants could be measured due to signal overlap. Closer inspection of the appropriate region between 3.10 and 3.50 ppm allowed the deduction that all signals split were of a large coupling constant. A NOE between the anomeric proton and H-5' confirmed that the hexose residue should be assigned as glucose. The presence of a glucose unit at C-1 of the iridoid structure is common (Fernandez *et al.*, 1995; Helfrich and Rimpler 2000).

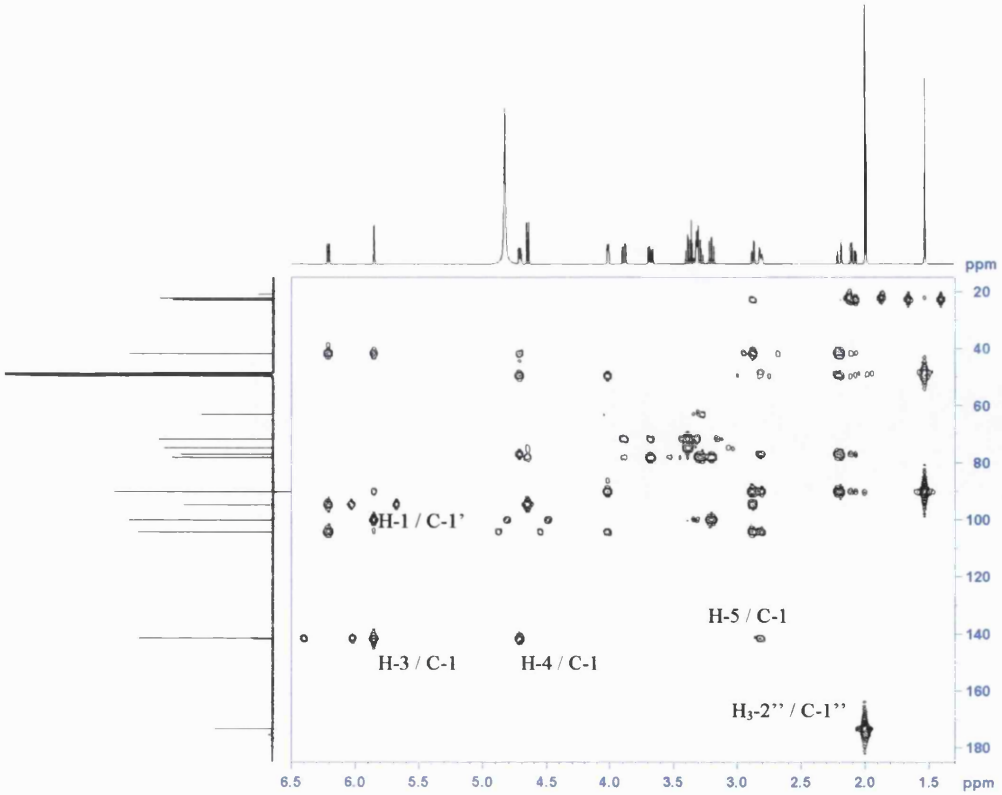

Figure 3.2.4.1D HMBC spectrum of **MS-5**

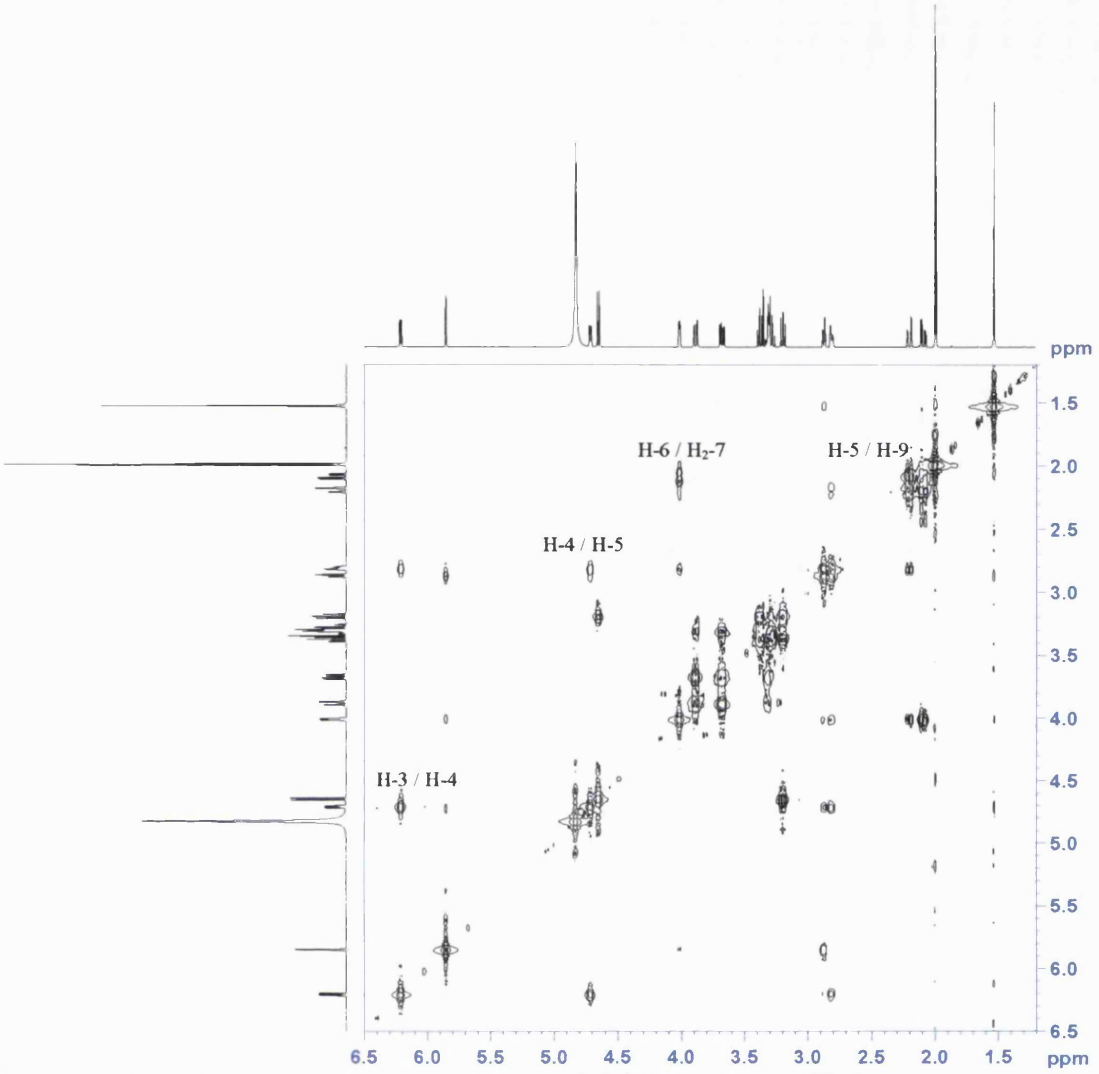

Figure 3.2.4.1E COSY spectrum of **MS-5**

The relative stereochemistry of **MS-5** was determined by NOESY spectra and coupling constant measurements. A NOE between H-5 and H-9 was detected indicating that these two protons are on the same face of the molecule. The large coupling constants measured (H-5 = 8.0 Hz and H-9 = 8.5 Hz) means that these protons must be *cis* (β-oriented). A NOE between H-4 and H-6 indicated that the oxymethine at H-6 is pseudoequatorial (α) and is equatorial with respect to H-5. This means that the hydroxyl attached at H-6 is β-oriented. A third NOE between methyl-10 and H_{α}-7 (δ_H 2.10 dd, J = 15.0, 5.0 Hz) showed that both the methyl and H_{α}-7 protons are on the same face of the molecule and in an α-orientation. A further NOE between methyl-10 and H-1, placed the proton attached at C-1 on the same face as the protons of methyl-10 in an α-orientation. So the acetyl and glucose moieties must be in a pseudoequatorial orientation (β). The relative stereochemistry of this molecule is

supported by Guiso *et al* (1974) with the exception of the orientation of the hydroxyl and methine proton at C-6. The orientations are opposite to that stated and so the compound is new and is the epimer of ajugoside, 6-*epi*-ajugoside.

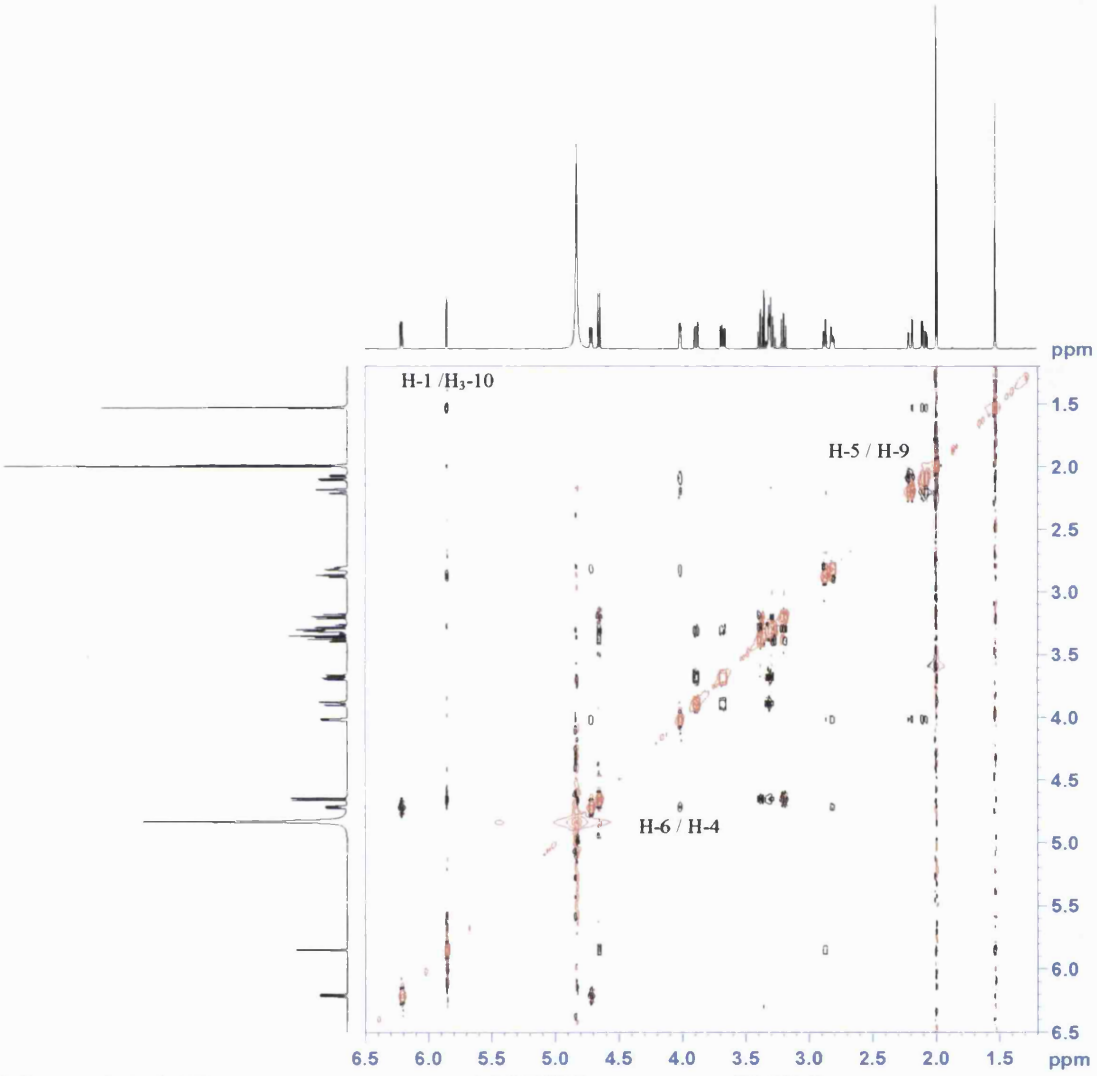

Figure 3.2.4.1F NOESY spectrum of **MS-5**

Table 5 ^{1}H and ^{13}C NMR data and ^{1}H-^{13}C long-range correlations of **MS-5** recorded in CD_3OD

Position	^{1}H	^{13}C	^{2}J	^{3}J
1	5.85 d (1.5)	94.6		C-3, C-5, C-8, C-1'
3	6.21 dd (6.5, 2.5)	141.5	C-4	C-1, C-5
4	4.72 dd (6.5, 1.0)	104.2	C-3, C-5	C-6, C-9
5	2.81 bd (8.0)	41.7	C-4, C-6, C-9	C-3, C-7, C-8
6	4.01 d (4.5)	76.9	C-7	C-4, C-8, C-9
7	2.10 dd (15.0, 5.0)	48.8	C-6, C-8	C-5, C-9
	2.21 d (15.0)			
8	-	90.1		
9	2.88 bd (8.5)	49.6	C-1, C-5, C-8	C-4, C-10
10	1.53 s	22.8	C-8	C-7, C-9
1'	4.65 d (8.0)	100.0		C-3', C-5', C-1
2'	3.19 t (8.0)	74.8	C-1', C-3'	
3'	3.38 t (8.5)	78.1	C-2', C-4'	
4'	3.29 m	71.7	C-3', C-5'	
5'	3.30 m	78.1		
6'	3.69 dd (12.0, 6.0)	63.0	C-5'	C-4'
	3.89 dd (11.5, 1.5)			
1"	-	173.3		
2"	2.00 s	22.3	C-1"	

3.2.4.2 Characterisation of MS-6 as 8-cinnamoyl ajugol (6-*epi*-laterioside)

MS-6 was isolated as an amorphous white powder from the chloroform extract. The molecular formula of **MS-6** was assigned as $C_{24}H_{30}O_{10}$ by HRCIMS $[M+NH_4]^+$ (496.2173). Signals for a C=C (1653 cm^{-1}) and hydroxyl (3648 cm^{-1}) groups were detected in the infrared spectrum. The ^{13}C spectrum provided evidence for 24 carbons whilst the ^1H spectrum again indicated the presence of an iridoid glycoside. The acetyl group present in **MS-5** was lacking in **MS-6** but a cinnamoyl residue was evident from the ^1H and ^{13}C NMR spectra.

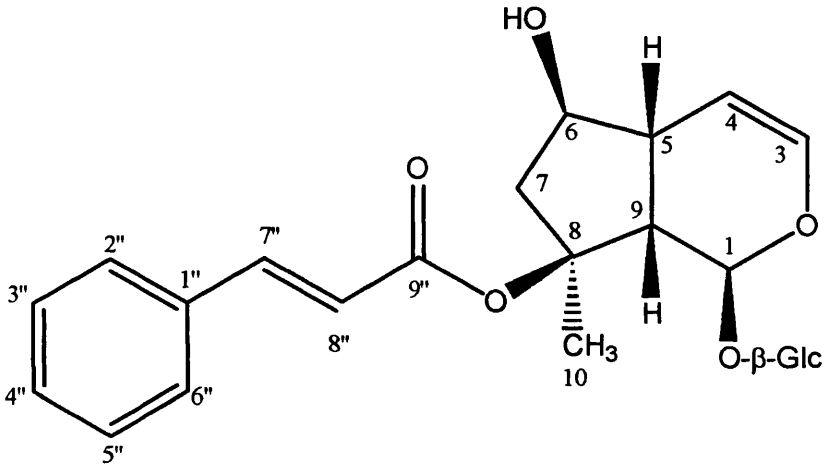

Figure 3.2.4.2A Structure of **MS-6**

The HMBC and COSY spectra provided similar signals as for **MS-5**, indicating another substituted iridoid glycoside. The only difference between **MS-6** and **MS-5** is the loss of the acetyl group attached at C-8, which was replaced by a cinnamoyl moiety. Again the downfield shift of C-8 (δ_C 90.3) indicated that the cinnamoyl group should be attached here. An hydroxyl group was attached at C-6 (δ_C 77.0) based on the upfield appearance of this carbon with respect to C-8. This was substantiated further by Ahmed *et al.*, (2003) who reported the downfield shift of C-8 when either an acetyl or cinnamoyl moiety was attached as compared to when an hydroxyl was positioned here. A greater downfield shift of H-6 would have also been expected had the cinnamoyl moiety been attached at C-6 to ~5.0-5.5 ppm. Had the cinnamoyl group been attached at C-6 a ^3J HMBC correlation should have been detected between H-6 and the carbonyl carbon, however this was absent. Whereas being positioned at C-8, an HMBC signal (^4J) would not be expected to be detected.

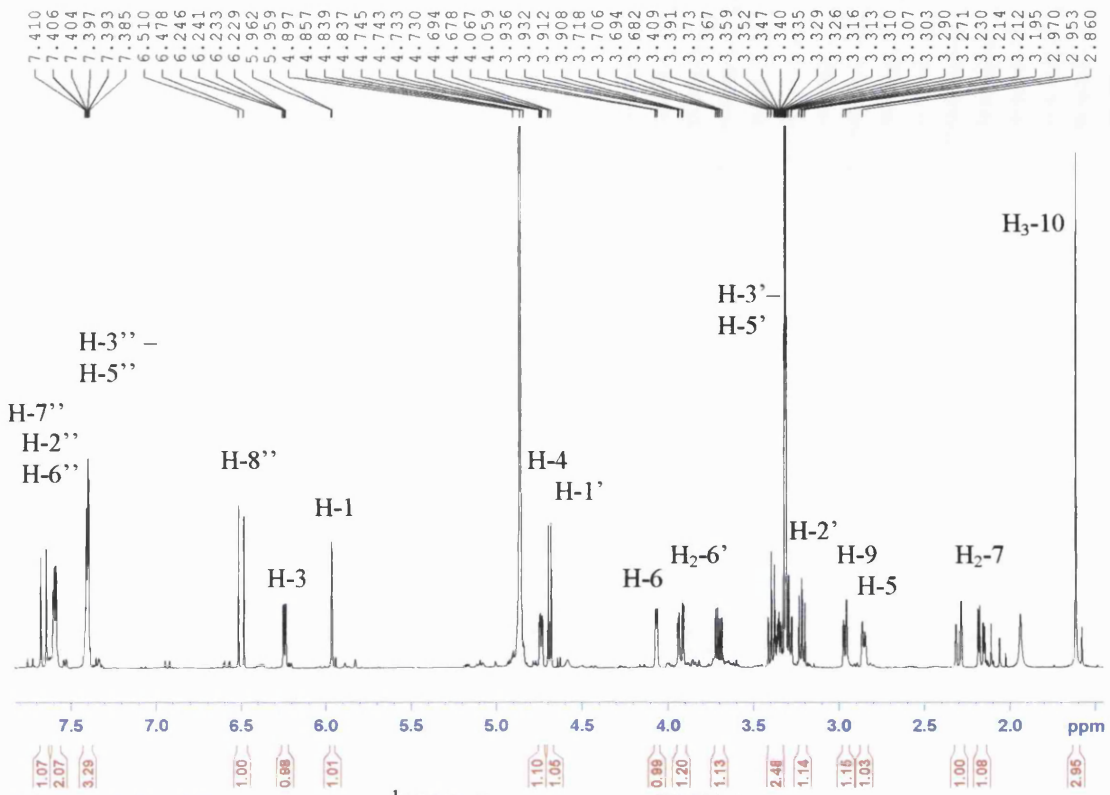

Figure 3.2.4.2B ^{1}H NMR spectrum of **MS-6**

The NOESY spectrum provided identical signals as observed for **MS-5**. A NOE between H-5 and H-9 placed these protons on the same face of the molecule. The large coupling constant (J = 8.5 Hz) meant that they are *cis* (β-oriented). A 1,3 interaction between the olefin, H-4, and H-6 placed this proton in a pseudoequatorial orientation (α). Therefore the hydroxyl group must be β-orientated. A third NOE between methyl-10 and H_{α}-7 (2.17 dd, J = 15.0, 4.5 Hz) placed these protons on the same face of the molecule (α). A further NOE between methyl-10 and H-1 placed this proton in an α-orientation.

The ^{1}H and ^{13}C NMR data for **MS-6** was in agreement with the literature for the 8-cinnamoyl ajugol iridoid glycoside also known as laterioside (Pardo *et al.*, 1998; Swiatek *et al.*, 1981). This is the first report of the full NMR data for 6-*epi*-laterioside.

Table 6 ^{1}H and ^{13}C NMR data and ^{1}H-^{13}C long-range correlations of **MS-6** recorded in CD_3OD

Position	^{1}H	^{13}C	^{2}J	^{3}J
1	5.96 d (1.5)	94.7		C-3, C-5, C-8, C-1'
3	6.24 dd (6.5, 2.5)	141.6	C-4	C-1, C-5
4	4.74 dd (6.5, 1.5)	104.2	C-3, C-5	C-6, C-9
5	2.85 bd (8.0)	41.8	C-4, C-6, C-9	C-3, C-8
6	4.06 d (4.0)	77.0		C-4, C-8, C-9
7	2.17 dd (15.0, 4.5)	48.9	C-6, C-8	C-5, C-9, C-10
	2.31 d (15.0)			
8	-	90.3		
9	2.97 bd (8.5)	49.7	C-1, C-5, C-8	C-4, C-10
10	1.61 s	23.0	C-8	C-7, C-9
1'	4.69 d (8.0)	100.2		C-1
2'	3.21 dd (9.0, 8.0)	74.9	C-1', C-3'	
3'	3.39 t (9.0)	78.1	C-2', C-4'	
4'	3.29 m	71.8	C-3', C-5'	C-6'
5'	3.35 m	78.2	C-4'	
6'	3.70 dd (12.0, 6.0)	63.1	C-5'	
	3.93 dd (12.0, 2.0)			
1"	-	135.8		
2"	7.59 m	129.2		C-4", C-6", C-7"
3"	7.40 m	130.0		C-1"
4"	7.40 m	131.4		C-2", C-6"
5"	7.40 m	130.0		C-1"
6"	7.59 m	129.2		C-2", C-4", C-7"
7"	7.67 d (16.0)	145.9	C-1", C-8"	C-2", C-6", C-9"
8"	6.51 d (16.0)	120.3	C-9"	C-1"
9"	-	168.7		

3.2.4.3 Characterisation of MS-7 as 6-*O*-α-L-rhamnopyranosylcatalpol

This compound was isolated as a colourless oil and a molecular formula of $C_{21}H_{32}O_{14}$ was assigned by ESI-MS. Peaks were detected for $[M+Na]^+$ (531.2) and $[M-H+2Na]^+$ (553.1). The ^1H NMR spectrum again indicated the presence of an iridoid glycoside, this time with two sugar moieties. The ^{13}C NMR spectrum showed 21 signals, fifteen of these were attributable to a catalpol and six to a rhamnopyranosyl group.

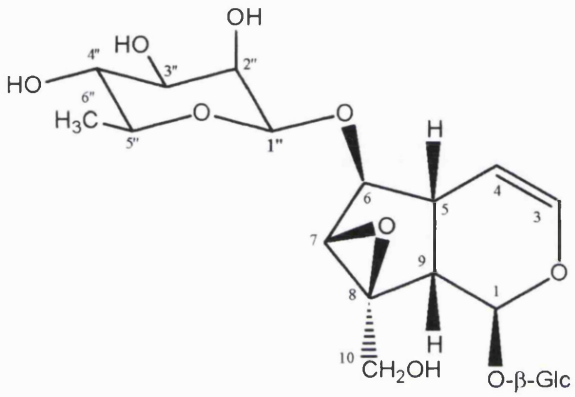

Figure 3.2.4.3A Structure of **MS-7**

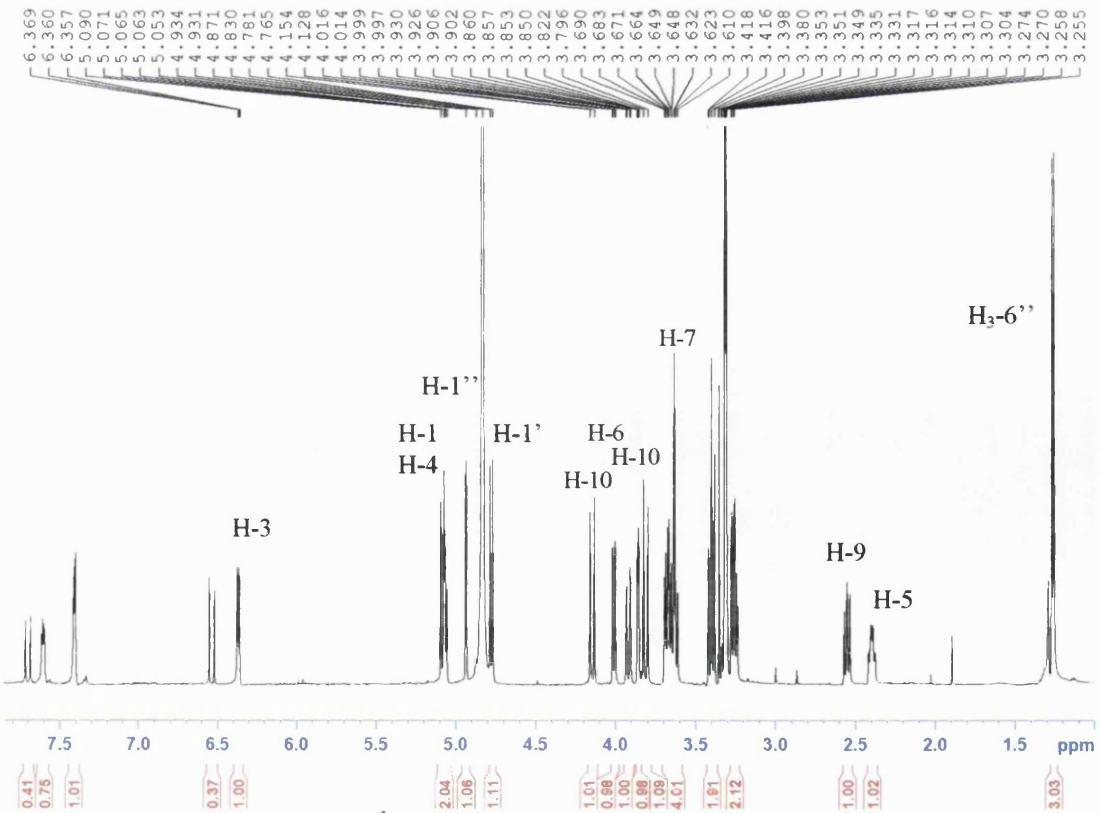

Figure 3.2.4.3B ^1H NMR spectrum of **MS-7**

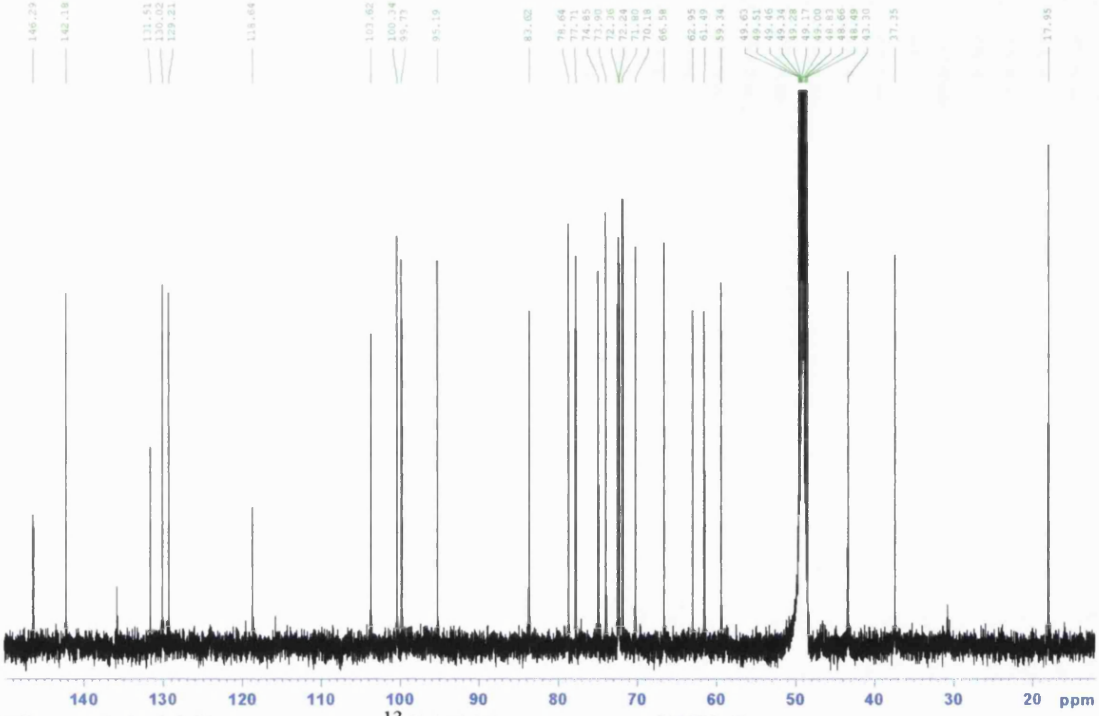

Figure 3.2.4.3C ^{13}C NMR spectrum of **MS-7**

Both the ^{1}H and ^{13}C spectra showed the presence of a cinnamate group. However, by comparing the integration of the cinnamate protons to those of the iridoid molecule (1:3) it is clear that this group is present only as an impurity. The cinnamate group may well have been attached to the iridoid structure at some point and then cleaved during the plant's own metabolism.

The HMBC and COSY spectra provided similar signals as for the previous iridoid glycosides discussed. Where **MS-7** differed from these compounds was at positions 6 and 8. A ^{2}J correlation between an oxymethylene (δ_H 3.82 d and δ_H 4.15 d, J = 13.0 Hz, H_2-10) and the quaternary carbon at position 8 (δ_C 66.6) placed this primary alcohol function here. The downfield chemical shift values of both C-8 and C-7 (δ_C 59.3) indicated that an oxygen is directly attached at these positions. This took the form of an epoxide rather than two hydroxyl groups based on the smaller chemical shift values observed for these two carbons and also the molecular weight calculated from ESI-MS. Had a free hydroxyl been placed at C-8, it would have resulted in the this carbon coming into resonance at ~79 ppm in the ^{13}C NMR spectrum (Ahmed *et al.*, 2003; Liva *et al.*, 2001). The formation of an epoxide between these two carbons is a relatively common feature and the chemical shifts are in close agreement with previously isolated iridoid glycosides (Hosny and Rosazza 1998).

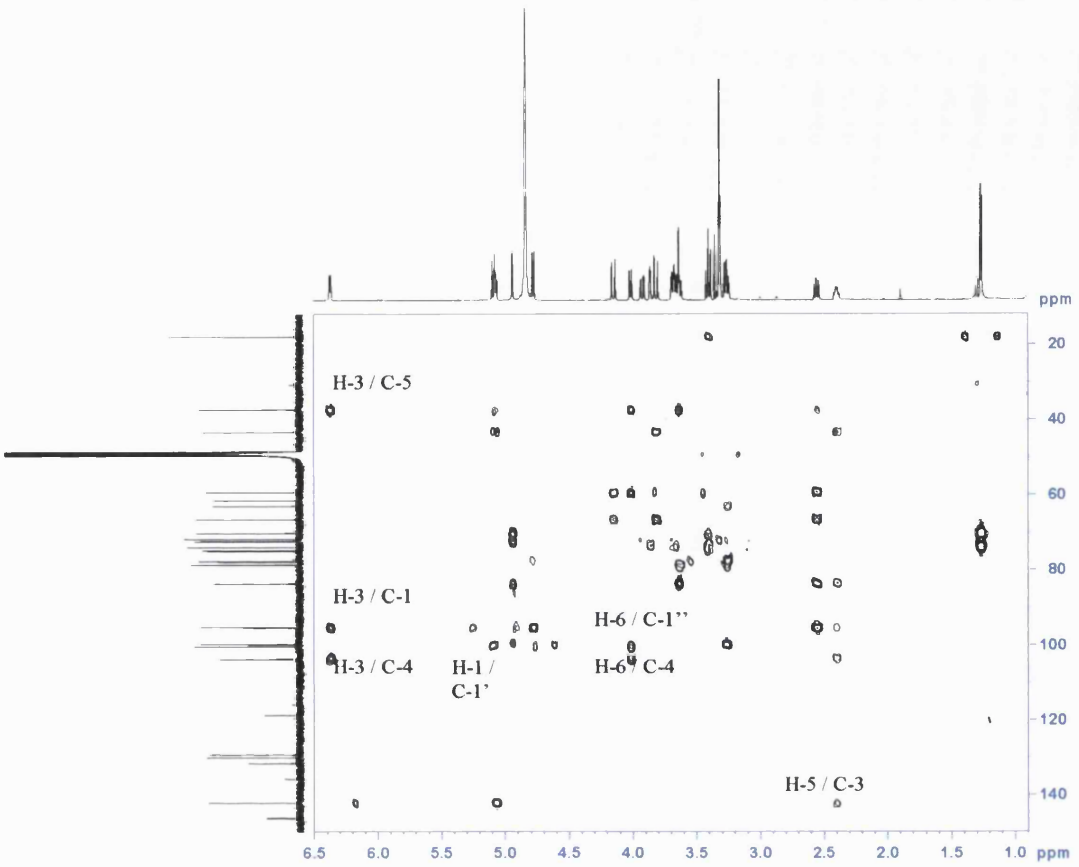

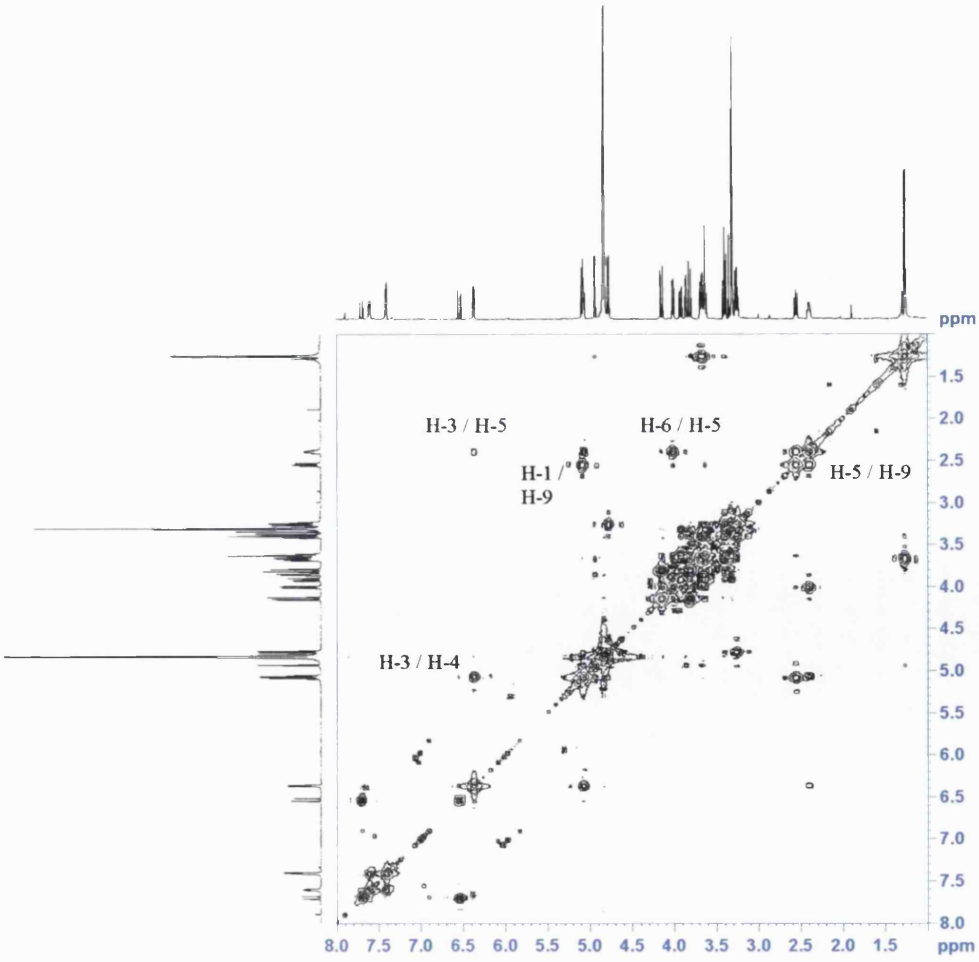

Figure 3.2.4.3D HMBC and COSY spectra of **MS-7**

The second difference between **MS-7** and **MS-5** is the attachment of a deoxyhexose sugar. The point of attachment for this moiety was found to be at position 6 of the iridoid molecule. Strong ^{3}J signals ($^{1}H \rightarrow ^{13}C$) were detected between H-6 (δ_H 4.01) and C-1'' and H-1'' (δ_H 4.93 d, J = 1.5 Hz) and C-6. The deoxyhexose sugar was identified as α-L-rhamnose. The anomeric proton showed signals towards C-2'', C-3'' and C-5''. A COSY correlation between H-1'' and H-2'' (δ_H 3.85 dd, J = 3.5, 1.5 Hz) fixed the oxymethine at this position. The methyl doublet belonging to the rhamnose (δ_H 1.26 d, J = 6.5 Hz, H_3-6'') exhibited ^{2}J and ^{3}J correlations towards C-5'' (δ_C 70.2, δ_H 3.66 m, H-5'') and C-4'' (δ_C 73.9, δ_H 3.39 t, J = 9.0, H-4'') respectively. Thus the ^{3}J correlation between H-1'' and C-3'' completed the rhamnose ring.

The relative stereochemistry of this compound was determined by NOESY correlations and the coupling constants calculated. The signals obtained were identical to those observed for **MS-5** and therefore possessing the same relative stereochemistry. The data for **MS-7** is in close agreement with that of the literature (Hosny and Rosazza 1998; Seifert *et al.*, 1989), therefore reaffirming the structure and relative stereochemistry of this compound which was previously isolated from *Verbascum pulverulentum* and *Gmelina arborea*.

Table 7 ^{1}H and ^{13}C NMR data and ^{1}H-^{13}C long-range correlations of **MS-7** recorded in CD_3OD

Position	^{1}H	^{13}C	^{2}J	^{3}J
1	5.09 m	95.2	C-9	C-3, C-5, C-1'
3	6.37 dd (6.0, 1.5)	142.2	C-4	C-1, C-5
4	5.06 d (6.0)	103.6	C-3	C-9
5	2.40 ddd (12.5, 8.0, 1.5)	37.4	C-4, C-6, C-9	C-1, C-3
6	4.01 d (8.0)	83.6	C-5, C-7	C-4, C-1"
7	3.63 s	59.3	C-6	C-5
8	-	66.6		
9	2.55 dd (9.5, 8.0)	43.3	C-1, C-5, C-8	C-6, C-7
10	3.82 d (13.0)	61.5	C-8	C7, C-9
	4.15 d (13.0)			
1'	4.78 d (8.0)	99.7		C-3', C-1
2'	3.25 m	74.9	C-1'	
3'	3.39 t (9.0)	77.7	C-2', C-4'	
4'	3.25 m	71.8	C-5'	C-6'
5'	3.32 m	78.6	C-4'	
6'	3.61 (12.5, 6.5)	63.0		
	3.92 dd (12.0, 1.5)			
1"	4.93 d (1.5)	100.3	C-2"	C-3", C-5", C-6
2"	3.85 dd (3.5, 1.5)	72.4		C-4"
3"	3.68 m	72.2	C-4"	
4"	3.39 t (9.0)	73.9	C-5"	C-6"
5"	3.66 m	70.2	C-4"	
6"	1.26 d (6.5)	18.0	C-5"	C-4"

3.2.4.4 Characterisation of MS-8 as 6-*O*-α-L-(4''-*trans*-3''',4'''-dimethoxycinnamoyl)-rhamnopyranosyl catalpol (buddlejoside A_8)

MS-8 was isolated as a colourless oil and ESI-MS enabled a molecular formula of $C_{32}H_{42}O_{17}$ to be assigned. Signals detected in the mass spectrum included $[M+Na]^+$ (721.0) and $[M-H+2Na]^+$ (743.0). The infrared spectrum provided evidence for a conjugated enone system (1652 cm^{-1}) and a broad signal at 3356 cm^{-1} for hydrogen bonded hydroxyl groups. The ^1H and ^{13}C spectra once more showed the presence of a 6-rhamnopyranosyl catalpol derivative, found in **MS-7**.

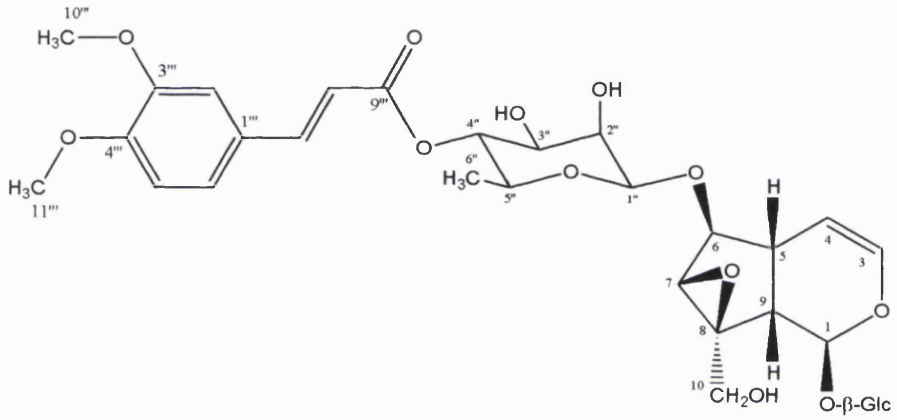

Figure 3.2.4.4A Structure of **MS-8**

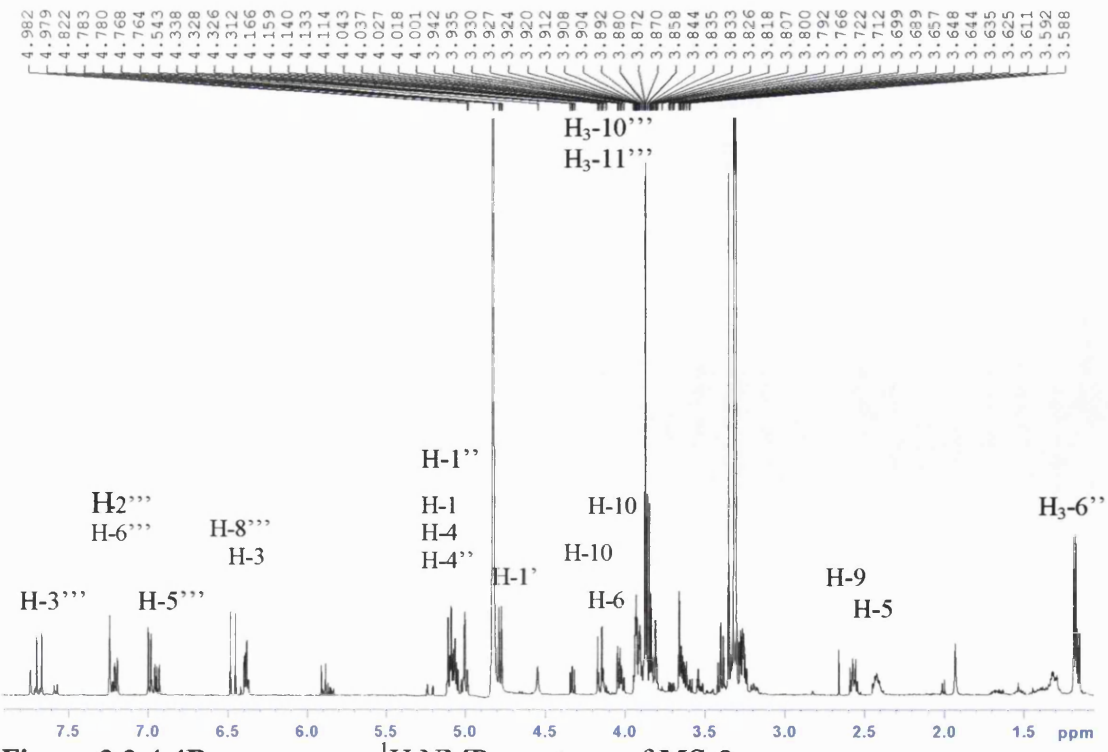

Figure 3.2.4.4B ^1H NMR spectrum of **MS-8**

The HMBC and COSY signals confirmed the presence of a 6-rhamnopyranosyl catalpol skeleton. The assignment of the rhamnose moiety was resolved by HMBC. H_3-6'' gave ^2J and ^3J correlations to C-5'' and C-4'' respectively, whilst the anomeric proton gave ^3J correlations to C-3'' and C-5''. A ^3J correlation between H-4'' (δ_H 5.07 m, δ_C 75.4) and C-2'' completed the rhamnose unit. The cinnamate moiety was assigned at C-4'' of the rhamnose unit due to the deshielded nature of the oxymethine proton H-4''. A signal in the HMBC spectrum from H-4'' to C-9''' was not detected but this was the only proton that exhibited a greater chemical shift than would be expected had an hydroxyl been attached. This was indicative of an ester linkage and therefore the cinnamate group was unambiguously attached at C-4''.

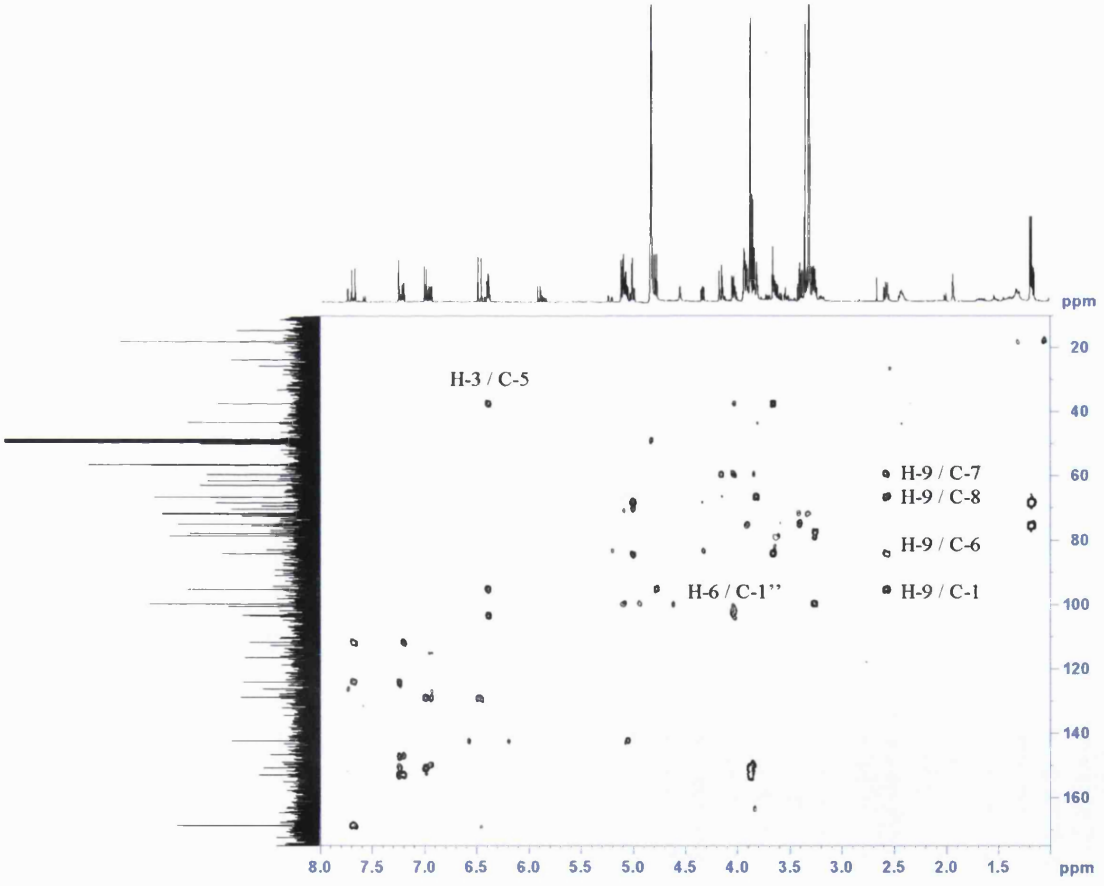

Figure 3.2.4.4C HMBC spectrum of **MS-8**

Once more the relative stereochemistry of **MS-8** was found to be the same as the iridoids already discussed as identical signals were detected. The NMR data for **MS-8** was in close agreement with that of the literature for buddlejoside A_8, isolated from *Buddleja japonica* (Miyase *et al.*, 1991).

Table 8 ^1H and ^{13}C NMR data and ^1H-^{13}C long-range correlations of **MS-8** recorded in CD_3OD

Position	^1H	^{13}C	^2J	^3J
1	5.10 m	95.2		C-1'
3	6.38 dt (6.0, 2.0)	142.3	C-4	C-1, C-5
4	5.06 m	103.5	C-3	
5	2.42 m	37.4		
6	4.04 d (8.0)	84.2	C-5, C-7	C-4, C-1"
7	3.65 s	59.5	C-6	C-5
8	-	66.6		
9	2.56 dd (9.5, 7.5)	43.4	C-1, C-8	C-6, C-7
10	3.83 d (14.0)	68.3	C-8	C-7
	4.16 d (13.0)			
1'	4.78 d (7.5)	99.8		C-1
2'	3.25 m	74.9	C-1', C-3'	
3'	3.40 t (9.0)	77.7	C-2'	
4'	3.27 m	71.8	C-3', C-5'	
5'	3.32 m	78.7		
6'	3.63 m	63.0		
	3.90 m			
1"	4.99 bs	100.5		C-3", C-5", C-6
2"	3.93 m	72.5		
3"	3.66 m	70.3		
4"	5.07 m	75.4		C-2"
5"	3.82 m	68.3		
6"	1.18 d (6.0)	17.9	C-5"	C-4"
1"'	-	128.9		
2"'	7.24 d (2.0)	111.7	C-3"'	C-4"', C-6"', C-7"'
3"'	-	150.8		
4"'	-	152.9		
5"'	6.99 d (8.5)	112.7		C-1"', C-3"'
6"'	7.20 dd (8.5, 2.0)	124.1		C-2"', C-4"', C-7"'
7"'	7.69 d (15.5)	146.8		C-2"', C-6"', C-9"'
8"'	6.47 d (16.0)	116.5	C-9"'	C-1"'
9"'	-	168.7		
10"'	3.87 s	56.4		C-3"'
11"'	3.87 s	56.6		C-4"'

3.2.4.5 Characterisation of MS-9 as 6-*O*-α-L-(2'',4''-diacetyl-3''-*trans*-cinnamoyl)-rhamnopyranosyl catalpol (scrospioside A)

MS-9 was isolated as a white amorphous powder from the chloroform extract of *S. deserti*. A molecular formula of $C_{34}H_{42}O_{17}$ was assigned on the basis of ESI-MS in negative mode. The mass spectrum yielded peaks corresponding to $[M-H]^-$ (721.1), $[M+Na]^-$ (745.1) and $[M-H+2Na]^-$ (767.1). The ^{13}C spectrum provided 34 signals and as with **MS-7**, fifteen of these were attributable to a catalpol group and six to a rhamnopyranosyl group. The remaining 13 carbon signals provided evidence for a cinnamoyl and two acetyl (δ_H 2.03 s and δ_H 2.16 s) groups. The ^1H spectrum verified the presence of an iridoid glycoside including the presence of a rhamnose unit with a similar spectrum to that of **MS-7**.

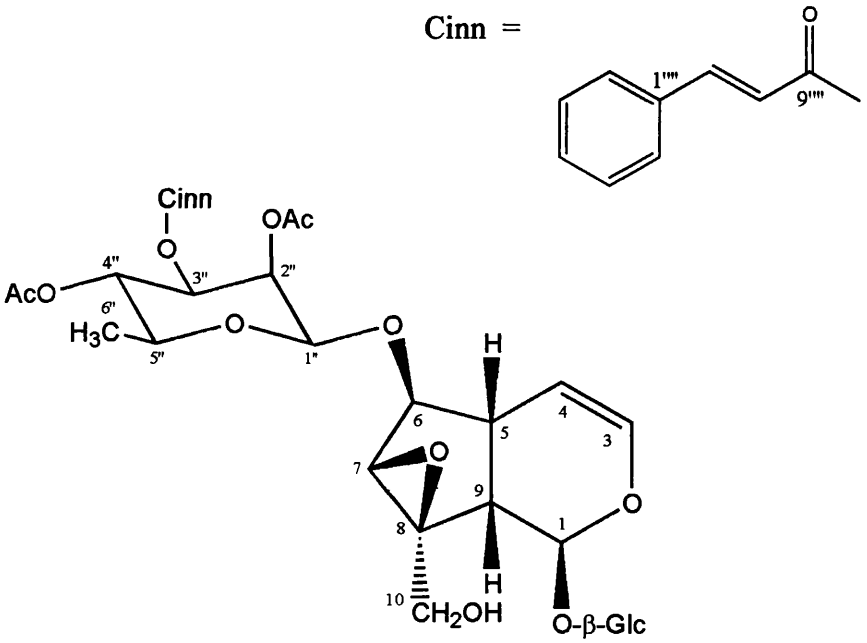

Figure 3.2.4.5A Structure of **MS-9**

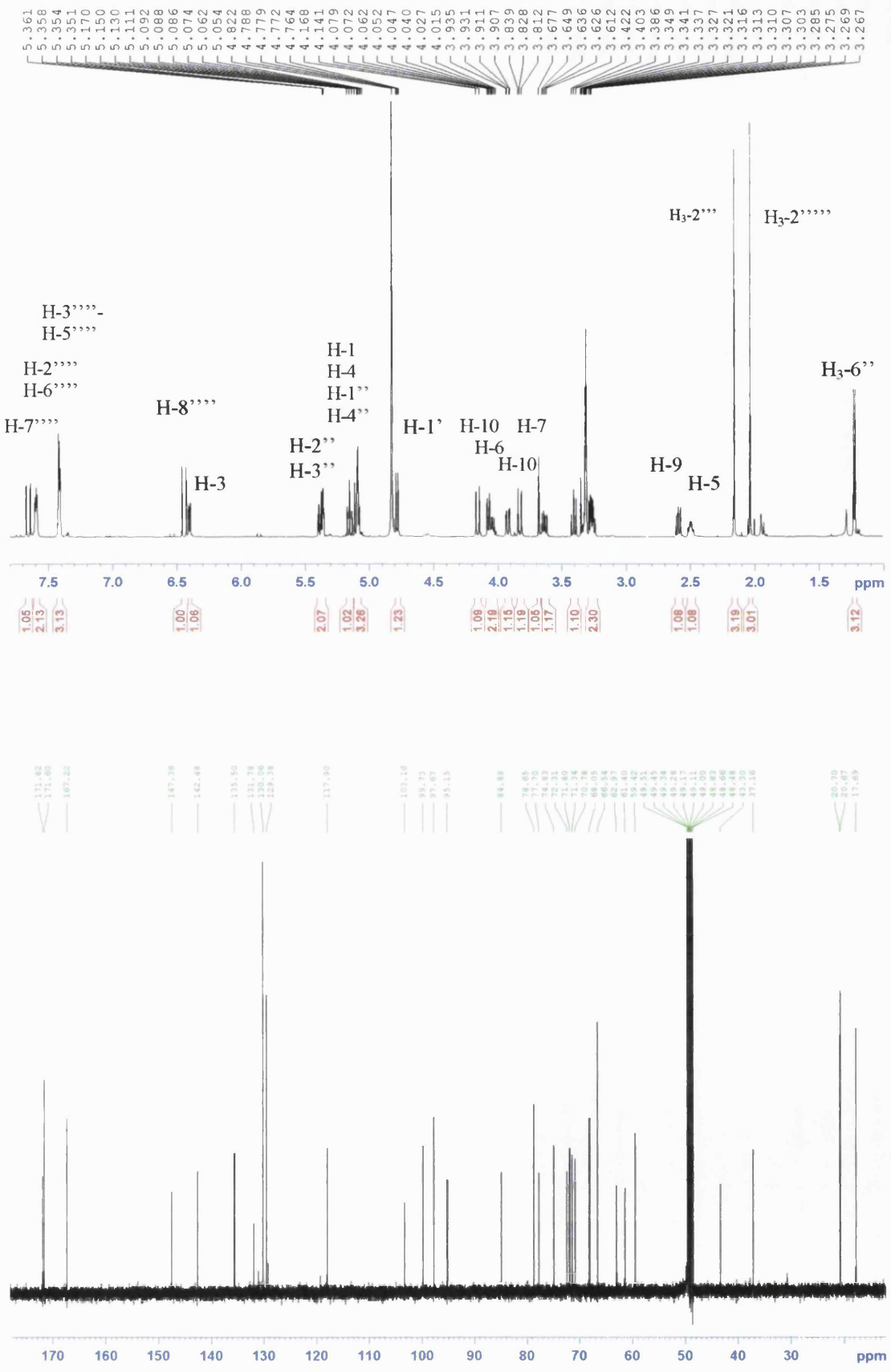

Figure 3.2.4.5B ^{1}H and ^{13}C NMR spectra of **MS-9**

The HMBC and COSY yielded identical signals as found for **MS-7** providing evidence for a 6-*O*-rhamnopyranosylcatalpol skeleton. The difference between **MS-7** and **MS-9** appears to be with the trisubstitution of the rhamnose moiety. This was apparent by the downfield chemical shift values observed in the ^{1}H spectrum for the three oxymethines directly attached to the acetyl or cinnamate groups. Each of these groups exerted a greater deshielding effect than an hydroxyl, normally associated with the rhamnose. The rhamnose moiety was solved mainly by HMBC connectivites and supported by the COSY spectrum. Beginning with the anomeric proton (δ_H 5.08 m, δ_C 97.7), this showed two ^{3}J signals to C-3'' (δ_H 5.39 m, δ_C 70.8) and C-5'' (δ_H 4.04 dd, J = 10.0, 6.5 Hz, δ_C 68.1). The position of C-5'' was confirmed by a ^{2}J signal from the methyl, H_3-6'' (δ_H 1.23 d, δ_C 17.7). A ^{3}J signal from this methyl to C-4'' (δ_H 5.15 t, δ_C 72.3) placed this oxymethine carbon here. A COSY correlation between C-3'' and C-4'' reaffirmed the position of these two oxymethine carbons. The third downfield oxymethine (δ_H 5.35 m, δ_C 71.3) was therefore placed at position 2 of the rhamnose unit. This was confirmed by a ^{3}J HMBC signal between H-2'' and C-4''.

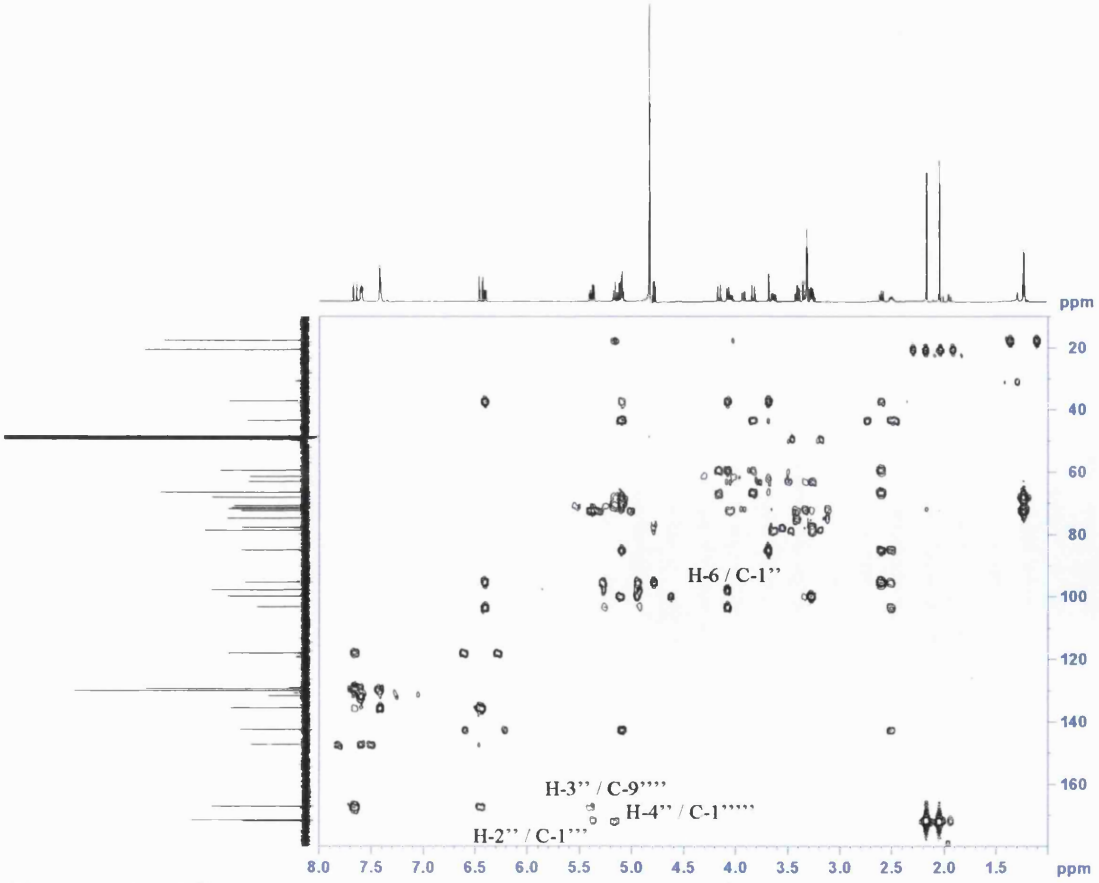

Figure 3.2.4.5C HMBC spectrum of **MS-9**

The assignment of the acetyl and cinnamate groups could now be made now that the structure of the rhamnose was determined. This was achieved by signals detected in the HMBC spectrum. ^{3}J correlations from H-2'' and H-4'' to methyl bearing carbonyls (δ_C 171.6, C-1''' and δ_C 171.8, C-1''''') enabled an acetyl group to be placed at these two positions. Another ^{3}J signal from H-3'' to a third carbonyl (δ_C 167.2, C-9'''') provided evidence to assign a cinnamate group here. This was shown to be of the *trans* type based on the large coupling (16.0 Hz) calculated for the olefins α (δ_H 6.45 d, δ_C 117.9) and β (δ_H 7.66 d, δ_C 147.4) to the carbonyl.

The relative stereochemistry of **MS-9** was found to be the same as the previously discussed iridoid glycosides as the NOESY spectrum provided identical signals as those described for **MS-5**. The NMR data for **MS-9** was in close agreement with that published for this compound, isolated from the roots of *Scrophularia korainensis* (Pachaly *et al.*, 1994). **MS-9** has also been isolated from the roots of *Scrophularia spicata* in Yunnan, where the plant is used in folk medicine (Zhang *et al.*, 1992).

Table 9 ^{1}H and ^{13}C NMR data and ^{1}H-^{13}C long-range correlations of **MS-9** recorded in CD_3OD

Position	^{1}H	^{13}C	^{2}J	^{3}J
1	5.11 m	95.2		C-1'
3	6.40 dd (6.0, 1.5)	142.5	C-4	C-1
4	5.08 m	103.2	C-3, C-5	C-6, C-9
5	2.50 m	37.2	C-4, C-6, C-9	C-1, C-3
6	4.08 d (8.5)	84.9	C-5, C-7	C-4, C-1"
7	3.67 s	59.4	C-6, C-8	C-5, C-9, C-10
8	-	66.5		
9	2.59 dd (10.0, 8.0)	43.3	C-1, C-5, C-8	C-6, C-7
10	3.83 d (13.0)	61.4	C-8	C-7, C-9
	4.16 d (13.0)			
1'	4.78 d (7.5)	99.7		C-3', C-5', C-1
2'	3.27 m	74.8	C-1'	C-4'
3'	3.40 t (9.5)	77.7		
4'	3.25 m	71.8		C-6'
5'	3.34 m	78.7	C-4', C-6'	C-1'
6'	3.63 dd (12.0, 6.5)	63.0	C-5'	
	3.93 dd (11.5, 1.5)			
1"	5.08 m	97.7		C-3", C-5", C-6
2"	5.35 m	71.3		C-4", C-1'''
3"	5.39 m	70.8	C-4"	C-9''''
4"	5.15 t (10.0)	72.3	C-3", C-5"	C-6", C-1'''''
5"	4.04 dd (10.0, 6.5)	68.1	C-4"	
6"	1.23 d (6.5)	17.7	C-5"	C-4"
1'''	-	171.6		
2'''	2.03 s	20.7	C-1'''	
1''''	-	135.5		
2''''	7.59 m	129.4		C-4''''
3''''	7.41 m	130.1		C-1''''
4''''	7.41 m	131.8	C-3'''', C-5''''	
5''''	7.41 m	130.1		C-1''''
6''''	7.59 m	129.4		C-4''''
7''''	7.66 d (16.0)	147.4	C-1'''', C-8''''	C-2'''', C-6'''', C-9''''
8''''	6.45 d (16.0)	117.9	C-9''''	C-1''''
9''''	-	167.2		
1'''''	-	171.8		
2'''''	2.16 s	20.7	C-1'''''	

3.2.4.6 Characterisation of MS-10 as 6-*O*-α-L-(2''-acetyl-3'',4''-*trans*-dicinnamoyl)-rhamnopyranosyl catalpol (scropolioside B)

MS-10 was isolated as a white amorphous solid and a molecular formula of $C_{41}H_{46}O_{17}$ was assigned on the basis of HRCIMS which gave the $[M+Na]^+$ ion at *m/z* 833.2628 (calculated for $C_{41}H_{46}O_{17}Na$: 833.2633). The ^{13}C NMR spectrum showed signals for 41 carbons, including three carbonyl carbons. Two anomeric carbons were also detected, confirming the presence of two sugar moieties. The ^1H NMR spectrum was very similar to that of **MS-9**, the only difference being the presence of a second cinnamate group taking the place of one of the acetate units in **MS-9**. Therefore **MS-10** is another highly substituted iridoid glycoside.

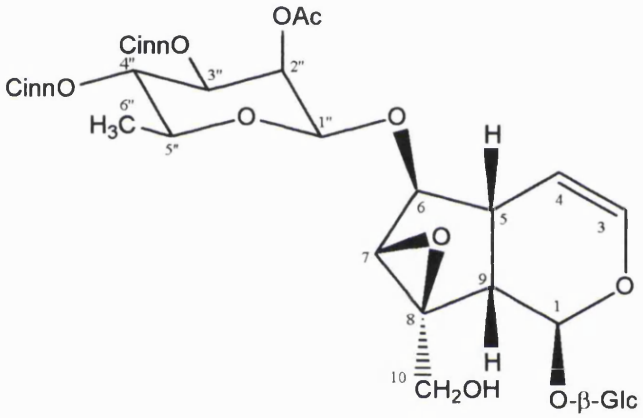

Figure 3.2.4.6A Structure of **MS-10**

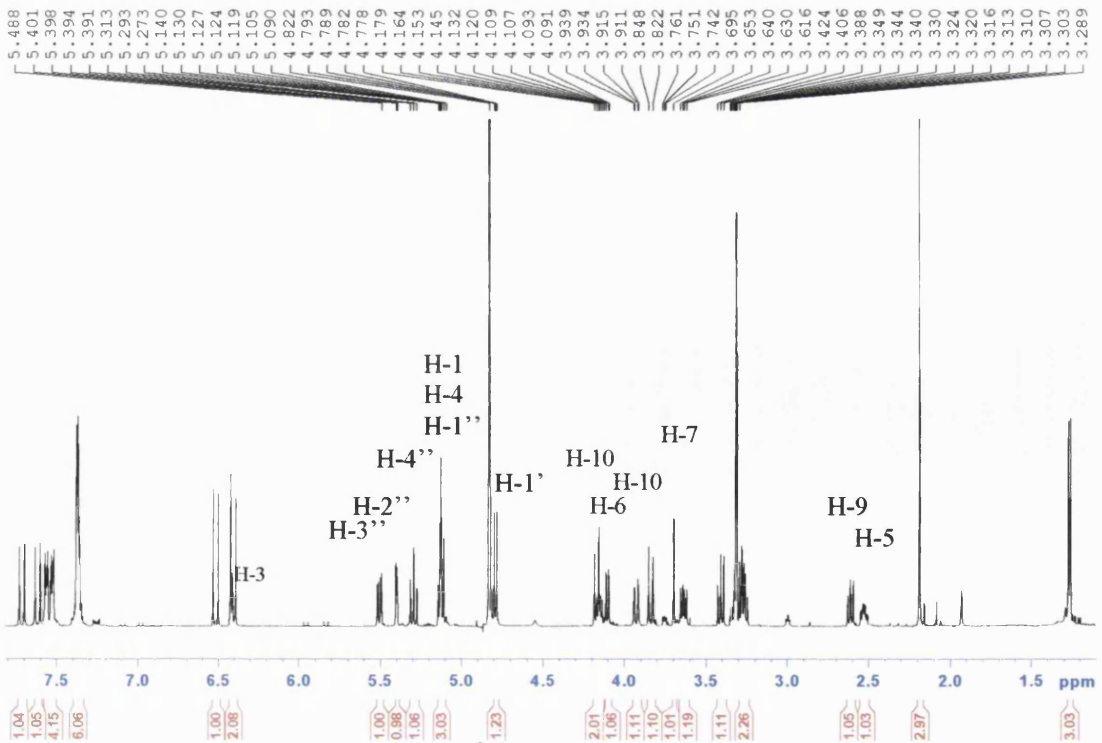

Figure 3.2.4.6B ^1H spectrum of **MS-10**

The HMBC and COSY spectra provided similar signals for the iridoid nucleus as in **MS-5**. The difference being that the methyl group at C-10 was oxidised to the primary alcohol along with the epoxide formation between C-7 and C-8. A glucose residue was attached to C-1 of the iridoid nucleus whilst a rhamnose moiety was placed at C-6. This was based on ^{3}J HMBC correlations from the anomeric protons to the respective carbons of the iridoid nucleus. The rhamnose moiety was assigned by both HMBC and COSY correlations. H-1'' showed a COSY correlation to H-2'', which in turn gave a signal to H-3''. H-3'' also exhibited a strong COSY correlation to H-4''. Methyl-6'' showed ^{2}J and ^{3}J signals to C-5'' and C-4'' respectively, completing the rhamnose moiety. Due to the deshielded nature of the oxymethine protons at C-2'', C-3'' and C-4'' it was clear that the cinnamate and acetate groups must be attached to the rhamnose residue as opposed to the glucose. A ^{3}J correlation between H-4'' and C-9''''' placed one of the cinnamate groups here. A second weak ^{3}J signal between H-2'' and C-1''' enabled the acetate group to be assigned at position 2 of the rhamnose residue. This left the second cinnamate group to be assigned at H-3''. Although no HMBC signal was detected the fact that H-3'' was the only deshielded proton remaining meant that the cinnamate group must be assigned here.

The relative stereochemistry of **MS-10** was found to be the same as the previously discussed iridoid glycosides as the NOESY spectrum provided identical signals as those described for **MS-5** - **MS-9**. The NMR data, including the stereochemistry, for **MS-10** was in close agreement with the published literature (Calis *et al.*, 1988). **MS-10** has also been referred to as scropoloside B (Bhandari *et al.*, 1992).

Table 10 ^{1}H and ^{13}C NMR data and ^{1}H-^{13}C long-range correlations of **MS-10** recorded in CD_3OD

Position	^{1}H	^{13}C	^{2}J	^{3}J
1	5.10 m	95.2	C-9	C-3, C-5, C-1'
3	6.40 m	142.5	C-4	C-1, C-5
4	5.13 m	103.2	C-3	C-6, C-9
5	2.53 m	37.2	C-4, C-6	
6	4.10 dd (8.0, 1.0)	85.0	C-5, C-7	C-4, C-8, C-1"
7	3.69 s	59.5	C-6	C-5
8	-	66.6		
9	2.60 dd (9.5, 7.5)	43.4	C-5, C-8	C-6, C-7
10	3.84 d (13.0)	61.4	C-8	C-7, C-9
	4.17 d (13.0)			
1'	4.79 d (8.0)	99.8	C-2'	C-1
2'	3.27 m	74.9	C-3'	
3'	3.40 t (8.5)	77.7	C-2'	
4'	3.25 m	71.8	C-3', C-5'	C-6'
5'	3.33 m	78.7		
6'	3.64 dd (11.5, 6.5)	63.0	C-5'	
	3.93 dd (11.5, 2.0)			
1"	5.12 m	97.8	C-2"	C-3", C-5", C-6
2"	5.39 dd (3.5, 1.5)	71.5	C-3"	C-4", C-1"'
3"	5.50 dd (10.5, 3.5)	70.9	C-4"	
4"	5.29 t (10.0)	72.5	C-3", C-5"	C-6", C-9"''
5"	4.13 dd (9.5, 6.5)	68.3		
6"	1.28 d (6.0)	17.8	C-5"	C-4"
1"'	-	171.6		
2"'	2.18 s	20.7	C-1"'	
1"''	-	135.5		
2"''	7.52 m	129.4		C-4"'', C-6"''
3"''	7.37 m	130.0		C-1"''
4"''	7.37 m	131.7		C-2"'', C-6"''
5"''	7.37 m	130.0		C-1"''
6"''	7.52 m	129.4		C-2"'', C-4"''
7"''	7.63 d (16.0)	147.4	C-8"''	C-2"'', C-6"'', C-9"''
8"''	6.41 d (16.0)	117.9	C-9"''	C-1"''
9"''	-	167.3		
1""'	-	135.5		
2""'	7.57 m	129.4		C-4""', C-6""'
3""'	7.37 m	130.0		C-1""'
4""'	7.37 m	131.8		C-2""', C-6""'
5""'	7.37 m	130.0		C-1""'
6""'	7.57 m	129.4		C-2""', C-4""'
7""'	7.72 d (16.0)	147.6	C-8""'	C-2""', C-6""', C-9""'
8""'	6.52 d (16.0)	117.9	C-9""'	C-1""'
9""'	-	167.7		

3.2.4.7 MS-11 proposed as 6-*O*-α-L-(3''-acetyl-2''-*trans*-cinnamoyl)-rhamnopyranosyl catalpol (scorodioside)

MS-11 was isolated as a colourless oil. ESI-MS in the positive mode yielded a peak assigned to $[M+Na]^+$ (703.0). Together with information derived from the 1D NMR data, this enabled a molecular formula of $C_{32}H_{40}O_{16}$ to be assigned. The ^{13}C NMR spectrum provided signals for 32 carbons, which included four olefinic, three acetal and two carbonyl carbons. The ^1H NMR spectrum gave signals indicating the presence of an iridoid natural product. This included an acetal proton (δ_H 5.09 m, H-1), two *cis* olefinic protons (δ_H 6.39 dd, J = 6.0, 1.5 Hz, H-3 and δ_H 5.12 m, H-4) and two methine protons located at the ring junction of the iridoid molecule (δ_H 2.49 m, H-5 and δ_H 2.58 dd, J = 10.0, 8.0 Hz, H-9). **MS-11** also gave signals for glucose and rhamnose moieties as well as cinnamate and acetate groups.

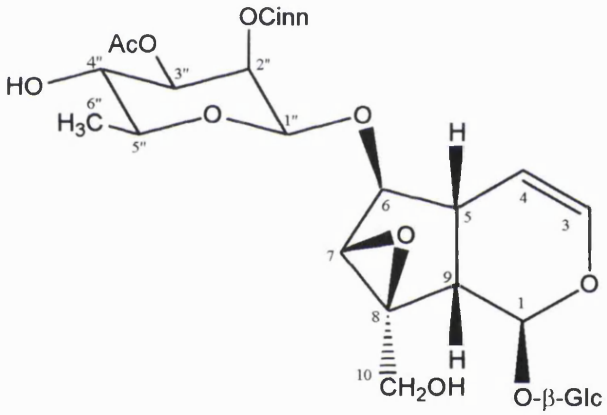

Figure 3.2.4.7A Structure of **MS-11**

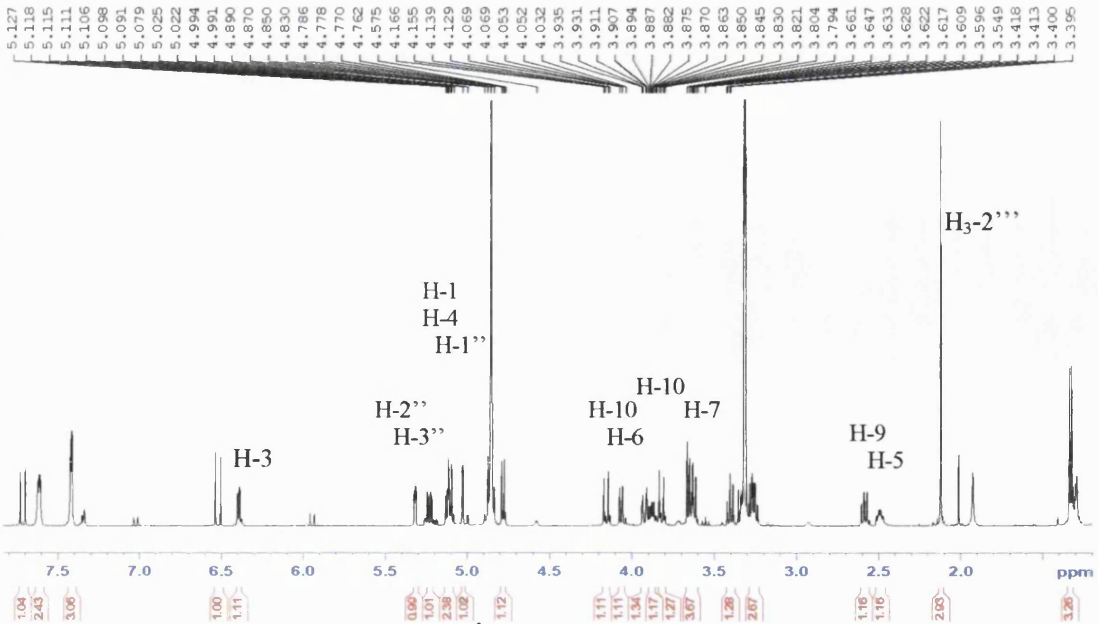

Figure 3.2.4.7B ^1H spectrum of **MS-11**

The HMBC and COSY spectra provided similar signals as previously isolated iridoids. Glucose and rhamnose moieties were also attached at C-1 and C-6 of the iridoid molecule based on ^3J correlations from the anomeric protons to these carbons. The COSY spectrum exhibited a weak signal between H-1'' and H-2'' as well as signals from H-2'' to H-3'' and finally from H-3'' to H-4''. The HMBC gave ^2J and ^3J correlations from H_3-6'' to C-5'' and C-4'' respectively, thus confirming the arrangement of the hexose residue. However the positioning of the acetyl and cinnamoyl groups could not be positively assigned by HMBC or NOE correlations. HMBC experiments ranging from 0.1 – 20.0 Hz were carried out. In all instances ^3J signals from the oxymethine protons towards the carbonyl carbons of the acetyl and cinnamoyl groups could not be detected. From the assignment of the rhamnose unit, these groups must be attached at C-2'' and C-3'' due to the highly deshielded oxymethine protons (δ_H 5.31, H-2'' and δ_H 5.23, H-3''). Whilst no ^3J correlations between the oxymethine protons H-2'' and H-3'' and the carbonyl carbons could be detected, the NMR data was in close agreement with that of scorodioside (Fernandez *et al.*, 1995). This indicates that **MS-11** is 6-*O*-α-L-(3''-acetyl-2''-*trans*-cinnamoyl)-rhamnopyranosyl catalpol.

The relative stereochemistry of **MS-11** was found to be the same as the previously discussed iridoid glycosides as the NOESY spectrum provided identical signals as those described for **MS-5** - **MS-10**. The stereochemistry of **MS-11** was identical to that of the acylated iridoid glycoside, scorodioside (Fernandez *et al.*, 1995).

Table 11 ^{1}H and ^{13}C NMR data and ^{1}H-^{13}C long-range correlations of **MS-11** recorded in CD_3OD

Position	^{1}H	^{13}C	^{2}J	^{3}J
1	5.09 m	95.2		C-1'
3	6.39 dd (6.0, 1.5)	142.4	C-4	C-1, C-5
4	5.12 m	103.4	C-3	
5	2.49 m	37.2		
6	4.06 dd (8.0, 0.5)	84.4	C-5, C-7	C-4, C-1"
7	3.66 d (7.0)	59.4	C-6	C-5
8	-	66.5		
9	2.58 dd (10.0, 8.0)	43.3	C-1, C-8	C-4, C-7
10	3.83 d (13.0)	61.4	C-8	C-7, C-9
	4.16 d (13.5)			
1'	4.78 d (8.0)	99.7	C-2'	C-1
2'	3.24 m	74.8	C-3'	
3'	3.40 t (9.0)	77.0	C-2'	
4'	3.26 m	71.8	C-3', C-5'	
5'	3.32 m	78.7		
6'	3.62 m	63.0	C-5'	C-4'
	3.93 dd (12.0, 2.0)			
1"	5.02 d (1.5)	97.6	C-2"	C-3", C-5", C-6
2"	5.31 dd (3.5, 1.5)	71.6		
3"	5.23 dd (9.5, 3.0)	73.1		
4"	3.61 m	71.5	C-3"	
5"	3.88 dd (9.5, 6.0)	70.3		
6"	1.33 d (6.5)	18.0	C-5"	C-4"
1'''	-	171.7		
2'''	2.12 s	20.7	C-1'''	
1''''	-	135.7		
2''''	7.60 m	129.1		C-4''''
3''''	7.41 m	130.0		C-1''''
4''''	7.41 m	131.6		
5''''	7.41 m	130.0		C-1''''
6''''	7.60 m	129.1		C-4''''
7''''	7.72 d (16.0)	146.8		C-2'''', C-6'''', C-9''''
8''''	6.53 d (16.0)	118.6		C-1''''
9''''	-	167.8		

3.2.4.8 Biosynthesis of iridoids

Iridoids are a class of natural product within the monoterpene family. Iridoids are biosynthesised from either geraniol or nerol (Dewick 2002). Labelling studies have indicated that 1-deoxy-D-xylulose is the precursor for isopentenyl pyrophosphate biosynthesis and not mevalonate (Contin *et al.*, 1998). Geranyl pyrophosphate is first oxidised to the hydroxyl at C-10 before being further oxidised to the dialdehyde, 10-oxogeranial. Cyclisation of 10-oxogeranial leads to the formation of the important intermediate iridodial. Glucosylation of iridodial *via* a glucosyltransferase is the next step in the proposed biosynthetic pathway of the iridoid glycosides isolated. The methyl group attached at C-4 is then oxidised to the carboxylic acid and then removed by a decarboxylase enzyme. **MS-5** and **MS-6** are proposed to be formed by hydroxylation at C-6 and C-8 followed by acetylation or addition of a cinnamate moiety at C-8 respectively.

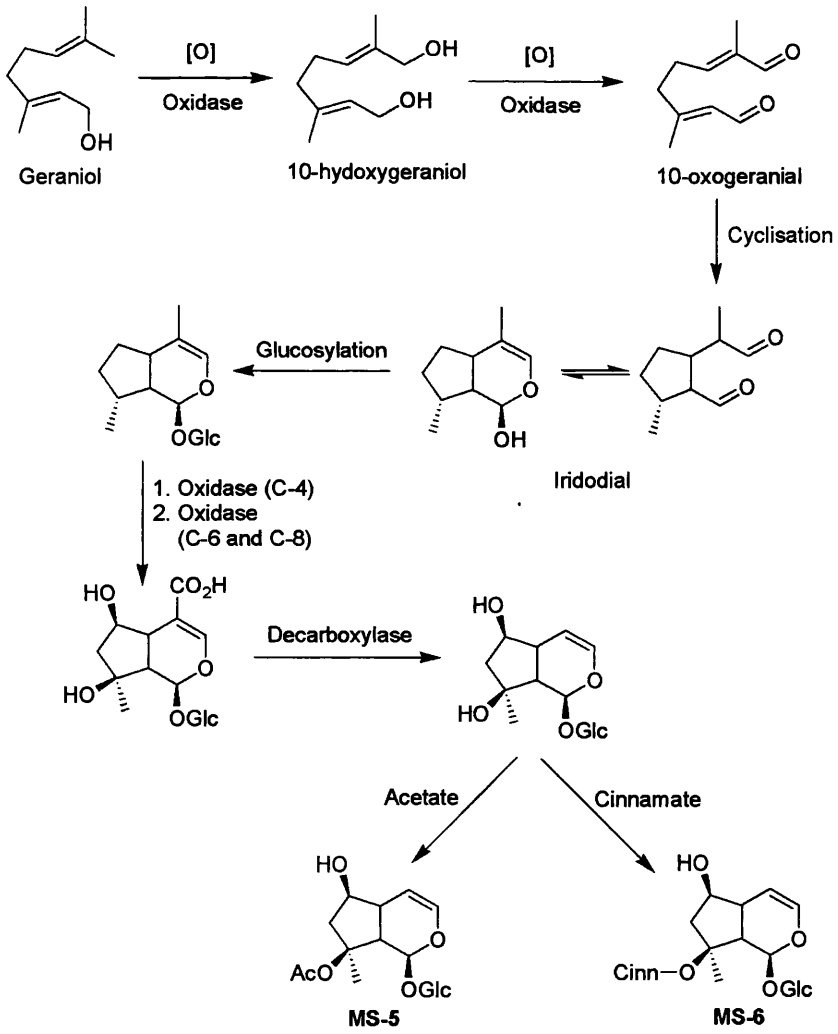

Scheme 1A Biosynthesis of MS-5 and MS-6 from geraniol. Adapted from Contin *et al.*, (1998).

The remaining iridoids, **MS-7 - MS-11**, were isolated as the 7,8 epoxides and with the C-10 methyl group oxidised to the primary alcohol. Another feature of these iridoids was the glycosylation at the C-6 hydroxyl group with a rhamnose moiety. The rhamnose moiety was also subject to substitution with acetate and cinnamate moieties. The biosynthetic pathway is proposed from deoxyloganic acid, thus oxidation of the methyl group at C-10 occurs prior to the decarboxylation step shown in **Scheme 1A**.

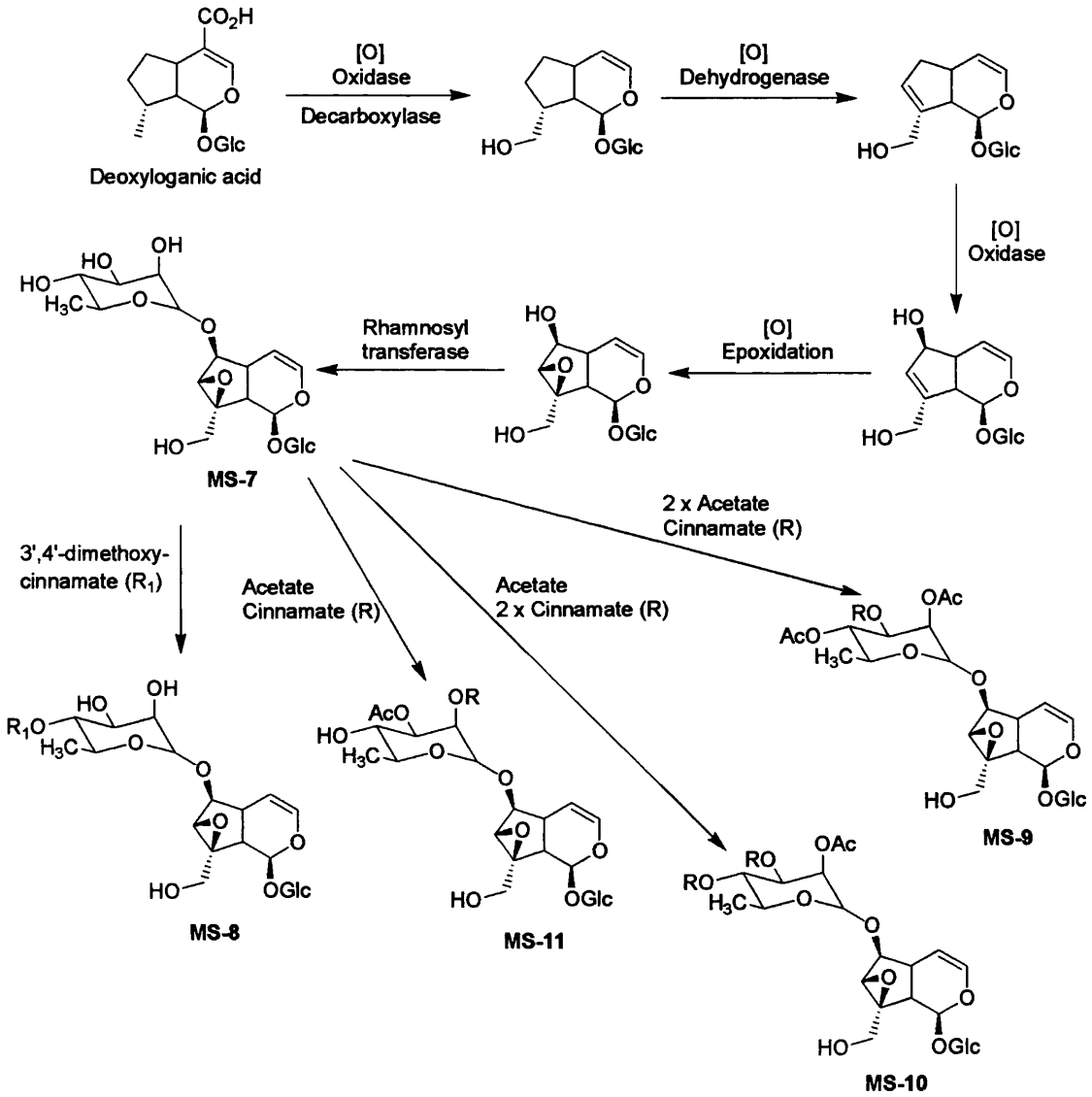

Scheme 1B **Proposed biosynthesis of MS-7 – MS-11 from the iridoid precursor deoxyloganic acid.**

3.3 Sesquiterpenes

3.3.1 Characterisation of MS-12 as 2α,6α-dimethyltetracyclo-decal-3-en-2,12-diol-8α,13-olide (pulicrispiolide)

MS-12 was isolated as a pale yellow oil from the hexane extract of *P. crispa*. Accurate mass measurement yielded an ion at *m/z* 246 $[M-H_2O]^+$ (246.1264) which gave the expected formula less a water molecule of $C_{15}H_{18}O_3$. The ^1H and ^{13}C NMR data provided signals for two olefinic protons, three methylene groups, two oxymethine groups, two methyl groups and a carbonyl carbon.

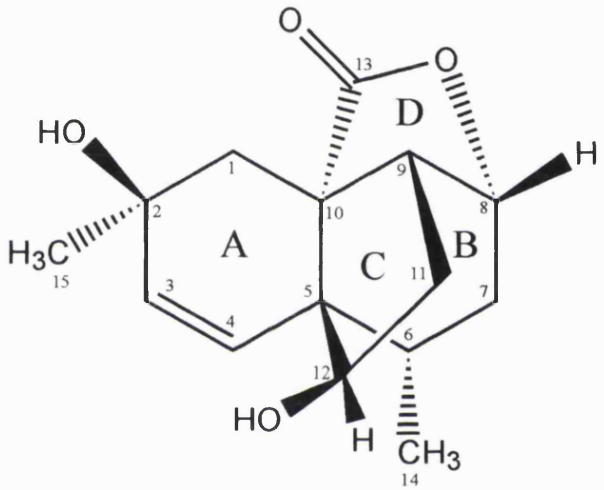

Figure 3.3.1A Structure of **MS-12**

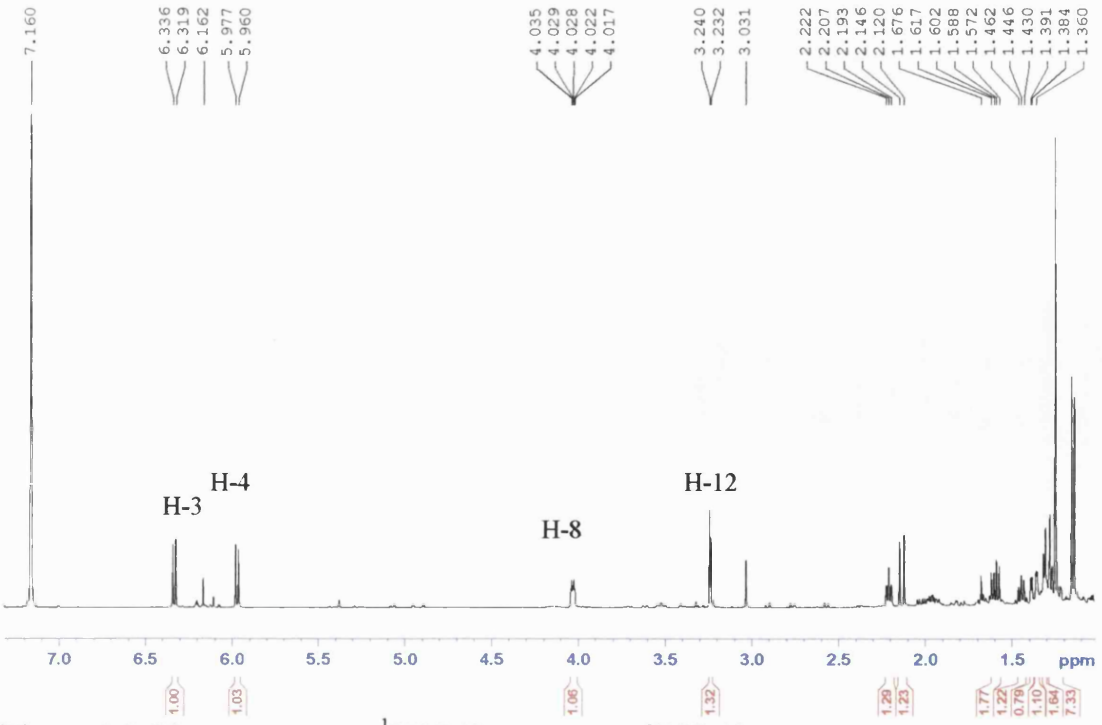

Figure 3.3.1B ^1H NMR spectrum of **MS-12**

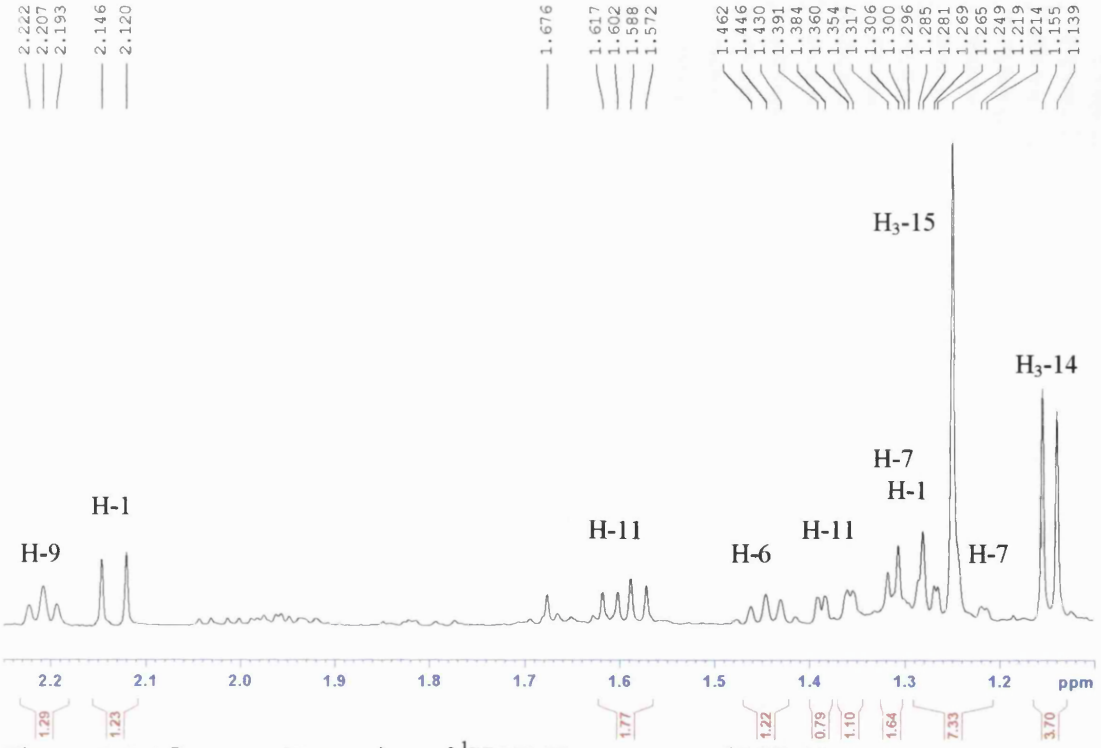

Figure 3.3.1C Expansion of ^{1}H NMR spectrum of **MS-12**

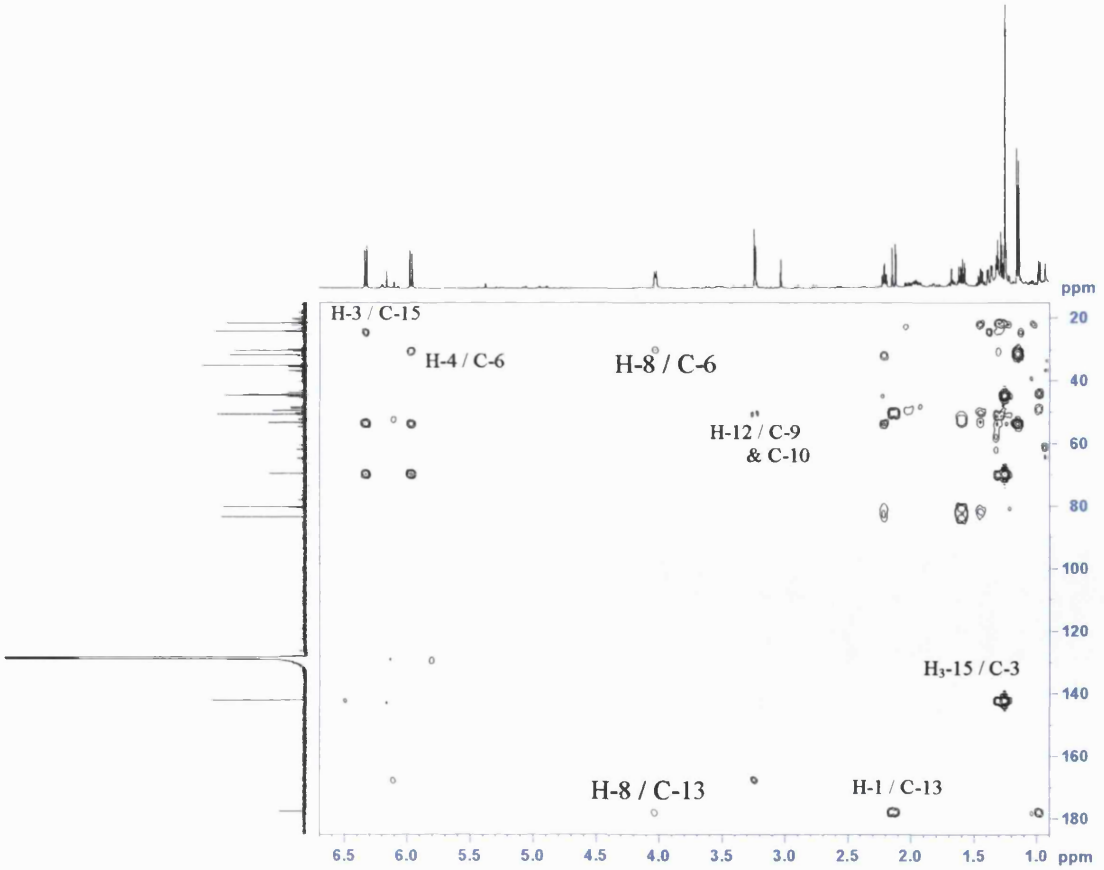

Figure 3.3.1D HMBC spectrum of **MS-12**

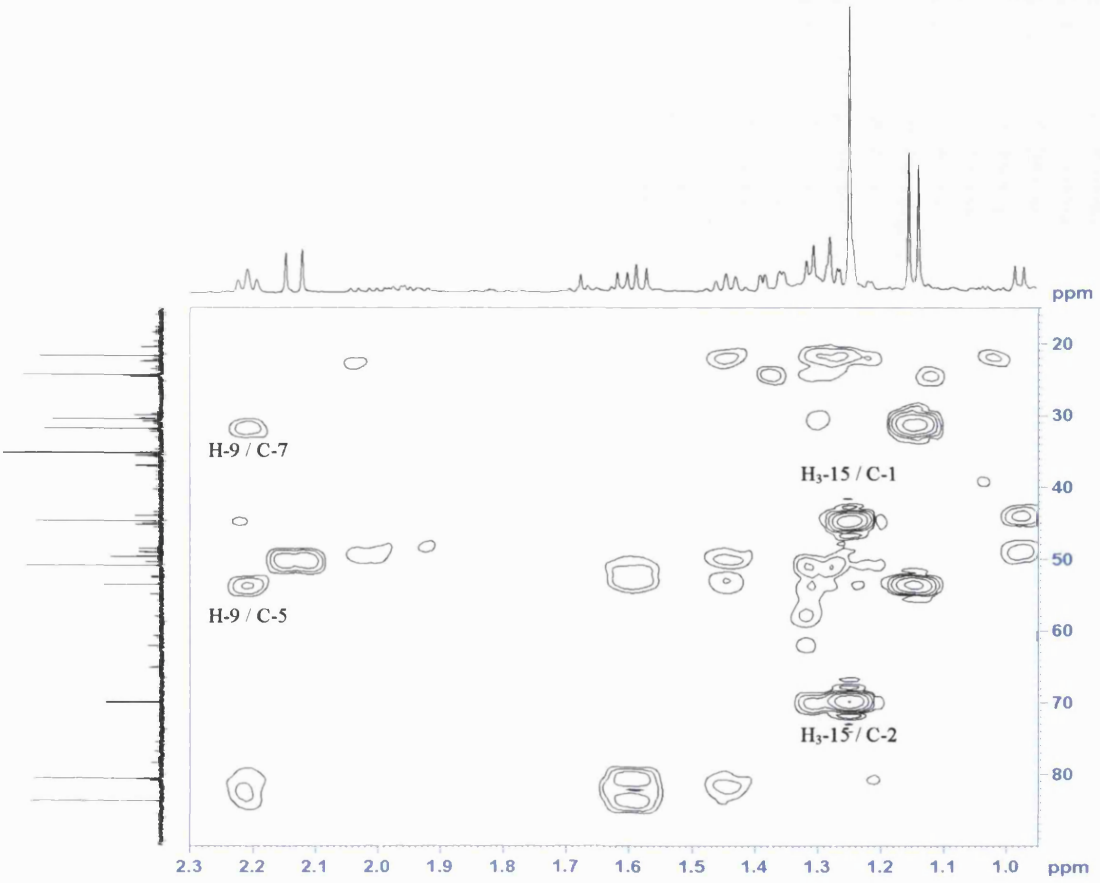

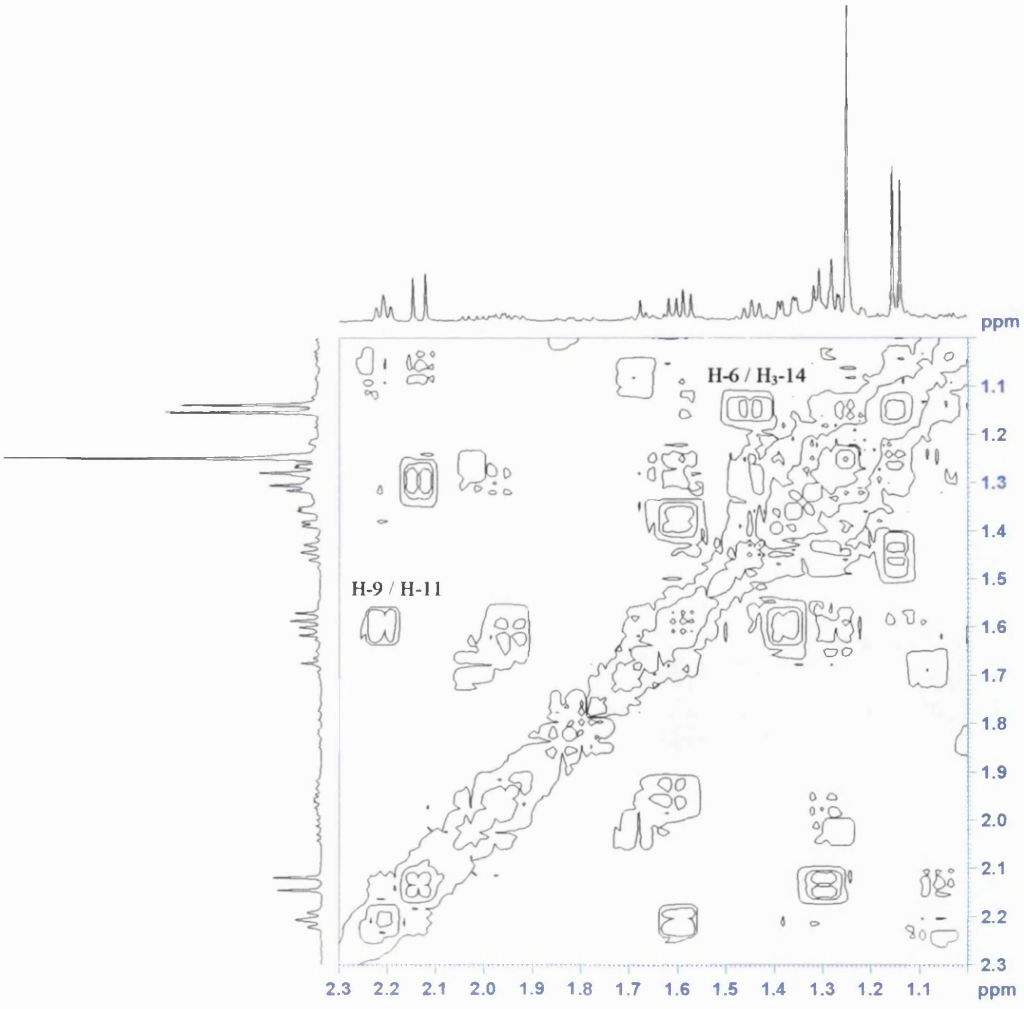

Figure 3.3.1E Expansion of HMBC and COSY spectra of **MS-12**

From the HMBC data methyl-15 (δ_H 1.25) appeared as a singlet and gave a ^2J correlation to a quaternary carbon, C-2 (δ_C 69.8) and ^3J correlations to a methylene group (C-1) and an olefinic group (δ_H 6.34 d, J = 8.5 Hz, δ_C 142.2, C-3). Due to the downfield appearance of C-2 an hydroxyl was placed here. The olefinic proton, H-3, exhibited a COSY correlation to its olefinic partner, H-4 (δ_H 5.98 d, J = 8.5 Hz, δ_C 129.2, C-4) and both showed an HMBC signal to a quaternary carbon placed at C-5 (δ_C 53.5). The ^{13}C resonance for C-5 is characteristic for a quaternary carbon at a ring junction (Zdero *et al.*, 1989). The olefinic proton, H-4, also showed a ^3J correlation to a methine carbon (δ_C 30.4, C-6), which in turn exhibited a ^2J and COSY correlation to a second methyl group (δ_H 1.16 d, J = 7.5 Hz, δ_C 21.7, C-14). Methyl-14 showed a ^3J correlation to C-5 and a methylene group at C-7. COSY correlations between H_2-7 and a deshielded proton H-8 (δ_H 4.03 dt, J = 7.5, 2.5 Hz) and H-8 and H-9 (δ_H 2.21 bt, J = 7.5 Hz) placed these groups here. ^2J and ^3J correlations between H_2-1 and H-6 respectively, to a quaternary carbon C-10 (δ_C 49.6) completed rings A and B of this sesquiterpene. The methine proton H-9 exhibited a COSY correlation towards the methylene protons of H_2-11 which in turn gave a COSY correlation to a deshielded methine proton H-12 (δ_H 3.24 d, J = 4.0 Hz, δ_C 83.7). Again due to the downfield appearance of C-12 an hydroxyl group was placed here. ^3J HMBC signals between H-9 and C-5, H-9 and C-12 and also H_2-11 and C-5 confirmed that C-12 should be connected to C-5 forming a cyclopentane ring (ring C). This was further reinforced by a ^3J signal between H-12 and C-10. Ring D was identified as being a 5-membered lactone ring system. The position of the carbonyl (δ_C 177.7, C-13) was determined by two ^3J correlations between H_2-1 and C-13 and also H-8 and C-13, placing the carbonyl group at this position. This left the oxygen atom of the lactone group to be attached at C-8, which would verify why this group is so highly deshielded. The HMBC data established the presence of a sesquiterpene with a novel skeleton and a molecular formula of $C_{15}H_{20}O_4$ was confirmed by mass spectrometry where an ion at *m/z* 246.1264 $[M\text{-}H_2O]^+$ (calculated for $C_{15}H_{18}O_3$: 246.1256) was detected.

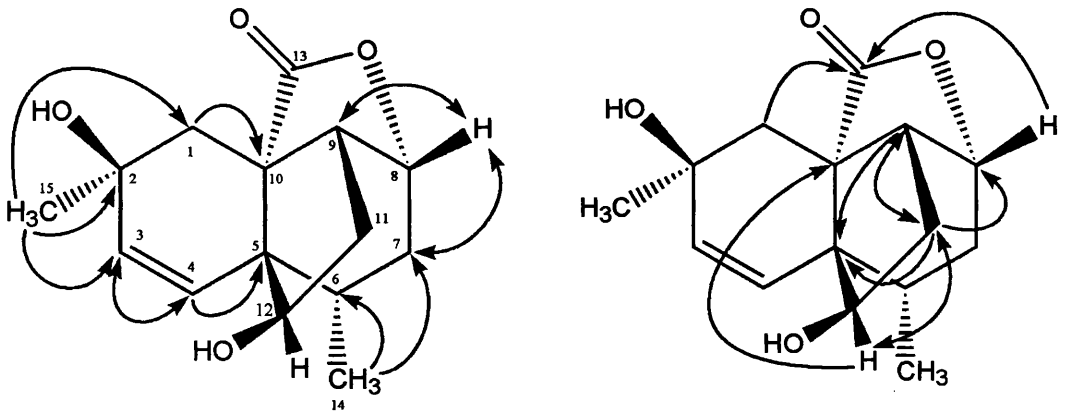

Figure 3.3.1F HMBC and COSY correlations for **MS-12**

The relative stereochemistry of **MS-12** was established by correlations obtained in the NOESY spectrum. The cyclopentane ring (ring C) was positioned β with respect to the plane of rings A and B, whilst the 5-membered lactone ring was α-orientated. H-6 showed a 1,3 interaction with H-12 meaning H-6 must be β-oriented. Therefore H-12 must be orientated towards ring B, with the hydroxyl group attached to this carbon being orientated towards ring A. This was supported by a strong NOE between H-4 and H_3-14, placing this methyl group in an α-orientation. An NOE between H-3 and H_3-15 placed this methyl group in an α-orientation. Finally, NOE's between H_2-1β and H-9 and between H-9 and H-8 placed these protons in a β-orientation, thus completing the relative stereochemistry of this novel sesquiterpene skeleton. Attempts to crystalise **MS-12** to determine the absolute stereochemistry by X-ray crystallography were unsuccessful. **MS-12** is therefore assigned as 2α,6α-dimethyltetracyclo-decal-3-en-2,12-diol-8α,13-olide (pulicrispiolide) and this is the first report of this novel sesquiterpene skeleton.

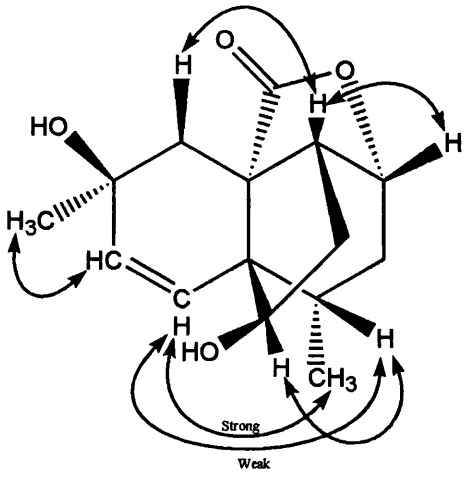

Figure 3.3.1G NOE correlations of **MS-12**

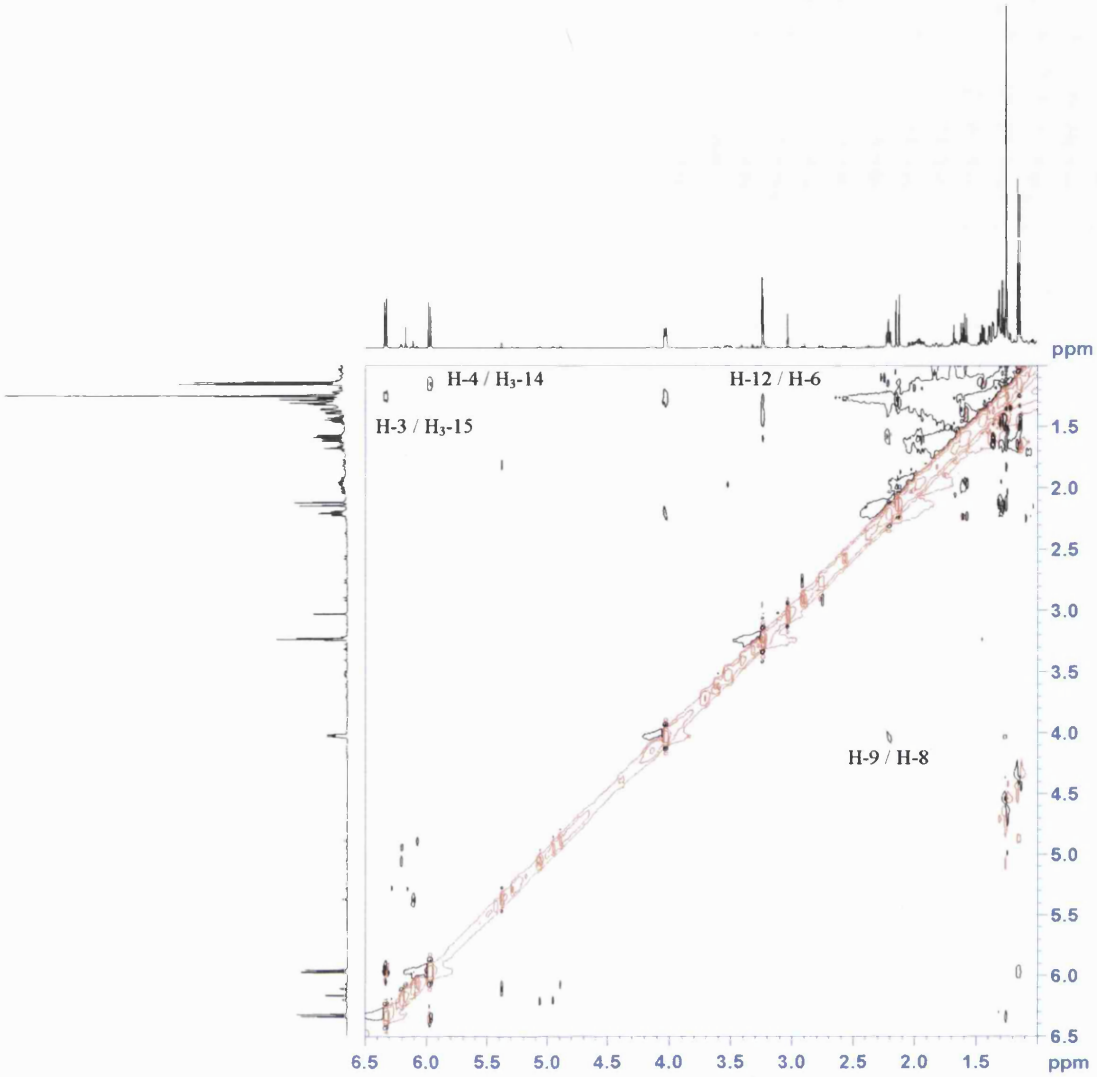

Figure 3.3.1H NOESY spectrum of **MS-12**

Table 12 ^{1}H and ^{13}C NMR data and ^{1}H-^{13}C long-range correlations of **MS-12** recorded in C_6D_6

Position	^{1}H	^{13}C	^{2}J	^{3}J
1	1.31 d (13.0)	44.7	C-2, C-10	C-3, C-5, C-9, C-13, C-15
	2.15 d (13.5)			
2	-	69.8		
3	6.34 d (8.5)	142.2	C-2	C-5, C-15
4	5.98 d (8.5)	129.2	C-5	C-2, C-6
5	-	53.5		
6	1.45 t (8.0)	30.4	C-5, C-7, C-14	C-8, C-10, C-12
7	1.26 m	31.8	C-6, C-8	C-5, C-9, C-14
	1.36 bd (2.5)			
8	4.03 dt (7.0, 2.5)	80.5		C-6, C-13
9	2.21 bt (7.5)	50.9	C-8	C-1, C-5, C-7, C-12
10	-	49.6		
11	1.39 d (4.0)	35.2	C-9, C-12	C-5, C-8
	1.60 dd (15.0, 8.5)			
12	3.24 d (4.0)	83.7		C-9, C-10
13	-	177.7		
14	1.16 d (7.5)	21.7	C-6	C-5, C-7
15	1.25 s	24.3	C-2	C-1, C-3

3.3.2 Proposed biosynthesis of MS-12

The biosynthesis of **MS-12** is proposed to occur from the enzyme-catalysed addition of one mole of dimethylallyl pyrophosphate to one mole of geranyl pyrophosphate leading to the formation of the cyclic intermediate **1**. Double bond migration results in the formation of **2**, which then undergoes cyclisation to form the decal-4-ene carbocation (**3**). Migration of the carbocation followed by electrophilic addition is proposed to yield the tricyclic intermediate **4**. A Wagner-Meerwein shift of the methyl group from C-9 to C-10 followed by two hydride shifts is proposed to form the intermediate **7**.

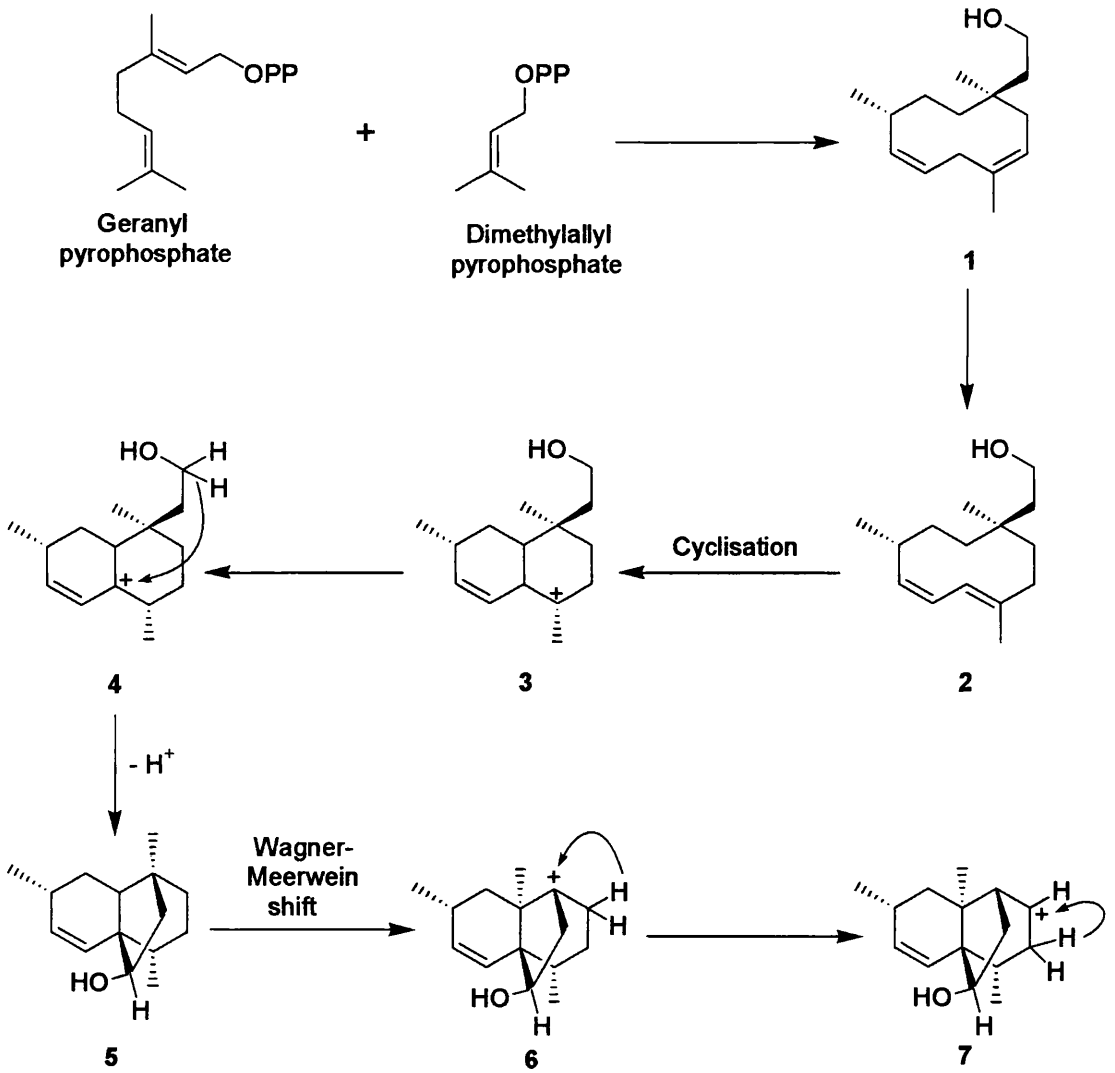

Scheme 2A Formation of intermediate 7 in the proposed biosynthetic pathway of 2α,6α-dimethyltetracyclo-decal-3-en-2,12-diol-8α,13-olide (**MS-12**).

Stabilisation of the carbocation by the loss of a proton leads to the formation of a double bond between C-7 and C-8 (**8**), which can then undergo addition of water across the double bond to form **9**. Oxidation of the methyl group attached at C-10 leads to the carboxylic acid (**10**), which can then undergo lactonisation with the hydroxyl group attached at C-8 resulting in a loss of water to form the tetracyclic intermediate **11**. Finally, oxidation at position 2 of the molecule to yield the hydroxyl is proposed to yield 2α,6α-dimethyltetracyclo-decal-3-en-2,12-diol-8α,13-olide (**MS-12**).

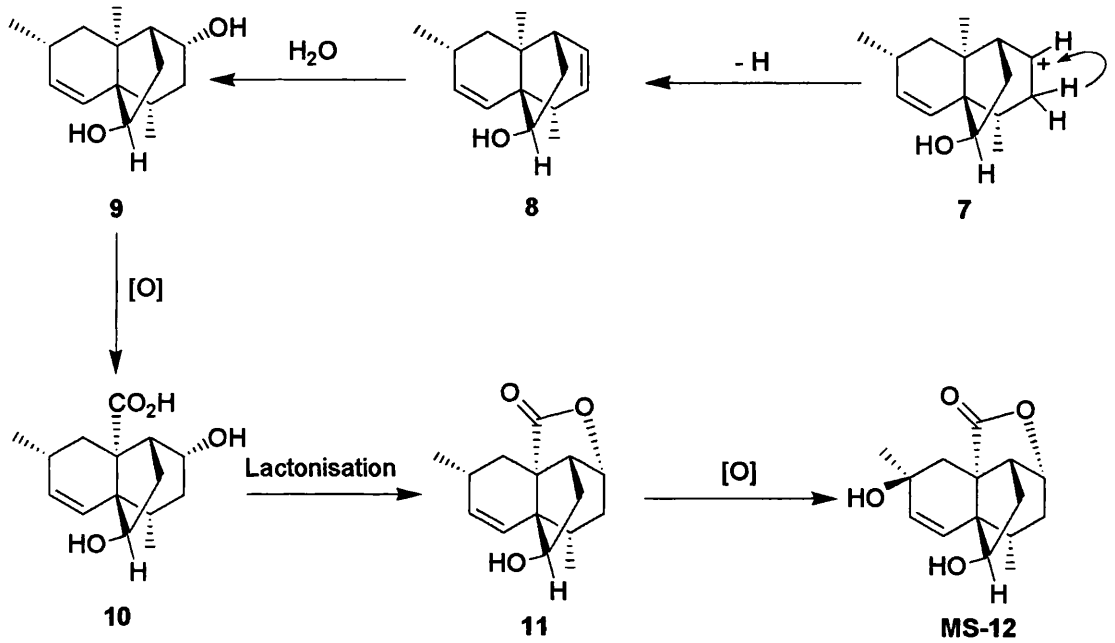

Scheme 2B Proposed biosynthetic pathway of 2α,6α-dimethyltetracyclo-decal-3-en-2,12-diol-8α,13-olide (**MS-12**) from intermediate **7**.

3.3.3 Characterisation of MS-13 as spathulenol

MS-13 was isolated as a colourless oil from the hexane extract of *A. monosperma*. The molecular formula was established from the ^{1}H and ^{13}C NMR data acquired. The ^{1}H spectrum provided signals indicative of a sesquiterpene. This included signals for an *exo*-methylene (δ_H 4.68 dd, J = 14.5, 1.0 Hz), three methyl singlets and four methylene groups. The presence of two highly shielded methine protons (δ_H 0.46 and δ_H 0.71) indicated they were part of a cyclopropane ring system (Iwabuchi *et al.*, 1989). The ^{13}C NMR spectrum yielded 15 signals of which three were quaternary carbons. This included olefinic (δ_C 153.4) and oxygen (δ_C 81.0) bearing quaternary carbons. Three methyl and four methine carbons were also detected along with five methylene carbons which included an *exo*-methylene.

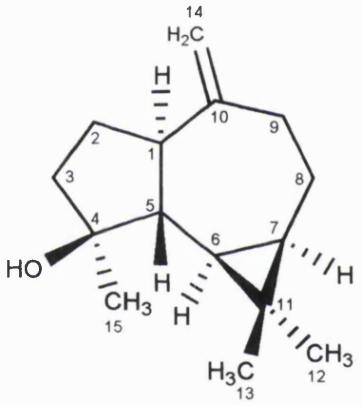

Figure 3.3.3A Structure of **MS-13**

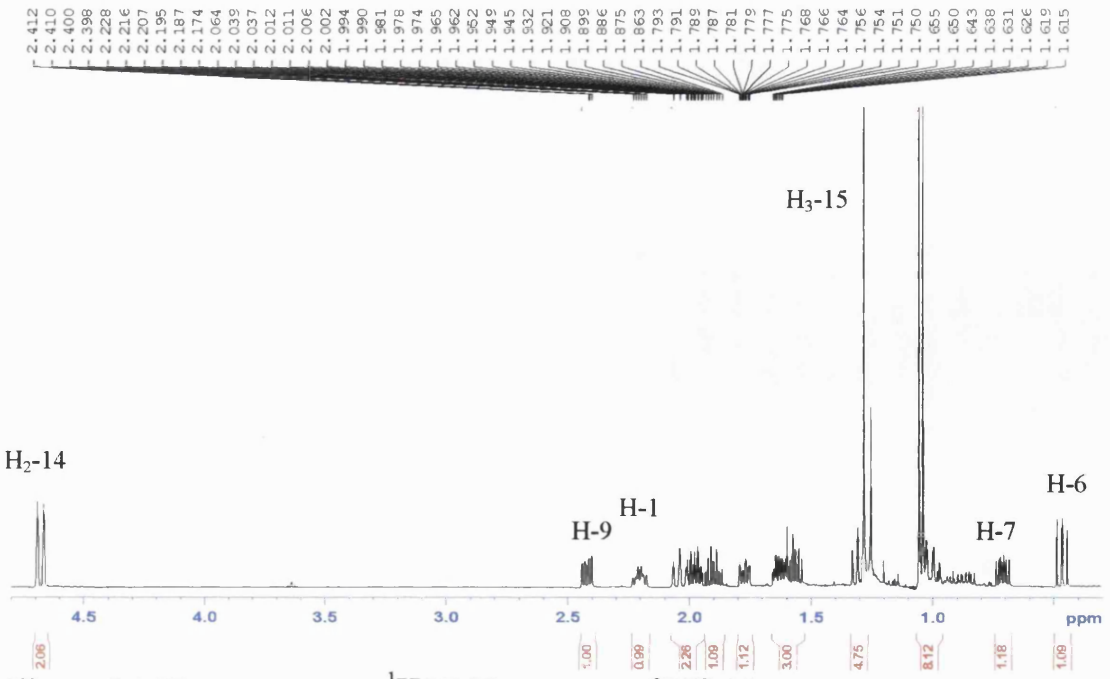

Figure 3.3.3B ^{1}H NMR spectrum of **MS-13**

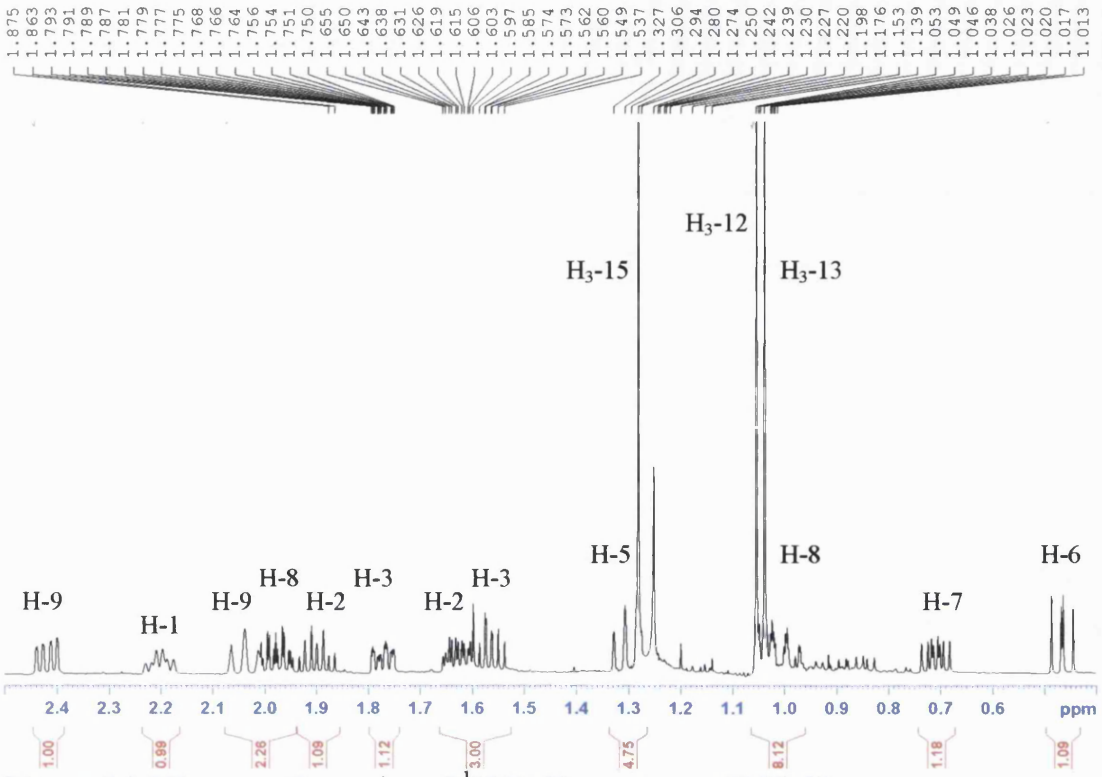

Figure 3.3.3C Expansion of ^{1}H NMR spectrum of **MS-13**

The olefinic protons of the *exo*-methylene gave a ^{2}J signal to an olefinic quaternary carbon and ^{3}J signals to a methine (δ_H 2.20, δ_C 53.4, C-1) and methylene (δ_H 2.04 and 2.42, δ_C 38.9, C-9) carbons. In the COSY spectrum, the methylene coupled to a second methylene group (δ_H 1.00 and 1.98, δ_C 24.8, C-8), which in turn coupled to a highly shielded methine proton (δ_H 0.71, δ_C 27.5, C-7). This methine proton showed a further coupling towards a second shielded methine proton (δ_H 0.46, δ_C 29.9, C-6), which indicated they were part of a cyclopropane ring. This was confirmed by a ^{2}J correlation from H-6 to a shielded quaternary carbon (δ_C 20.3, C-11). Two methyl groups (δ_H 1.05, H-12, δ_H 1.04, H-13) appearing as singlets in the ^{1}H NMR spectrum were directly attached to this carbon based on ^{2}J signals detected in the HMBC. The cyclopropane ring was completed with ^{3}J signals from the protons of H_3-13 towards C-6 and C-7. The COSY spectrum showed H-6 coupled to another methine, H-5, which in turn coupled to H-1, thus completing the 7-membered ring. An HMBC signal from H-6 to a downfield quaternary carbon placed it at C-4. An hydroxyl was placed at this carbon due to its downfield appearance in the ^{13}C NMR spectrum. A methyl group (δ_H 1.28 s, H_3-15) was also placed on this carbon based on a ^{2}J correlation in the HMBC. H_3-15 also exhibited ^{3}J correlations to the methine group at C-5, confirming its position here, as well as to a methylene group (δ_H 1.56

and 1.78, H_2-3). COSY signals from H-1 to H_2-2 and H_2-3 to H_2-2 completed the cyclopentane ring and the structure of the sesquiterpene.

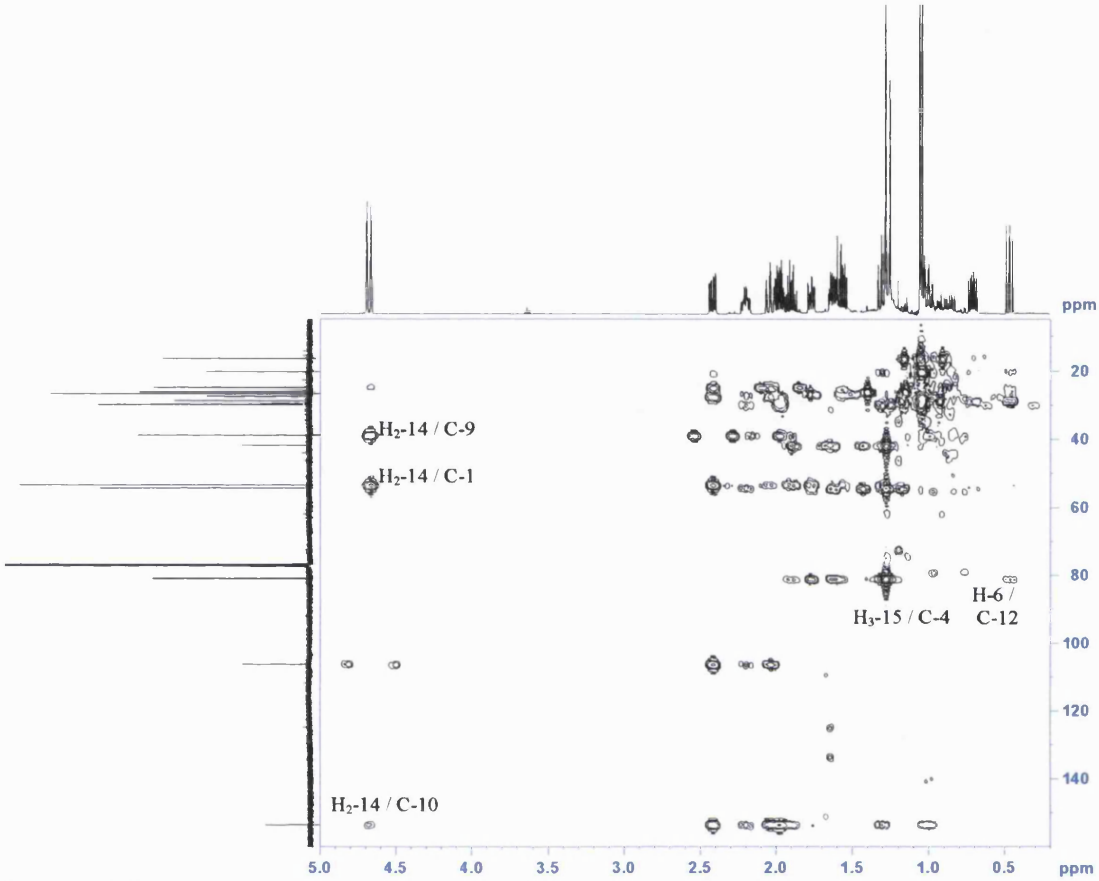

Figure 3.3.3D HMBC spectrum of **MS-13**

The NOESY spectrum enabled **MS-13** to be assigned as spathulenol. An NOE between H-6 and H-7 placed both of these protons on the same face of the molecule (α) and the large coupling constant measured (J = 9.0 Hz) confirmed that they are *cis*. H-6 also showed 1,3 interactions with H_3-12 and H_3-15 placing these methyl groups in an α-orientation as well. Therefore the hydroxyl group at C-4 must be β-oriented. The methine proton, H-1, gave NOE's to H_3-15 and H-6, placing them on the same face of the molecule (α). An NOE between H_3-13 and H-5 placed these protons in a β-orientation and completed the relative stereochemistry of this compound. The full NMR data was in close agreement with the literature for spathulenol, which has previously been isolated from the peel oil of *Citrus junos* (Inagaki and Abe 1985), *Salvia sclarea* (Maurer and Hauser 1983) and *Panax ginseng* (Iwabuchi *et al.*, 1989).

Only partial ^{1}H NMR data were reported by the last two groups along with the full ^{13}C NMR data. However this was in close agreement with the data recorded in this thesis.

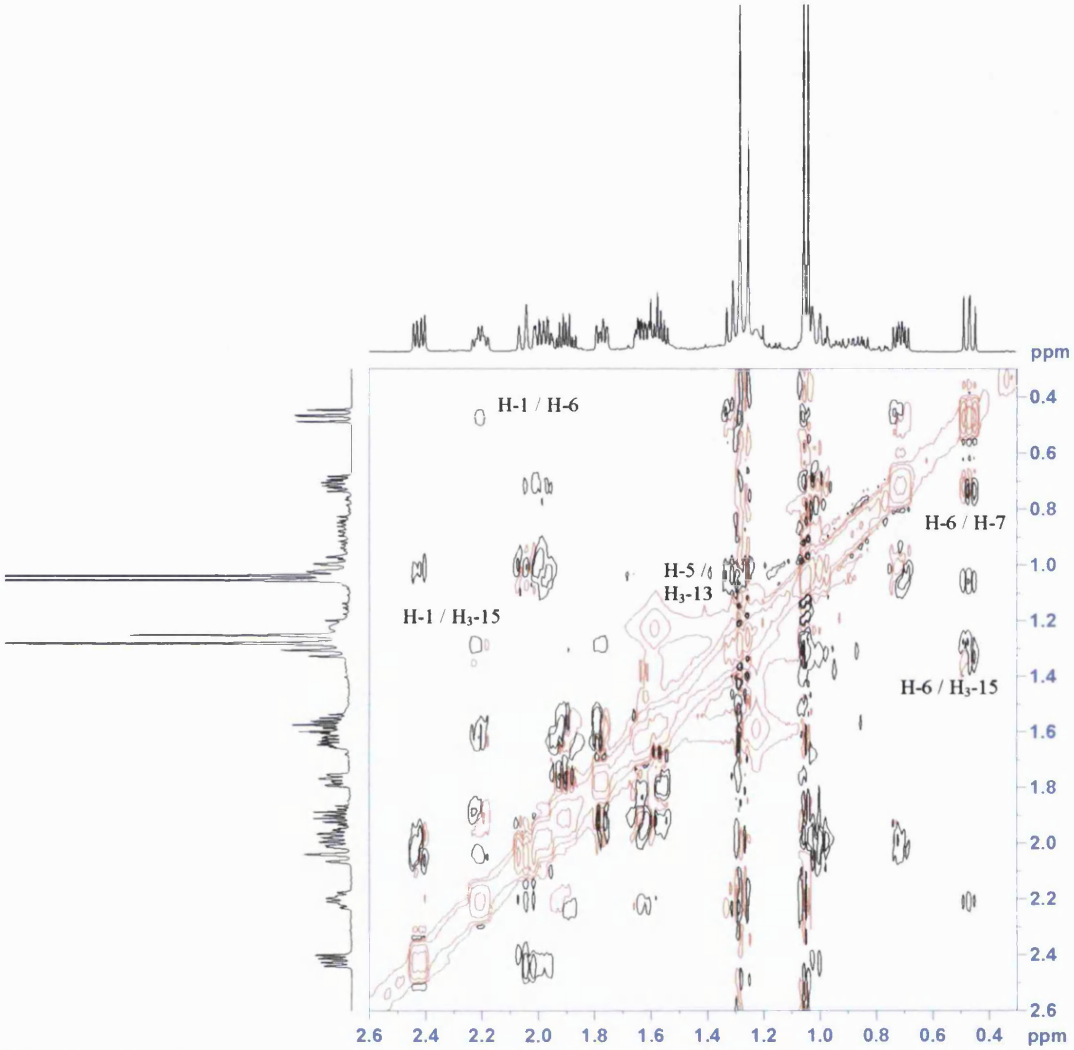

Figure 3.3.3E NOESY spectrum of **MS-13**

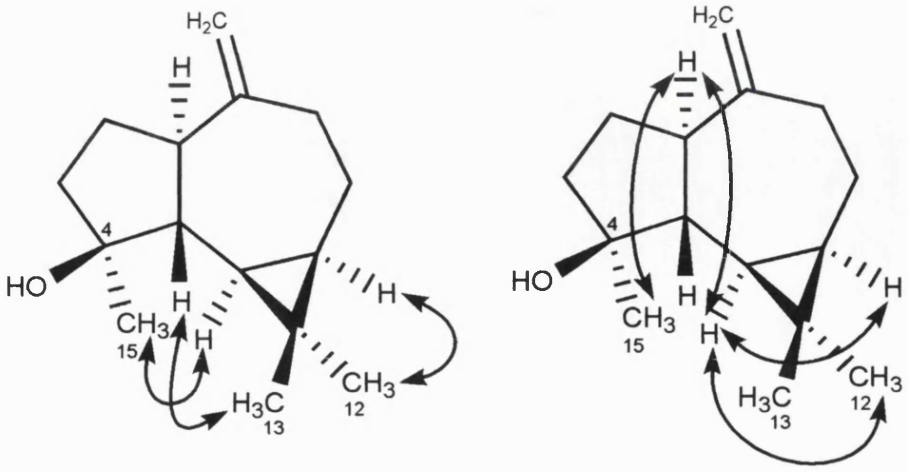

Figure 3.3.3F NOE correlations of **MS-13**

Table 13 ^{1}H and ^{13}C NMR data and ^{1}H-^{13}C long-range correlations of **MS-13** recorded in $CDCl_3$

Position	^{1}H	^{13}C	^{2}J	^{3}J
1	2.20 dt (10.5, 6.0)	53.4	C-2, C-5, C-10	C-6, C-9, C-14
2	1.63 m	26.7	C-1, C-3	C-4, C-5, C-10
	1.91 dq (11.5, 6.0)			
3	1.56 m	41.7	C-2, C-4	C-1, C-5
	1.78 m			
4	-	81.0		
5	1.30 m	54.3	C-1, C-6	C-10
6	0.46 dd (11.5, 9.5)	29.9	C-11	C-4, C-12
7	0.71 ddd (11.0, 9.0, 6.0)	27.5		C-12
8	1.00 m	24.8	C-7, C-9	C-6, C-10
	1.98 m			
9	2.04 t (13.0)	38.9	C-8, C-10	C-1, C-7, C-14
	2.42 ddd (13.5, 6.0, 0.5)			
10	-	153.4		
11	-	20.3		
12	1.05 s	28.7	C-11	C-13
13	1.04 s	16.3	C-11	C-6, C-7, C-12
14	4.68 dd (14.5, 1.0)	106.3	C-10	C-1, C-9
15	1.28 s	26.1	C-4	C-3, C-5

3.3.4 Characterisation of MS-14 as *rel*-1β,3α,6β-trihydroxyeudesm-4-ene

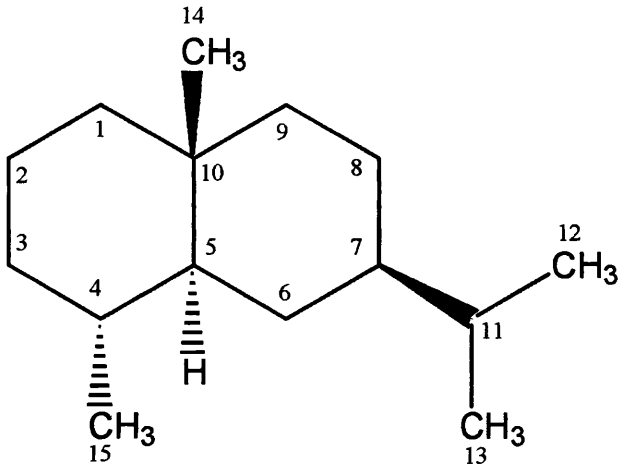

Figure 3.3.4A Eudesmane skeleton

MS-14 was isolated as a colourless oil from the hexane extract of *A. monosperma*. HREIMS gave a molecular ion which solved for $C_{15}H_{26}O_3$ $[M]^+$ (254.1864). The ^1H and ^{13}C NMR spectra gave signals indicative of a eudesmane sesquiterpene (Garcia-Granados *et al.*, 1985; Zhao *et al.*, 1997). From the spectra, it could be deciphered that the sesquiterpene was composed of 4 methyl groups, 3 oxymethine groups, 3 quaternary carbons, two of which were olefinic, 3 methylene and two methine groups.

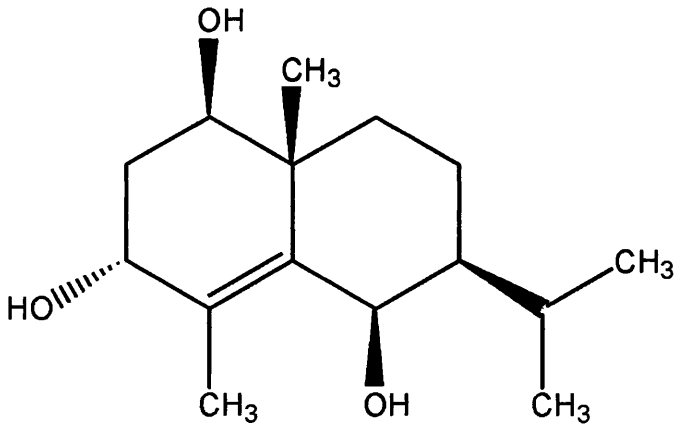

Figure 3.3.4B Structure of **MS-14**

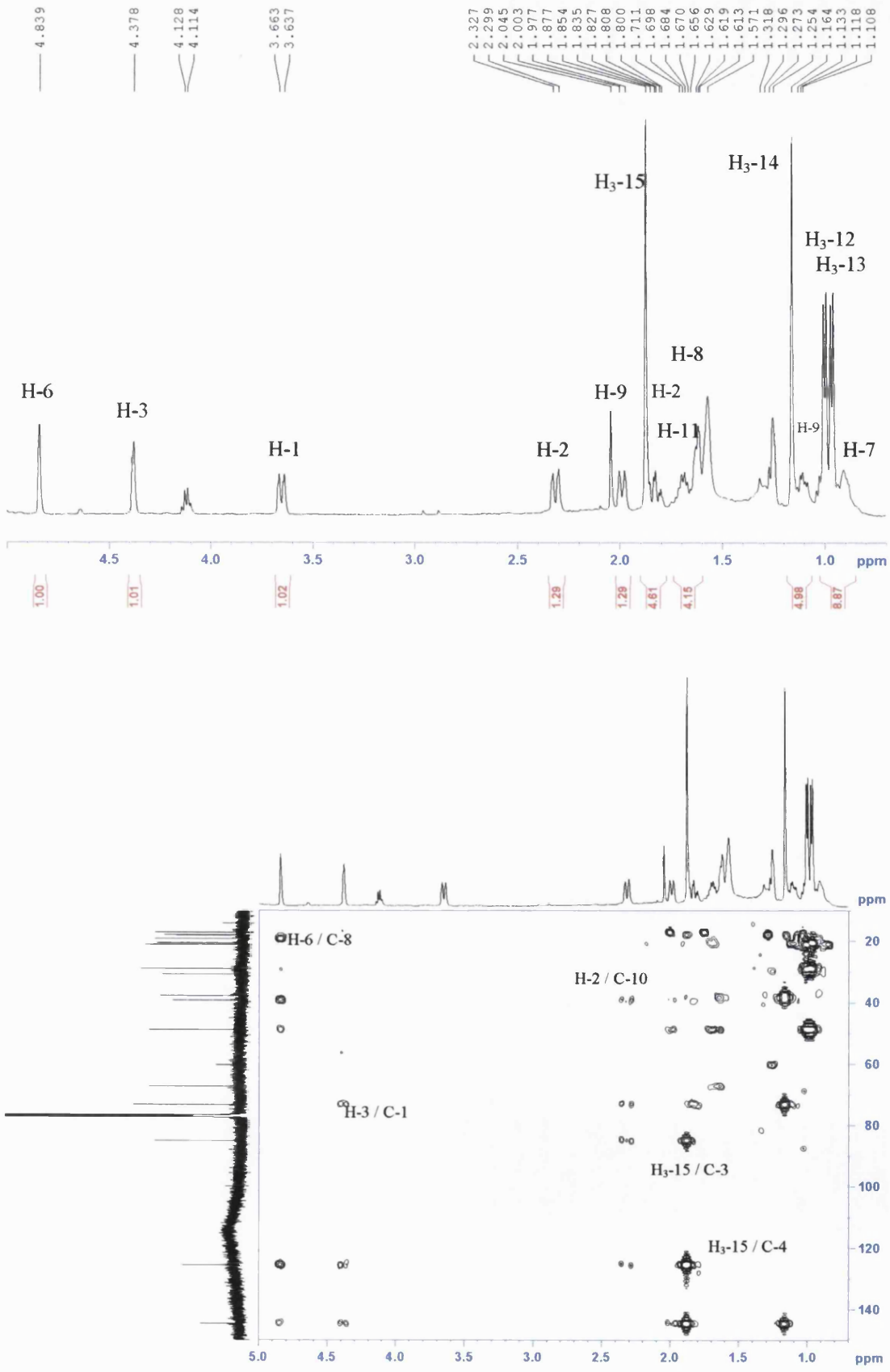

Figure 3.3.4C ^{1}H and HMBC spectra of **MS-14**

From the HMBC data a deshielded methyl singlet (δ_H 1.88, H_3-15) showed a ^2J correlation to an olefinic quaternary carbon (δ_C 125.5, C-4) and ^3J correlations to a second olefinic quaternary carbon (δ_C 144.7, C-5) and an oxymethine carbon (δ_C 85.1, C-3). The oxymethine proton (δ_H 4.38) appeared as a broad singlet and coupled to two protons of a methylene group (δ_H 1.83 m, 2.31 bd, J = 14.0 Hz, H_2-2). These protons in turn coupled to a deshielded methine proton, which appeared as a broad doublet (δ_H 3.65, J = 12.9 Hz, H-1). The methylene protons also gave a ^3J correlation to a quaternary carbon (δ_C 39.2, C-10), placing this carbon at the ring junction of the 4-eudesmene skeleton. A second methyl singlet (δ_H 1.16, H_3-14) showed a ^2J correlation to this quaternary carbon as well as ^3J correlations to the oxymethine carbon, C-1 and the olefinic quaternary carbon C-5, thus completing ring A. A third signal to a methylene carbon (δ_H 1.11 m, 1.99 d, J = 12.6 Hz, δ_C 37.7, C-9) placed this group here. In the COSY spectrum, the two methylene protons coupled to a further two protons of a methylene (δ_H 1.62 m, H_2-8), which in turn coupled to a shielded methine proton (δ_H 0.91 m, H-7). Ring B of the 4-eudesmene skeleton was completed by placing an oxymethine group at position 6 (δ_H 4.84 s, δ_C 67.4). The oxymethine proton exhibited a COSY correlation to H-7 as well as ^2J correlations in the HMBC spectrum to C-5 and C-7 and ^3J signals to C-4, C-8 and C-10, confirming the placement of this group at this position. An isopropyl group was placed at C-7 due to a COSY coupling between H-7 and a methine proton (δ_H 1.70, H-11). Two methyl doublets exhibited ^2J and ^3J correlations to C-11 and C-7 respectively. This confirmed the presence of an isopropyl group, which is a common feature of eudesmane sesquiterpenes found in the Asteraceae.

The deshielded nature of the methine groups C-1, C-3 and C-6 and the accurate mass determination, indicating a molecular formula of $C_{15}H_{26}O_3$, suggested that hydroxyl groups must be placed here.

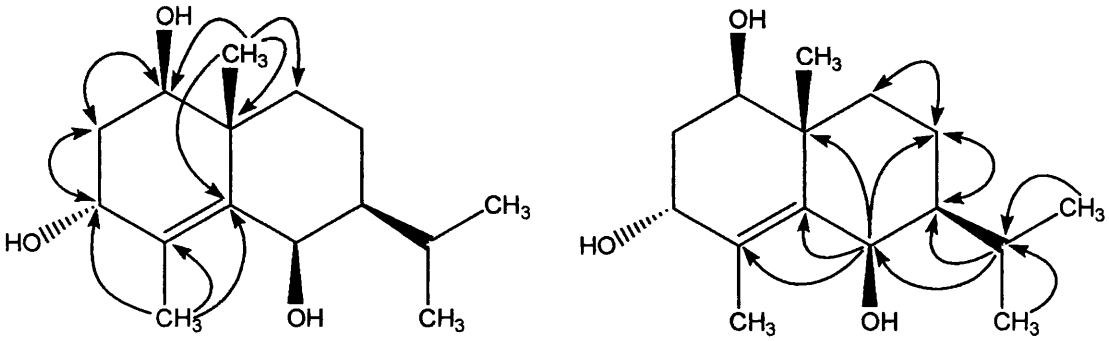

Figure 3.3.4D HMBC and COSY correlations for **MS-14**

The large coupling constant measured for H-1 (12.9 Hz) means that this proton must be axial. Whereas H-3 and H-6 appeared as broad and sharp singlets respectively, therefore the lack of a measurable coupling placed these protons in an equatorial configuration.

A NOE between H-1 and H_{α}-9, placed these protons in an axial configuration (α-orientation). A second NOE between H_{β}-2 and H_3-14 placed these groups in an axial configuration on the opposite face of the molecule (β). A 1,3 interaction between H-3 and H_3-15 confirmed that this proton should be in an equatorial (β) position therefore the hydroxyl must be α-oriented. A lack of material meant that the absolute stereochemistry could not be determined. This novel compound is therefore assigned as *rel*-1β,3α,6β-trihydroxyeudesm-4-ene and has recently been published (Stavri *et al.*, 2004a).

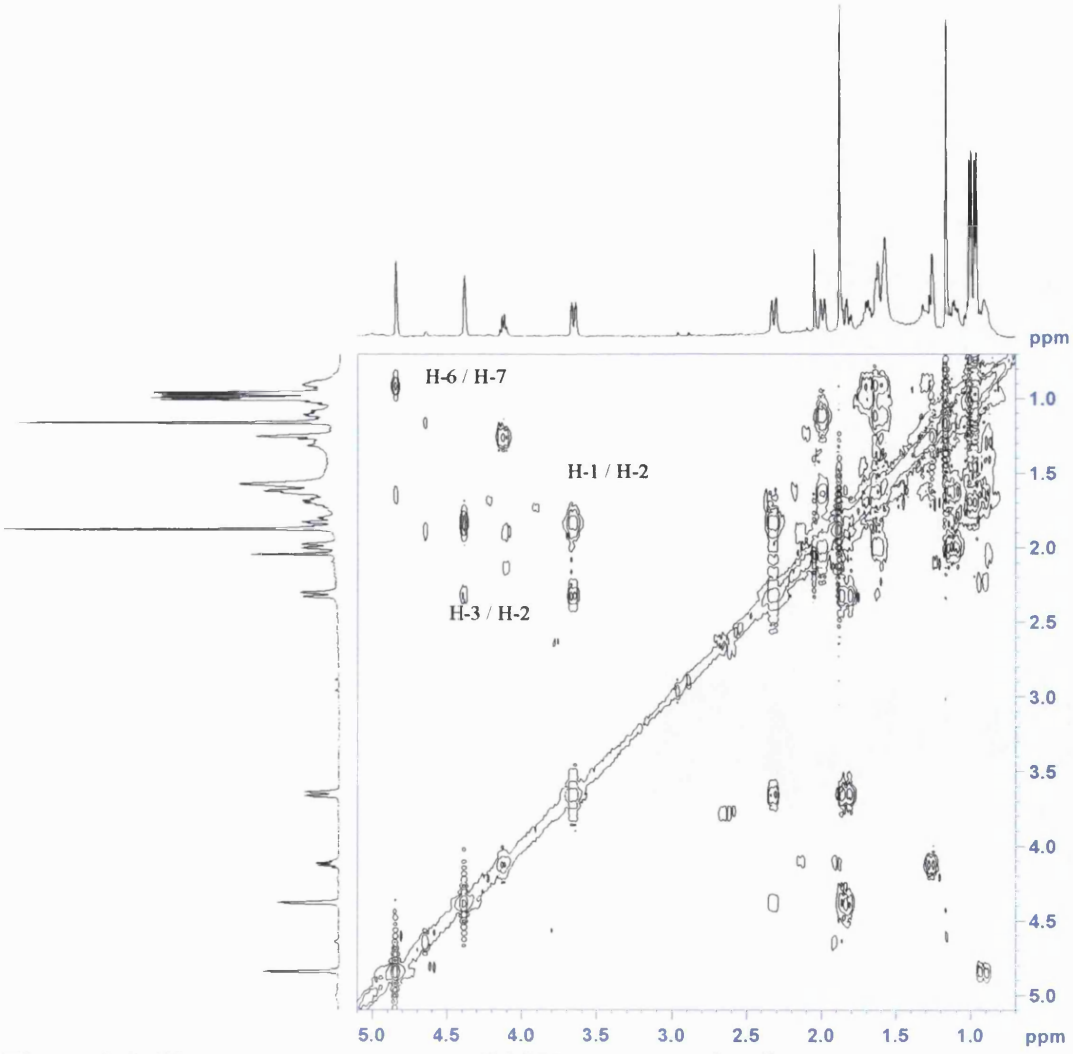

Figure 3.3.4E COSY spectrum of **MS-14**

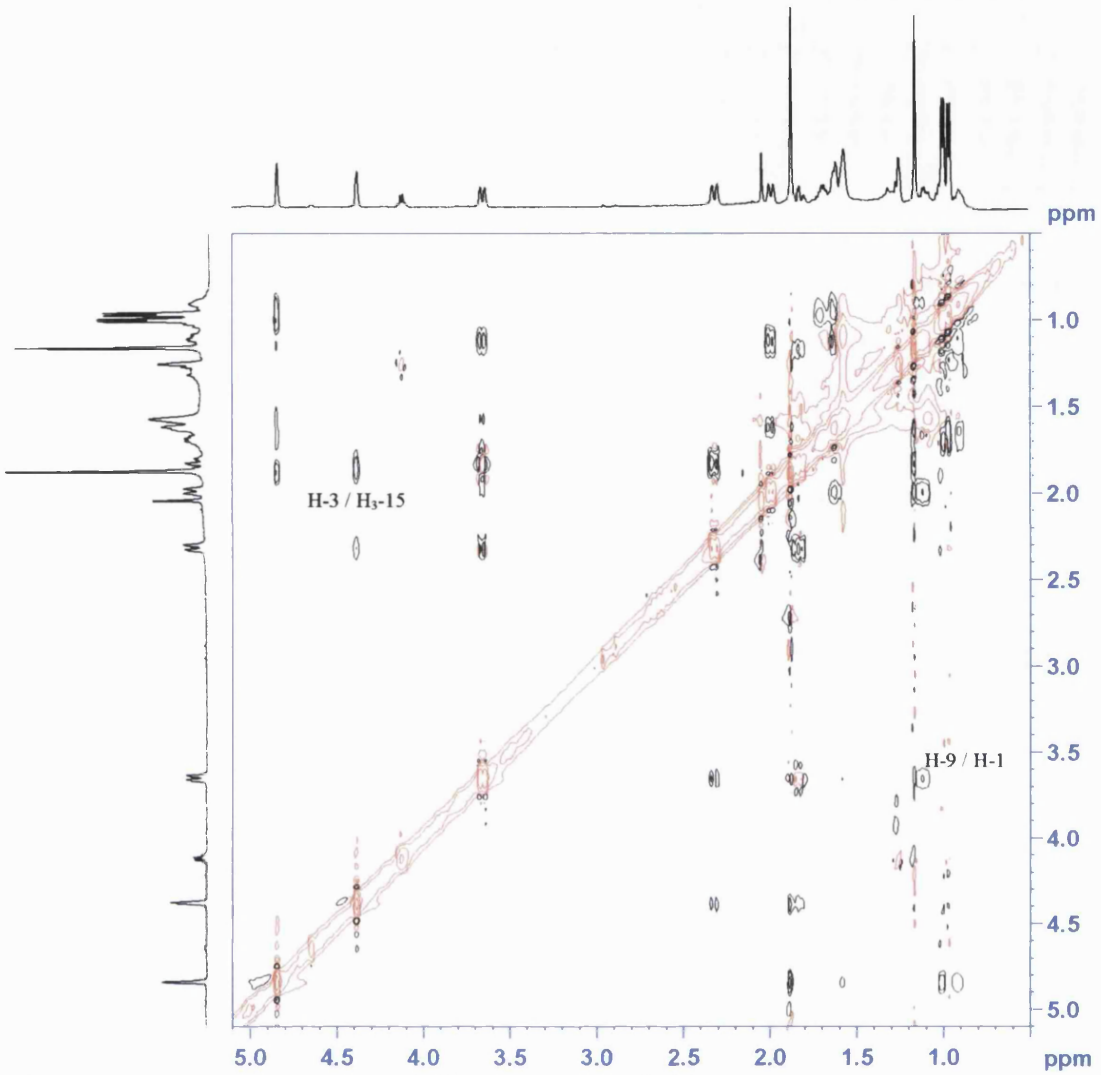

Figure 3.3.4F NOESY spectrum of **MS-14**

Table 14 ^{1}H and ^{13}C NMR data and ^{1}H-^{13}C long-range correlations of **MS-14** recorded in $CDCl_3$

Position	^{1}H	^{13}C	^{2}J	^{3}J
1	3.65 bd (12.9)	73.3		
2	1.83 m	30.8	C-1, C3	C-4, C-10
	2.31 bd (14.0)			
3	4.38 bs	85.1	C-4	C-1, C-5
4	-	125.5		
5	-	144.7		
6	4.84 s	67.4	C-5, C-7	C-4, C-8, C-10, C-11
7	0.91 m	48.9	C-8	
8	1.62 m	19.2	C-7, C-9	C-6, C-10
9	1.11 m	37.7		C-7, C-14
	1.99 bd (12.6)			
10	-	39.2		
11	1.70 m	28.9	C-7	C-6
12	1.00 d (6.3)	20.7	C-11	C-7, C-13
13	0.97 d (6.3)	21.2	C-11	C-7, C12
14	1.16 s	18.0	C-10	C-1, C-5, C-9
15	1.88 s	17.2	C-4	C-3, C-5

3.3.5 Characterisation of guaianolides from *Pulicaria crispa*

3.3.5.1 Characterisation of MS-15 as 1,2-dehydro-1,10α-dihydropseudoivalin

MS-15 was isolated as a colourless oil and solved for a molecular formula of $C_{15}H_{20}O_3$ by ESI-MS. The ^1H and ^{13}C NMR spectra provided evidence to indicate **MS-15** was a guaianolide sesquiterpene. The ^1H NMR spectrum showed characteristic signals for an *exo*-methylene (δ_H 5.73, 6.20, H_2-13), an olefin (δ_H 5.37 t, H-2) and two methyl groups (δ_H 1.22, H_3-14 and δ_H 1.25, H_3-15). Fifteen signals were detected in the ^{13}C spectrum, which included a carbonyl carbon (δ_C 172.1, C-12) and four olefinic carbons. The ^1H and ^{13}C NMR data were similar to those of previously isolated guaianolide sesquiterpenes. This natural product class is common among species belonging to the genus *Pulicaria* (syn. *Francoeuria*) (Abdel-Mogib *et al.*, 1990; Zdero *et al.*, 1988).

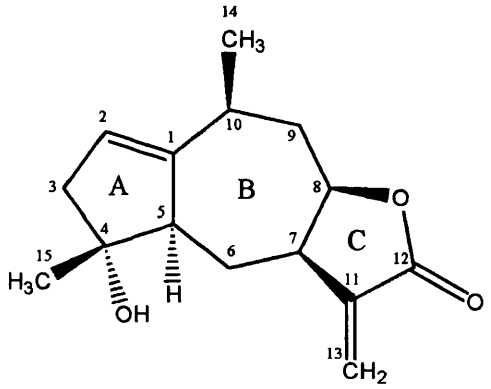

Figure 3.3.5.1A Structure of **MS-15**

Assuming a guaianolide skeleton the *exo*-methylene protons, H_2-13, provided a ^2J correlation to a quaternary carbon (δ_C 142.4, C-11) and ^3J signals to a methine (δ_C 43.3, C-7) and carbonyl carbons. H-7 provided two strong COSY correlations towards H-6 (δ_H 1.46 and 1.99) and H-8 (δ_H 4.82 m, δ_C 82.6). The highly deshielded nature of this methine meant that it must be directly attached to an oxygen and so was placed here, β to the carbonyl. This completes ring C. The methine, H-8, gave a COSY correlation to H_2-9 which in turn showed a signal to H-10 (δ_H 2.24 bs). Methyl-14 (δ_H 1.22 d) showed three strong correlations to a methine (H-10), methylene (H_2-9) and an olefinic quaternary carbon (δ_C 151.1, C-1), fixing them at these positions. Its olefinic partner was placed at postion 2 (δ_H 5.37 t, J = 1.5 Hz, δ_C 120.3). No signal was detected in the HMBC spectrum, however this was the last olefinic carbon still to be accounted for. A COSY correlation between H-2 and a methylene (δ_H 2.37 dd, J = 16.0 Hz, H_2-3) placed this group here. A ^3J and ^2J HMBC signal from H-2 and H_2-3

respectively, towards a quaternary carbon (δ_C 82.1) placed it at C-4. Methyl-15 (δ_H 1.25 s) appeared as a singlet and gave three HMBC signals to a quaternary carbon (C-4), a methylene carbon (C-3) and a methine carbon (δ_C 59.7, C-5). Due to the deshielded nature of C-4, a hydroxyl was placed here. Two ^3J signals from H-2 and H_2-3 to C-5 and a ^2J signal from H-5 to C-1 enabled this ring to be completed (ring A). COSY correlations between H-5 and H-7 towards H-6 completed the heptacyclic ring B and that structure of **MS-15**.

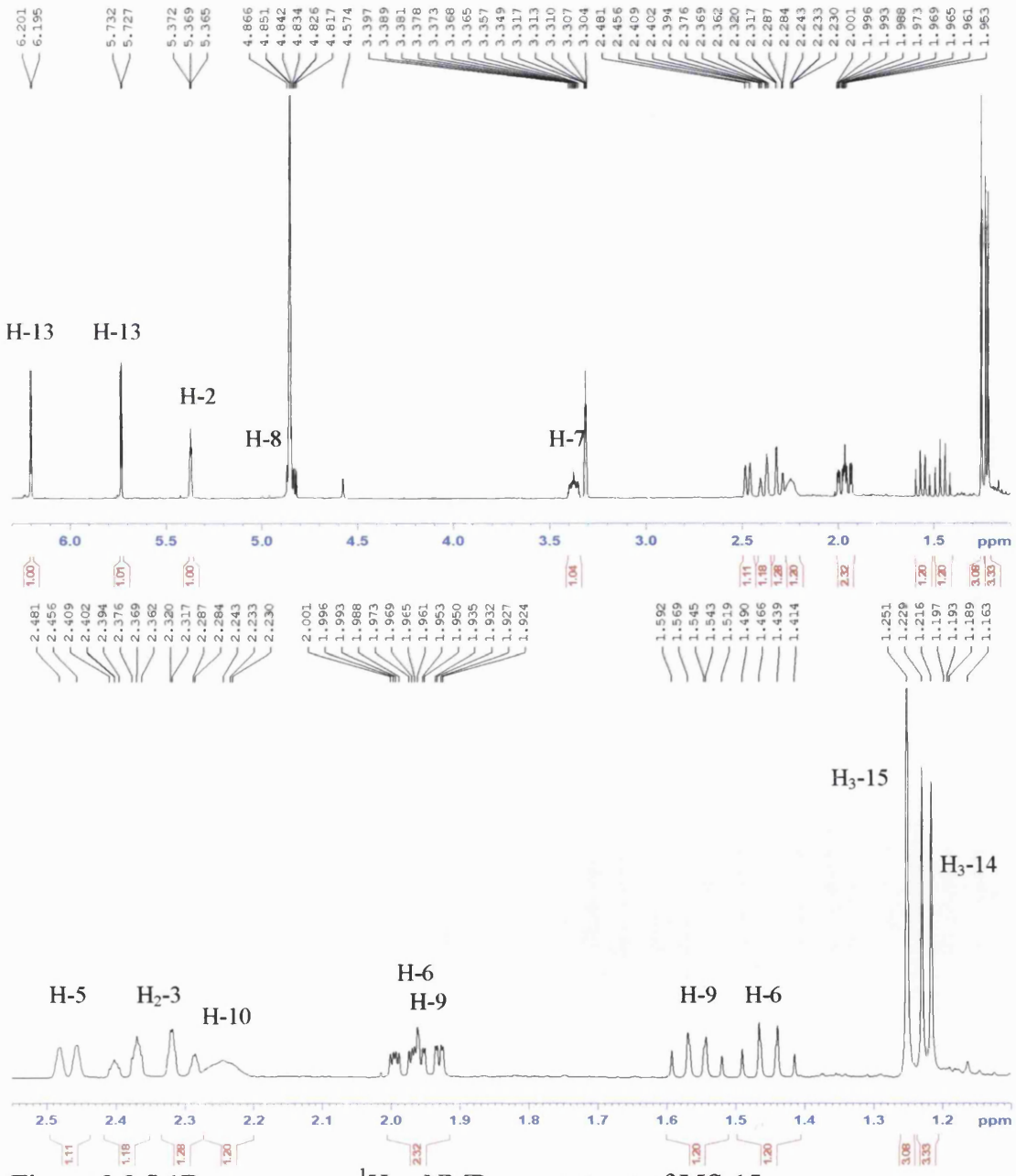

Figure 3.3.5.1B ^{1}H NMR spectrum of **MS-15**

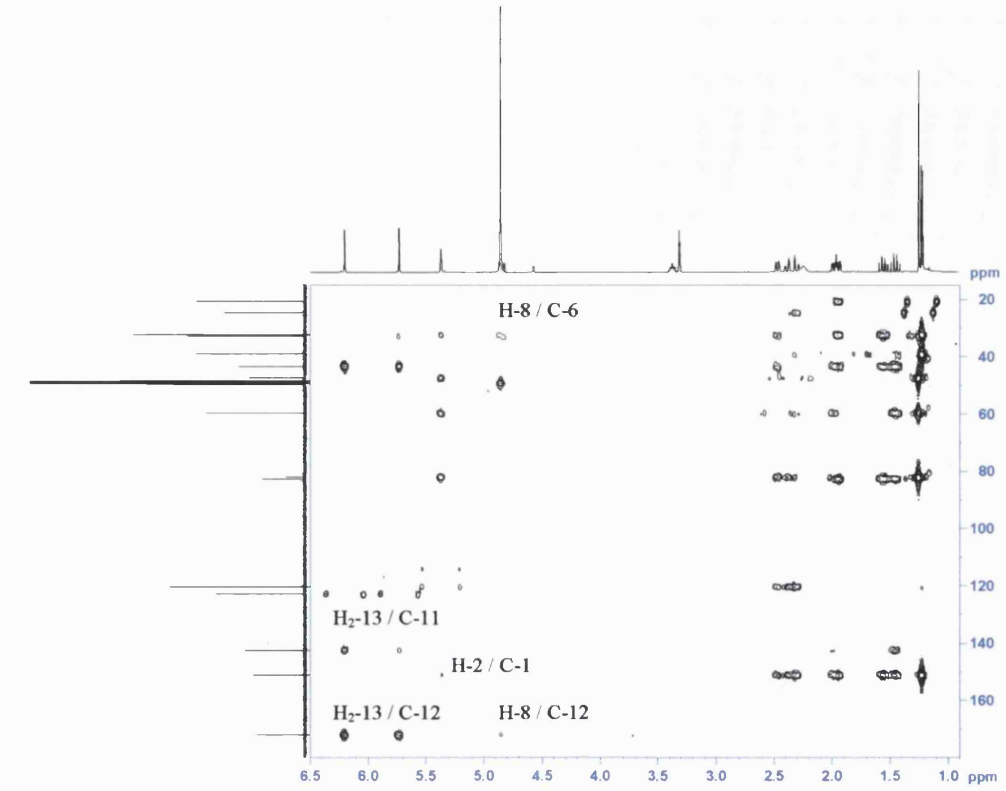

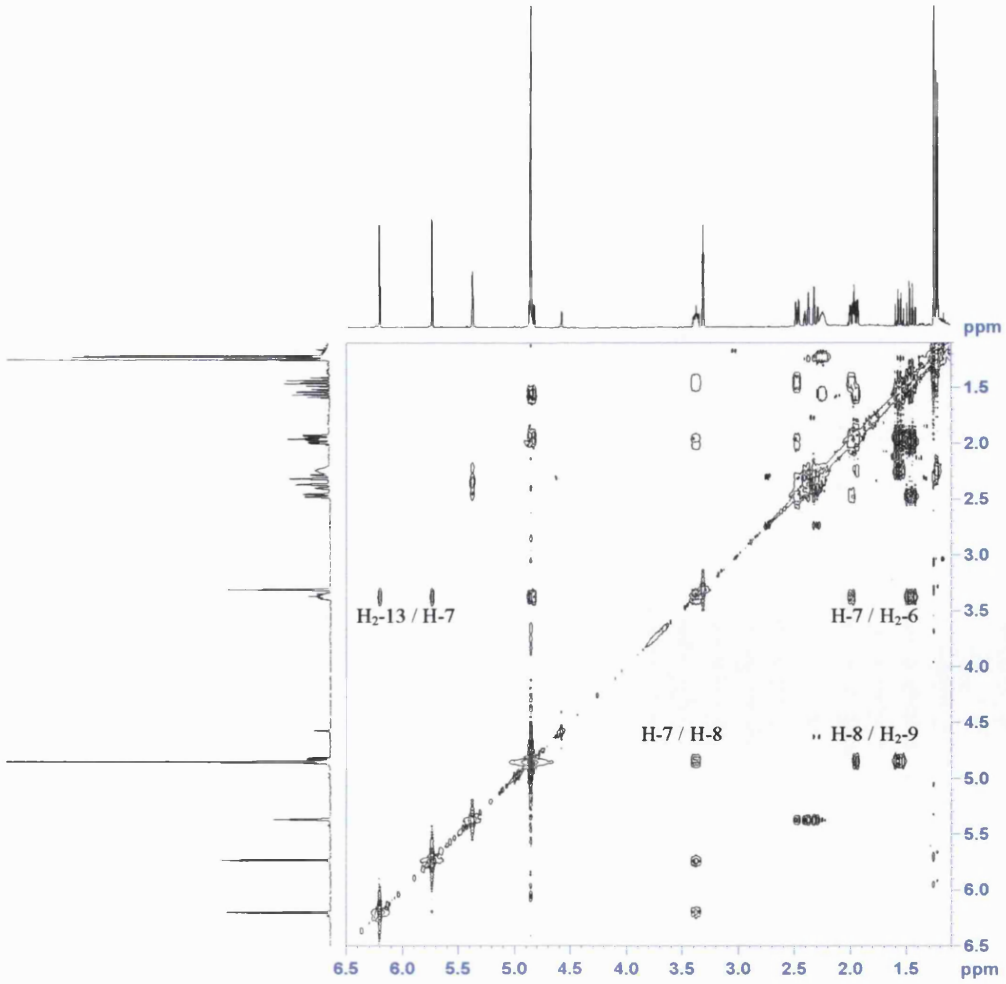

Figure 3.3.5.1C HMBC and COSY spectra of **MS-15**

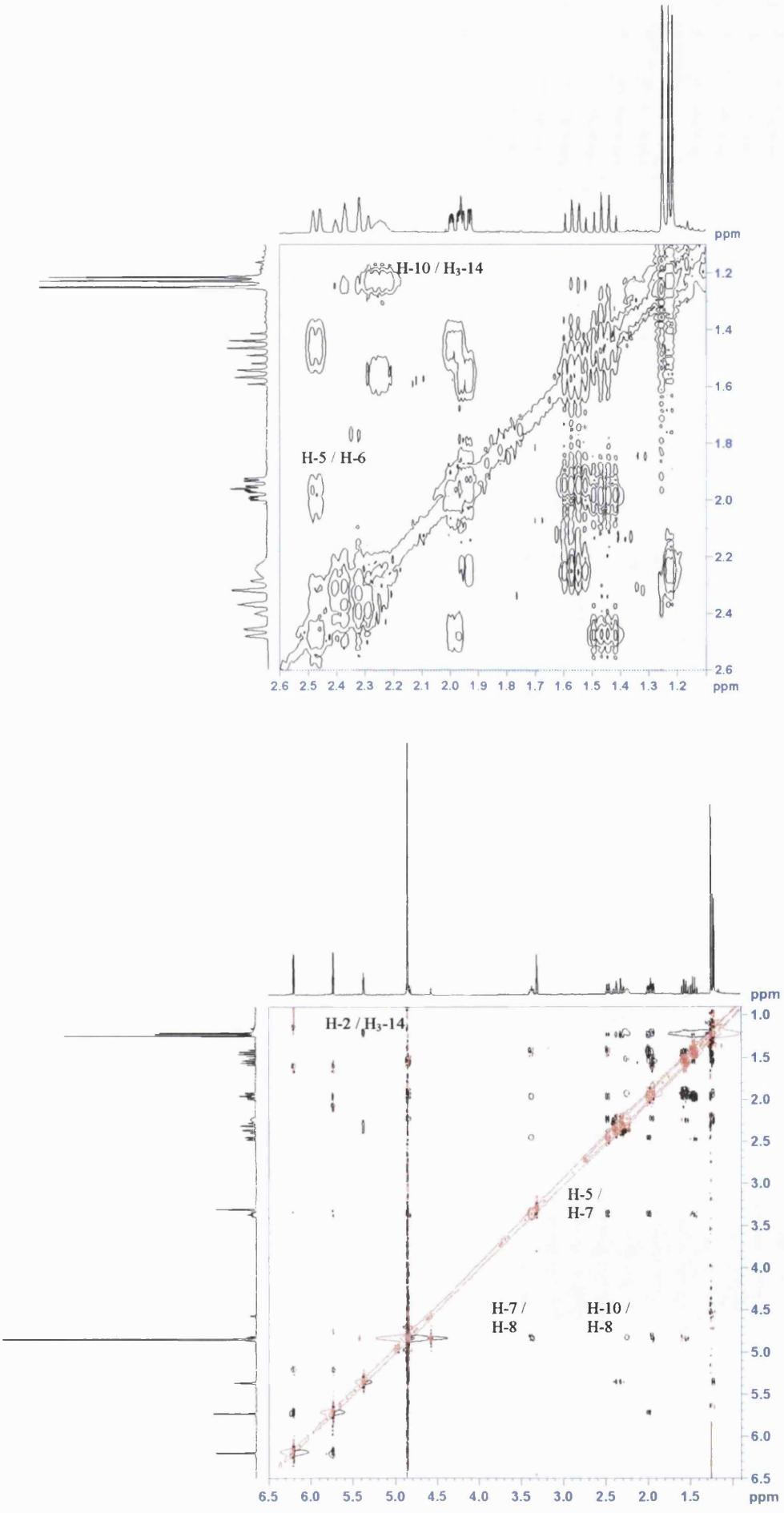

Figure 3.3.5.1D COSY and NOESY spectra of **MS-15**

The relative stereochemistry of **MS-15** was determined by NOESY and ^1H NMR. An NOE between H-2 and H_3-14 meant that this methyl group should be β-oriented. NOE's detected between H-10 and H-8 and H-8 and H-7 showed that these protons are on the same face of the molecule and α oriented. The orientation of the lactone ring must therefore be assigned as β. A fourth NOE between H-7 and H-5 also placed this proton on the same face of the molecule as H-10, H-8 and H-7. This was further corroborated by a 1,3 interaction between H-10 and H-5 and so this proton must be α orientated. Methyl-15 was positioned in a β orientation due to a 1,3 interaction with H_α-6 (δ_H 1.99 m). **MS-15** has previously been isolated from *Pulicaria sicula* and the measurement of a positive specific rotation confirmed the stereochemistry as 1,2-dehydro-1,10α-dihydropseudoivalin (Zdero *et al.*, 1988). Whilst 1,2-dehydro-1,10α-dihydropseudoivalin has previously been reported by Zdero *et al.*, (1988), this is the first report of the ^{13}C NMR data for this compound and the first report of the full NMR data in deuterated methanol.

Table 15 ^1H and ^{13}C NMR data and ^1H-^{13}C long-range correlations of **MS-15** recorded in CD_3OD

Position	^1H	^{13}C	^2J	^3J
1	-	151.1		
2	5.37 t (1.5)	120.3	C-1, C-3	C-4, C-5, C-10
3	2.37 dd (16.0)	47.5	C-2, C-4	C-1, C-5, C-15
4	-	82.1		
5	2.48 d (12.5)	59.7	C-1, C-4, C-6	C-2, C-7
6	1.46 dd (12.5)	32.7	C-5, C-7	C-1, C-8, C-11
	1.99 m			
7	3.37 ddd (12.0, 9.5, 4.0)	43.3		
8	4.82 m	82.6		C-6, C-12
9	1.56 dd (12.0)	39.1	C-8, C-10	C-1, C-7, C-14
	1.93 m			
10	2.24 bs	32.4		
11	-	142.4		
12	-	172.1		
13	5.73 d (2.5)	122.9	C-11	C-7, C-12
	6.20 d (3.0)			
14	1.22 d (6.5)	20.6	C-10	C-1, C-9
15	1.25 s	24.7	C-4	C-3, C-5

3.3.5.2 Characterisation of MS-16 as 2α,4α-dihydroxy-10β-methyl-guaia-1(5),11(13)-dien-8β,12-olide

MS-16 was isolated as a colourless oil and a molecular formula of $C_{15}H_{20}O_4$ $[M]^+$ (264.1355) was solved by HREIMS. The ^1H and ^{13}C NMR spectra were similar to those of **MS-15**, which indicated that **MS-16** was a closely related guaianolide sesquiterpene.

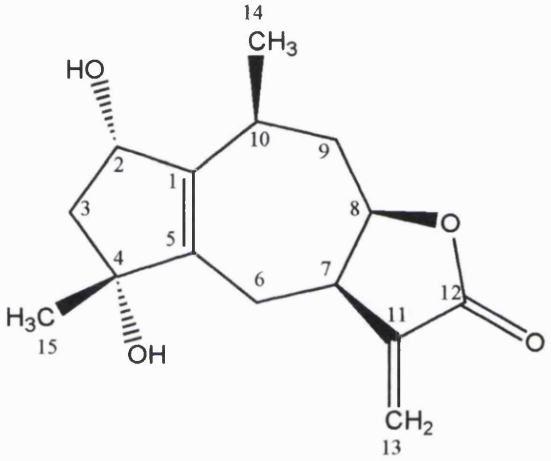

Figure 3.3.5.2A Structure of **MS-16**

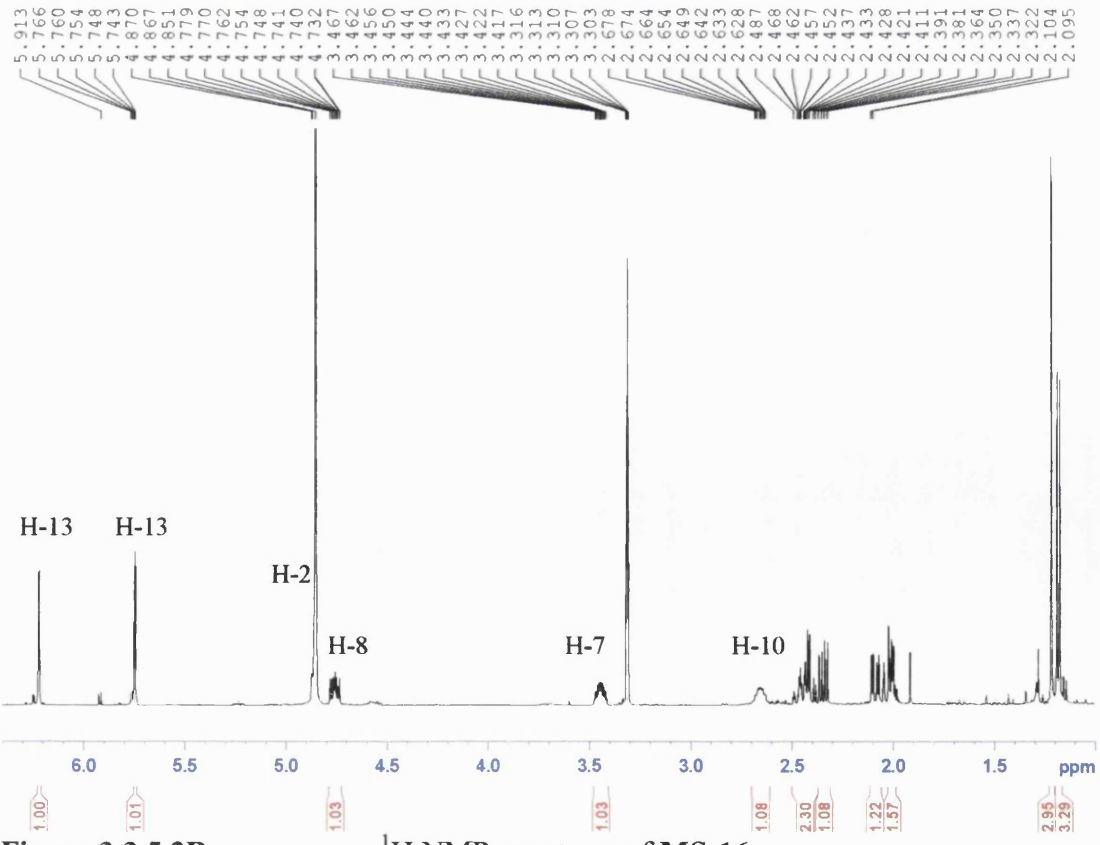

Figure 3.3.5.2B ^1H NMR spectrum of **MS-16**

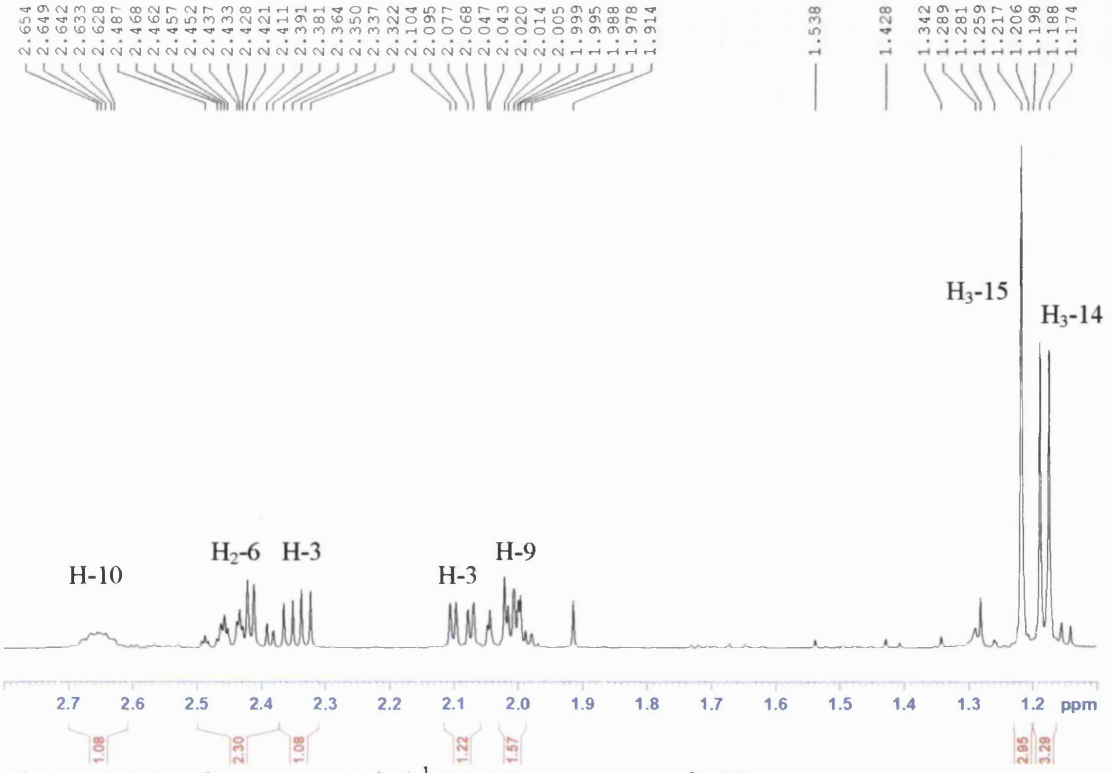

Figure 3.3.5.2.C Expanded ^{1}H NMR spectrum of **MS-16**

MS-16 was found to be different from **MS-15** at positions C-1, C-2 and C-5. Assuming identical HMBC and COSY correlations for the rest of the molecule, the assignment of the three unknown carbons was achieved primarily by HMBC signals from the two methyl groups. Methyl-15 (δ_H 1.21 s) exhibited HMBC signals to a quaternary and methylene carbons as in **MS-15**. However, it also showed a ^{3}J correlation to an olefinic quaternary carbon (δ_C 144.9) which could be placed at C-5. A ^{2}J signal from H_2-6 to this carbon also further corroborated that this carbon should be placed here. Methyl-14 (δ_H 1.18) again appeared as a doublet and provided HMBC signals towards a methine and methylene carbons as for **MS-15**. It also showed a ^{3}J correlation towards another olefinic quaternary carbon (δ_C 140.8, C-1). This was further confirmed by three ^{3}J signals from H_2-3, H_2-6 and H_2-9 to this carbon. The remaining methine was placed at C-2 (δ_C 87.4, δ_H 4.86) due to a strong COSY correlation between this proton and the methylene protons at C-3. Due to the downfield nature of the methine (C-2) and the molecular weight of this compound an hydroxyl was positioned here. The oxymethine would also be shifted further downfield because it is allylic, and this is the case when compared to **MS-17** (3.59 s, H-2) which lacks the double bond between C-1 and C-5.

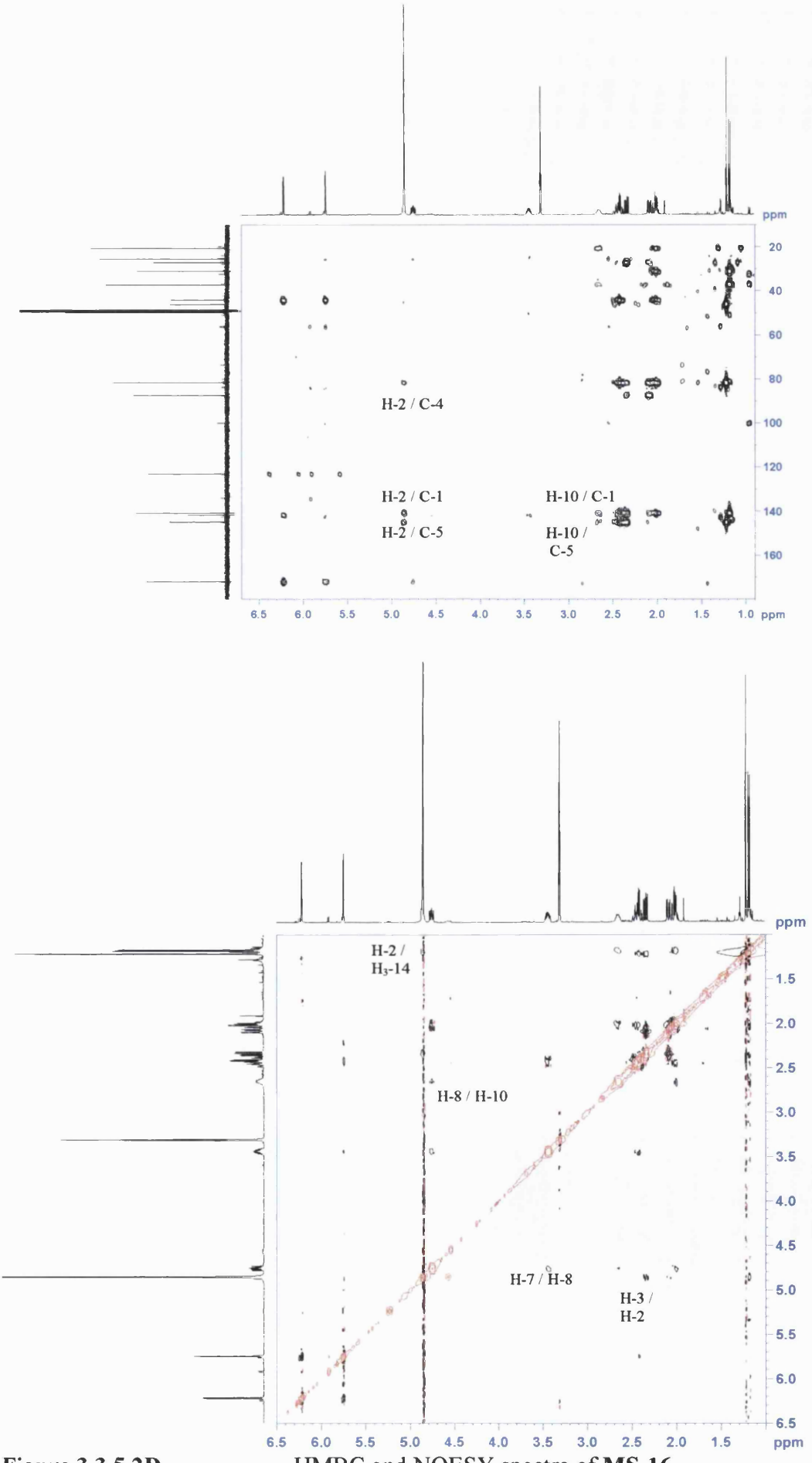

Figure 3.3.5.2D HMBC and NOESY spectra of **MS-16**

The relative stereochemistry of **MS-16** was again determined by inspection of the ^{1}H and NOESY spectra. An NOE between H-7 and H-8 showed that these two protons are on the same face of the molecule. As only the coupling constants could be measured for H-8 and not for H-7, a model of this molecule indicated that these protons should be *cis* (α-oriented). This correlates well with one of the coupling constants measured for H-8 of 8.5 Hz and helped to confirm the *cis* orientation. A similar coupling constant measured for **MS-15** also corroborated this assignment. A 1,3 NOE interaction between H-8 and H-10 allowed the assignment of this proton as being α, therefore methyl-14 must be positioned in a β-orientation. A third NOE between methyl-14 and H-2 placed this proton in a β-orientation and so the hydroxyl attached to this carbon must be α. An NOE between H-2 and the downfield proton of the methylene at position 3 (δ_H 2.35) meant that this proton must be on the same face of the molecule (β). Thus a 1,3 interaction between H_β-3 and methyl-15 showed that this group should also be assigned as β. This is further confirmed by a NOE between methyl-15 and both protons attached at C-6. **MS-16** is therefore assigned as 2α,4α-dihydroxy-10β-methyl-guaia-1(5),11(13)-dien-8β,12-olide and is reported here for the first time.

Table 16 ^{1}H and ^{13}C NMR data and ^{1}H-^{13}C long-range correlations of **MS-16** recorded in CD_3OD

Position	^{1}H	^{13}C	^{2}J	^{3}J
1	-	140.8		
2	4.86 m	87.4	C-1	C-4, C-5
3	2.09 dd (13.5, 4.5)	46.0	C-2, C-4	C-1, C-5, C-15
	2.35 dd (13.5, 7.0)			
4	-	81.6		
5	-	144.9		
6	2.41 dd (15.0, 5.0)	25.5	C-5, C-7	C-1, C-4, C-8
	2.46 ddt (15.0, 5.0, 2.5)		C-5, C-7	C-1, C-4, C-8
7	3.44 m	44.1		
8	4.76 ddd (12.5, 8.5, 4.5)	81.5		
9	1.99 m	37.2	C-8, C-10	C-1, C-7, C-14
10	2.65 m	31.0	C-1, C-9, C-14	C-5
11	-	141.6		
12	-	172.0		
13	5.75 d (2.5)	123.1	C-11	C-7, C-12
	6.21 d (3.0)			
14	1.18 d (7.0)	20.6	C-10	C-1, C-9
15	1.21 s	27.0	C-4	C-3, C-5

3.3.5.3 Characterisation of MS-17 as 4-*epi*-1α,2α-epoxy-1,10α-dihydropseudoivalin

MS-17 was isolated from the hexane extract of *P. crispa* as a pale yellow oil and HREIMS enabled a molecular formula of $C_{15}H_{20}O_4$ $[M]^+$ (264.1363) to be assigned. The ^{13}C NMR spectrum indicated the presence of 15 carbons, including a carbonyl, olefinic and two oxyquaternary carbons. The ^1H NMR spectrum provided signals for an *exo*-methylene group, two methyl groups and two deshielded methine protons. The proton spectrum provided evidence to suggest that **MS-17** is a guaianolide due to the similarity observed with the spectra of previously isolated guaianolide sesquiterpenes **MS-15** and **MS-16**.

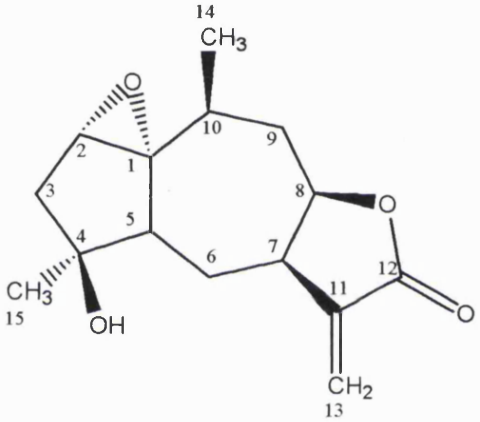

Figure 3.3.5.3A Structure of **MS-17**

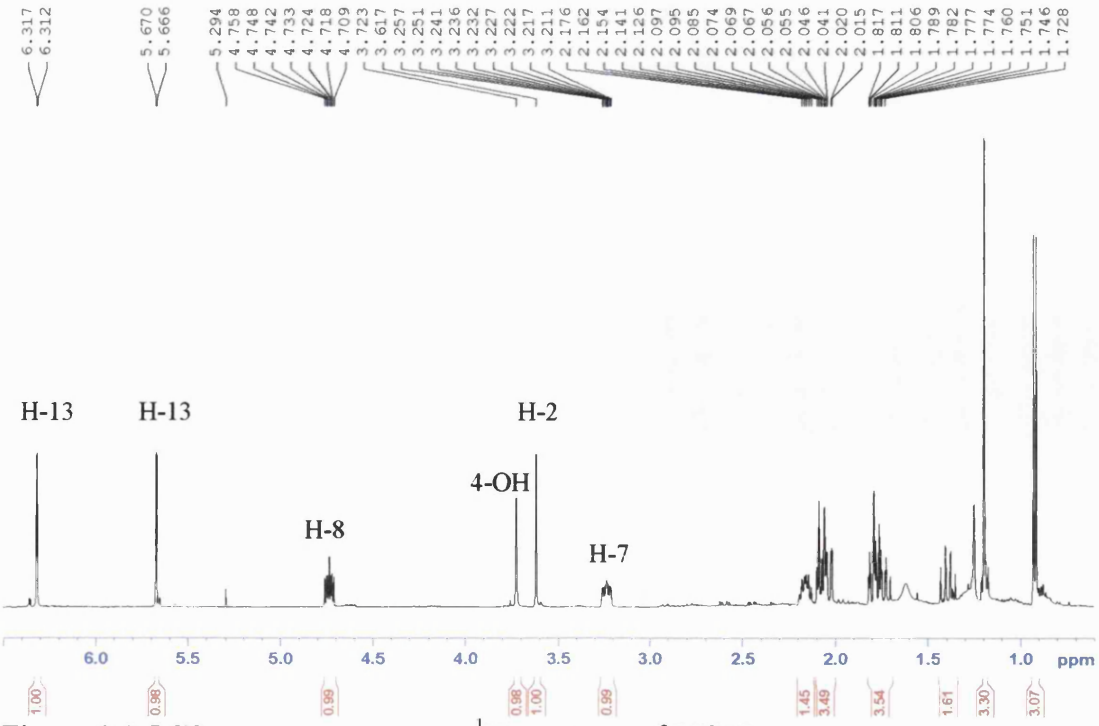

Figure 3.3.5.3B ^1H spectrum of **MS17**

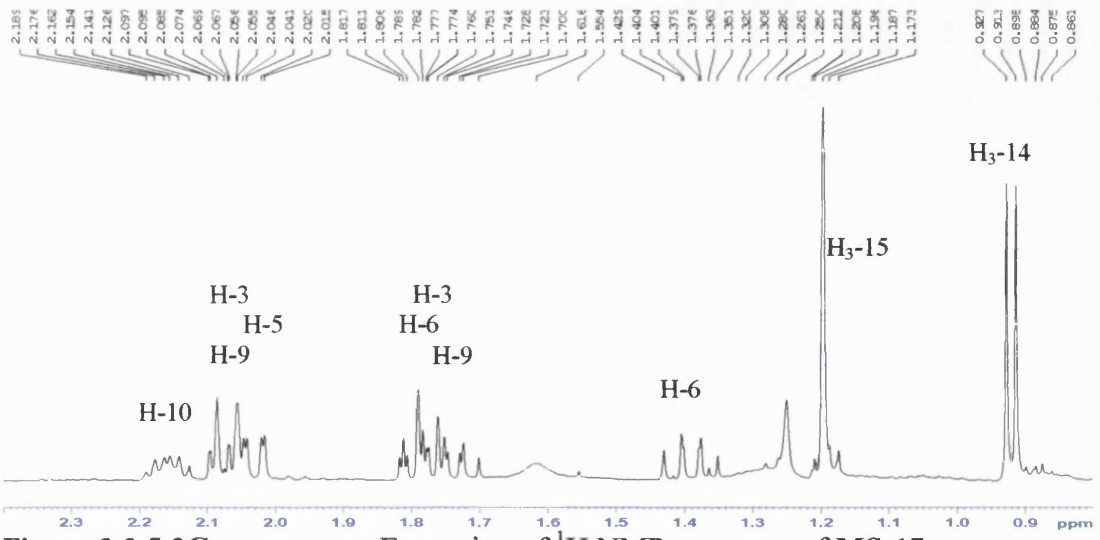

Figure 3.3.5.3C Expansion of ^{1}H NMR spectrum of **MS-17**

The structure of **MS-17** was closely related to that of **MS-16**, except for the absence of the double bond between C-1 and C-5 and the absence of an hydroxyl group attached at C-2. Instead ring A of **MS-17** was saturated with the formation of an epoxide between C-1 and C-2. The remainder of the guaianolide structure was the same as that of **MS-16** with similar HMBC and COSY correlations. The epoxide carbons (δ_C 72.4, C-1 and δ_C 59.6, C-2) were detected upfield and this is characteristic for epoxide carbons, especially C-2. The hydroxyl proton was also detected in the ^{1}H spectrum as a sharp singlet and provided information as to the carbon it was attached to, with a ^{2}J correlation to C-4 and a ^{3}J correlation to C-15. This further corroborated the structure of the cyclopentane ring (ring A). The ^{1}H NMR data for **MS-17** is in close agreement with that of the literature (Zdero *et al.*, 1988). However, the NOESY spectrum provided evidence to indicate that **MS-17** was in fact the epimer of the guaianolide isolated by Zdero *et al.*, (1988) at the C-4 position.

From the NOESY spectrum, a 1,3 interaction between H-8 and H-10 and a second NOE between H-8 and H-7 indicated these protons are on the same face of the molecule in an α-orientation. Again as with **MS-16**, the large coupling constant measured for H-8 (7.5 Hz) further verified that this proton should be *cis* with respect to H-7 (α). H-7 showed an NOE to H-5, which in turn gave a 1,3 interaction with the methyl protons attached to C-15. This means both H-5 and H_3-15 must also be on the same face of the molecule as H-7 in an α-orientation. The methylene protons attached at C-6 each gave an NOE to H_3-15 and a molecular model of this molecule showed that these protons are equidistant apart from the methyl protons further confirming the

relative stereochemical assignment at C-4. The hydroxyl group must therefore be in a β-orientation. This is the point of difference between the relative stereochemistry of **MS-17** and that assigned by Zdero *et al.*, (1988). The guaianolide described in the literature was described with the methyl group in a β-orientation and the hydroxyl group in an α-orientation. As H-10 was assigned as being α-oriented, this places the methyl group at C-14 in a β-orientation. The methyl protons gave a 1,3 interaction to H-2 placing this proton on the same face of the molecule as H_3-14 (β). Thus the epoxide must be α-oriented and this follows the representation of the epimeric form of the molecule described by Zdero *et al.*, (1988). **MS-17** is therefore assigned as 4-*epi*-1α,2α-epoxy-1,10α-dihydropseudoivalin and is reported here for the first time.

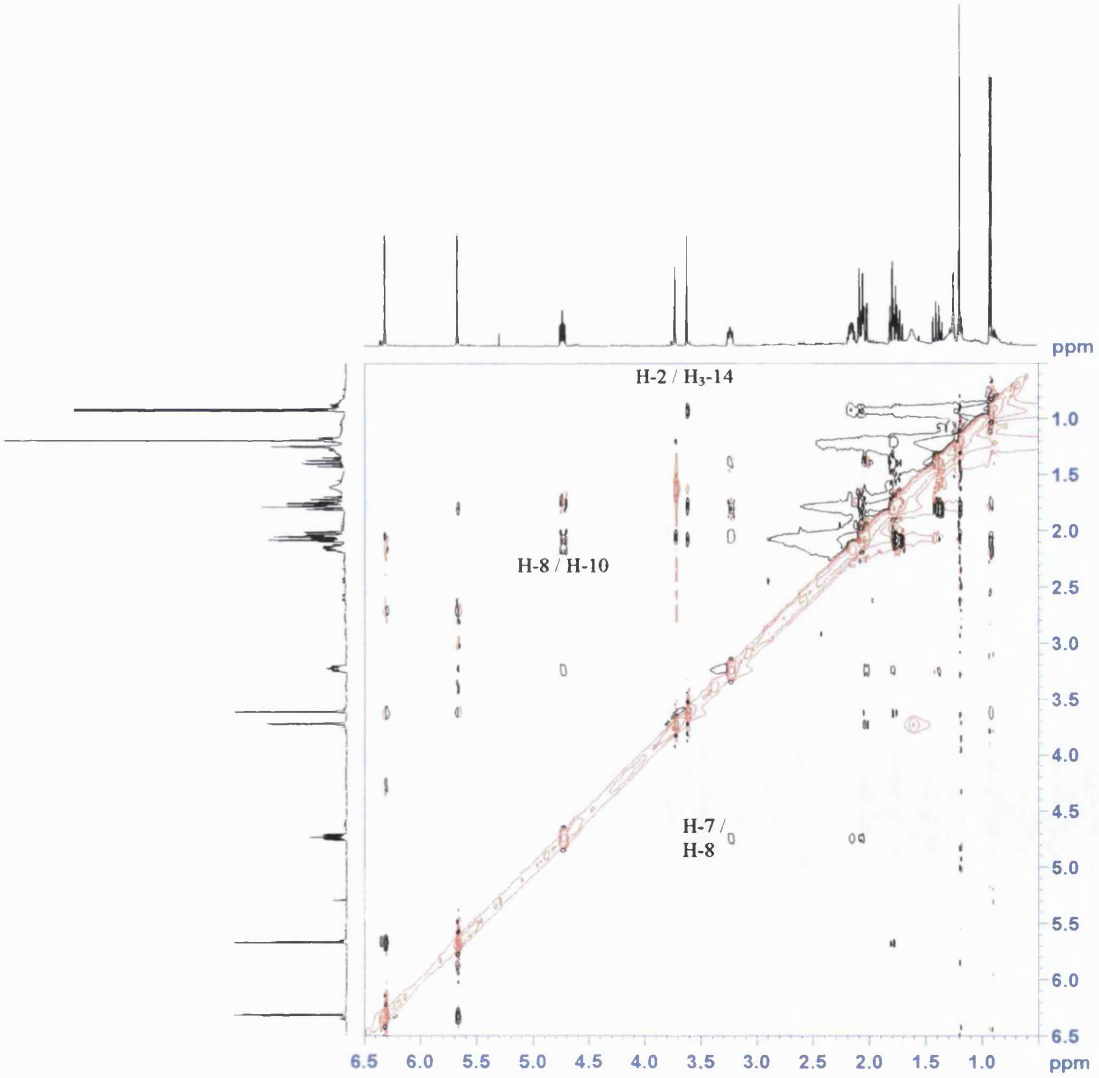

Figure 3.3.5.3D NOESY spectrum of **MS-17**

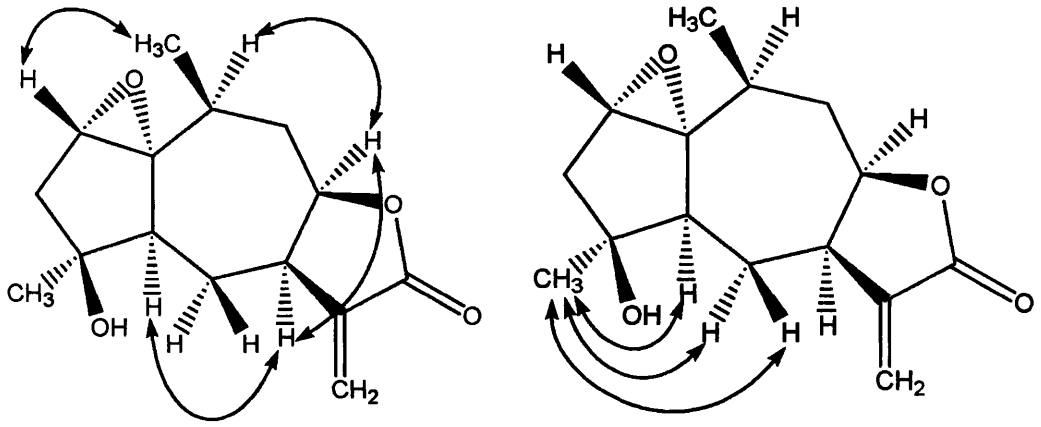

Figure 3.3.5.3E NOE correlations for **MS-17**

Table 17 ^{1}H and ^{13}C NMR data and ^{1}H-^{13}C long-range correlations of **MS-17** recorded in $CDCl_3$

Position	^{1}H	^{13}C	^{2}J	^{3}J
1	-	72.4		
2	3.59 s	59.6	C-3	C-4
3	1.77 d (14.5)	40.6	C-2, C-4	C-1, C-5, C-15
	2.06 d (15.0)			
4	-	78.2		
5	2.02 dd (13.0, 2.0)	54.9	C-1, C-6	C-2
6	1.38 m	30.6	C-5, C-7	C-1, C-8, C-11
	1.79 m			
7	3.21 m	41.9	C-6, C-11	C-12
8	4.72 ddd (12.0, 7.5, 4.5)	79.1		C-6
9	1.73 d (14.0)	35.3	C-8, C-10	C-1, C-7, C-14
	2.07 dd (13.5, 0.5)			
10	2.14 m	30.0	C-1, C-9, C-14	C-2, C-8
11	-	140.1		
12	-	169.5		
13	5.65 d (2.0)	123.3	C-11	C-7, C-12
	6.29 d (2.5)			
14	0.90 d (7.0)	17.2	C-10	C-1, C-9
15	1.17 s	23.5	C-4	C-3, C-5
4-OH	3.70 s	-	C-4	C-15

3.3.5.4 Characterisation of MS-18 as 5,10-*epi*-2,3-dihydroaromatin

MS-18 was isolated as a white amorphous powder and the accurate EI-MS in the positive mode provided the molecular ion of *m/z* 248.1412 to establish a molecular formula of $C_{15}H_{20}O_3$. The ^{13}C NMR spectrum yielded signals for 15 carbons, including two carbonyl carbons, an *exo*-methylene and an olefinic quaternary carbon. The ^{1}H NMR spectrum provided signals indicative of a guaianolide sesquiterpene. This included signals for a pair of *exo*-methylene protons, two methyl and four methylene groups.

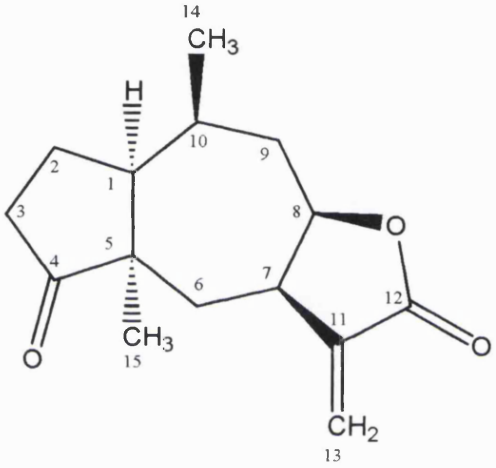

Figure 3.3.5.4A Structure of **MS-18**

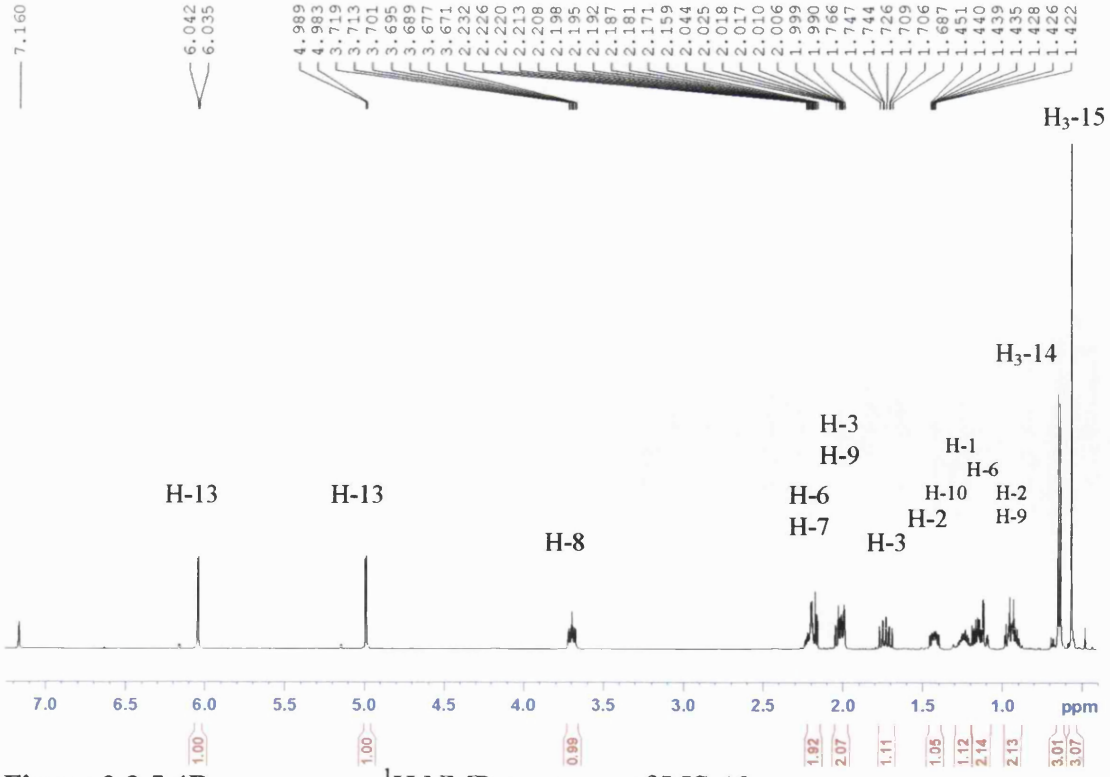

Figure 3.3.5.4B ^{1}H NMR spectrum of **MS-18**

The HMBC spectrum provided similar signals as for the previous guaianolide sesquiterpenes discussed, the notable differences occurring at ring A. The position of methyl-15 strongly indicates that a Wagner-Meerwein rearrangement had taken place, moving this group from C-4 to C-5 of the molecule. The normal biosynthetic pathway (**Scheme 3A**) from the C_{15} precursor farnesyl pyrophosphate would place this methyl group at C-4. However, in the case of **MS-18**, C-4 has been oxidised to a keto carbonyl. Methyl-15 appeared as a singlet and gave a ^2J correlation to a quaternary carbon C-5 (δ_C 50.2) as well as ^3J correlations to C-1 (δ_C 48.6), C-6 (δ_C 35.4) and the keto carbonyl C-4 (δ_C 222.4). The keto carbonyl was highly deshielded and this was due to the highly strained nature of the cyclopentane ring (ring A). The methylene protons at C-3 showed a COSY correlation with H_2-2, which in turn gave a further COSY correlation to H-1. The methine proton, H-1, also gave a COSY correlation to H-10, which in turn gave a COSY signal to H_2-9. The methylene protons attached at C-9 then gave a COSY signal to the oxymethine proton, H-8. A COSY correlation between H-8 and H-7 indicated that they should be placed at the ring junction of ring B and C. This was confirmed by an allylic coupling detected between H-7 and the *exo*-methylene protons H_2-13. The COSY correlations detected for **MS-18** were similar to those of the previously discussed guaianolides (**MS-15 – MS-17**).

The relative stereochemistry of **MS-18** was achieved by NOE's detected in the NOESY (**Figure 3.3.5.4E**) spectrum along with the coupling constants measured. An NOE between H-8 and H-7 placed these protons on the same face of the molecule in an α-orientation. The large coupling constant measured (9.0 Hz) also indicated that these protons are *cis*. A second NOE between H-8 and H-10 (**Figure 3.3.5.4D**) also placed this proton on the same face of the molecule (α), therefore methyl-14 must be β-oriented. This was further confirmed by NOE's between both H_2-2α and H_2-2β to methyl-14. A molecular model showed that the methylene protons are equidistant with respect to methyl-14, whereas if the methyl group were α-orientated this would not be possible. An NOE between H-8 and H-1 also placed this proton in an α-orientation, thus confirming the relative stereochemistry at this position. Finally, methyl-15 exhibited NOE's with H-10 and H_2-3α placing this group on the same face of the molecule as H-1, H-7, H-8 and H-10 (α).

MS-18 has been isolated previously (Abdel-Mogib *et al.*, 1990; Bohlmann and Mahanta 1979; Rustaiyan *et al.*, 1987), however the relative stereochemistry of this compound differs from all these compounds referred to in at least one position. All

published literature quote the ^{1}H NMR data in deuterated chloroform, which suffers from signal overlap. However, for the purpose of comparing the ^{1}H NMR data with that of the literature, **MS-18** was also analysed in deuterated chloroform (**Table 18B**). The ^{1}H NMR data for **MS-18** was in agreement with that of the literature for 2,3-dihydroaromatin (**Figure 3.3.5.4C**) (Merfort and Wendisch 1993) with the exception of H-7 and H-8 which were reported to be further downfield. The downfield values reported for these protons are consistent with previous literature articles for guaianolides that have these protons in a *cis* (α) arrangement (Zdero *et al.*, 1988), whereas they appear more upfield when H-7 (~2.75 ppm) and H-8 (~4.30 ppm) are *trans* (Abdel-Mogib *et al.*, 1990; Rustaiyan *et al.*, 1987). However, the NOESY experiment for **MS-18** acquired in deuterated benzene indicated that H-7 and H-8 should be *cis* (α-oriented). **MS-18** differs from 2,3-dihydroaromatin at positions 5 and 10 where the methyl groups attached to these carbons are opposite in both instances i.e α- and β-oriented respectively. The guaianolide **MS-18** is reported here for the first time as 5,10-*epi*-2,3-dihydroaromatin.

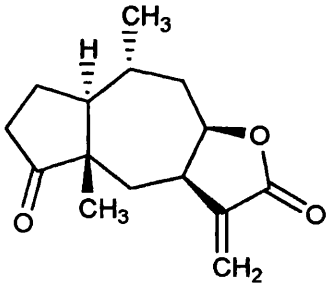

Figure 3.3.5.4C Structure of 2,3-dihydroaromatin

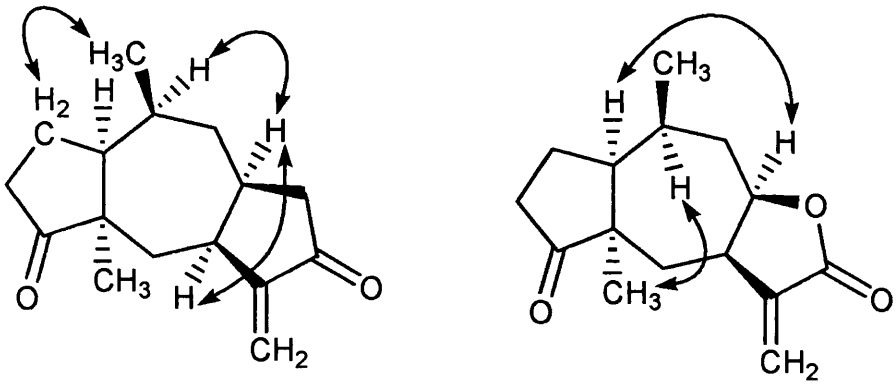

Figure 3.3.5.4D Key NOE's detected for **MS-18**

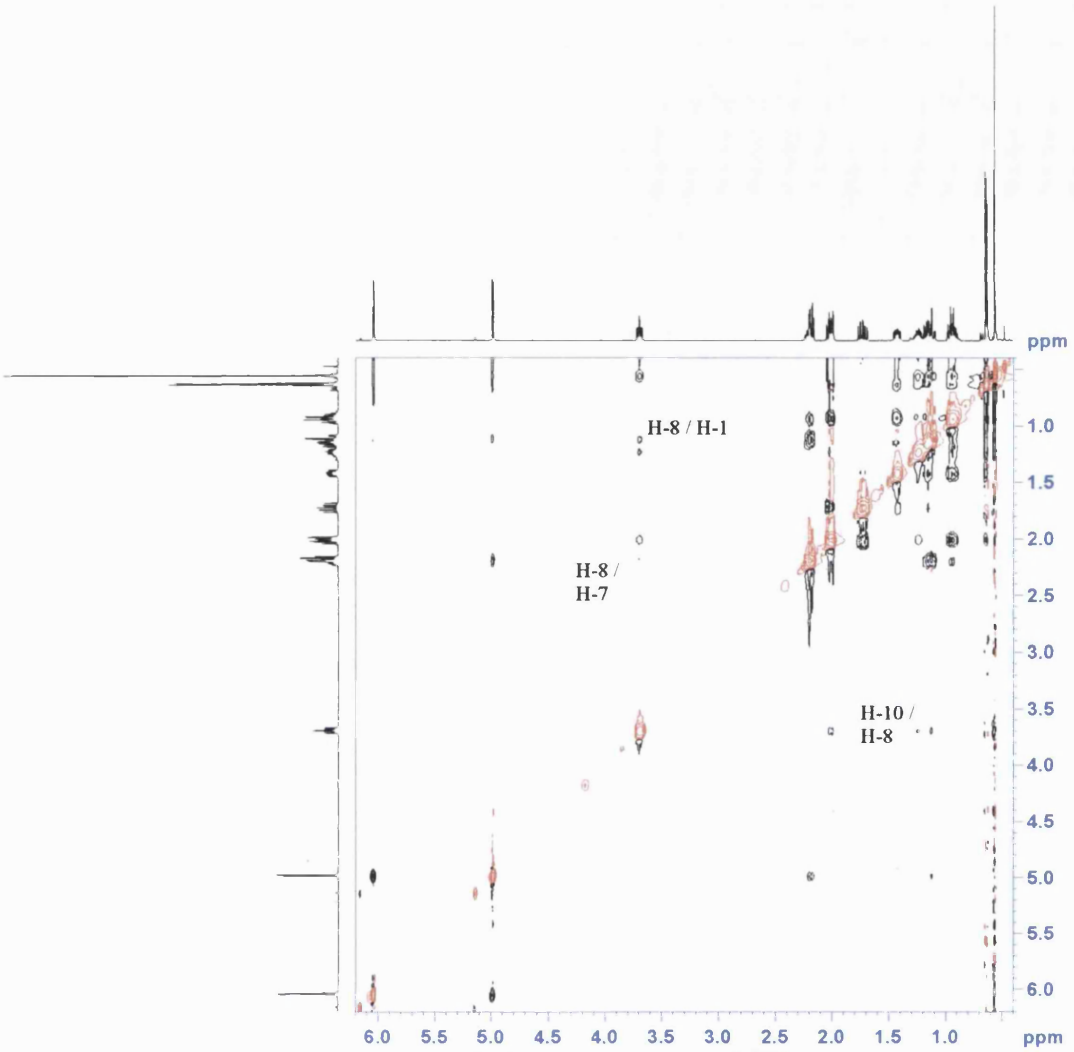

Figure 3.3.5.4E NOESY spectrum of **MS-18**

Table 18A ^{1}H and ^{13}C NMR data and ^{1}H-^{13}C long-range correlations of **MS-18** recorded in C_6D_6

Position	^{1}H	^{13}C	^{2}J	^{3}J
1	1.16 m	48.6	C-2, C-10	C-15
2	0.97 ddd (9.0, 3.0)	24.6	C-3	C-5, C-4
	1.42 dddd (12.5, 9.5, 6.5, 1.0)			
3	1.72 ddd	35.6	C-2, C-4	C-1
	2.01 m			
4	-	222.4		
5	-	50.2		
6	1.11 dd (13.0, 2.5)	35.4	C-5, C-7	C-4, C-8, C-15
	2.19 m			
7	2.21 m	45.1		
8	3.69 ddd (12.0, 9.0, 3.0)	81.0		C-6
9	0.95 d (12.5)	44.8	C-8, C-10	C-1, C-7, C-14
	2.02 m			
10	1.24 m	30.0		C-2
11	-	142.1		
12	-	169.9		
13	4.99 d (3.0)	119.3	C-11	C-7, C-12
	6.04 d (3.5)			
14	0.64 d (6.5)	20.4	C-10	C-1, C-9
15	0.56 s	22.4	C-5	C-1, C-4, C-6

Table 18B ^{1}H and ^{13}C NMR data for **MS-18** and 2,3-dihydroaromatin recorded in $CDCl_3$

	MS-18		2,3-dihydroaromatin (Merfort and Wendisch, 1993)	
Position	^{1}H	^{13}C	^{1}H	^{13}C
1	1.89 m	48.7	1.94 m	49.4
2	1.58 s	24.1	1.51 m	22.7
	2.09 m		2.07 m	
3	2.15 m	35.2	2.17 m	35.5
	2.43 m		2.45 m	
4	-	222.4	-	219.3
5	-	50.0	-	50.1
6	1.48 dd (15.0, 11.5)	34.5	1.51 dd (14.9, 11.8)	34.9
	2.48 m		2.48 dd (14.9, 6.2)	
7	2.77 m	44.7	3.06 m	39.3
8	4.24 ddd (12.5, 9.5, 3.0)	80.8	4.76 ddd (12.1, 9.3, 3.1)	77.1
9	1.39 ABq (12.0)	44.1	1.61 m	37.1
	2.43 m		2.42 m	
10	1.89 m	29.6	1.94 m	28.9
11	-	140.2	-	139.5
12	-	169.8	-	169.6
13	5.47 d (3.0)	120.0	5.67 d (2.0)	123.3
	6.15 d (3.5)		6.27 d (2.5)	
14	1.00 s	22.0	0.93 s	19.3
15	1.06 d (6.0)	19.9	1.13 d (6.8)	17.8

3.3.5.5 Possible biosynthetic pathway for the eudesmanolide and guaianolides MS-14 – MS-18

Guaianolides are a class of sesquiterpene lactone that are commonly found within the Asteraceae family, including the genus *Pulicaria*. They are biosynthesised from the sesquiterpene precursor farnesyl pyrophosphate by a series of oxidation and cyclisation steps. The initial step in this pathway is the cyclisation of farnesyl pyrophosphate to germacrene A by germacrene A synthase. The next step is the oxidation of the isopropenyl side chain to the carboxylic acid followed by a postulated hydroxylation at C-8 of the germacratrien-12-oic acid and then lactonisation. From here, further cyclisation leads to the formation of the guaianolide sesquiterpene lactones. Subsequent oxidation and rearrangement reactions of this guaianolide are proposed to yield the guaianolides **MS-15 – MS-18** isolated from *P. crispa*.

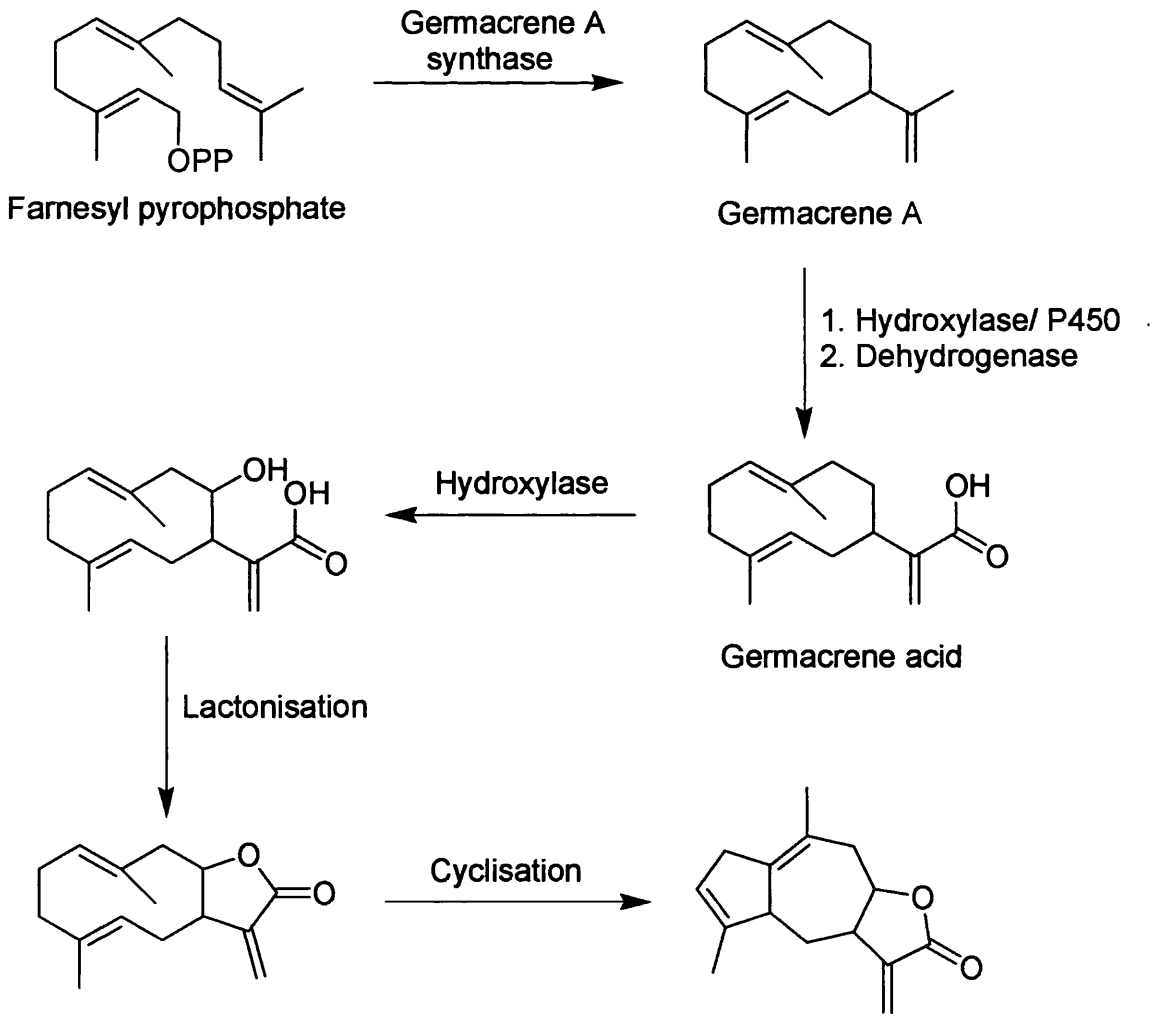

Scheme 3A Proposed biosynthetic pathway of 1(10),3-guaiadien-12,8-olide. Adapted from Kraker *et al.*, (2002).

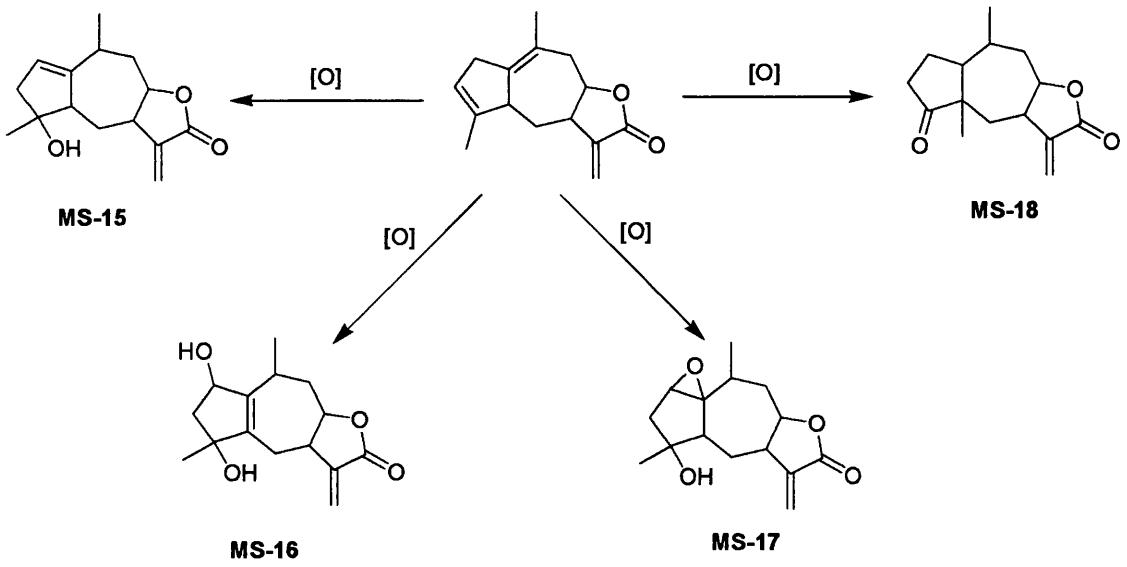

Scheme 3B **Biosynthesis of MS-15 – MS-18**

The biosynthesis of **MS-14** (eudesmanolide) is also proposed to be derived from germacrene A. Cyclisation by the enzyme germacrane cyclase results in the formation of the eudesmane skeleton. Reduction of the isopropenyl side chain by a hydrogenase to yield an isopropyl group, followed by oxidation at C-1, C-3 and C-6 by a hydroxylase would thus form **MS-14**.

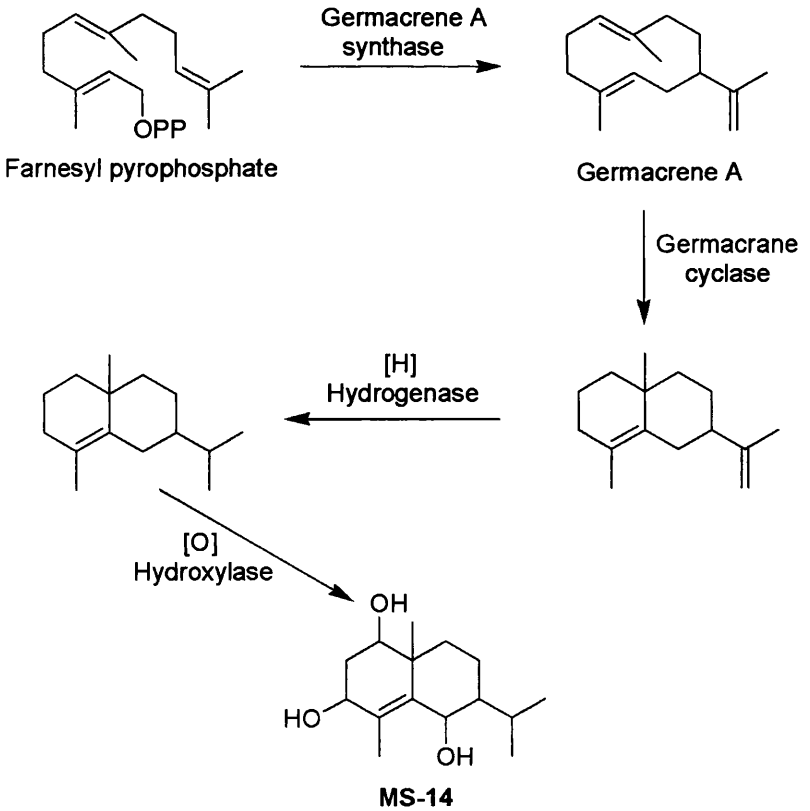

Scheme 3C **Proposed biosynthetic pathway of MS-14**

3.4 Diterpene

3.4.1 Characterisation of MS-19 as paniculoside V

MS-19 was isolated from the methanol extract of *P. crispa* as a colourless solid. The ESI-MS showed the $[M+Na]^+$ ion at *m/z* 665. Together with the NMR data this suggested the presence of a kaurane diterpene diglycoside, which had previously been isolated from plants belonging to the Asteraceae family (Catalan *et al.*, 2003). The ^1H and ^{13}C spectra showed signals for an *exo*-methylene group (δ_H 4.93 and δ_H 5.30), two anomeric protons (δ_H 4.44 and δ_H 5.42), nine oxymethine groups, two methyl groups (δ_H 0.98 and δ_H 1.23) and a carbonyl carbon (δ_C 178.5).

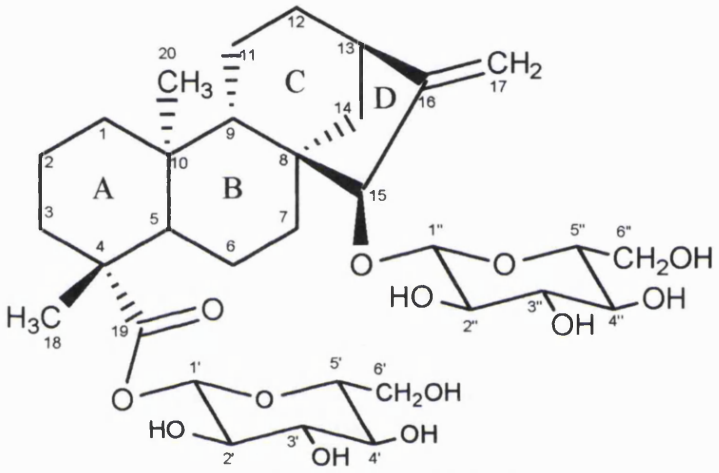

Figure 3.4.1A Structure of **MS-19**

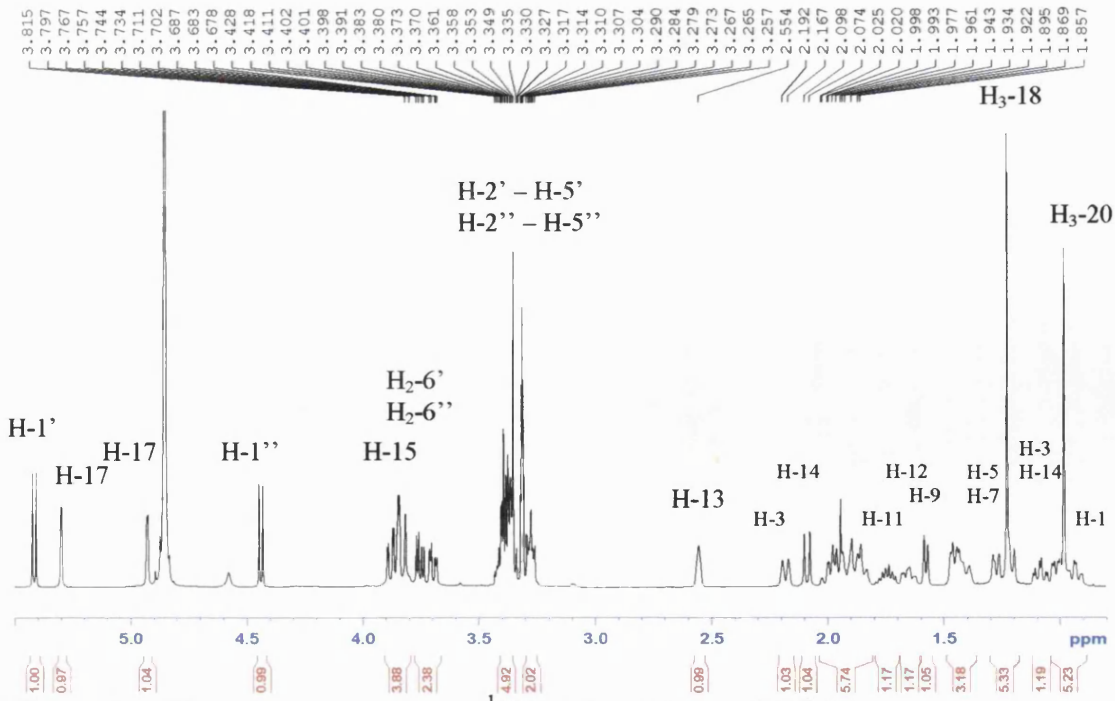

Figure 3.4.1B ^1H NMR spectrum of **MS-19**

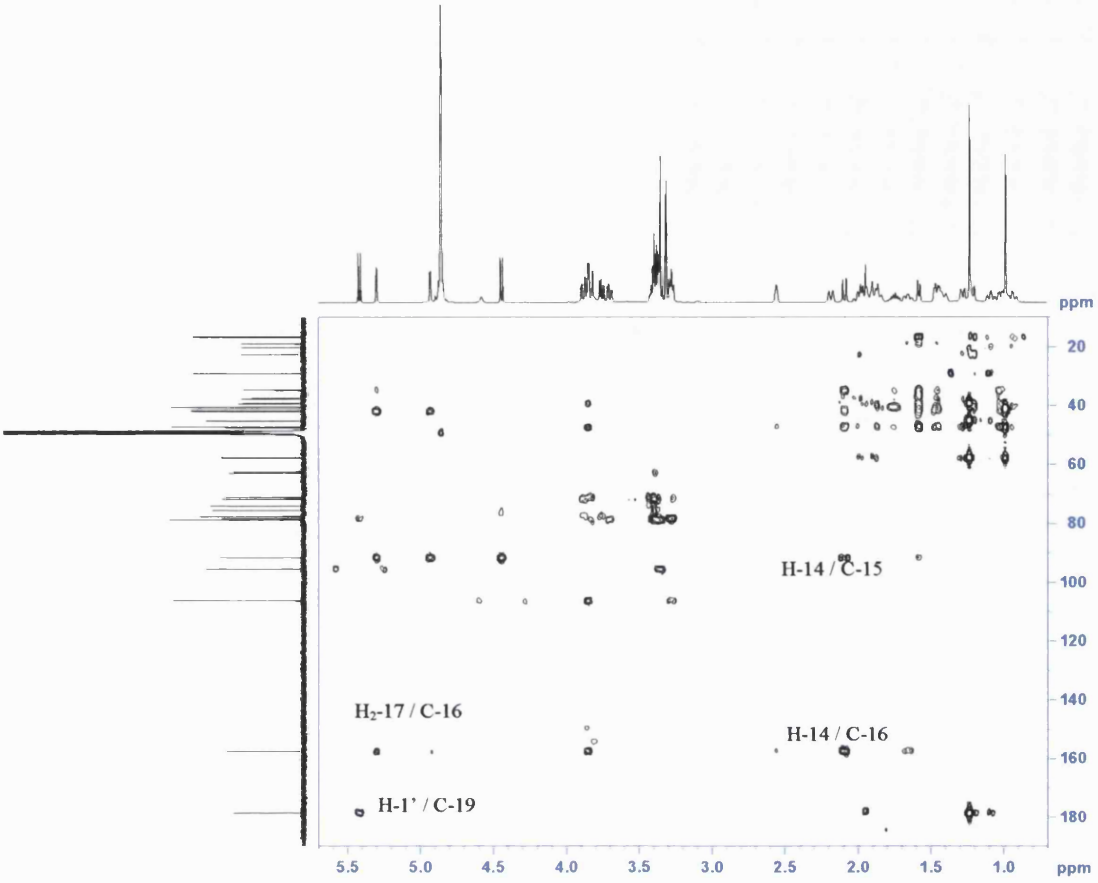

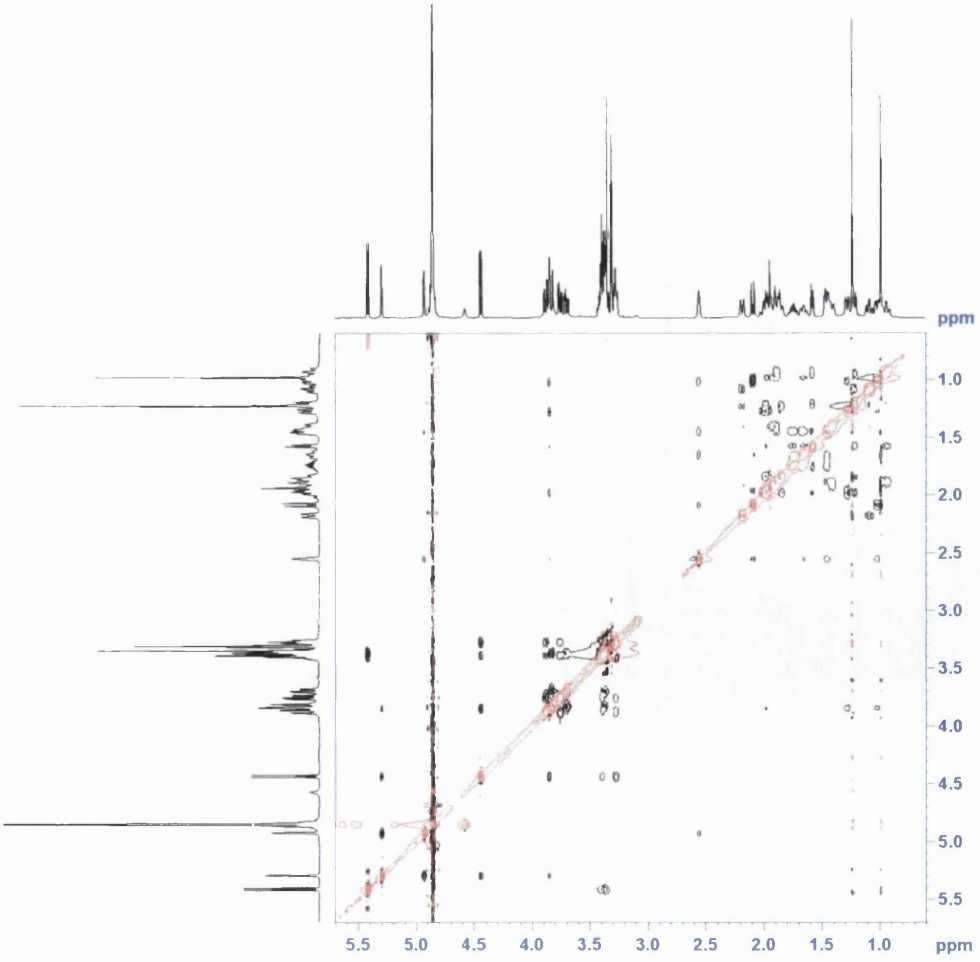

Figure 3.4.1C HMBC and NOESY spectra of **MS-19**

The HMBC and COSY spectra enabled the structure of the kaurane diterpene to be completed. Methyl-20 (δ_H 0.98) appeared as a singlet and gave a ^2J correlation to a quaternary carbon (δ_C 40.6, C-10), placing this at the ring junction of the molecule. Methyl-20 also gave ^3J signals to C-1, C-5 and C-9. COSY correlations between the methylene protons H_2-1, H_2-2 and H_2-3 placed these groups here. Ring A was completed by placing a quaternary carbon at C-4 (δ_C 45.2). This was confirmed by a second methyl singlet (δ_H 1.23, H_3-18), which gave a ^2J signal to C-4 and ^3J signals to C-3 and C-5. Methyl-18 also gave a ^3J signal to C-19 (δ_C 178.5) placing the carbonyl carbon adjacent to C-4. The more deshielded anomeric proton (δ_H 5.42, H-1') showed a ^3J correlation to C-19 indicating the hexose residue is attached *via* the oxygen atom of the carboxyl group. The methine proton H-5 showed a ^2J signal to C-6 with H_2-6 in turn exhibiting a COSY correlation to H_2-7. H_2-7 also gave a ^3J correlation to C-9, and a ^2J correlation from H-9 to a quaternary carbon C-8 completed ring B. H-9 gave HMBC signals to C-11, C-12 and C-14 confirming its position at the ring junction of rings B and C. C-12 was a methylene group which gave a COSY signal to a methine proton (δ_H 2.55 bs, H-13), which in turn gave a COSY signal to H_2-14, completing ring C. The methine proton also gave a ^2J correlation to an olefinic quaternary carbon (δ_C 157.5, C-16) which was also correlated to by the protons of an *exo*-methylene group (δ_H 4.93 and δ_H 5.30, H_2-17), placing this group at C-16. The *exo*-methylene protons also showed a ^3J signal to an oxymethine group (δ_C 91.7, C-15) which was connected to C-8. This was further corroborated by ^3J signals from H-9 and H_2-14 to C-15, completing ring D of the kaurane molecule. A second hexose residue was attached at C-15 by an ether link, based on a ^3J correlation from the second, more upfield anomeric proton (δ_H 4.44, H-1''). It was not possible to determine the nature of the hexose residues from the NMR data acquired due to signal overlap. However, hydrolysis of the hexose residues from the aglycone moiety followed by GC-MS analysis enabled the identification to be made as glucose in both cases.

The relative stereochemistry of this compound was assigned by NOE's from the NOESY spectrum. The methyl protons H_3-20 showed NOE's to H_2-1α, H_2-2α, H-5 and H_2-14α, with respect to ring C, indicating that the methyl group is α-oriented. Methyl-18 showed NOE's to H_2-3 and H_2-6, implying that this group should be β-orientated whilst the carbonyl must be α-oriented. H-9 exhibited a 1,3 interaction with H_2-12β, thus placing this proton in a β-orientation. Paniculoside V (= crispioside A)

has previously been isolated from *Francoeuria crispa* (= *Pulicaria crispa*) (Abdel-Mogib *et al.*, 1990) and *Stevia paniculata* (Asteraceae) (Yamasaki *et al.*, 1977) and the NMR data for **MS-19** was in close agreement with the literature values published.

Table 19 ^{1}H and ^{13}C NMR data and ^{1}H-^{13}C long-range correlations of **MS-19** recorded in CD_3OD

Position	^{1}H	^{13}C	^{2}J	^{3}J
1	0.94 dt (14.0, 4.5)	41.8	C-2	C-5, C-9, C-20
	1.90 m			
2	1.87 m	20.3	C-3	C-10
3	1.09 dt (13.5, 4.0)	39.1	C-2, C-4	C-19
	2.19 bd (12.5)			
4	-	45.2		
5	1.22 d (12.0)	57.7	C-4, C-6	C-20
6	2.00 m	22.6	C-5	
7	1.29 d (13.0)	39.3	C-6	C-5, C-9
	1.96 m			
8	-	47.2		
9	1.58 d (8.0)	47.4	C-8, C-10, C-11	C-1, C-7, C-12, C-14, C-15, C-20
10	-	40.6		
11	1.46 m	19.0	C-9, C-12	C-8, C-10, C-13
	1.74 m			
12	1.44 m	34.7	C-11, C-13	C-9, C-14, C-16
	1.65 bdt (12.5, 3.0)			
13	2.55 bs	41.8	C-16	C-8
14	1.02 dd (12.5, 5.0)	37.5	C-8, C-13	C-9, C-12, C-15, C-16
	2.10 d (12.0)			
15	3.85 m	91.7		
16	-	157.5		
17	4.93 d (2.5)	106.3	C-16	C-13, C-15
	5.30 s			
18	1.23 s	29.1	C-4	C-3, C-5, C-19
19	-	178.5		
20	0.98 s	16.7	C-10	C-1, C-5, C-9
1'	5.42 d (8.0)	95.6		C-19
2'	3.35 m	74.1		
3'	3.41 m	78.7		
4'	3.40 m	71.1		
5'	3.41 m	78.7		
6'	3.70 dd (12.0, 4.5)	62.4		
	3.85 m			
1"	4.44 d (8.0)	106.3		C-15
2"	3.27 m	75.5		
3"	3.35 m	78.4		
4"	3.38 m	71.6		
5"	3.26 m	77.6		
6"	3.76 dd (11.5, 5.0)	62.9		
	3.89 dd (11.5, 2.5)			

3.5 Triterpenes and sterols

3.5.1 Characterisation of MS-20 as β-sitosterol

MS-20 was isolated from the hexane extract of *I. pes-caprae* as a colourless oil and the ^{1}H and ^{13}C NMR spectra suggested a molecular formula of $C_{29}H_{50}O$. **MS-20** was identified as β-sitosterol by comparison of the ^{1}H and ^{13}C NMR data with that of the literature (Horibe *et al.*, 1989; Matsumoto *et al.*, 1983) for this compound.

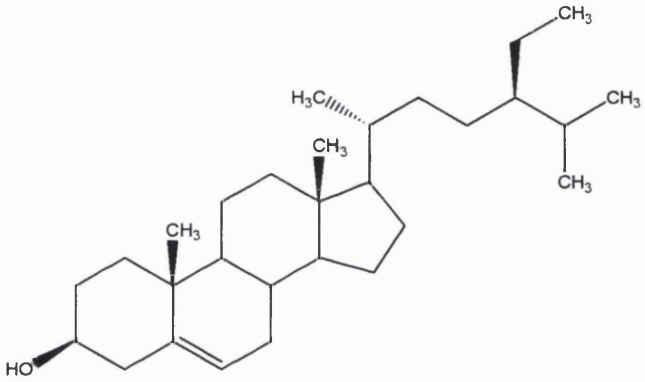

Figure 3.5.1A Structure of **MS-20**

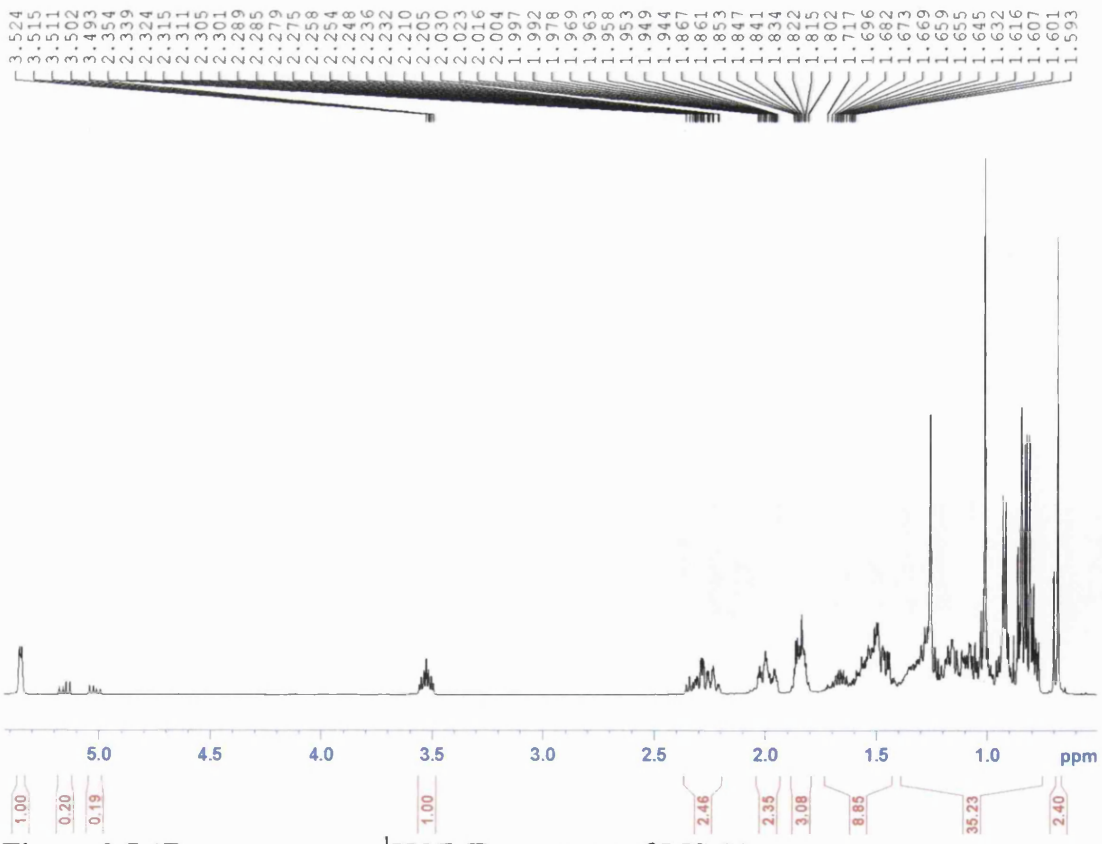

Figure 3.5.1B ^{1}H NMR spectrum of **MS-20**

3.5.2 Characterisation of MS-21 as lupeol

MS-21 was also isolated from the hexane extract of *I. pes-caprae*. It was purified as a colourless oil and a molecular formula of $C_{30}H_{50}O$ was proposed from the ^{1}H and ^{13}C NMR data. The ^{1}H NMR spectrum provided signals for an *exo*-methylene (δ_H 4.69 and δ_H 4.57) along with a downfield methyl appearing as a singlet (δ_H 1.68), which is indicative of an isopropenyl group present in the structure (Gibbons 1994). The ^{1}H (methyl and *exo*-methylene groups) and ^{13}C NMR data for **MS-21** when compared favourably with the literature for lupeol were in close agreement (Goad and Akihisa 1997; Sholichin *et al.*, 1980).

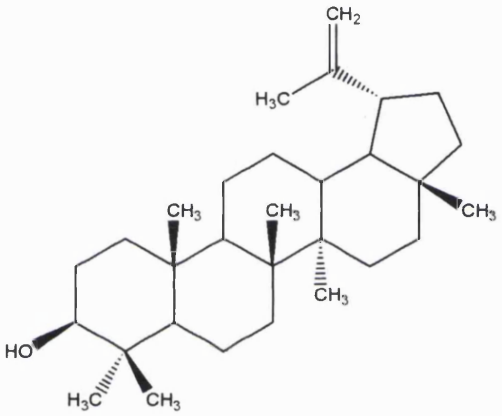

Figure 3.5.2A Structure of **MS-21**

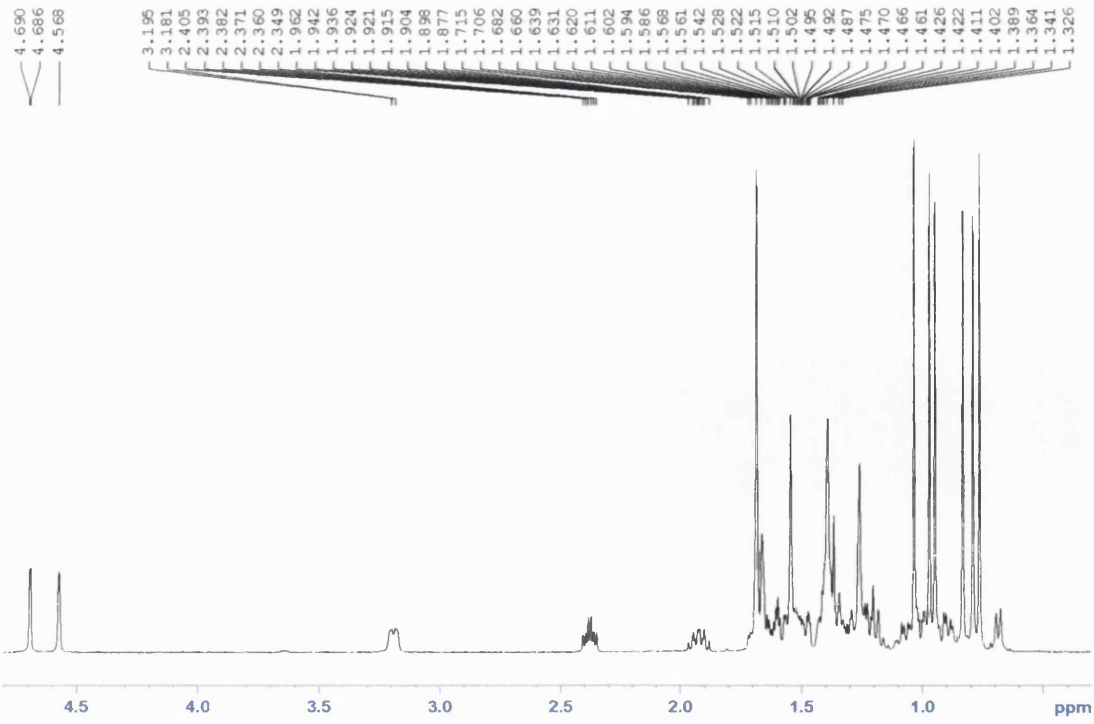

Figure 3.5.2B ^{1}H NMR spectrum of **MS-21**

3.5.3 Characterisation of MS-22 as α-amyrin

The ^{1}H and ^{13}C NMR spectra indicated a molecular formula of $C_{30}H_{50}O$. This compound was isolated as a colourless oil from the hexane extract of *I. pes-caprae*. The ^{1}H NMR spectrum exhibited a signal for an olefinic proton (δ_H 5.12 t, $J = 4.0$ Hz, H-12) and two olefinic carbons (δ_C 124.3, C-12 and 139.3, C-13) in the ^{13}C NMR spectrum. The 1D spectra provided signals for 6 quaternary carbons and 8 methyl groups, of which six appeared as singlets and two as doublets. The NMR data acquired for **MS-22** correlated closely with that of the literature for α-amyrin (Goad and Akihisa 1997; Seo *et al.*, 1981), and **MS-22** is therefore assigned as α-amyrin.

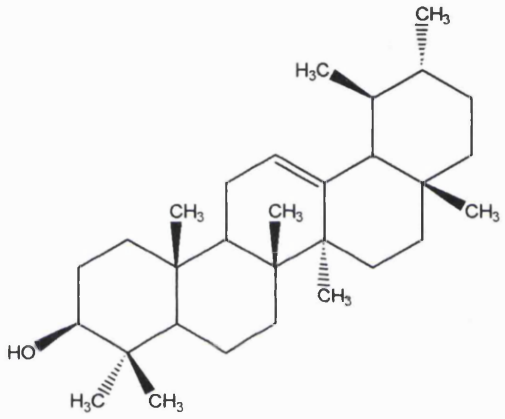

Figure 3.5.3A Structure of **MS-22**

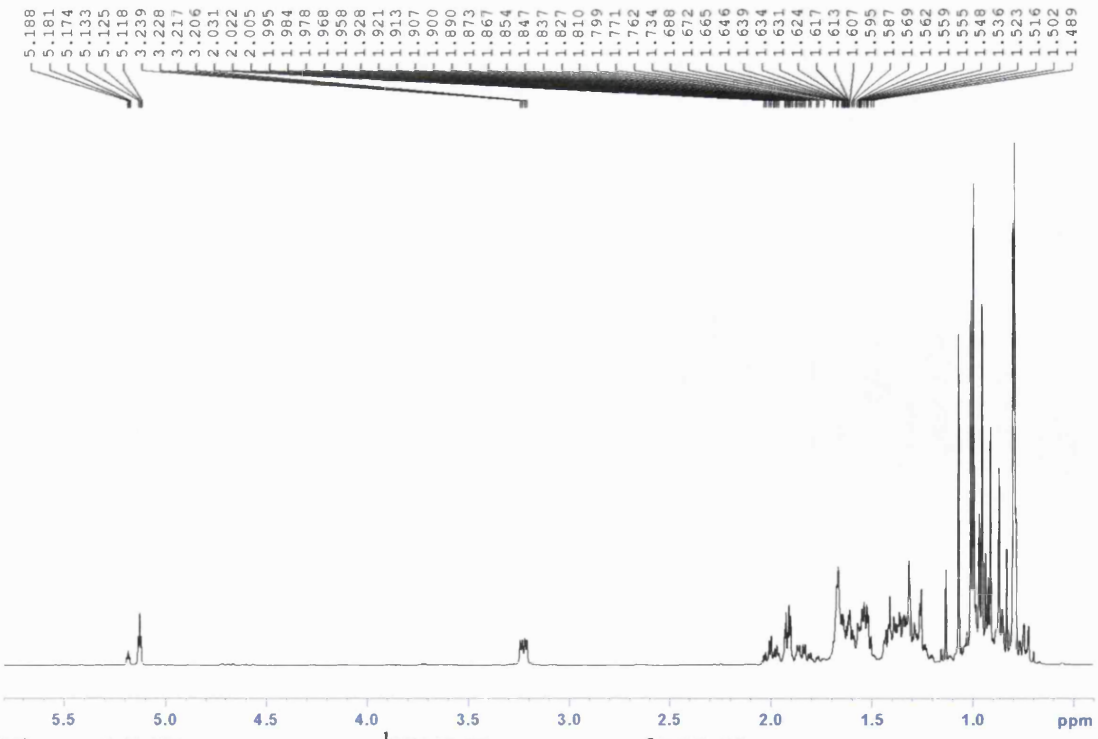

Figure 3.5.3B ^{1}H NMR spectrum of **MS-22**

3.5.4 Biosynthesis of sterols and triterpenes

Steroids and triterpenes are derived from the same C_{30} precursor, squalene (Mann 1996). The 'building blocks' for this precursor are the C_5 isoprenoids, isopentenyl pyrophosphate (IPP) and dimethylallyl pyrophosphate (DMAPP). Two farnesyl pyrophosphate units joined in an unusual 'head-to-head' manner are required for squalene biosynthesis (Mann 1996). Labelling experiments have shown that mevalonate is the preferred precursor for both sterol and pentacyclic triterpene biosynthesis rather than deoxyxylulose (Flores-Sanchez *et al.*, 2002). The polycyclic structures formed from squalene are initiated by acid-catalysed ring opening of 2,3-oxidosqualene (Mann 1996). The cyclisation of 2,3-oxidosqualene, which is in the 'chair-boat-chair-boat' conformation, leads to the production of a protosteryl cation **(Scheme 4A)**. In plants, this is then converted to cycloartenol by cycloartenol synthase.

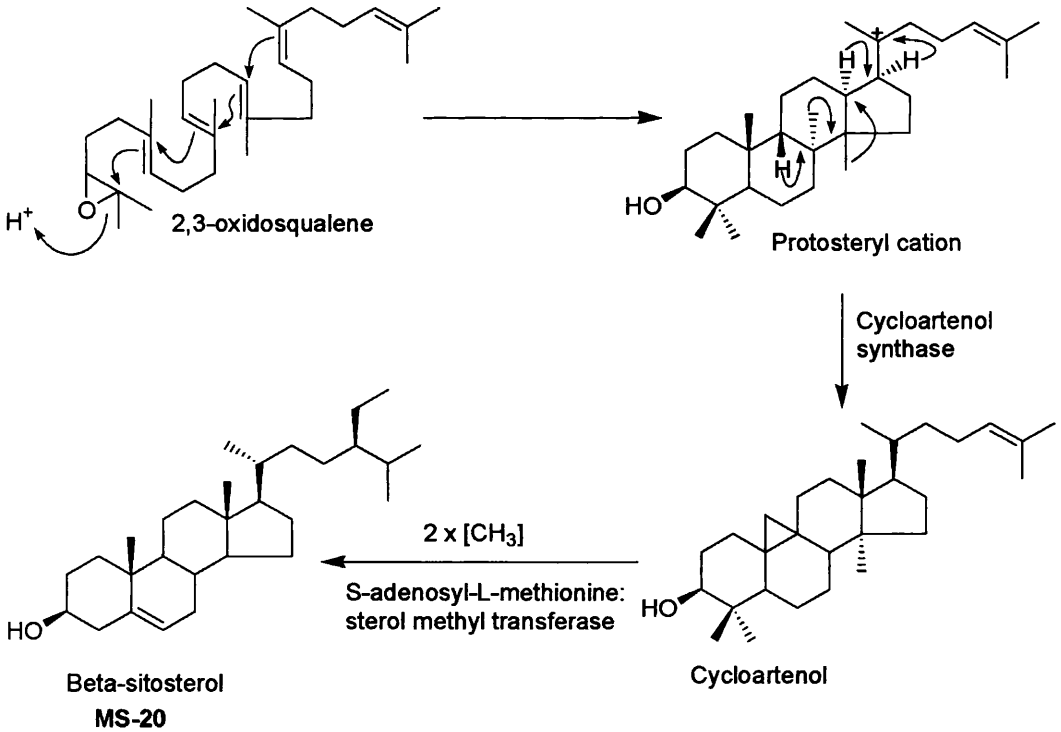

Scheme 4A Biosynthesis of β-sitosterol (MS-20) from 2,3-oxidosqualene. Adapted from Gibbons (1994).

The triterpenes, such as lupeol (Path A: lupane series) and α-amyrin (Path B: amyrin series), are produced *via* the dammarenyl cation, which is in the 'chair-chair-chair-boat' conformation. It is also the intermediate for the production of dammarene-like triterpenes.

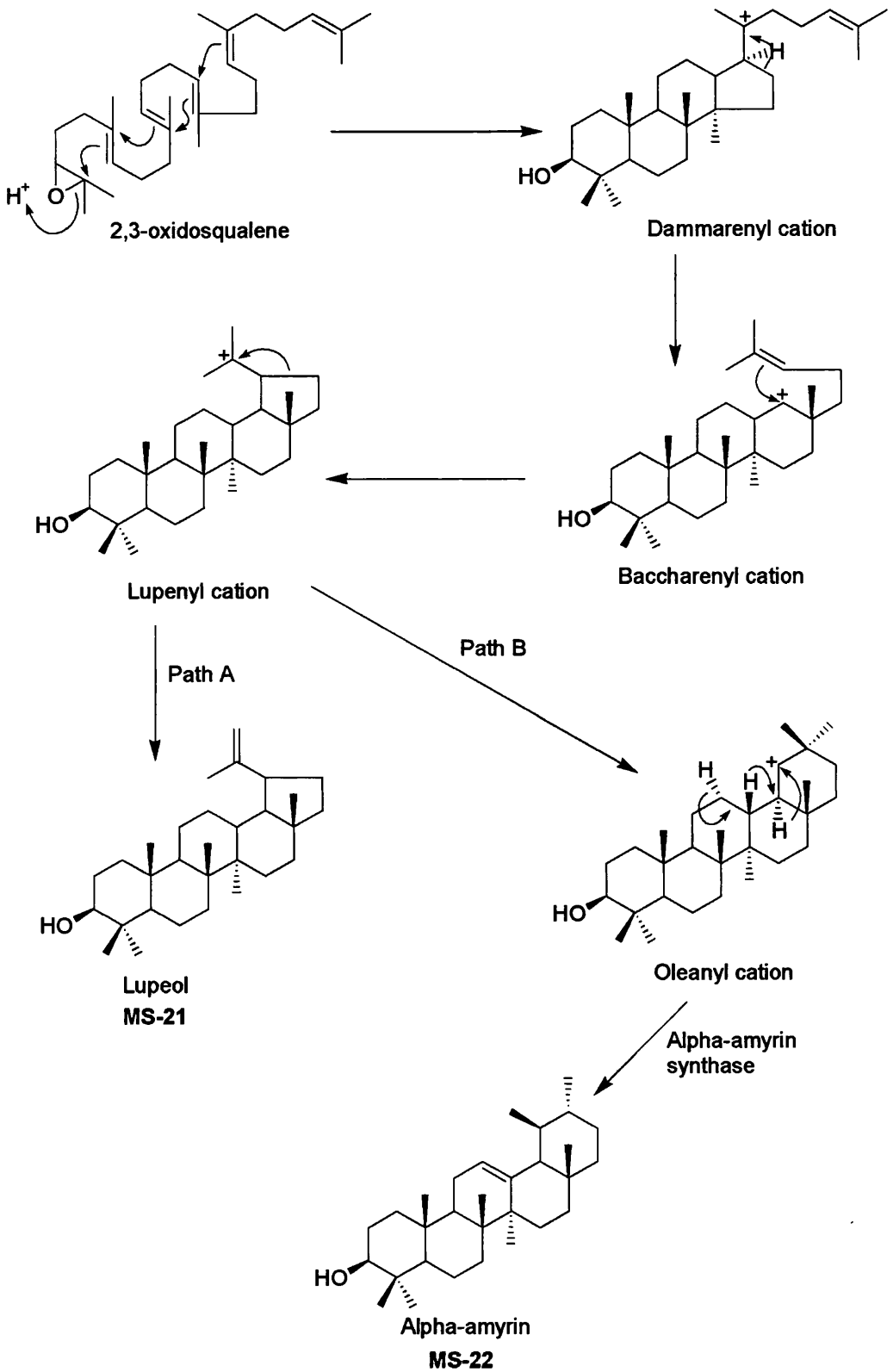

Scheme 4B **Biosynthesis of lupeol (MS-21) and α-amyrin (MS-22) from 2,3-oxidosqualene. Adapted from Haralampidis *et al.*, (2002).**

3.6 Polyacetylenes

3.6.1 Characterisation of MS-23 as falcarindiol

MS-23 was isolated as a pale yellow oil from the hexane extract of *A. graveolens*. The ^{13}C NMR spectrum provided four quaternary carbon signals at δ_C 68.7, 70.3, 78.2, 79.8 ppm. These signals are characteristic for the polyacetylene natural product class (Bernart *et al.*, 1996). This was corroborated by a weak absorption at 2235 cm^{-1} in the infrared spectrum, which is also characteristic of an alkyne (Williams and Fleming 1995). The presence of four signals indicates there are two alkyne bonds within this molecule. The ^1H spectrum also provided signals for a vinyl group (δ_H 5.27 dt, 5.49 dt H_2-1 and δ_H 5.94 ddd, H-2), two oxymethines (δ_H 4.94 dd, H-3 and δ_H 5.21 d, H-8) and two olefins (δ_H 5.53 dt, H-9 and δ_H 5.62 dt, H-10).

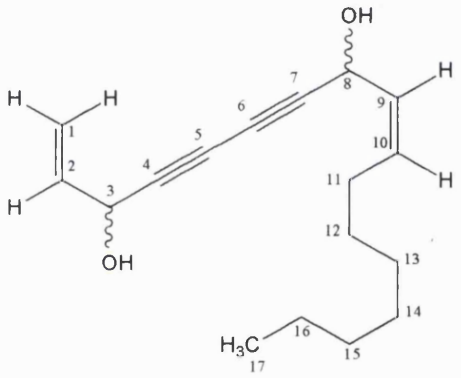

Figure 3.6.1A Structure of **MS-23**

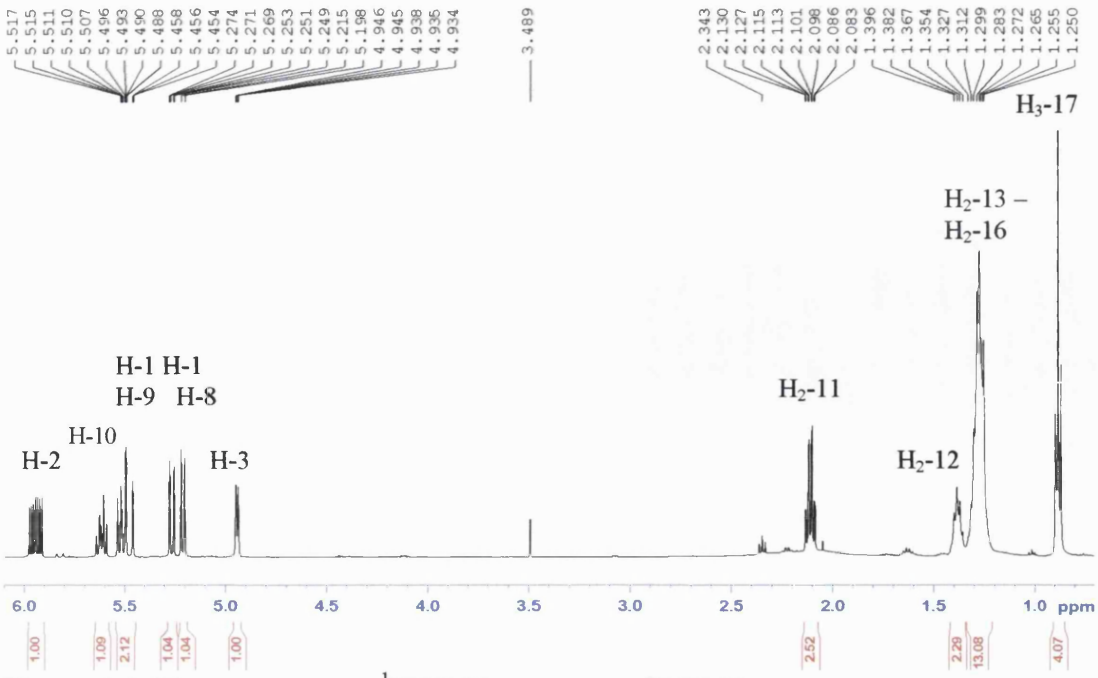

Figure 3.6.1B ^1H NMR spectrum of **MS-23**

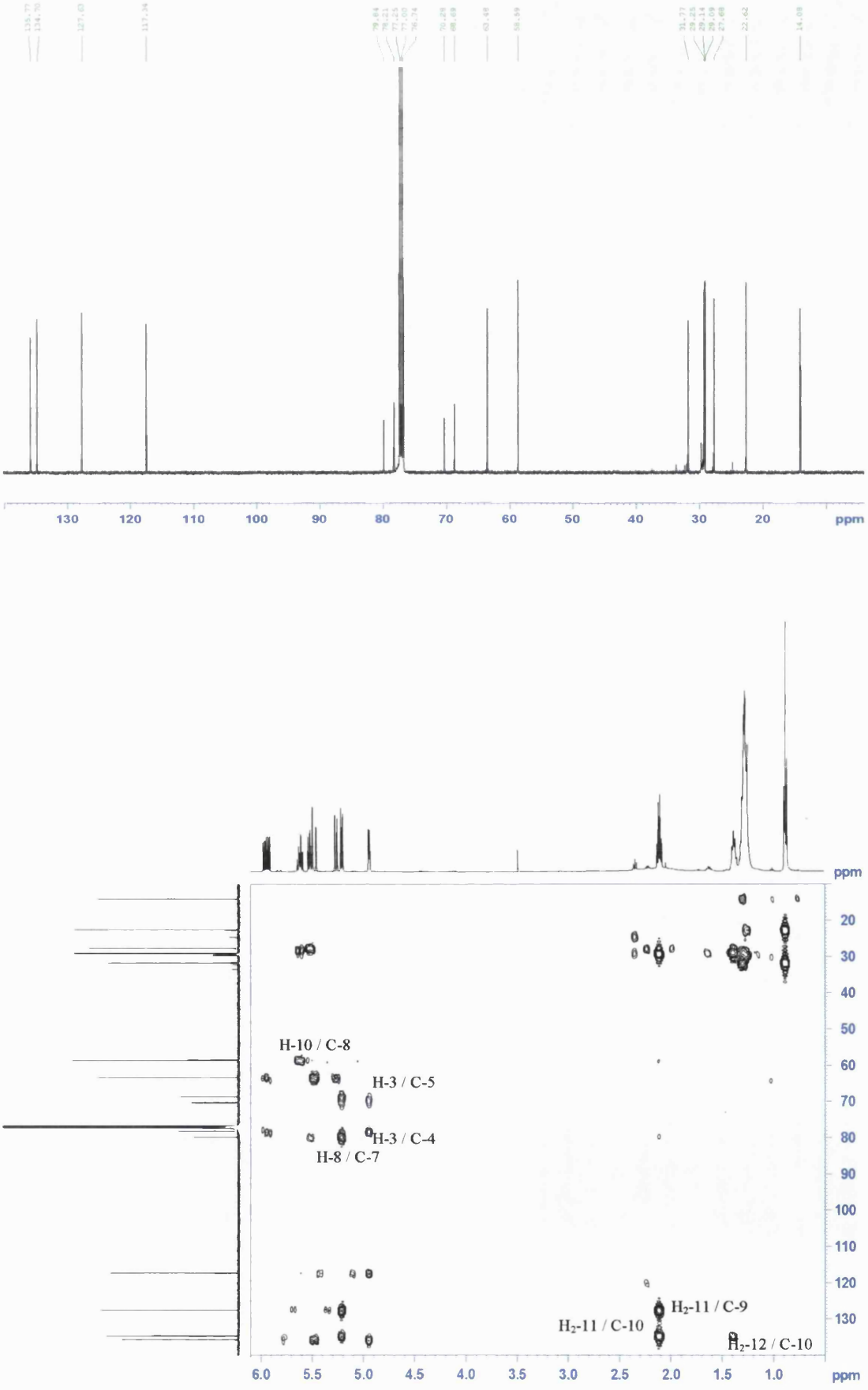

Figure 3.6.1C ^{13}C NMR and HMBC spectra of **MS-23**

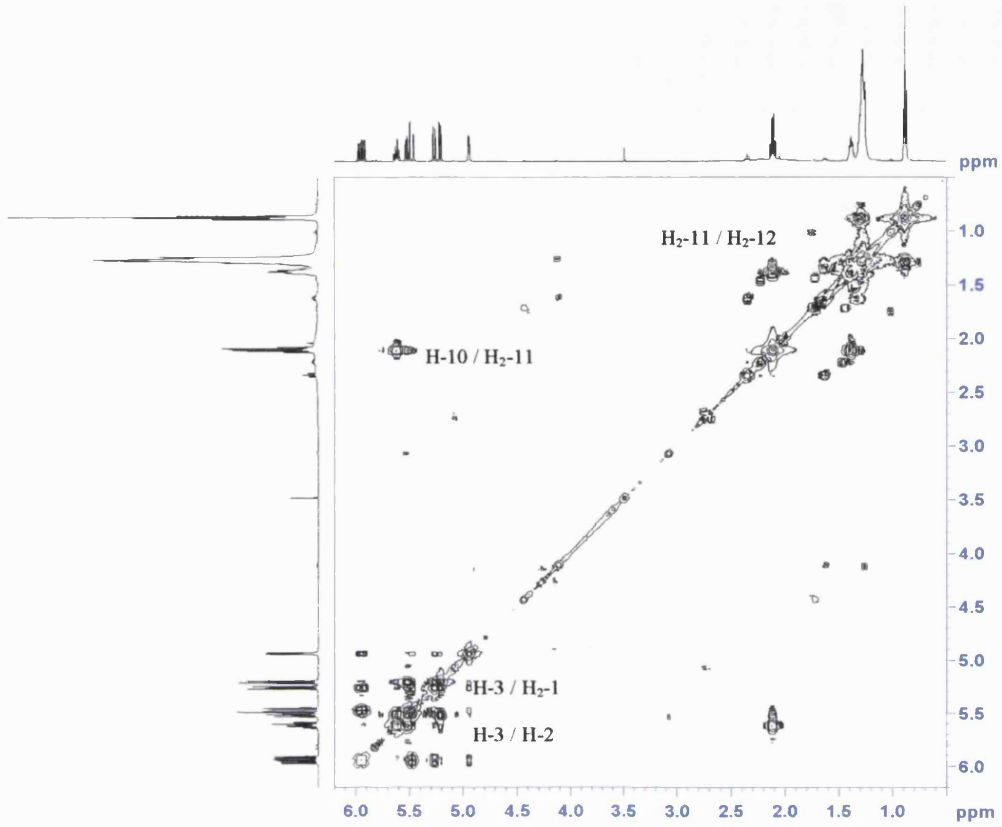

Figure 3.6.1D COSY spectrum of **MS-23**

The *exo*-methylene of the vinyl group showed a COSY correlation to its olefinic partner, which in turn gave a signal to one of the oxymethines (δ_H 4.94, H-3). This was confirmed by ^2J and ^3J correlations in the HMBC spectrum between these three groups. H_2-1 also gave a long range COSY correlation to H-3. The oxymethine proton displayed ^2J and ^3J signals to two of the acetylenic carbons (δ_C 78.2, C-4 and δ_C 70.3, C-5) placing them here. The second oxymethine proton (H-8) gave HMBC signals to the remaining acetylenic carbons (C-6 and C-7) as well as to two olefinic carbons (C-9 and C-10). The olefinic proton H-9 also gave a ^3J signal to C-7. Due to the shielded nature of these acetylenic carbons and the lack of any other signals towards them, this implies that these carbons are conjugated. COSY correlations between H-8, H-9 and H-10 confirmed the position of these groups within the molecule. A further coupling between H-10 and the most downfield methylene protons placed this group at H_2-11. The COSY spectrum showed that these protons coupled to methylene protons at δ_H 1.38 (H_2-12) which in turn coupled to the methylene envelope at δ_H 1.27, which contained four methylene groups. A terminal methyl group (δ_H 0.88 t, H_3-17) completed the diacetylenic molecule, exhibiting signals towards the methylene envelope. The data was consistent with that of the

literature for this compound (Furumi *et al.*, 1998), confirming the isolation of the C_{17} polyacetylene, falcarindiol. Due to a paucity of falcarindiol, the absolute stereochemistry at C-3 and C-8 could not be determined. However, a positive specific rotation ($[\alpha]_D^{23}$ +72.6°) enabled two of the four stereoisomers to be dispelled leaving two possible stereoisomers. The literature describes 3*S*,8*S*-falcarindiol as having a positive specific rotation (Bernart *et al.*, 1996; Kobaisy *et al.*, 1997), whilst the 3*R*,8*S* stereoisomer has been described as having a negative specific rotation ($[\alpha]_D^{25}$ -130°) (Lechner *et al.*, 2004). The alternative laevoisomer must therefore be the 3*R*,8*R* enantiomer, which has previously been described as dextrorotatory (Lechner *et al.*, 2004). The dextrorotatory falcarindiol corresponds to the 3*S*,8*S* stereoisomer, therefore the alternative dextroisomer must be the 3*S*,8*R* stereoisomer. This enables the stereochemistry of **MS-23** at positions 3 and 8 to be assigned as either the 3*S*,8*S* or 3*S*,8*R* stereoisomer.

Table 20 ^1H and ^{13}C NMR data and ^1H-^{13}C long-range correlations of **MS-23** recorded in $CDCl_3$

Position	^1H	^{13}C	^2J	^3J
1	5.27 dt (10.5, 1.5) 5.49 dt (17.0, 1.5)	117.3	C-2	C-3
2	5.94 ddd (17.0, 10.0, 5.5)	135.8	C-3	C-4
3	4.94 dd (5.5, 0.5)	63.5	C-2, C-4	C-1, C-5
4	-	78.2		
5	-	70.3		
6	-	68.7		
7	-	79.8		
8	5.21 d (8.5)	58.6	C-7, C-9	C-6, C-10
9	5.53 dt (8.5, 1.5)	127.6		C-7, C-11
10	5.62 ddt (11.0, 8.0, 1.5)	134.7	C-11	C-8
11	2.11 ddd (15.0, 7.5, 1.5)	27.7	C-10, C-12	C-9, C13
12	1.38 m	29.1	C-13	C-10, C14
13	1.27 m	29.3		
14	1.27 m	29.1		
15	1.27 m	31.8		
16	1.27 m	22.6		
17	0.88 t (7.0)	14.1	C-16	C-15

3.6.2 Characterisation of MS-24 as 3*R*,8*R*-16,17-dehydrofalcarindiol

MS-24 was isolated as a pale yellow oil from the hexane extract of *A. monosperma*. A molecular formula of $C_{17}H_{22}O_2$ was established by ESI-MS in the positive mode $[M+H]^+$ (259.0). This compound showed good similarity with falcarindiol with respect to both ^1H and ^{13}C NMR spectra. **MS-24** differed from falcarindiol as it exhibited signals indicating the presence of two vinyl groups. This accounted for the presence of two downfield methylene groups at δ_H 2.05, H_2-15 and δ_H 2.11, H_2-11. The four acetylenic carbons, two remaining olefins and two oxymethine groups were also present.

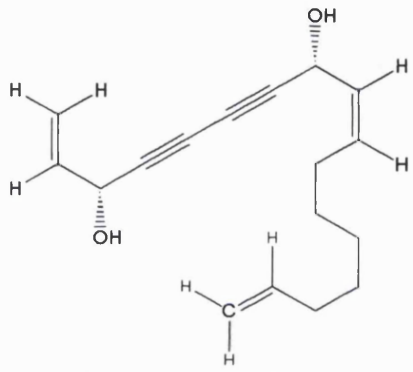

Figure 3.6.2A Structure of **MS-24**

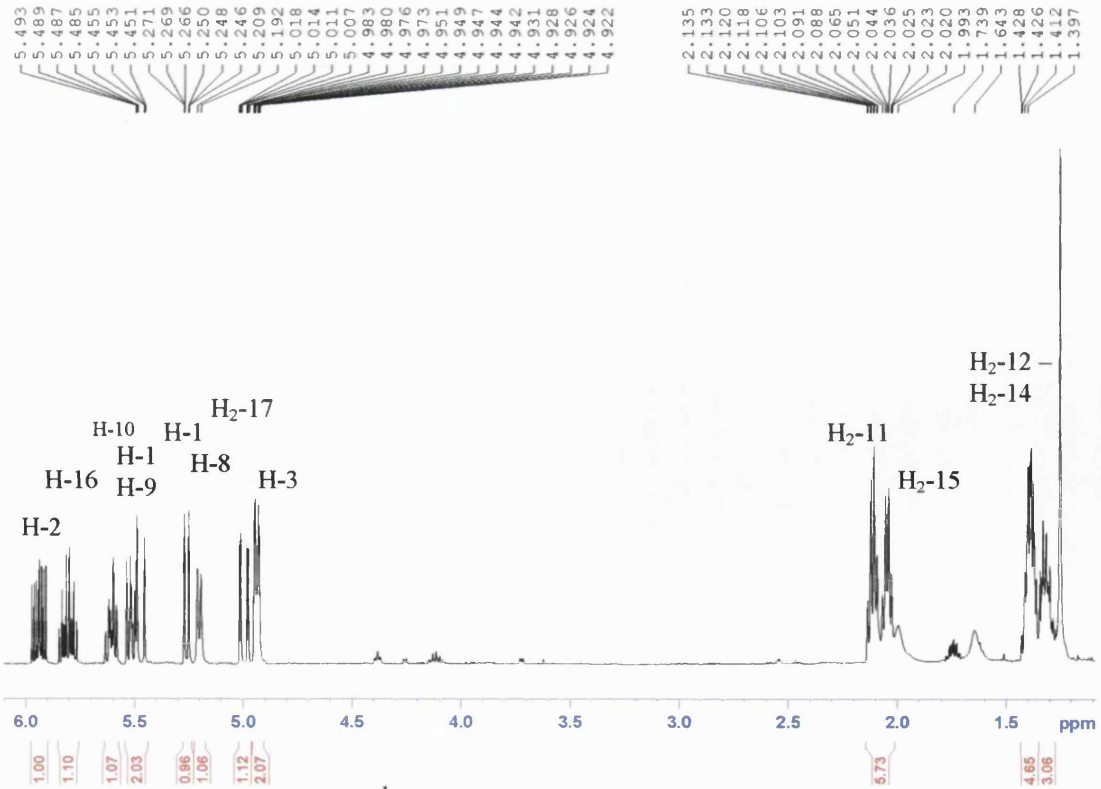

Figure 3.6.2B ^1H NMR spectrum of **MS-24**

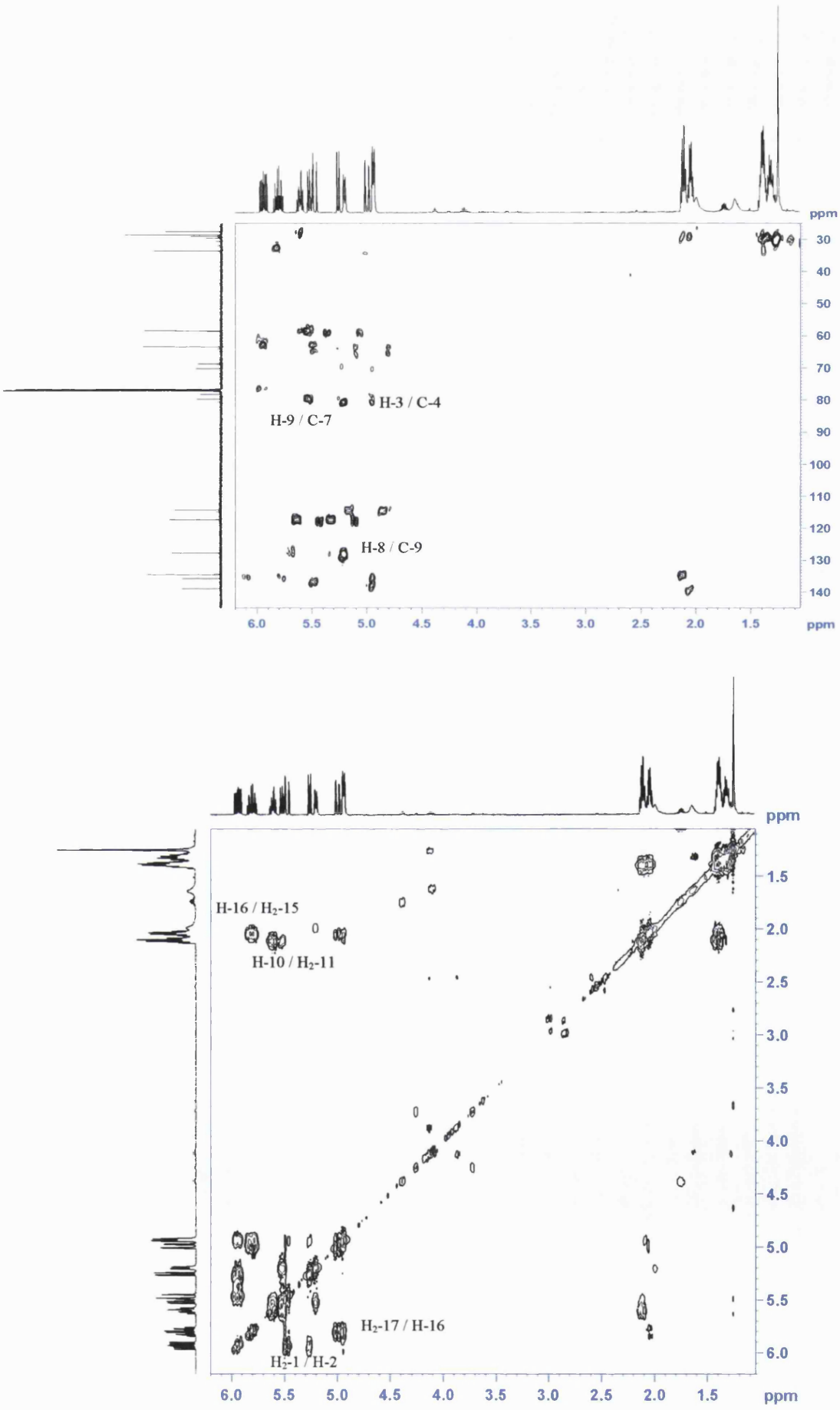

Figure 3.6.2C HMBC and COSY spectra of **MS-24**

The COSY spectrum showed a correlation between H_2-17 (δ_H 5.00 dd, δ_C 114.3, C-17) and H-16 (δ_H 5.81 ddt, δ_C 139.0, C-16), which in turn coupled to a downfield methylene (δ_H 2.05 m, δ_C 33.7, C-15). These protons also exhibited a long range correlation to the *exo*-methylene protons as well as an upfield methylene group (δ_H 1.38, H_2-14). The remainder of the molecule was identical to falcarindiol and similar signals in both the HMBC and COSY spectra enabled the assignments to be made for the same reasons as for the aforementioned compound. **MS-24** was therefore assigned as 16,17-dehydrofalcarindiol and the NMR data correlated closely to that published for this compound (Bernart *et al.*, 1996). The absolute stereochemistry of **MS-24** was determined by Mosher's ester methodology, by esterifying the two hydroxyl groups attached to the chiral carbons with either *R*- or *S*-MPA (methoxyphenylacetic acid). The $\delta\Delta^{R,S}$ values (δ_R-δ_S) for H_2-1 and H-2 and also H-9 and H-10 were positive, indicating *R*-stereochemistry at both C-3 and C-8. This is the first report of the absolute stereochemistry of 16,17-dehydrofalcarindiol assigned as 3*R*,8*R*.

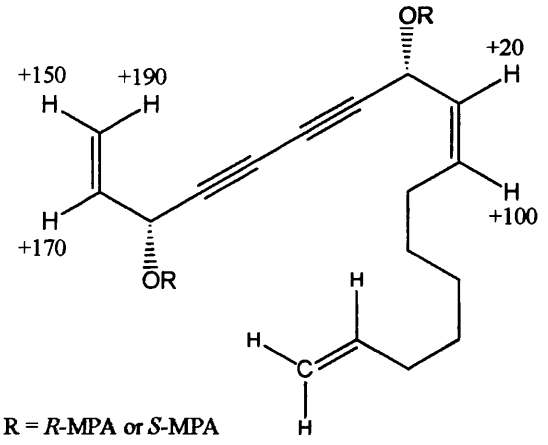

Figure 3.6.2D Δδ values [Δδ (in ppb) = $\delta_R - \delta_S$] obtained for the (*R*)- and (*S*)-MPA esters of **MS-24**

Table 21 ^{1}H and ^{13}C NMR data and ^{1}H-^{13}C long-range correlations of **MS-24** recorded in $CDCl_3$

Position	^{1}H	^{13}C	^{2}J	^{3}J
1	5.25 dt (10.5, 1.0)	117.3	C-2	C-3
	5.45 dt (17.0, 1.0)			
2	5.93 ddd (17.0, 10.5, 1.5)	135.8	C-3	
3	4.93 m	63.5	C-2, C-4	C-1, C-5
4	-	78.3		
5	-	70.3		
6	-	68.7		
7	-	79.8		
8	5.20 d (8.5)	58.6	C-7, C-9	C-6, C-10
9	5.53 ddt (10.5, 8.5, 1.0)	127.8	C-8	C-7
10	5.61 ddt (10.5, 7.5, 1.0)	134.5		C-8
11	2.11 m	27.6	C-10	C-9
12	1.38 m	29.1	C-13	C-10, C-14
13	1.33 m	28.7	C-12, C-14	
14	1.38 m	28.6	C-13	C-12, C-16
15	2.05 m	33.7	C-16	C-17
16	5.81 ddt (17.0, 10.0, 7.0)	139.0		
17	4.95 m	114.3	C-16	C-15
	5.00 dd (17.5, 1.5)			

3.6.3 Characterisation of MS-25 as 16,17-dehydrofalcarinol

MS-25 was isolated as a yellow oil from the chloroform extract of *A. monosperma*. The ^{1}H and ^{13}C NMR spectra were almost identical to that of 16,17-dehydrofalcarindiol. The only difference between the spectra of these two compounds being the presence of a downfield methylene group (δ_H 3.02 d, δ_C 17.7, C-8) instead of an oxymethine group (δ_H 5.21 d, δ_C 58.6, C-8) found in 16,17-dehydrofalcarindiol.

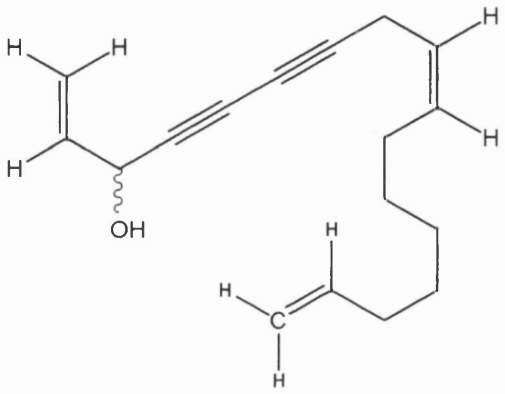

Figure 3.6.3A Structure of **MS-25**

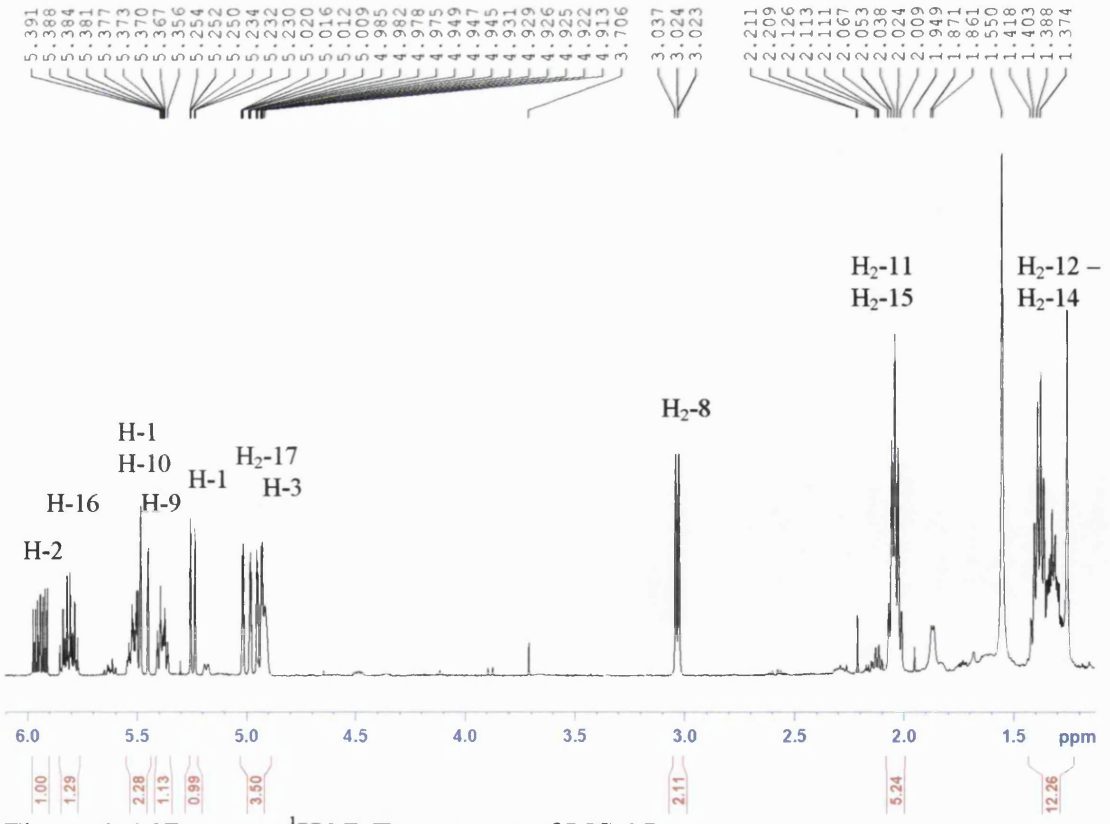

Figure 3.6.3B ^{1}H NMR spectrum of **MS-25**

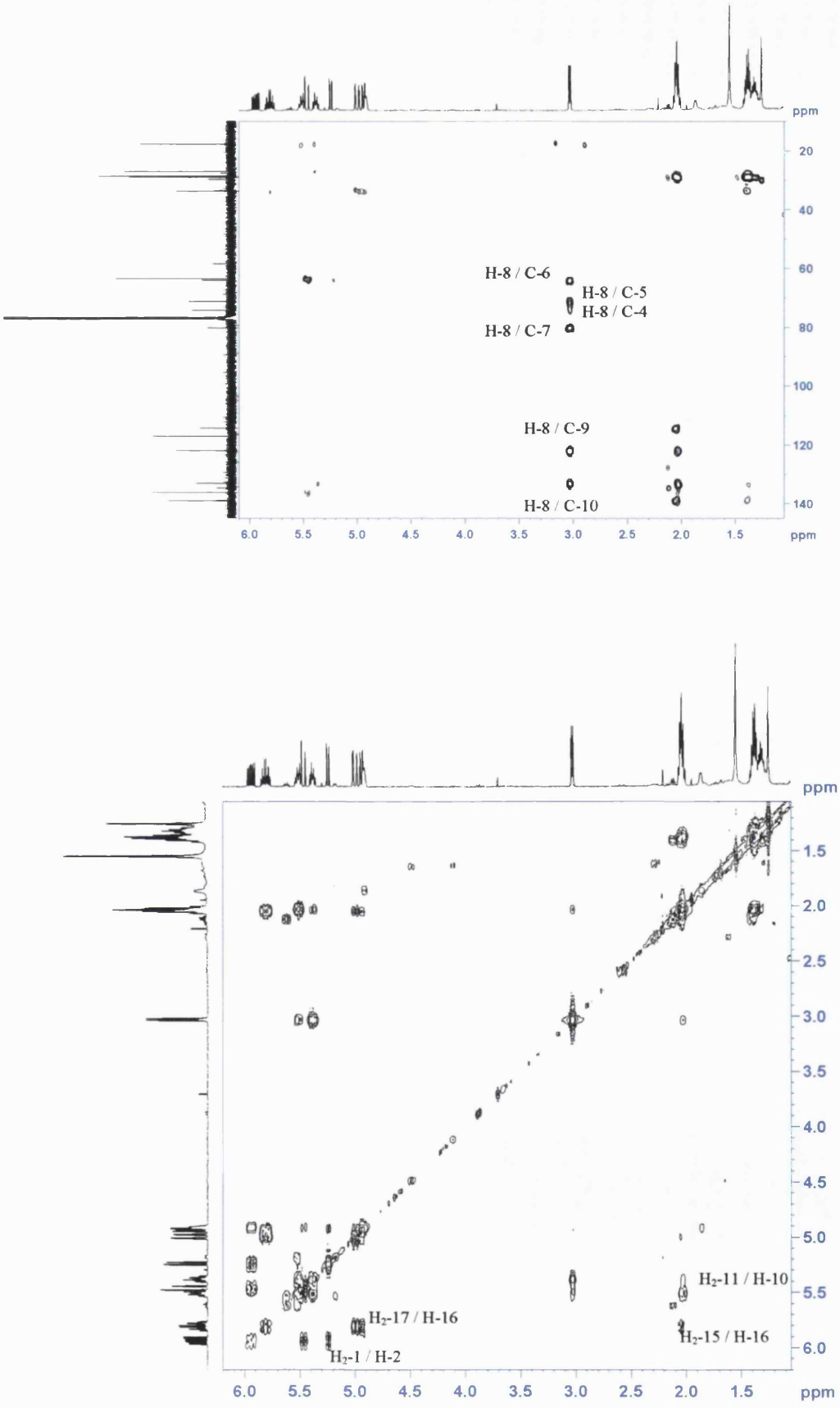

Figure 3.6.3C HMBC and COSY spectra of **MS-25**

The COSY spectrum clearly shows a coupling between H_2-8 and the olefinic proton H-9, with a coupling constant of 7.0 Hz, as well as a long range coupling to H-10. The HMBC provided ^2J and ^3J correlations between H_2-8 and the acetylenic carbons at C7 and C-6 respectively. This confirms the positioning of the methylene group here. The HMBC spectrum yielded similar signals as those detected for 16,17-dehydrofalcarindiol. The COSY spectrum further supports the assignments for 16,17-dehydrofalcarinol and the NMR data for this compound was in close agreement with that published (Bernart *et al.*, 1996).

Table 22 ^1H and ^{13}C NMR data and ^1H-^{13}C long-range correlations of **MS-25** recorded in $CDCl_3$

Position	^1H	^{13}C	^2J	^3J
1	5.23 d (10.0)	117.0		C-3
	5.46 d (17.5)			
2	5.92 ddd (17.0, 10.0, 5.5)	136.1		
3	4.92 dd (10.5, 1.0)	63.6		
4	-	74.2		
5	-	71.3		
6	-	64.0		
7	-	80.2		
8	3.02 d (7.0)	17.7	C-7, C-9	C-6, C-10
9	5.37 ddt (10.5, 7.0, 1.5)	122.0	C-8	C-11
10	5.51 ddt (10.5, 7.5, 1.5)	133.0		C-8
11	2.04 m	27.1	C-10, C-12	C-9, C-13
12	1.29 m	28.8	C-13	C-14
13	1.35 m	28.7	C-12, C-14	
14	1.23 m	29.1		
15	2.04 m	33.7	C-14, C-16	C-13, C-17
16	5.79 ddt (17.0, 10.5, 6.5)	139.0	C-15	
17	4.96 m	114.3		C-15
	5.00 d (17.0, 2.0)			

3.6.4 Characterisation of MS-26 as 1,3*R*,8*R*-trihydroxydec-9-en-4,6-yne

MS-26 was isolated as a colourless oil from the chloroform extract of *A. monosperma*. A molecular formula of $C_{10}H_{12}O_3$ was established by HREIMS *m/z* 180.0788. The ^1H and ^{13}C spectra provided signals for an *exo*-methylene (δ_H 5.19 and δ_H 5.40, H_2-10), an olefinic proton (δ_H 5.91, H-9), two oxymethine protons (δ_H 4.56, H-3 and δ_H 4.88, H-8), a methylene group (δ_H 1.89, H_2-2) and an oxymethylene group (δ_H 3.70, H_2-1). This was in addition to four acetylenic quaternary carbons, which gave similar resonances to the polyacetylenes already discussed. The presence of these acetylenic carbons was confirmed by a weak absorption at 2357 cm^{-1} in the IR spectrum.

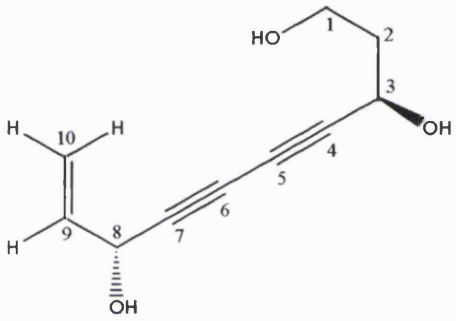

Figure 3.6.4A Structure of **MS-26**

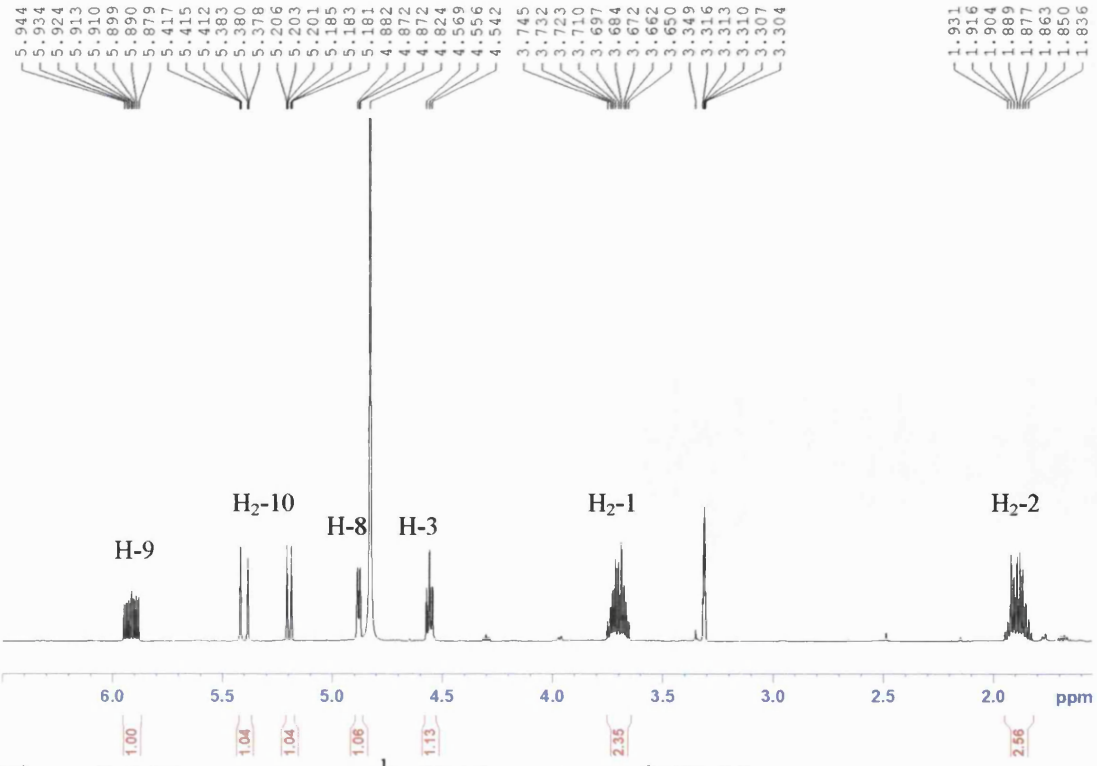

Figure 3.6.4B ^1H NMR spectrum of **MS-26**

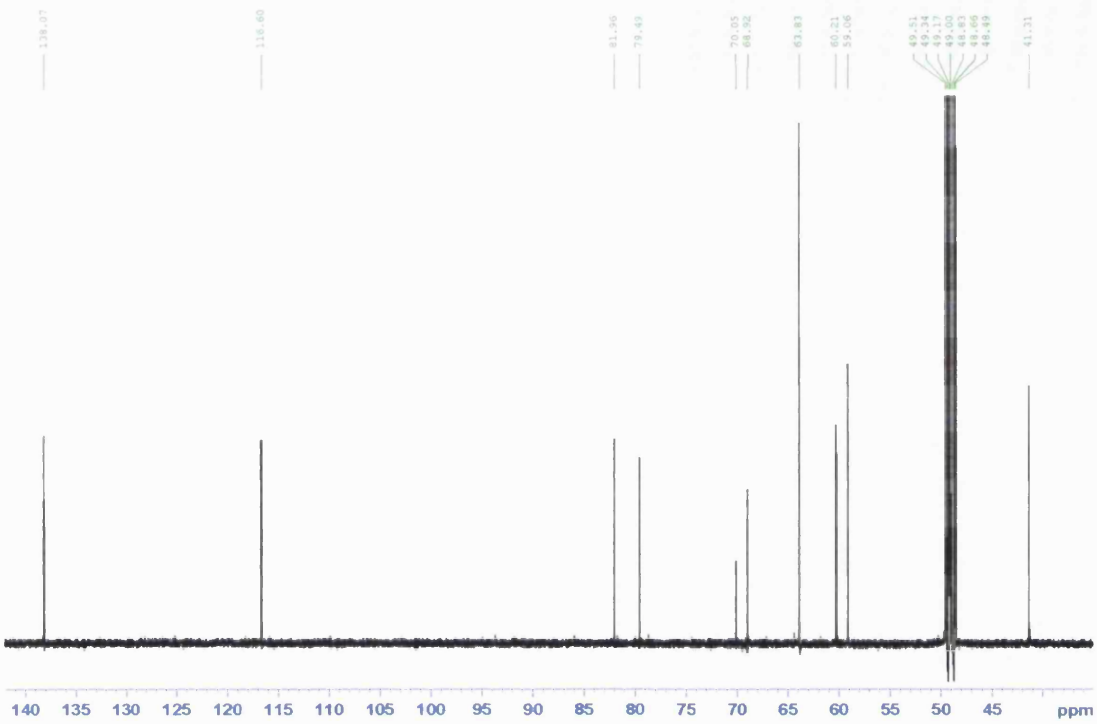

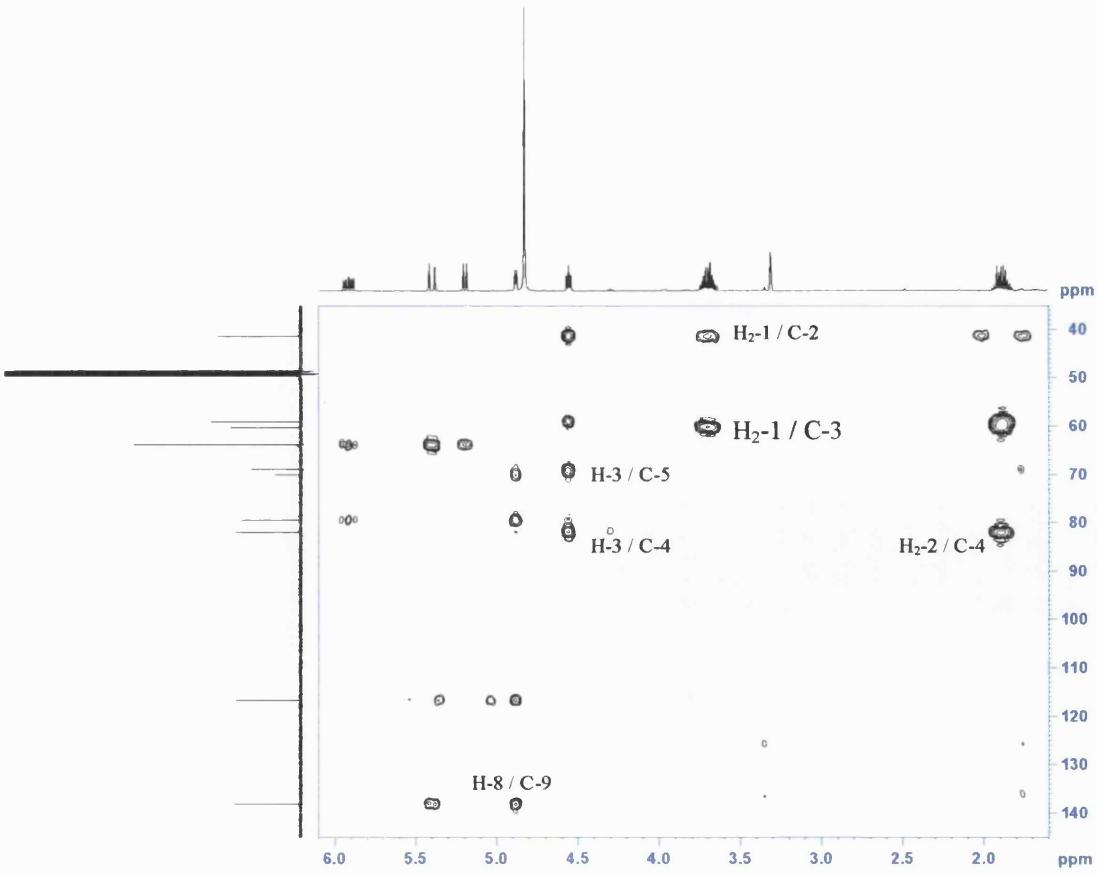

Figure 3.6.4C ^{13}C NMR and HMBC spectra of **MS-26**

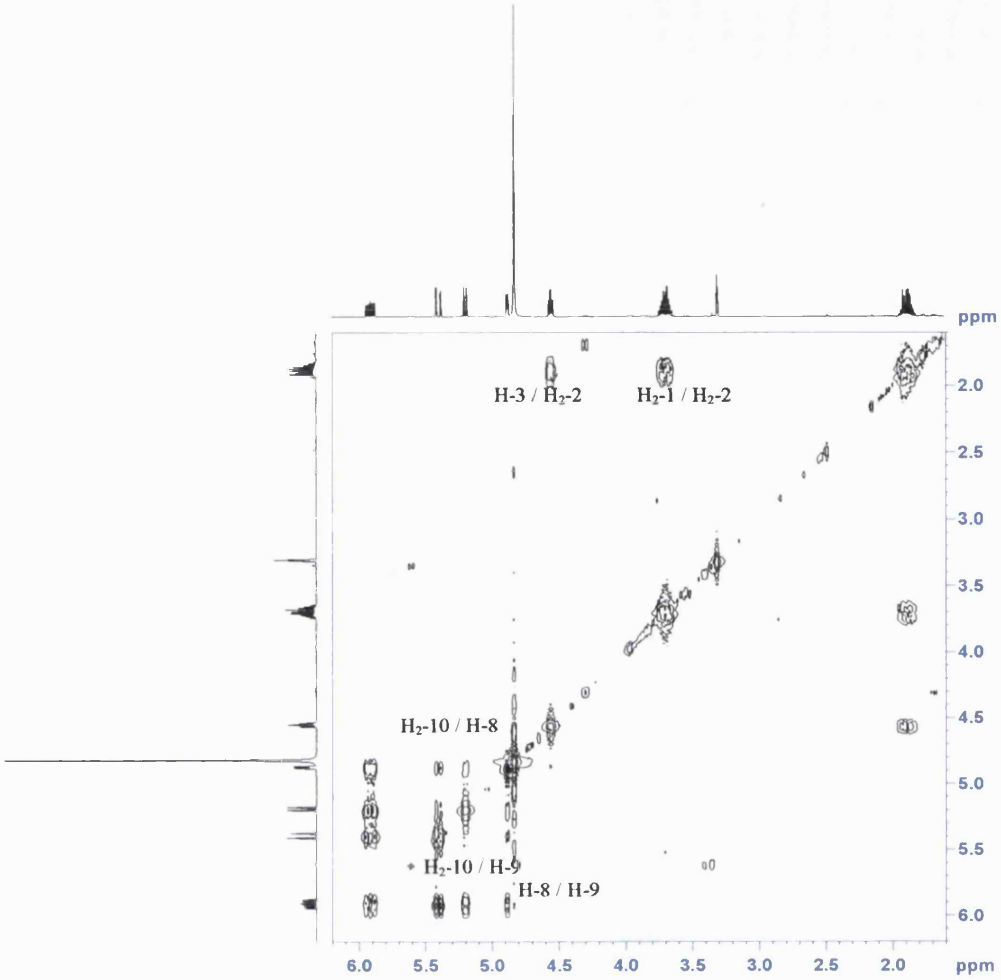

Figure 3.6.4D COSY spectrum of **MS-26**

The *exo*-methylene protons gave a COSY correlation to the olefin, which in turn coupled to an oxymethine proton (**Figure 3.6.4D**). This proton exhibited a ^{2}J and ^{3}J correlation to two of the acetylenic carbons positioned at C-7 and C-6 respectively. The COSY spectrum also showed a signal between an oxymethylene and methylene protons, which in turn coupled to a second oxymethine (δ_H 4.56 t, J = 6.9 Hz, H-3) (**Table 23**). The HMBC yielded ^{2}J and ^{3}J correlations between H-3 and the remaining acetylenic carbons (C-4 and C-5). The HMBC signals exhibited, and the shielded nature of these acetylenic carbons indicates that they should be conjugated and connected. This is not uncommon and is a feature of falcarinol, dehydrofalcarindiol and falcarindiol (Bernart *et al.*, 1996; Furumi *et al.*, 1998; Kobaisy *et al.*, 1997). Due to the downfield appearance of the two oxymethines and oxymethylene groups in both the ^{1}H and ^{13}C NMR spectra, hydroxyls were placed at these carbons. This was supported by the HREIMS for this compound.

The absolute stereochemistry of this compound was determined by Mosher's ester methodology. The primary alcohol was first protected with *tert*-butyl dimethylsilyl (TBDMS), whilst the compound was treated with (*R*)-(-)- and (*S*)-(+)-methoxyphenylacetic acid (MPA) in two separate reactions to give the bis-(*R*)- and bis-(*S*)-MPA esters (Stavri *et al.*, 2004a). The $\delta\Delta^{R,S}$ values ($\delta_R - \delta_S$) are shown in **Figure 3.6.4E**. The $\delta\Delta^{R,S}$ values for H_2-1 and H_2-2 were positive, indicating *R* configuration at C-3 (Stavri *et al.*, 2004a). The $\delta\Delta^{R,S}$ values for H-9 and H_2-10 were also positive, indicating *R* stereochemistry at C-8 as well (Stavri *et al.*, 2004a). **MS-26** was assigned as the new C_{10} polyacetylene 1,3*R*,8*R*-trihydroxydec-9-en-4,6-yne.

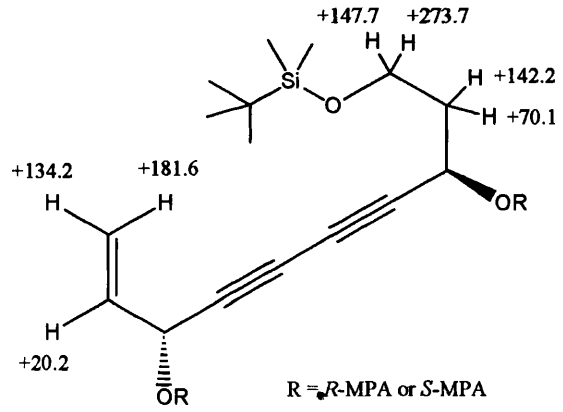

Figure 3.6.4E Δδ values [Δδ (in ppb) = $\delta_R - \delta_S$] obtained for the (*R*)- and (*S*)-MPA esters of the TBDMS-protected polyacetylene (**MS-26**).

Table 23 ^1H and ^{13}C NMR data and ^1H-^{13}C long-range correlations of **MS-26** recorded in CD_3OD

Position	^1H	^{13}C	^2J	^3J
1	3.70 m	59.1	C-2	C-3
2	1.89 m	41.3	C-1, C-3	C-4
3	4.56 t (6.9)	60.2	C-2, C-4	C-1, C-5
4	-	82.0		
5	-	68.9		
6	-	70.1		
7	-	79.5		
8	4.88 d (5.4)	63.8	C-7, C-9	C-6, C-10
9	5.91 ddd (17.0, 10.1, 5.4)	138.1	C-8	C-7
10	5.19 d (10.1)	116.1	C-9	C-8
	5.40 bd (17.0)			

3.6.5 Characterisation of MS-27 as 3(ζ),8(ζ)-dihydroxydec-9-en-4,6-yne-1-*O*-β-D-glucopyranoside

MS-27 was isolated as a pale yellow oil from the methanol extract of *A. monosperma*. A molecular formula of $C_{16}H_{22}O_8$ was assigned by ESI-MS $[M+Na]^+$ (365.1). The ^1H and ^{13}C NMR spectra provided similar signals as for **MS-26** as well as signals for an hexose. This indicated that **MS-27** was the glycoside of **MS-26**. Signals for the aglycone moiety indicated the presence of an *exo*-methylene, an olefin, two oxymethine groups, a methylene and oxymethylene groups as well as four acetylenic quaternary carbons. The hexose gave signals for four oxymethine groups, an oxymethylene and an anomeric carbon (δ_C 104.5)

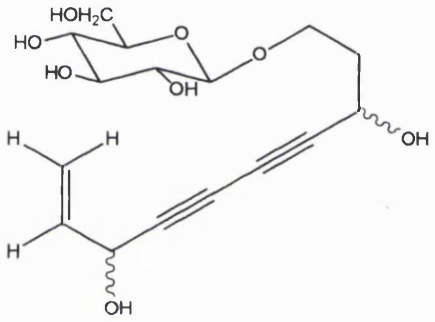

Figure 3.6.5A Structure of **MS-27**

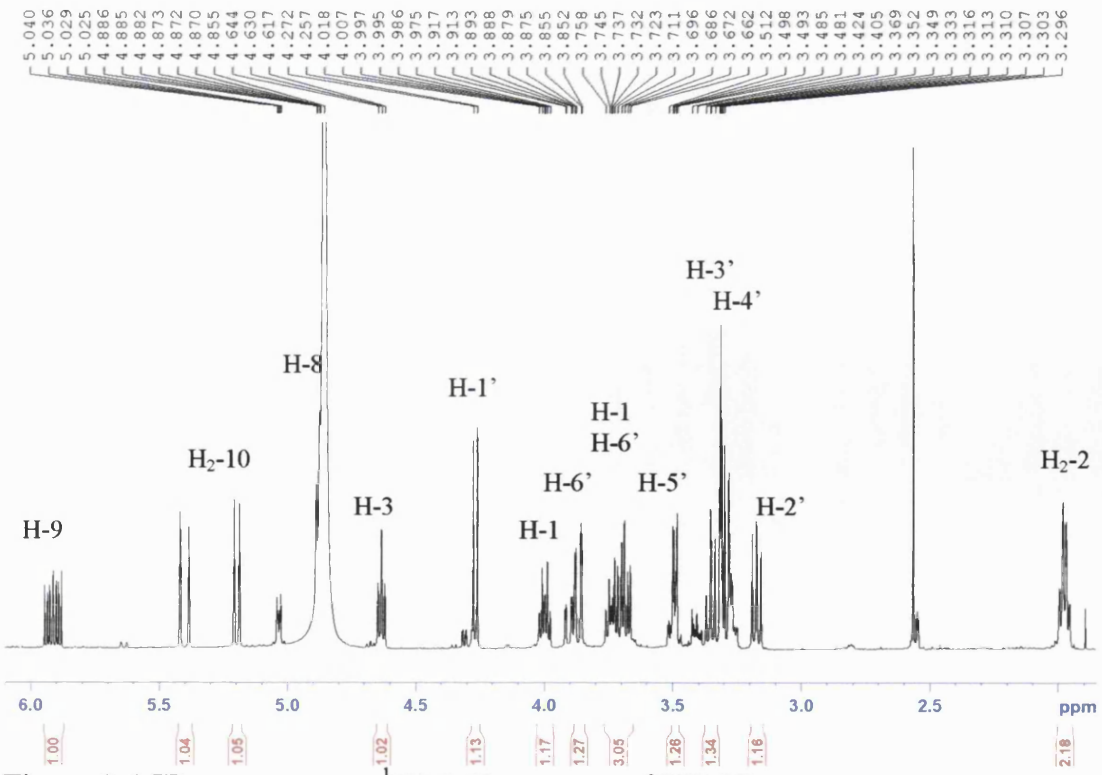

Figure 3.6.5B ^1H NMR spectrum of **MS-27**

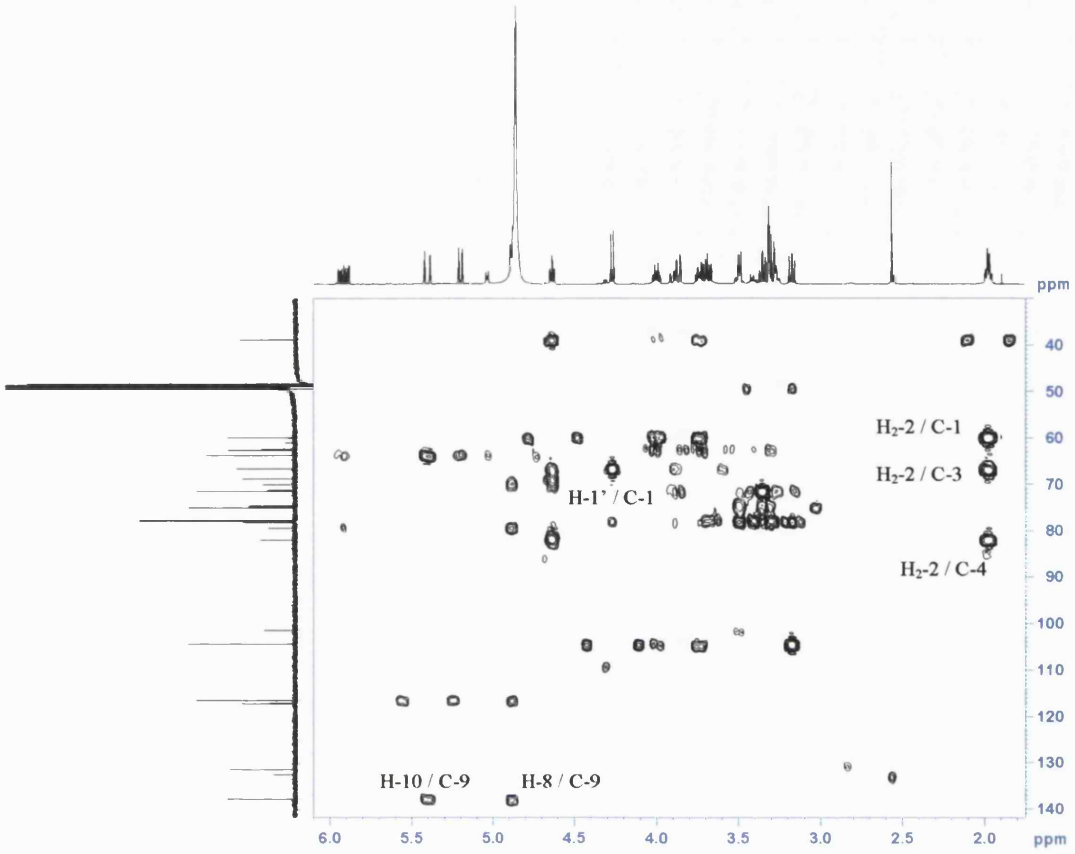

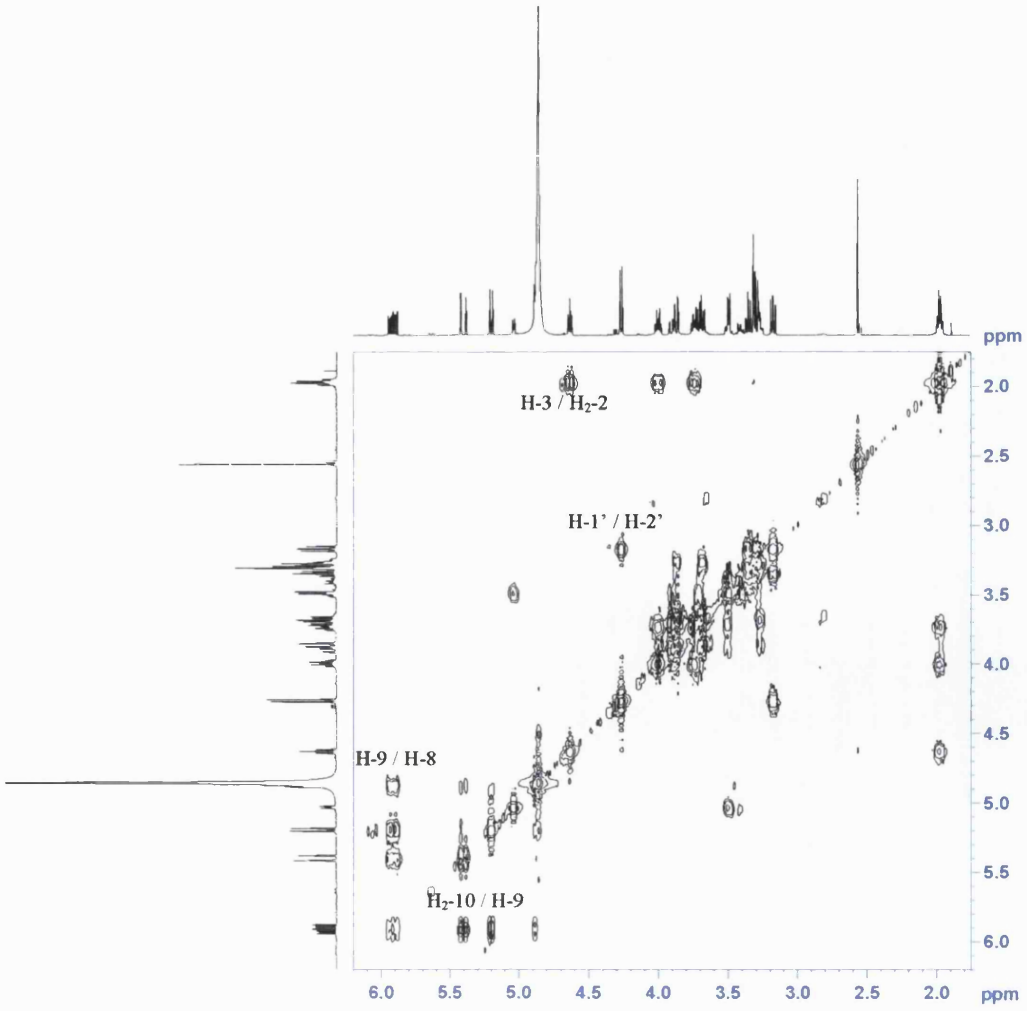

Figure 3.6.5C HMBC and COSY spectra of **MS-27**

Similar signals were detected in both the HMBC and COSY spectra as compared to **MS-26**. The point of attachment of the hexose was deemed to be at C-1 of the polyacetylene. A ^{3}J correlation between the anomeric proton and the oxymethylene carbon was detected in the HMBC spectrum. The COSY spectrum provided correlations between the anomeric proton (H-1') and H-2', H-2' to H-3', H-3' to H-4', H-4' to H-5' and H-5' to the oxymethylene protons (H_2-6'). The coupling between the anomeric proton and H-2' was large (7.5 Hz) as was the coupling between H-2' and H-3' (9.0 Hz). H-3' appeared as a double doublet with a second coupling of 8.0 Hz indicating axial configuration for H-1', H-2', H-3' and H-4'. An NOE between H-1' and H-5' indicated axial configuration for H-5' and this was further confirmed by a second NOE between H-3' and H-5' therefore the hexose was assigned as glucose.

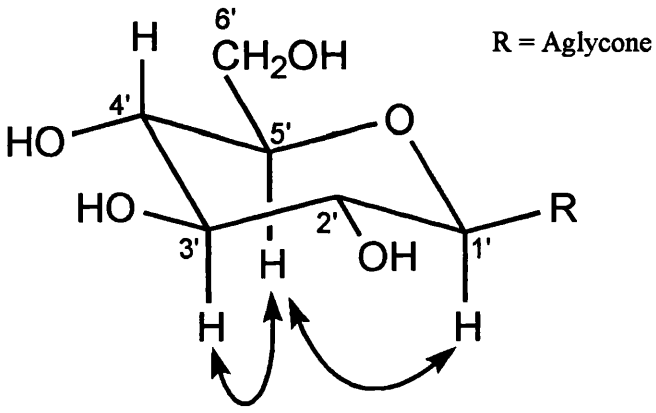

Figure 3.6.5D NOE correlations for the glycone moiety of **MS-27**

The absolute stereochemistry of **MS-27** at positions 3 and 8 has yet to be determined using Mosher ester methodology. It is proposed that the stereochemistry at these two positions will be the same as that of **MS-26** i.e. 3*R*,8*R*. A negative specific rotation was recorded ($[\alpha]_D^{25}$ -45.3°), which differs from that recorded for **MS-26** ($[\alpha]_D^{25}$ +127°). This can be explained by the stereocentres of the glucose moiety having a greater effect on the specific rotation than that of the aglycone stereocentres. **MS-27** is therefore assigned as 3(ζ),8(ζ)-dihydroxydec-9-en-4,6-yne-1-*O*-β-D-glucopyranoside and is reported here for the first time.

Table 24 ^{1}H and ^{13}C NMR data and ^{1}H-^{13}C long-range correlations of **MS-27** recorded in CD_3OD

Position	^{1}H	^{13}C	^{2}J	^{3}J
1	3.73 dt (11.0, 6.0)	66.7	C-2	C-3, C-1'
	3.99 dt (10.0, 6.0)			
2	1.97 dd (13.0, 7.0)	38.9	C-1, C-3	C-4
3	4.63 t (7.0)	60.0	C-2, C-4	C-1, C-5
4	-	82.0		
5	-	68.9		
6	-	70.1		
7	-	79.5		
8	4.88 m	63.8	C-7, C-9	C-6, C-10
9	5.91 ddd (17.0, 10.0, 5.5)	138.0	C-8	C-7
10	5.20 dt (10.0, 1.5)	116.6	C-9	C-8
	5.41 dt (17.0, 1.5)			
1'	4.27 d (7.5)	104.5		C-3', C-1
2'	3.17 dd (9.0, 8.0)	75.1	C-1', C-3'	
3'	3.35 dd (9.0, 8.0)	77.9	C-2'	C-5'
4'	3.28 m	71.6		
5'	3.50 m	78.0	C-4'	
6'	3.68 dd (12.0, 5.0)	62.7	C-5'	
	3.87 dd (11.5, 1.5)			

3.6.6 Biosynthesis of polyacetylenes

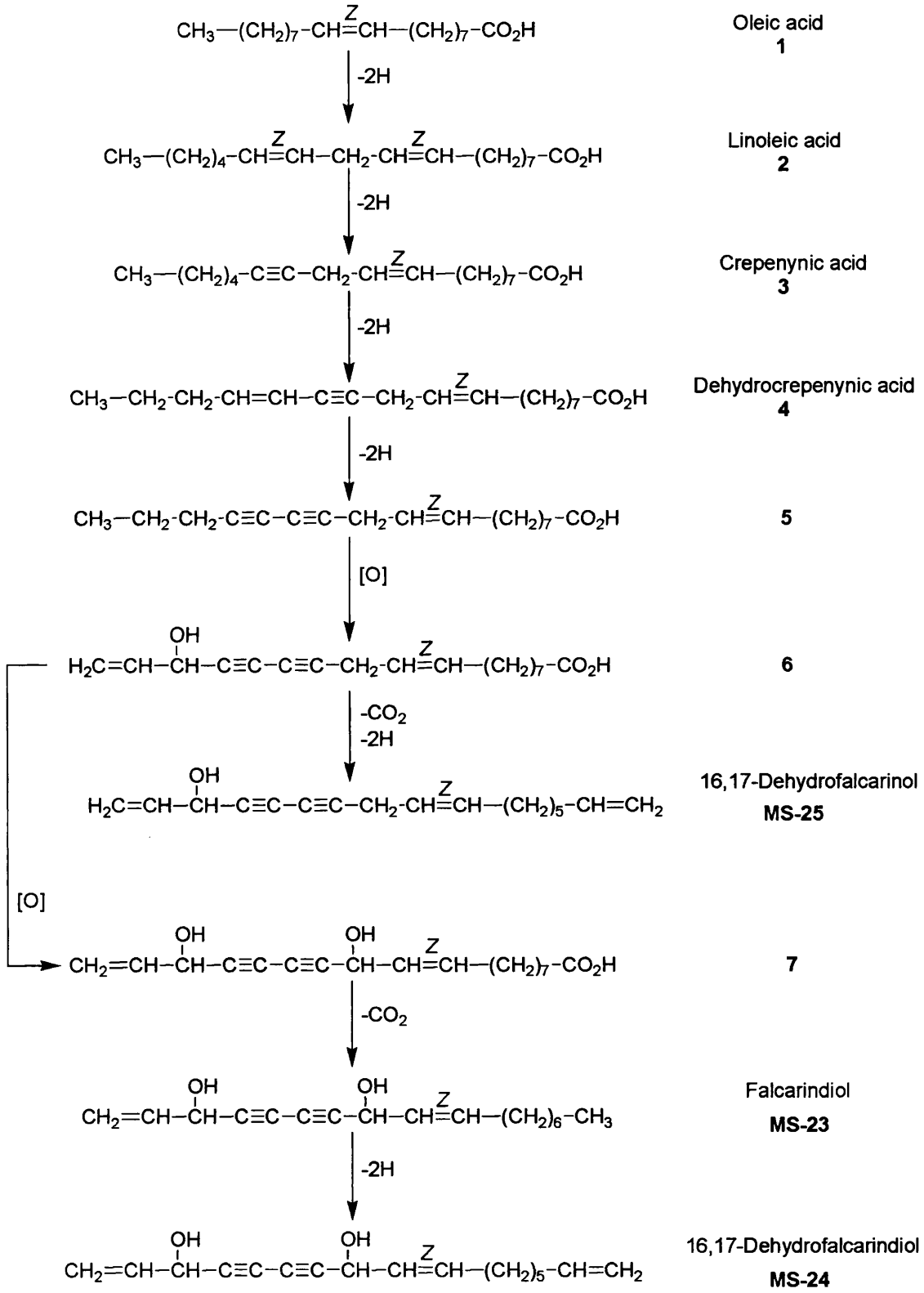

Scheme 5A **Proposed biosynthetic pathway for the C_{17} polyacetylenes MS-23 – MS-25 from the C_{18} unsaturated fatty acid oleic acid (1). Adapted from Hansen and Boll (1986).**

Polyacetylenes are a characteristic metabolite of both the Apiaceae and Asteraceae families. Their biosynthesis is proposed to be derived from the C_{18} fatty acid oleic acid with acetate as the starter molecule and malonate as the elongator molecule. It is then proposed that oleic acid undergoes a series of oxidative dehydrogenations to yield linoleic acid (**2**), crepenynic acid (**3**), dehydrocrepenynic acid (**4**) and 9(*Z*)-octadecen-12,14-diynoic acid (**5**). 16(*R*)-hydroxyoctadeca-9(*Z*)-17-dien-12,14-diynoic acid (**6**) could then be formed by allylic oxidation and dehydrogenation of **5** (Hansen and Boll 1986). There have only been a few C_{18} polyacetylenes isolated from Heliantheae, one of the largest tribes of the Asteraceae (Christensen and Lam 1991). This suggests that the C_{17} polyacetylenes are derived by a decarboxylation reaction, which would then yield 16,17-dehydrofalcarinol (**MS-25**). Falcarindiol (**MS-23**) and 16,17-dehydrofalcarindiol (**MS-24**) are proposed to be biosynthesised from **6** by undergoing further oxidation reactions and a decarboxylation step.

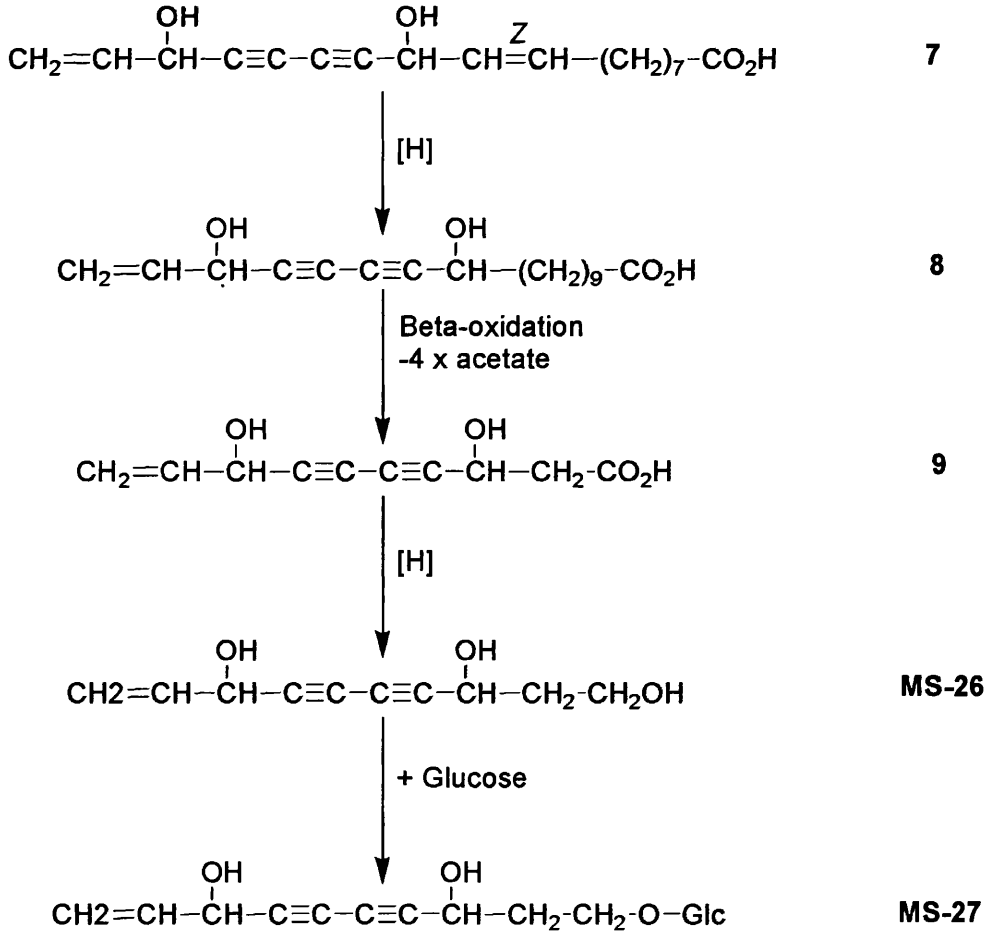

Scheme 5B **Proposed biosynthetic pathway of C_{10} polyacetylenes MS-26 and MS-27 from a C_{18} acetylene precursor**

Smaller C_{10} polyacetylenes are also proposed to be derived from oleic acid (**1**). However, this is proposed to be achieved *via* a hydrogenation reaction to yield **8** followed by a series of β-oxidation reactions of this acetylenic precursor. Following the formation of **MS-26**, this can then undergo an enzymatic glycosylation reaction by a glucosyltranferase to yield **MS-27**.

3.7 Furocoumarins

3.7.1 Characterisation of MS-28 as pangelin

This compound was isolated as a colourless amorphous solid from the hexane extract of *D. anethifolia*. The molecular formula of **MS-28** was determined as $C_{16}H_{14}O_5$ $[M+H]^+$ (287.0) by fast atom bombardment mass spectrometry in the positive mode. The ^1H NMR spectrum showed characteristic signals for a furocoumarin. This included signals for a pair of *cis* olefins linked α and β to a carbonyl (δ_H 6.30 d, J = 9.6 Hz, H-3 and δ_H 8.19 dd, J = 9.6, 0.8 Hz, H-4) as well as signals for a pair of furan olefins (δ_H 7.61 d, J = 2.4 Hz, H-2' and δ_H 6.98 dd, J = 2.4, 0.8 Hz, H-3'). The ^{13}C NMR spectrum supplied information for the presence of 16 carbons, indicating that this furocoumarin was prenylated.

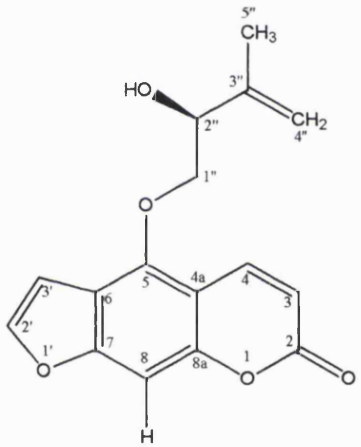

Figure 3.7.1A Structure of **MS-28**

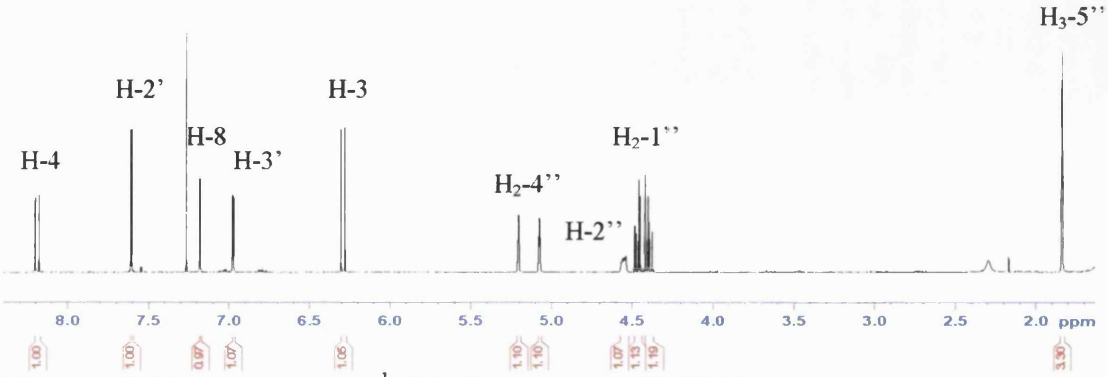

Figure 3.7.1B ^1H NMR spectrum of **MS-28**

A COSY and HMBC correlation between H-3 and H-4 and H-3 to C-2 (δ_C 161.0) placed these olefins α and β to the carbonyl, respectively. A ^3J signal from H-3 to a quaternary carbon (δ_C 107.4, C-4a) placed it at the ring junction. A ^3J signal from H-4 to a downfield quaternary carbon (δ_C 152.7, C-8a) indicated an oxygen should be directly attached, thus completing the six membered unsaturated lactone ring system. Another ^3J correlation from H-4 to C-5 (δ_C 148.5) and a weak 'zig zag' coupling to C-8 ($^5J_{HH}$ = 0.8 Hz) provided important information as to the positioning of these carbons within the aromatic ring system. H-8 provided two ^2J correlations to C-7 (δ_C 158.1) and C-8a and two ^3J correlations to C-6 (δ_C 114.2) and C-4a allowing the completion of the aromatic ring. A COSY correlation between H-2' and H-3' meant that these two olefin protons are coupled to each other. H-2' and H-3' gave HMBC correlations to C-6 and C-7 to complete the furan ring. The deshielded nature of C-2' and C-7 provided evidence that the oxygen of the furan ring is directly attached at these carbons. H-3' also gave a 'zig zag' coupling to H-8 ($^5J_{HH}$ = 0.8 Hz) although no signal was detected in the HMBC spectrum. This completed the structure of the linear furocoumarin. The ^1H, ^{13}C and HMBC spectra provided evidence for a 5-*O*-prenylated furocoumarin. The protons of a deshielded methylene (δ_H 4.40 dd, J = 10.0, 7.2 Hz, δ_H 4.47 dd, J = 10.0, 3.6 Hz, δ_C 75.7, C-1'') gave a ^3J correlation to C-5. The resonances of both carbons indicated that they are deshielded and so are coupled together *via* an ether link. A COSY correlation between H-1'' and H-2'' (δ_H 4.55 m, δ_C 74.3) placed this methine here. Due to the deshielded nature of this group an hydroxyl must be here. HMBC signals from H-1'' and H-2'' placed an olefinic quaternary carbon at C-3'' (δ_C 143.4). A methyl group (δ_H 1.85 dt, J = 0.8, 0.4 Hz) showing only long-range coupling, gave a ^2J correlation to C-3'' and ^3J correlations to C-2'' and an *exo*-methylene carbon (δ_C 113.4, δ_H 5.08 m and 5.21 m). Both the methyl and *exo*-methylene groups must be attached to the quaternary carbon, C-3'', completing the structure of the prenyl group. Measurement of a positive absolute rotation confirmed the assignment of the compound as pangelin (Ognyanov and Botcheva 1971; Stavri *et al.*, 2003). The ^1H NMR data for this compound was in close agreement with that published for pangelin, which was previously isolated from *Angelica pancici* (Ognyanov and Botcheva 1971). The ^{13}C data has not been published before and was recently described by us (Stavri *et al.*, 2003).

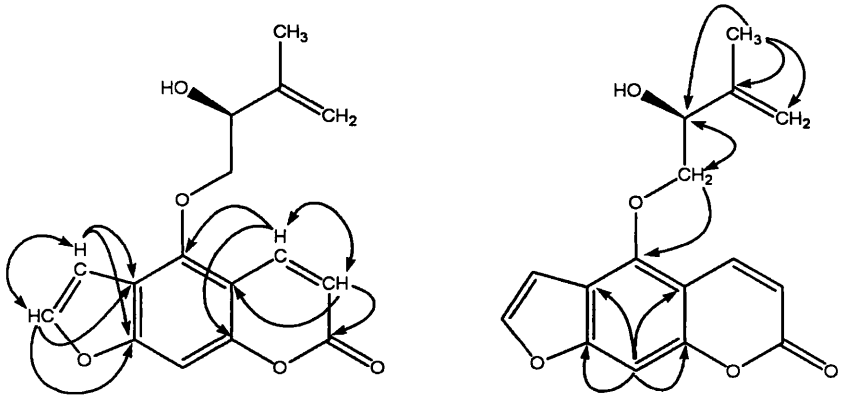

Figure 3.7.1C HMBC and COSY correlations for **MS-28**

Table 25 ^{1}H and ^{13}C NMR data and ^{1}H-^{13}C long-range correlations of **MS-28** recorded in $CDCl_3$ (400 MHz for ^{1}H and 100 MHz for ^{13}C)

Position	^{1}H	^{13}C	^{2}J	^{3}J
2	-	161.0		
3	6.30 d (9.6)	113.1	C-2	C-4a
4	8.19 dd (10.0, 0.8)	139.0		C-2, C-5, C-8a
4a	-	107.4		
5	-	148.5		
6	-	114.2		
7	-	158.1		
8	7.18 t (0.8)	94.8	C-7, C-8a	C-4a, C-6
8a	-	152.7		
2'	7.61 d (2.4)	145.2		C-6, C-7
3'	6.98 dd (2.4, 0.8)	104.7	C-2', C-6	C-7
1"	4.40 dd (10.0, 7.2)	75.7	C-2"	C-3", C-5
	4.47 dd (10.0, 3.6)			
2"	4.55 m	74.3	C-1", C-3"	C-4"
3"	-	143.4		
4"	5.21 m 5.08 m	113.4	C-3"	C-2", C-5"
5"	1.85 dt (0.8, 0.4)	18.7	C-3"	C-2", C-4"

3.7.2 Characterisation of MS-29 as oxypeucedanin hydrate (aviprin) (racemate)

MS-29 was isolated as a colourless amorphous solid from the chloroform extract of *A. graveolens*. A molecular formula of $C_{16}H_{16}O_6$ $[M+H-H_2O]^+$ (287.0) was assigned by ESI-MS. The ^1H and ^{13}C NMR spectra were very similar to that of pangelin indicating the presence of another linear furocoumarin. The ^1H spectrum differed from pangelin with respect to the 5-*O*-prenyl group attached to the furocoumarin. The presence of two methyl groups (both δ_H 1.70 s) and an oxymethine (δ_H 4.07 m) as well as the oxymethylene group found with pangelin were detected. The ^{13}C NMR spectrum also showed the presence of an oxygen bearing quaternary carbon (δ_C 71.4, C-3'').

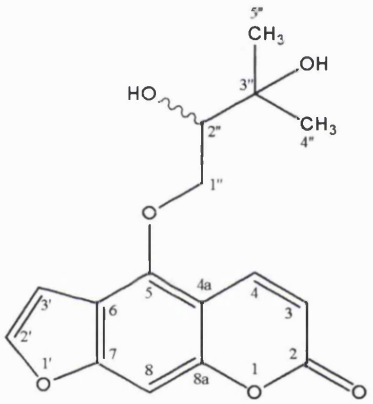

Figure 3.7.2A Structure of **MS-29**

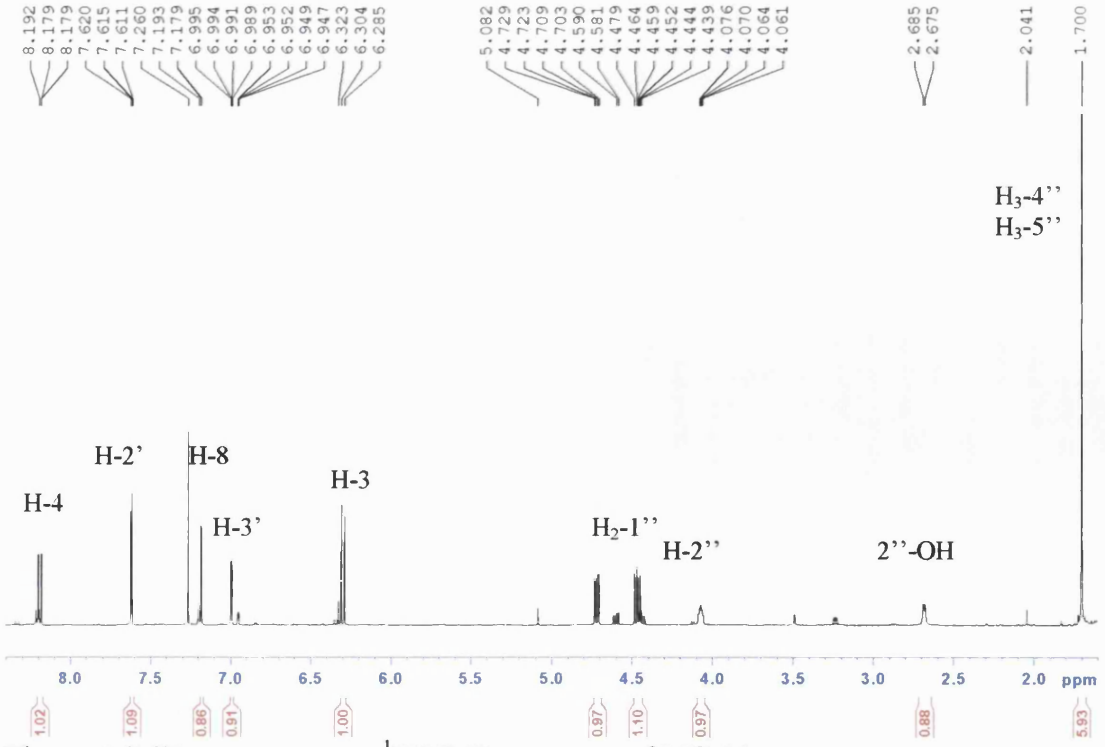

Figure 3.7.2B ^1H NMR spectrum of **MS-29**

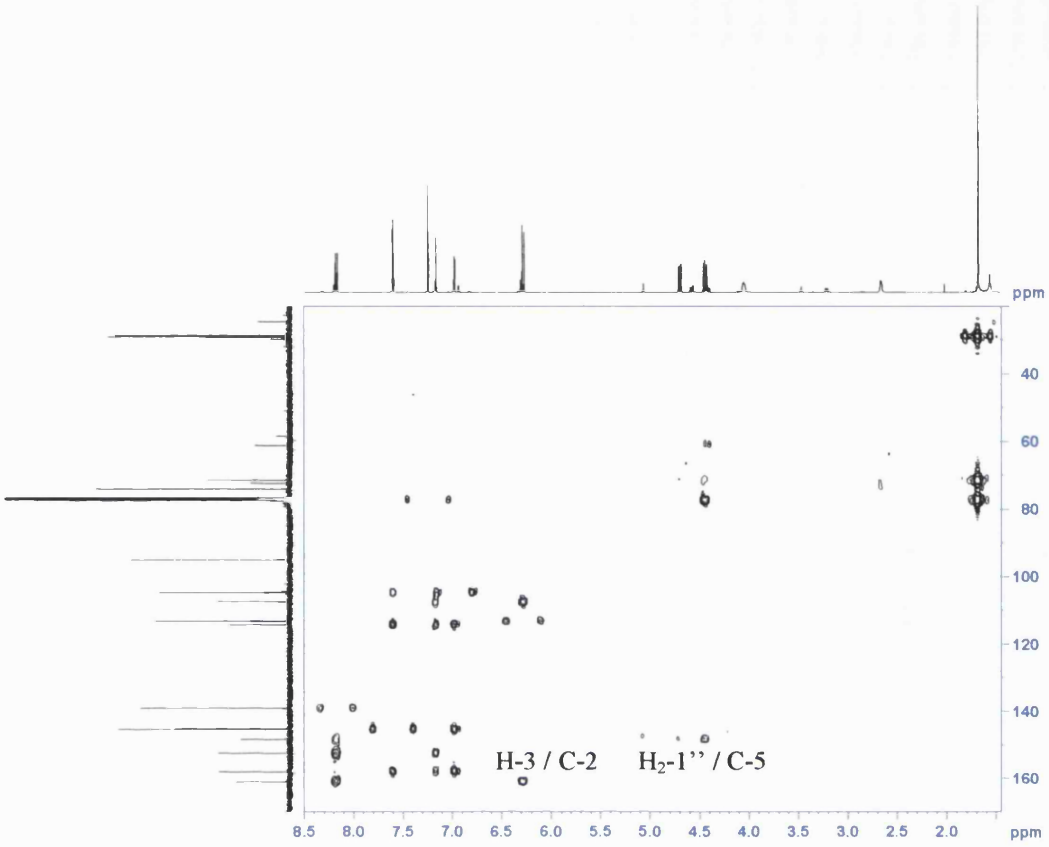

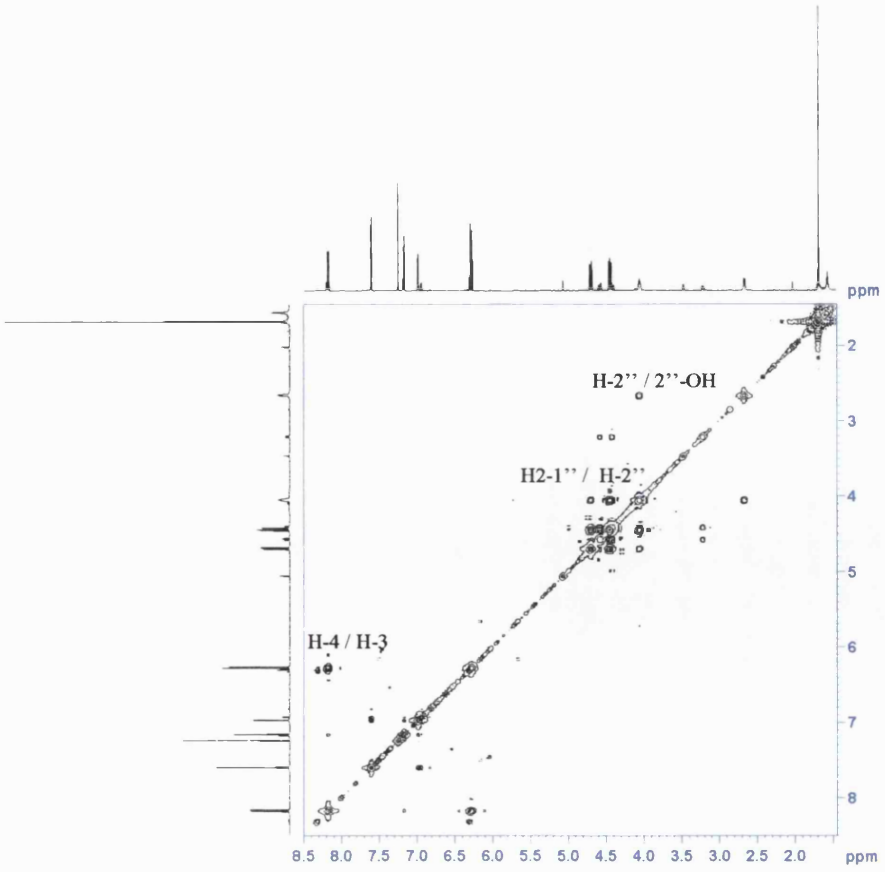

Figure 3.7.2C HMBC and COSY spectra of **MS-29**

The HMBC and COSY signals obtained for the furocoumarin portion of the molecule were identical to those detected for pangelin. This confirmed the presence of a 6,7 furocoumarin. The point of attachment of the prenyl group was again found to be at C-5 (δ_C 148.3). The deshielded nature of the two carbons, C-5 and C-1'' (δ_C 74.1) as well as the downfield position of the methylene protons suggested that the prenyl group (δ_H 4.46 and δ_H 4.72) is attached to the furocoumarin by an ether linkage. A ^3J correlation between H_2-1'' and C-5 confirmed the position of the prenyl group. A COSY signal between these methylene protons and a methine (δ_H 4.07 m) placed this group at position 2''. The downfield nature of this carbon indicated that an hydroxyl should be placed here. Both the methylene and methine protons gave an HMBC signal to a quaternary carbon, placing it at C-3''. Again an hydroxyl was attached to this carbon due to its downfield appearance in the ^{13}C spectrum. Finally, the two methyl groups gave ^2J correlations to C-3'' and the appearance of these groups as singlets meant that they must be directly attached to a quaternary carbon. This completed the structure of this 5-*O*-substituted linear furocoumarin. **MS-29** was optically inactive and therefore deemed to be a racemic mixture.

The ^{13}C NMR data for this compound was in close agreement with that published for oxypeucedanin hydrate, which was previously isolated from the roots of *Angelica officinalis* (Harkar *et al.*, 1984) and *Angelica dahurica* (Ishihara *et al.*, 2001). The ^1H NMR data (recorded in $CDCl_3$) for the furocoumarin was also in close agreement with the literature, but not for the prenyl group (**Table 26**: ^1H NMR data from literature in bold and parentheses) (Ishihara *et al.*, 2001). The downfield shift of the two methyl groups recorded in this thesis can be explained by a deshielding effect caused by the hydroxyl group at C-3''. The deshielding effect of this hydroxyl group must be equal for both the methyl groups. The hydroxyl group at C-2'' would also have a deshielding effect on the two methyl groups due to the close spatial proximity of these groups. Once more the deshielding effect of this hydroxyl group will be equal for both methyls as **MS-29** was isolated as a racemic mixture. This would account for the methyl protons appearing as a 6H singlet at δ_H 1.70 in the ^1H NMR spectrum.

Table 26 ^{1}H and ^{13}C NMR data and ^{1}H-^{13}C long-range correlations of **MS-29** recorded in $CDCl_3$. ^{1}H NMR chemical shifts reported by Ishihara *et al.*, (2001) of the prenyl group in parentheses in bold.

Position	^{1}H	^{13}C	^{2}J	^{3}J
2	-	161.0		
3	6.30 d (9.5)	113.1	C-2	C-4a
4	8.20 dd (10.0, 0.5)	139.0		C-2, C-5, C-8a
4a	-	107.4		
5	-	148.3		
6	-	114.1		
7	-	158.1		
8	7.18 s	94.9	C-7, C-8a	C-6, C-4a
8a	-	152.5		
2'	7.62 d (2.5)	145.3	C-3'	C-6, C-7
3'	6.99 dd (2.0, 1.0)	104.7	C-2', C-6	C-7
1"	4.46 dd (10.0, 7.5) **(4.45 dd)**	74.1	C-2"	C-3", C-5
	4.72 dd (10.0, 3.0) **(4.55 dd)**			
2"	4.07 m **(3.91 m)**	77.3		
3"	-	71.4		
4"	1.70 s **(1.10 s)**	28.7	C-3"	C-2", C-5"
5"	1.70 s **(1.17 s)**	29.1	C-3"	C-2", C-4"
2"-OH	2.68 bs	-		

3.7.3 Characterisation of MS-30 as (*R*)-(+)-oxypeucedanin

MS-30 was isolated as a colourless amorphous solid and a molecular composition of $C_{16}H_{14}O_5$ $[M+H]^+$ (287.1) was established by ESI-MS. The ^1H and ^{13}C NMR spectra were very similar to those of **MS-29**, the difference being with the upfield shift of the carbons at positions C-2'' and C-3'' in **MS-30** with respect to **MS-29** along with the more shielded and hence upfield position of the methine proton, H-2''. The signals in the ^1H and ^{13}C NMR spectra provided evidence for 16 carbons, which again take the form of a 5-*O*-substituted linear furocoumarin.

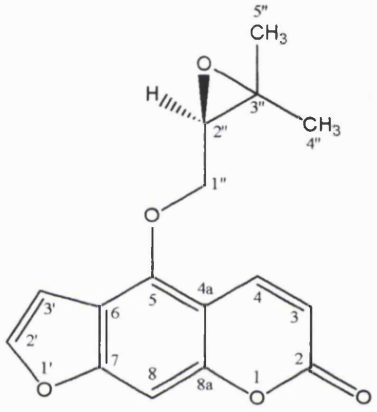

Figure 3.7.3A Structure of **MS-30**

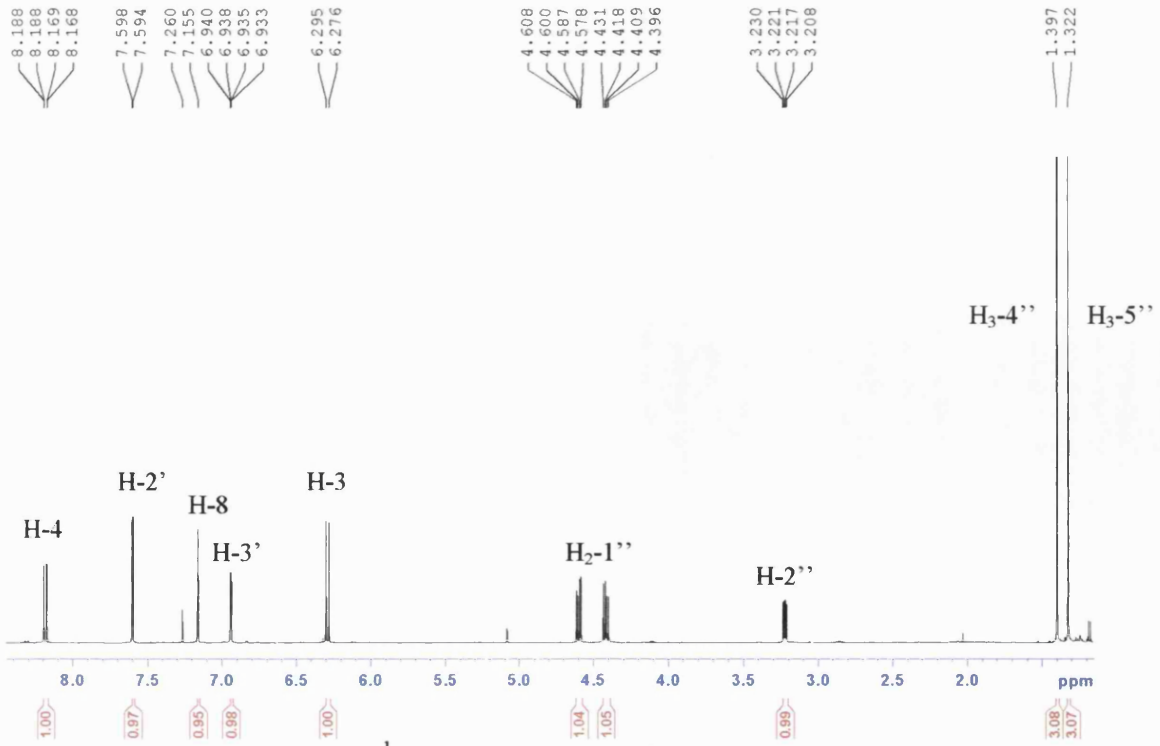

Figure 3.7.3B ^1H NMR spectrum of **MS-30**

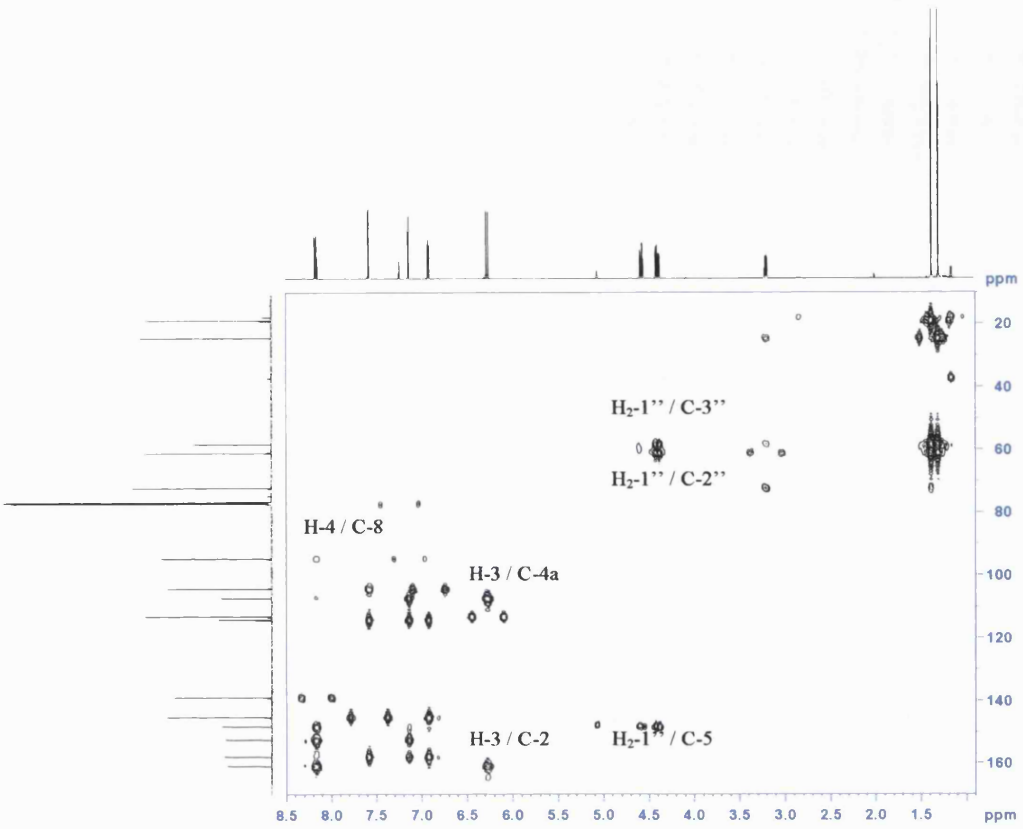

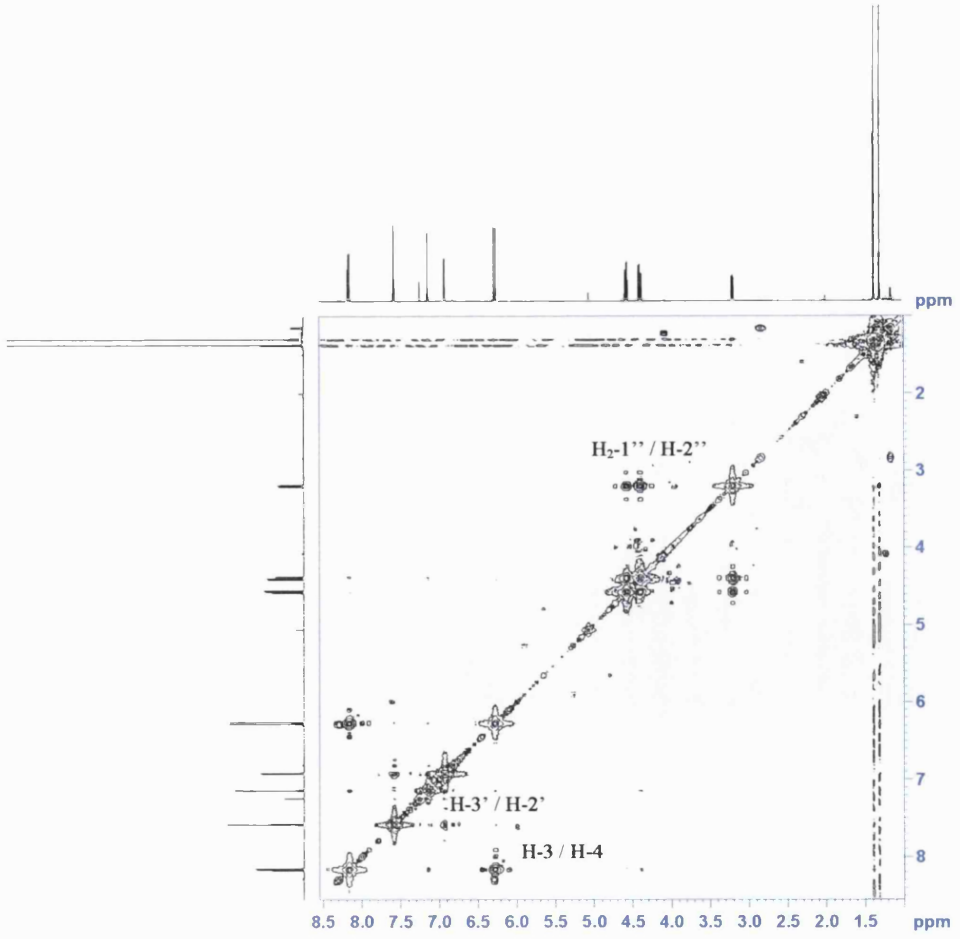

Figure 3.7.3C HMBC and COSY spectra of **MS-30**

The HMBC and COSY spectra confirmed the presence of a 6,7 furocoumarin with almost identical signals as for **MS-29**. The correlations for the prenyl group were also very similar. However, the upfield shift of C-2'' (δ_C 61.1) and C-3'' (δ_C 58.3) was characteristic for the presence of an epoxide between these two carbons. The information gained from the mass spectrum corroborated this assignment. The NMR data for this compound was in close agreement with that published for oxypeucedanin, which was also previously isolated from the roots of *Angelica officinalis* (Harkar *et al.*, 1984). Measurement of a positive absolute rotation, $[\alpha]_D^{23}$ +9.1° (*c* 1.755, $CHCl_3$), allowed **MS-30** to be assigned as (*R*)-(+)-oxypeucedanin (Lemmich *et al.*, 1971).

Table 27 ^1H and ^{13}C NMR data and ^1H-^{13}C long-range correlations of **MS-30** recorded in $CDCl_3$

Position	^1H	^{13}C	^2J	^3J
2	-	161.0		
3	6.30 d (10.0)	113.1	C-2	C-4a
4	8.19 dd (10.0, 0.5)	139.0		C-2, C-5, C-8a
4a	-	107.4		
5	-	148.3		
6	-	114.1		
7	-	158.0		
8	7.16 s	94.8	C-7, C-8a	C-6, C-4a
8a	-	152.5		
2'	7.60 d (2.0)	145.3	C-3'	C-6, C-7
3'	6.94 dd (2.5, 1.0)	104.5	C-2', C-6	C-7
1"	4.42 dd (11.0, 6.5)	72.3	C-2"	C-3", C-5
	4.60 dd (11.0, 4.0)			
2"	3.22 dd (6.5, 4.5)	61.1	C-1", C-3"	C-4"
3"	-	58.3		
4"	1.40 s	24.5	C-3"	C-2", C-5"
5"	1.32 s	19.0	C-3"	C-2", C-4"

3.7.4 Characterisation of MS-31 as 5-[4''-hydroxy-3''-methyl-2''-butenyloxy]-6,7-furocoumarin

MS-31 was isolated as a white amorphous solid and a molecular formula of $C_{16}H_{14}O_5$ $[M]^+$ (286.0840) was established by HREIMS. The ^1H and ^{13}C NMR spectra once more provided evidence to indicate the presence of a 5-*O*-prenylated furocoumarin. The signals for the furocoumarin were identical to those of the previous compounds of this natural product class. The prenyl group was composed of two oxymethylenes (δ_H 5.04 d, H_2-1'' and δ_H 4.20 s, H_2-4''), an olefin (δ_H 5.70 t, H-2'', δ_C 122.1) and a methyl group (δ_H 1.90 s, H_3-5''). The ^{13}C spectrum also showed the presence of an olefinic quaternary carbon (δ_C 141.4)

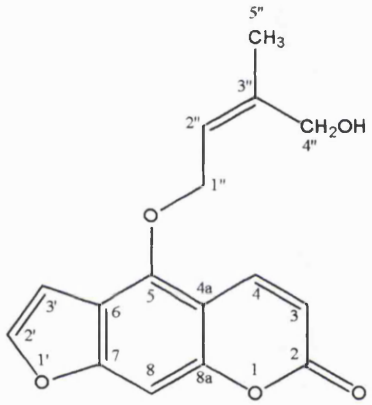

Figure 3.7.4A Structure of **MS-31**

Figure 3.7.4B ^1H NMR spectrum of **MS-31**

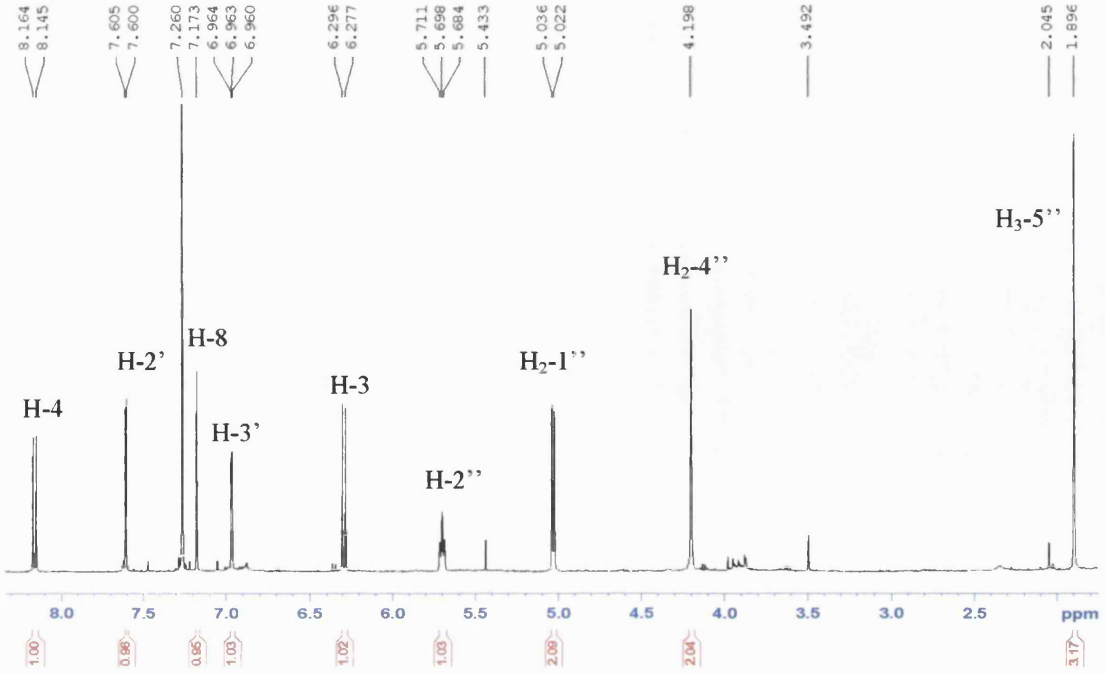

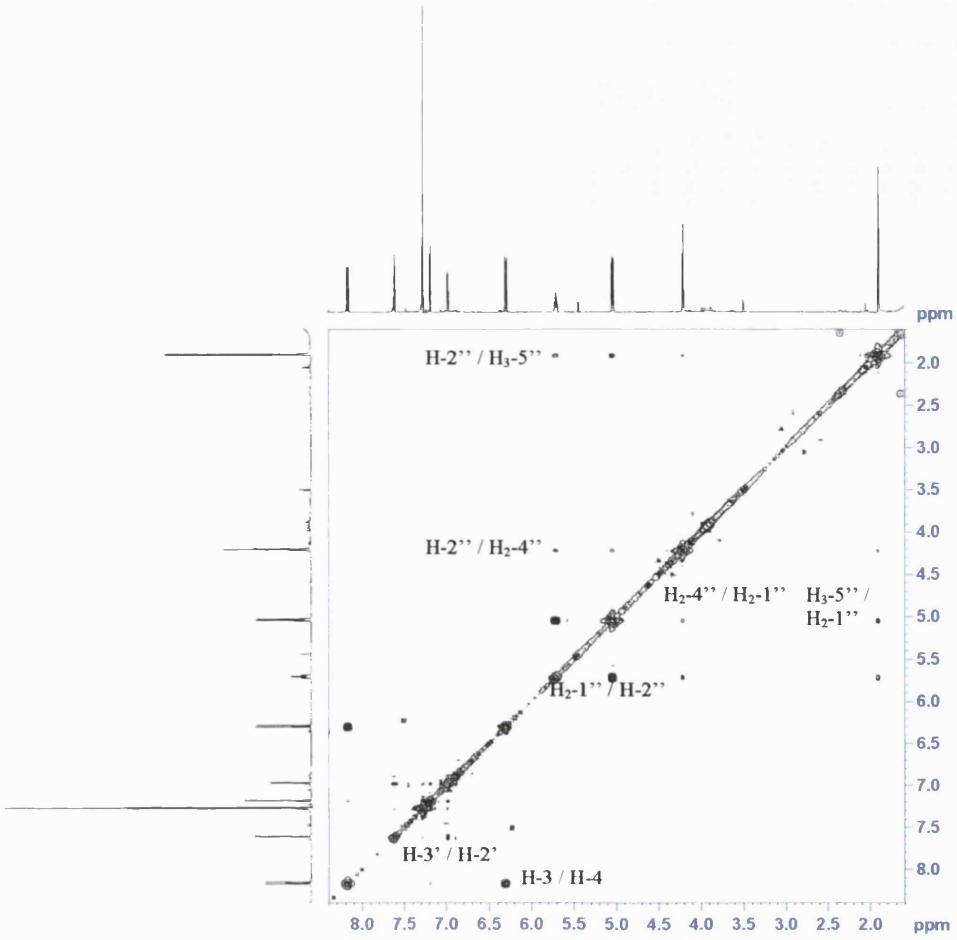

Figure 3.7.4C COSY spectrum of **MS-31**

From the HMBC, H_2-1'' gave a ^3J correlation to C-5 placing this prenyl group here. Whilst a COSY signal between H_2-1'' and H-2'' placed this olefin next to the oxymethylene. Both the oxymethylene and olefin gave an HMBC signal to an olefinic quaternary carbon and assigned at position C-3''. The remaining oxymethylene and methyl groups appeared as singlets in the ^{1}H spectrum and each gave a ^2J correlation to C-3'' and so must be directly attached to this quaternary carbon. Due to the downfield nature of the methylene protons (δ_H 4.20 s, H-4'') an hydroxyl was placed here. H_3-5'' and H_2-4'' both gave allylic correlations to H-2'', as well as towards each other. These groups also showed homo-allylic correlations to H_2-1'', confirming the structure of the prenyl group.

The NOESY spectrum enabled the stereochemistry of the prenyl group to be ascertained. An NOE between H-2'' and methyl-5'' placed these protons on the same side of the molecule. This was further confirmed by a second NOE between H_2-1'' and H_2-4''. There has been no previous report of a linear furocoumarin with this particular prenyl group attached at position 5 and so **MS-31** is new.

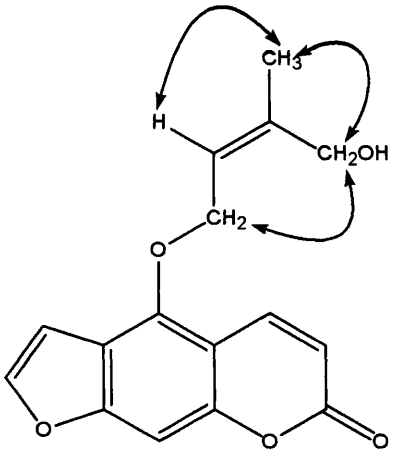

Figure 3.7.4D NOE correlations for **MS-31**

Table 28 ^{1}H and ^{13}C NMR data and ^{1}H-^{13}C long-range correlations of **MS-31** recorded in $CDCl_3$

Position	^{1}H	^{13}C	^{2}J	^{3}J
2	-	161.2		
3	6.30 d (9.5)	112.8	C-2	C-4a
4	8.16 d (10.0)	139.4		C-2, C-5, C-8a
4a	-	107.4		
5	-	148.6		
6	-	114.1		
7	-	158.1		
8	7.17 s	94.5	C-8a	C-6, C-4a
8a	-	152.7		
2'	7.61 d (2.5)	145.1		C-6, C-7
3'	6.96 dd (2.0, 0.5)	104.9	C-2', C-6	C-7
1"	5.04 d (6.0)	68.9	C-2"	C-3", C-5
2"	5.70 t (6.5)	122.1		
3"	-	141.4		
4"	4.20 s	61.9	C-3"	C-2", C-5"
5"	1.90 s	21.4	C-3"	C-2", C-4"

3.7.5 Biosynthesis of furocoumarins

Cinnamic acids are the precursors for coumarin biosynthesis. The incorporation of a mole of a C_5 isoprenoid such as DMAPP combined with the loss of three carbon atoms leads to the formation of both angular and linear furocoumarins. The formation of **MS-28** - **MS-31** occurs with an unusual *ortho*-hydroxylation of *p*-coumaric acid. The *trans* double bond then undergoes isomerisation to yield the *cis* geometric isomer, followed by a cyclisation step to form umbelliferone.

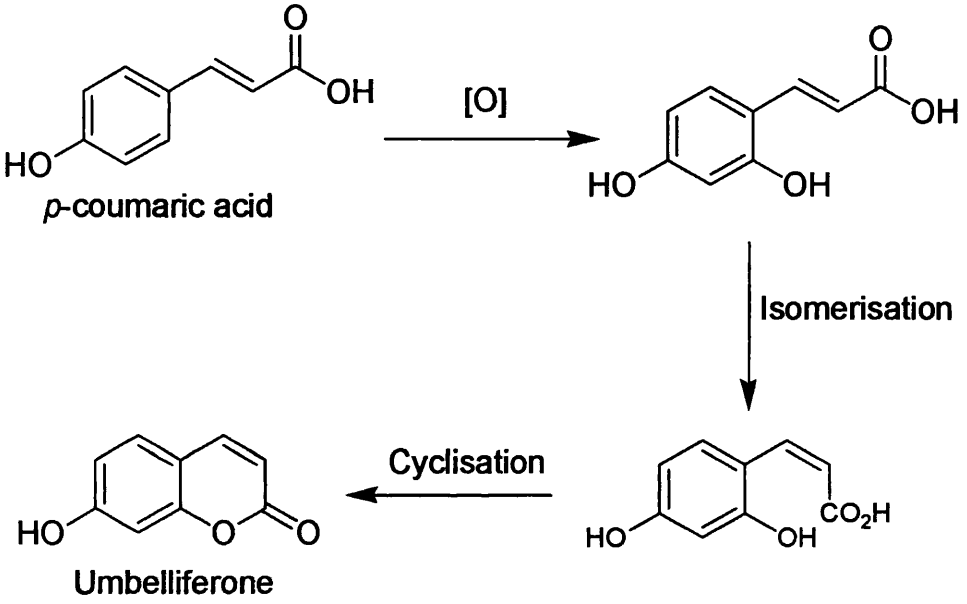

Scheme 6A **Biosynthesis of umbelliferone from the precursor *p*-coumaric acid.**

The formation of linear and angular furocoumarins occurs by prenylation at positions 6 and 8 of umbelliferone respectively. Labelling studies, in *Apium graveolens*, have shown that prenylation of umbelliferone is achieved *via* the mevalonate independent pathway, using 1-deoxy-D-xylulose-derived DMAPP (Stanjek *et al.*, 1999). Prenylation of umbelliferone is catalysed by dimethylallyl transferase to form demethylsuberosin. Oxidative attack at the double bond of demethylsuberosin by the P450-type enzyme marmesin synthase yields (-)-marmesin (Stanjek *et al.*, 1999). A second P450-type enzyme, psoralen synthase, catalyses the removal of the C-3'-H_{Si} hydrogen atom along with the propyloxy group to yield the linear furocoumarin psoralen. Oxidation at the C-5 position of psoralen, followed by

prenylation at this point is proposed as a biosynthetic route for the production of **MS-28 - MS-31**.

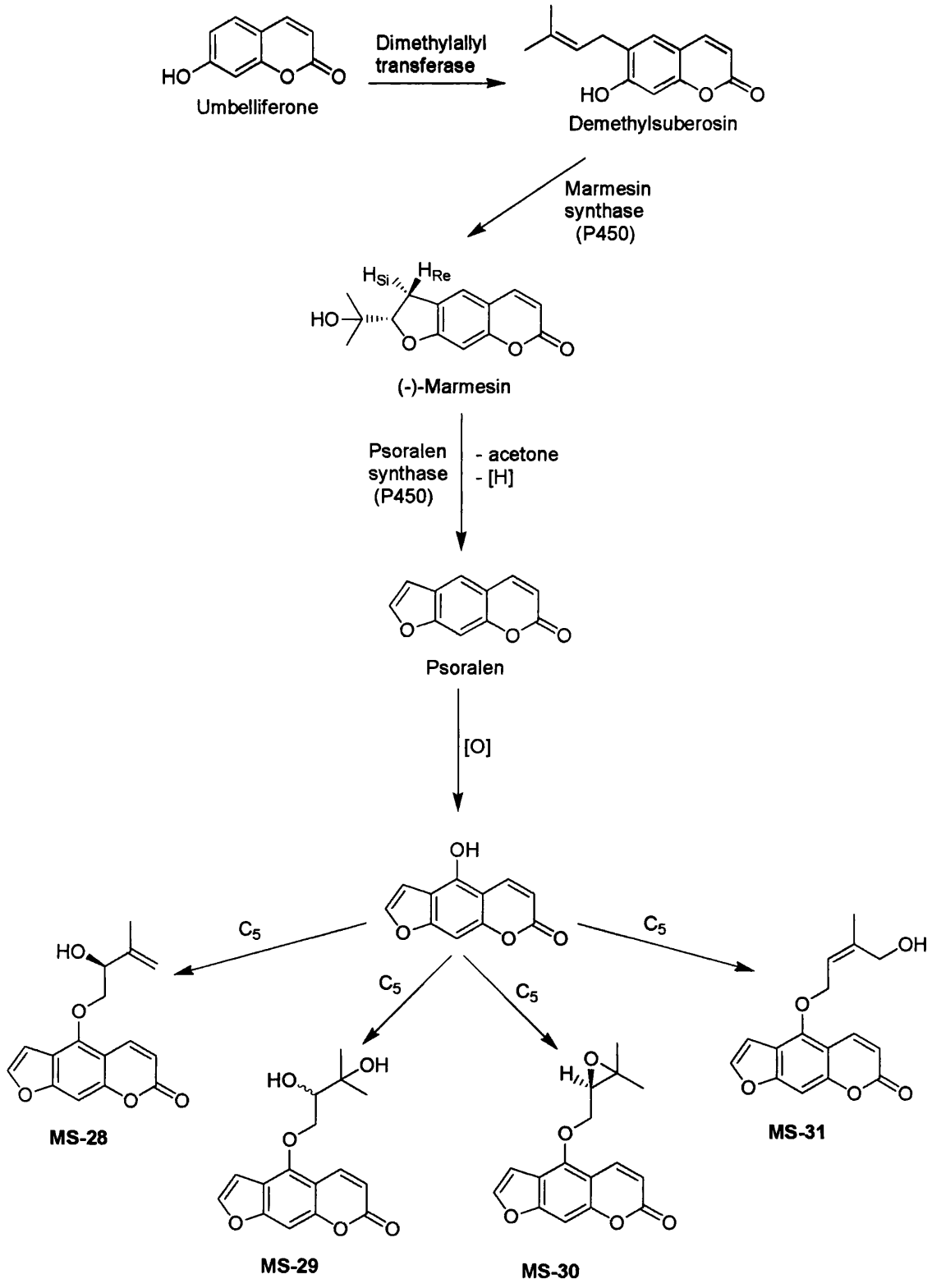

Scheme 6B **Biosynthesis of MS-28 – MS-31 from the coumarin umbelliferone. Adapted from Stanjek *et al.*, (1999).**

3.8 Flavonoids

3.8.1 Characterisation of MS-32 as 3',5-dihydroxy-4',6,7-trimethoxyflavone (eupatorin)

MS-32 was isolated as a yellow amorphous powder, and a molecular formula of $C_{18}H_{16}O_7$ $[M-H]^-$ (343.3) was established by ESI-MS. The ^1H NMR spectrum provided signals characteristic of a highly methoxylated flavone. Three methoxyl groups (δ_H 3.93 – 3.99) were detected along with five aromatic protons. The ^{13}C NMR spectrum yielded signals for 18 carbons, which included a carbonyl (δ_C 182.7, C-4) and 7 oxygen bearing aromatic quaternary carbons.

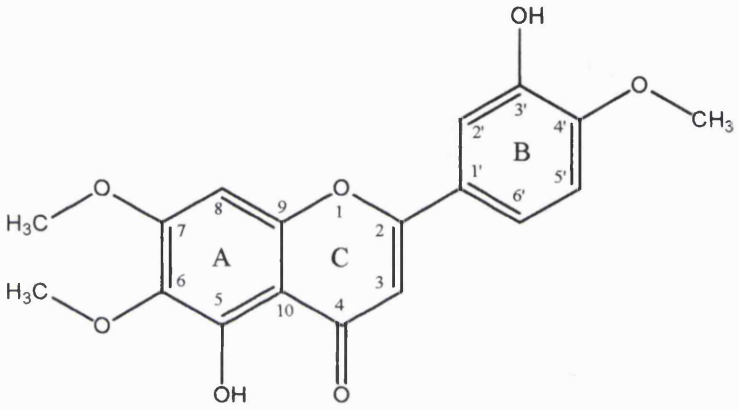

Figure 3.8.1A Structure of **MS-32**

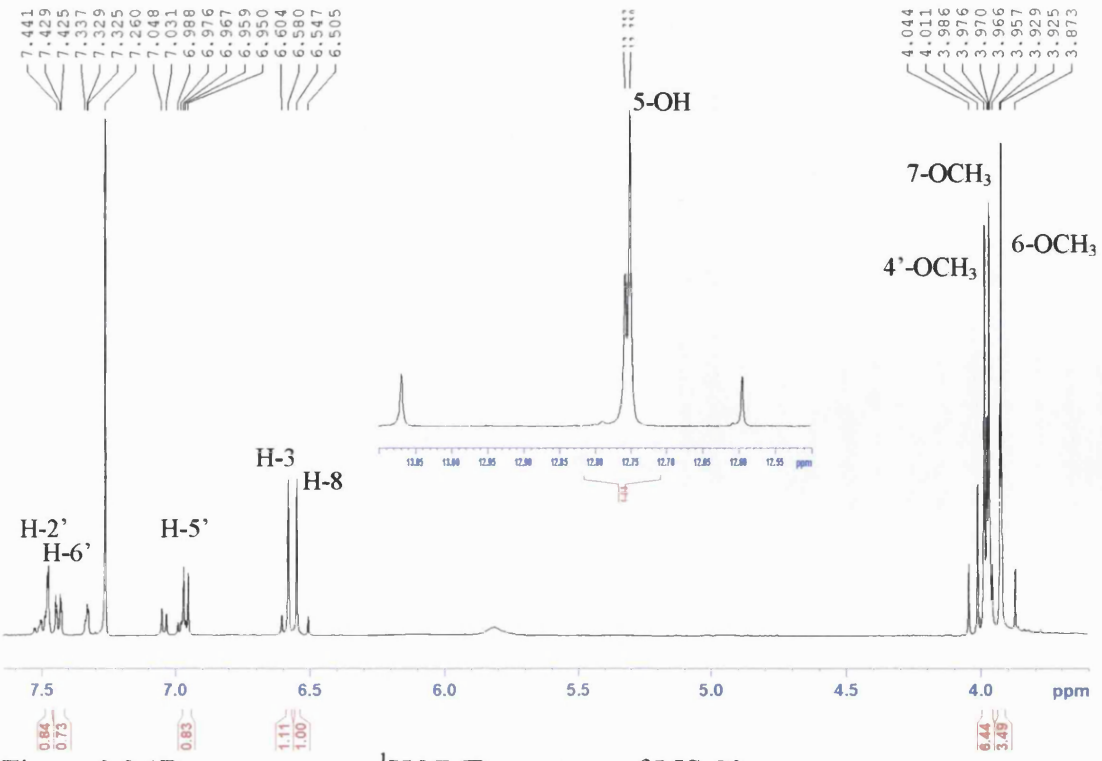

Figure 3.8.1B ^1H NMR spectrum of **MS-32**

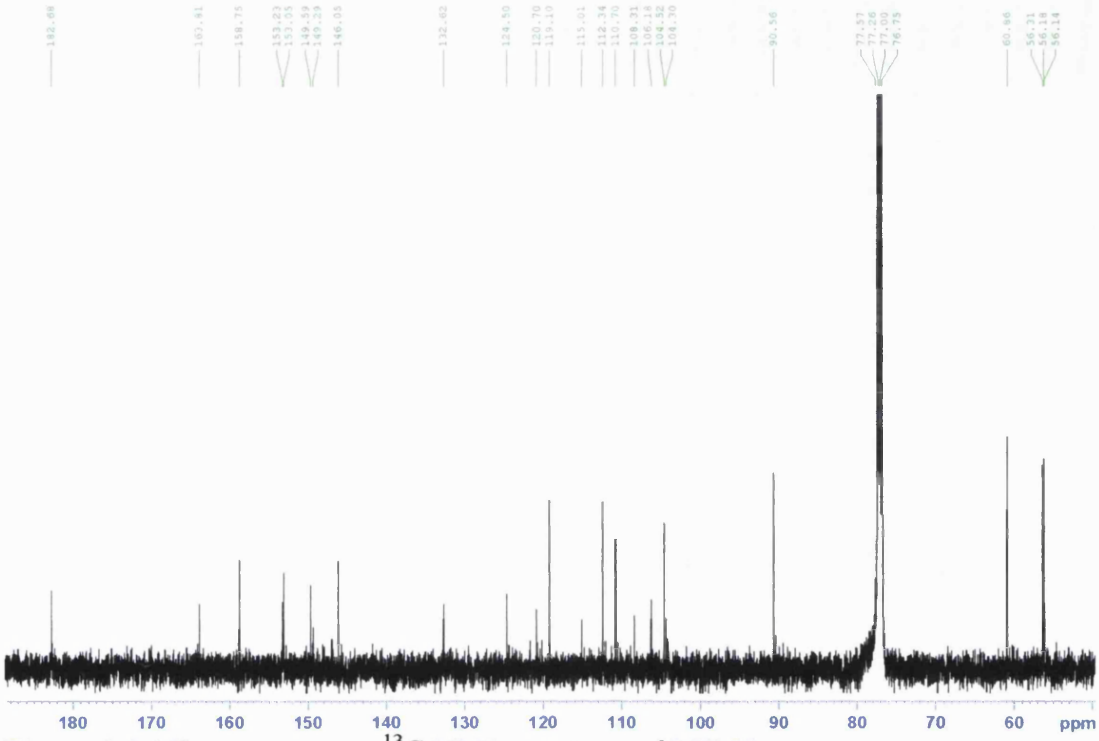

Figure 3.8.1C ^{13}C NMR spectrum of **MS-32**

The presence of an aromatic proton appearing as a singlet in the ^{1}H NMR spectrum is characteristic of H-8 (δ_H 6.55) of a flavone (Albach *et al.*, 2003). This proton showed ^{2}J signals to two oxygen bearing olefinic quaternary carbons (δ_C 158.8, C-7 and δ_C 153.1, C-9) and ^{3}J signals to a third oxygen bearing olefinic quaternary carbon (δ_C 132.6, C-6) and an olefinic quaternary carbon (δ_C 106.2, C-10). Ring A of the flavone was completed by HMBC correlations from the proton of an hydroxyl detected as a singlet at δ_H 12.75. This gave a ^{2}J correlation to a quaternary carbon (δ_C 153.2, C-5), placing the hydroxyl here. Two ^{3}J correlations to C-6 and C-10 confirmed the position of this quaternary carbon as being *para* with respect to H-8. The presence of a second proton singlet in the aromatic region of the ^{1}H NMR spectrum is characteristic of H-3 (δ_H 6.58) of a flavone (Albach *et al.*, 2003). This gave a ^{3}J correlation to C-10 and ^{2}J correlation to an oxygen bearing quaternary carbon (δ_C 163.8, C-2), completing ring C. The olefin is shielded because the group is positioned α with respect to the carbonyl of the flavone. As electrons are being attracted by the oxygen of the carbonyl, the electron density becomes higher thus providing a shielding effect. Ring B was composed of three aromatic protons arranged in an ABD spin system. This is characteristic of a 1',3',4'-trisubstituted ring system. The COSY spectrum showed that H-5' coupled to H-6' (J = 8.5 Hz), which in turn

gave a long range coupling to H-2' in the ^{1}H NMR spectrum of 2.0 Hz. In the HMBC spectrum H-2' and H-6' both gave ^3J correlations to an oxyquaternary carbon (δ_C 149.3) placing it at C-4'. H-5' also gave a ^3J correlation to a second oxyquaternary carbon (δ_C 146.1) placing it at C-3' as well as a quaternary carbon (δ_C 124.5) at C-1'. H-2' and H-6' both gave a ^3J correlation to C-2, finalising the point of attachment of ring B to ring C of the flavone. The protons of the methoxyl groups each gave ^3J signals to the carbons to which they were attached. Thus methoxyl groups were attached to C-6, C-7 and C-4'. This meant that hydroxyl groups had to be placed at C-5 and C-3', which was corroborated by the mass spectrum for this compound. **MS-32** is a known compound having previously been isolated from *Eupatorium altissimum* (Asteraceae) (Dobberstein *et al.*, 1977) and *Orthosiphon aristatus* (Lamiaceae) (Sumaryono *et al.*, 1991).

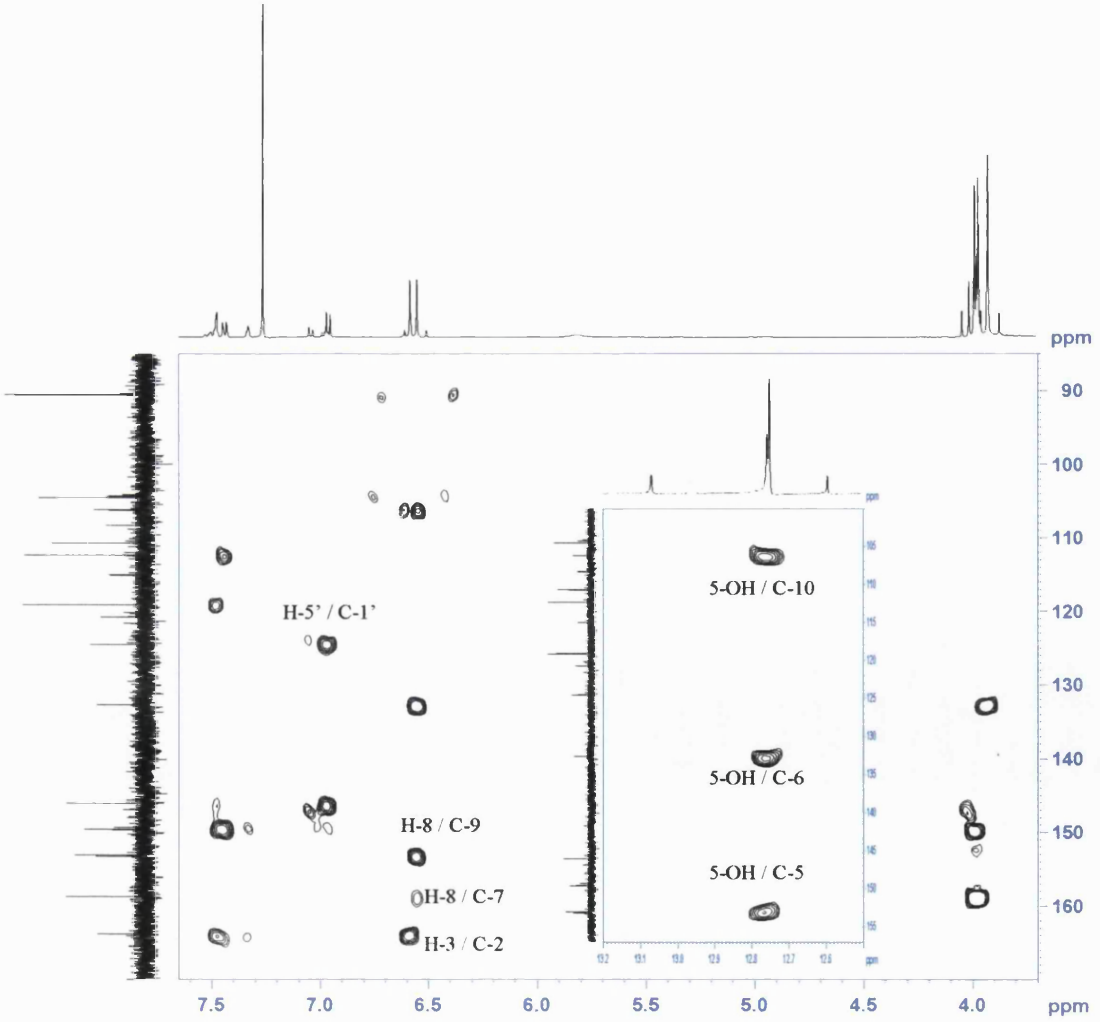

Figure 3.8.1D HMBC spectrum of **MS-32**

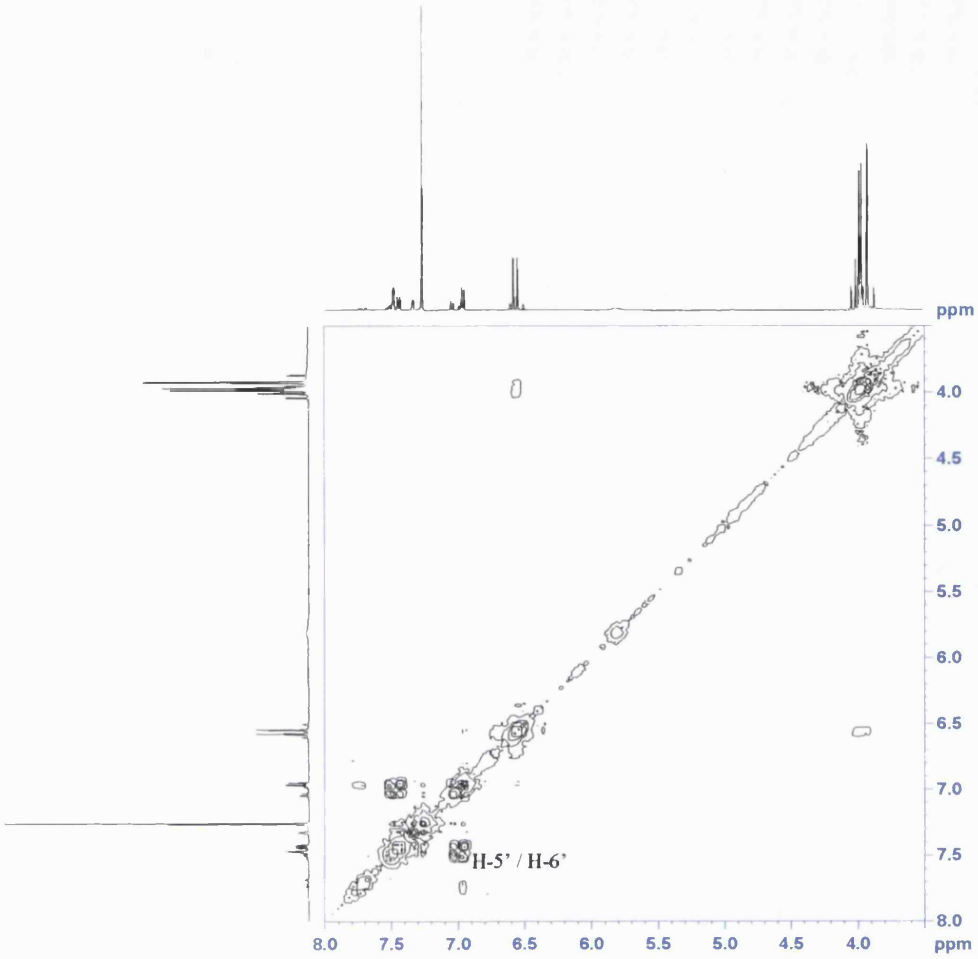

Figure 3.8.1E COSY spectrum of **MS-32**

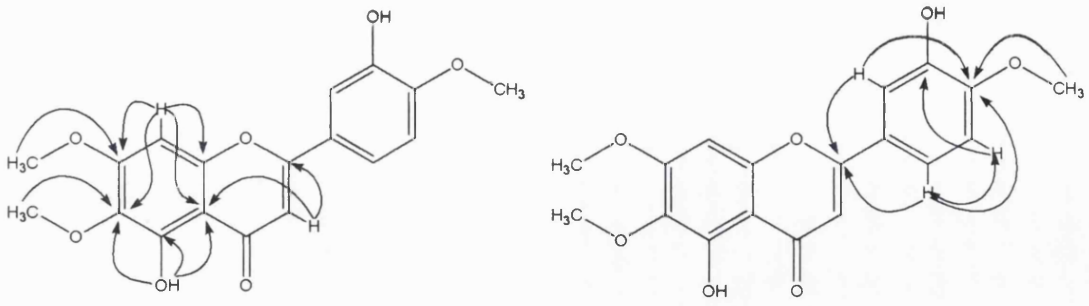

Figure 3.8.1F HMBC correlations for **MS-32**

Table 29 ^{1}H and ^{13}C NMR data and ^{1}H-^{13}C long-range correlations of **MS-32** recorded in $CDCl_3$

Position	^{1}H	^{13}C	^{2}J	^{3}J
1	-	-		
2	-	163.8		
3	6.58 s	104.5	C-2	C-10
4	-	182.7		
5	-	153.2		
6	-	132.6		
7	-	158.8		
8	6.55 s	90.6	C-7, C-9	C-6, C-10
9	-	153.1		
10	-	106.2		
1'	-	124.5		
2'	7.48 d (2.0)	112.3		C-4', C-6', C-2
3'	-	146.1		
4'	-	149.3		
5'	6.97 d (8.5)	110.7		C-1', C-3'
6'	7.44 dd (8.5, 2.5)	119.1		C-2', C-4', C-2
6-OCH_3	3.93 s	60.9		C-6
7-OCH_3	3.97 s	56.3		C-7
4'-OCH_3	3.99 s	56.1		C-4'
5-OH	12.75 s	-	C-5	C-6, C-10

3.8.2 Characterisation of MS-33 as 5-hydroxy-3',4',6,7-tetramethoxyflavone

MS-33 was isolated as a yellow amorphous powder, and a molecular formula of $C_{19}H_{18}O_7$ $[M+H]^+$ (359.1) was assigned by ESI-MS. The ^1H and ^{13}C NMR spectra were similar to that of eupatorin, the only difference being the presence of an extra methoxyl group (δ_H 3.99 s, δ_C 56.3, 3'-OCH_3).

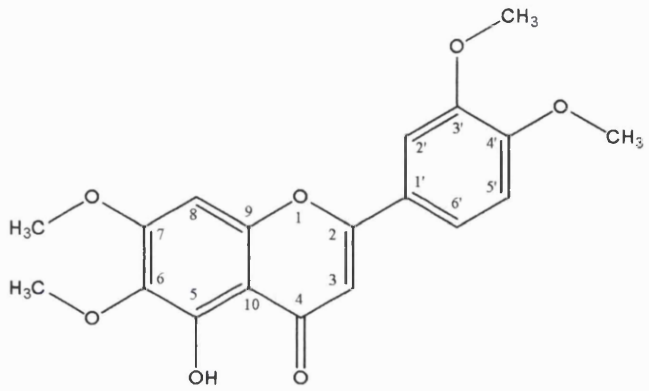

Figure 3.8.2A Structure of **MS-33**

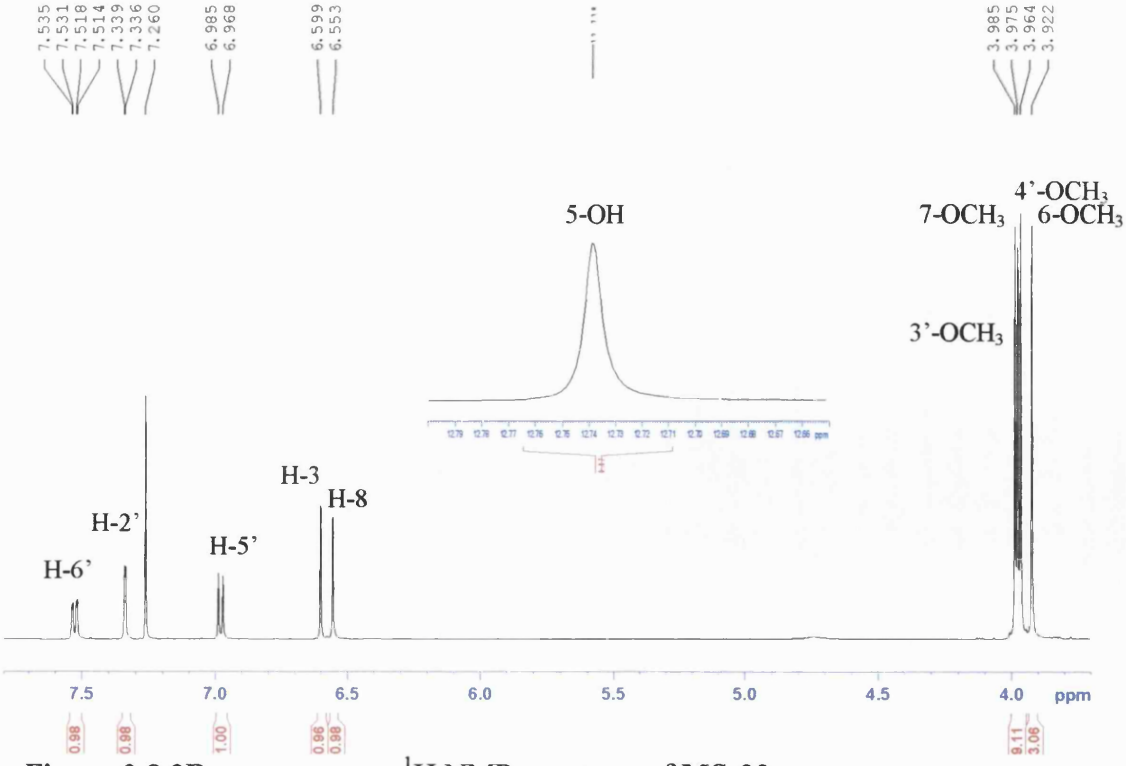

Figure 3.8.2B ^1H NMR spectrum of **MS-33**

The proton singlets at H-3 (δ_H 6.60) and H-8 (δ_H 6.55), described as being characteristic of a flavone in **MS-32** were again detected in **MS-33**, and gave identical HMBC signals. The presence of a downfield singlet (δ_H 12.74, 5-OH) was also indicative of a hydrogen bonded hydroxyl at position 5. The HMBC signals from the hydroxyl were the same as for **MS-32**, thus completing rings A and C. Ring B was again composed of three aromatic protons arranged in an ABD spin system (A: δ_H 6.99 d, J = 8.5 Hz, H-5'; B: δ_H 7.53 dd, J = 8.5, 2.0 Hz, H-6'; D: δ_H 7.34 d, J = 1.5 Hz H-2'). Substitution at positions 3 and 4 of ring B was confirmed by HMBC, which also placed methoxyl groups here. **MS-33** was previously isolated from the Asteraceae plants *Artemisia argyi* (Wu 1985) and *Eupatorium altissimum* (Dobberstein *et al.*, 1977) as well as from *Orthosiphon aristatus* (Lamiaceae) (Sumaryono *et al.*, 1991). The ^{1}H NMR data compared favourably with that of the literature (Dobberstein *et al.*, 1977). ^{1}H NMR data was also published by Wu (1985) and Sumaryono *et al.*, (1991) but in deuterated DMSO, however the ^{13}C NMR data was lacking in all three papers cited.

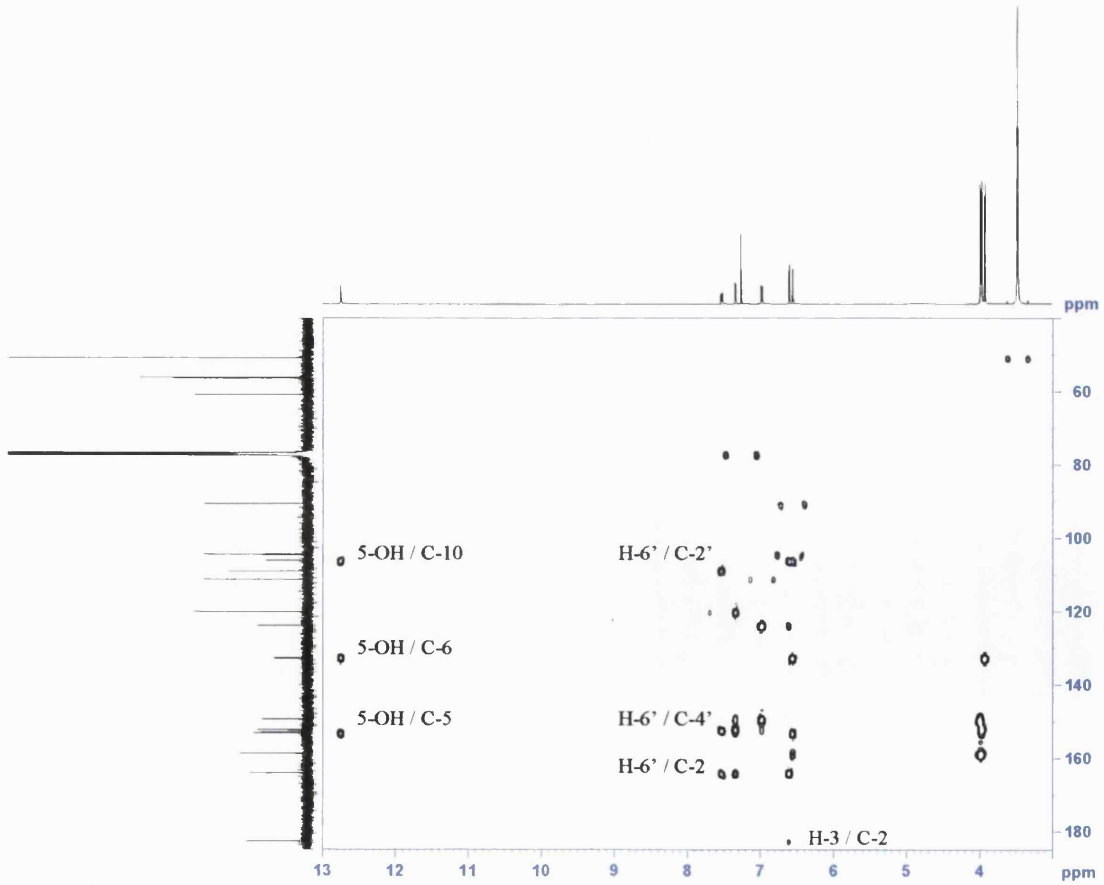

Figure 3.8.2C HMBC spectrum of **MS-33**

Table 30 ^{1}H and ^{13}C NMR data and ^{1}H-^{13}C long-range correlations of **MS-33** recorded in $CDCl_3$

Position	^{1}H	^{13}C	^{2}J	^{3}J
1	-	-		
2	-	164.1		
3	6.60 s	104.5	C-2	C-10, C-1'
4	-	182.7		
5	-	153.3		
6	-	132.8		
7	-	158.8		
8	6.55 s	90.7	C-7, C-9	C-6, C-10
9	-	153.1		
10	-	106.2		
1'	-	123.9		
2'	7.34 d (1.5)	109.1	C-3'	C-4', C-6', C-2
3'	-	149.5		
4'	-	152.4		
5'	6.99 d (8.5)	111.3	C-4'	C-1', C-3'
6'	7.53 dd (8.5, 2.0)	120.1		C-2', C-4', C-2
6-OCH_3	3.92 s	60.8		C-6
7-OCH_3	3.98 s	56.2		C-7
3'-OCH_3	3.99 s	56.3		C-3'
4'-OCH_3	3.97 s	56.1		C-4'
5-OH	12.74 s	-	C-5	C-6, C-10

3.8.3 Characterisation of MS-34 as quercetin-3-*O*-β-D-glucopyranoside

MS-34 was isolated as a yellow amorphous powder. ESI-MS yielded a peak at *m/z* 463.3 $[M-H]^-$, which enabled a molecular formula $C_{21}H_{20}O_{12}$ to be assigned based on the NMR data. The ^1H and ^{13}C NMR data provided signals characteristic for a flavonol glycoside. The ^1H spectrum revealed five aromatic protons, two of which exhibited long range couplings of 2.0 Hz characteristic of H-6 (δ_H 6.19 d, δ_C 100.3) and H-8 (δ_H 6.38 d, δ_C 95.0). The remaining three aromatic protons were arranged in an ABD spin system as for **MS-32** and **MS-33**. The presence of an anomeric proton (δ_H 5.12 d, H-1''), along with protons for 4 oxymethines and an oxymethylene was indicative of a hexose. The ^{13}C spectrum provided signals for 20 carbons, including a carbonyl (δ_C 179.5, C-4), and 8 oxygen bearing quaternary carbons.

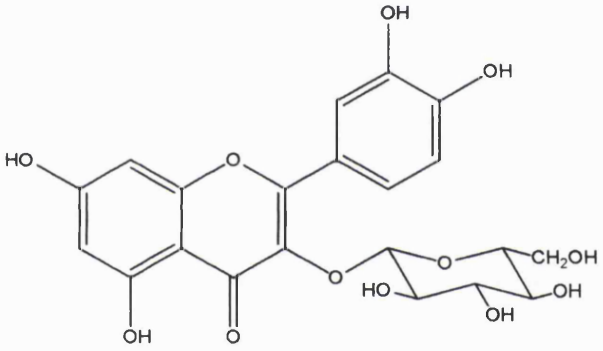

Figure 3.8.3A Structure of **MS-34**

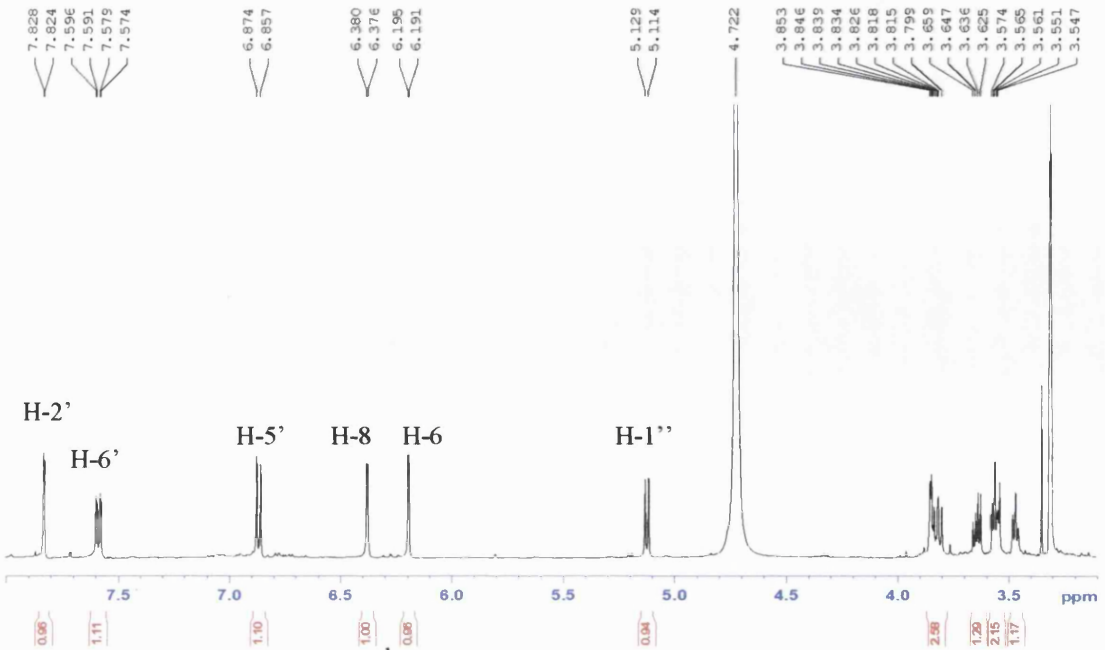

Figure 3.8.3B ^1H NMR spectrum of **MS-34**

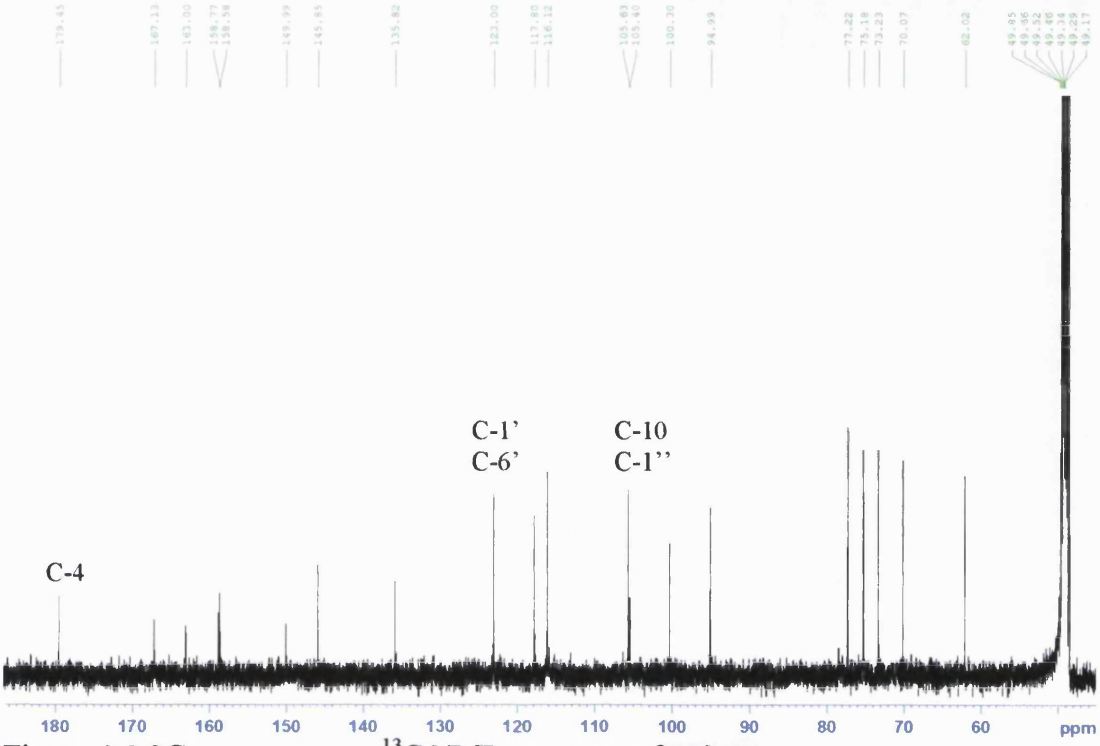

Figure 3.8.3C ^{13}C NMR spectrum of **MS-34**

The aromatic proton attached at C-8 gave ^{2}J correlations to C-7 (δ_C 167.1) and C-9 (δ_C 158.6) and ^{3}J correlations to C-6 (δ_C 100.3) and C-10 (δ_C 105.4). C-10 was also correlated to by H-6 placing this carbon at the ring junction of the benzopyranone system. The appearance of these two aromatic protons in the ^{1}H spectrum is indicative of a 5,7 disubstituted aromatic ring. The downfield resonance of these carbons led to hydroxyl groups being placed here. H-2' and H-6' each gave a ^{3}J correlation to C-2, placing this carbon here, whilst the anomeric proton of the hexose gave a ^{3}J signal to C-3 placing this carbon α with respect to the carbonyl. This accounts for the shielding effect observed for C-3 (δ_C 135.8) as opposed to C-2 (δ_C 158.8). H-2' (δ_H 7.82), H-5' (δ_H 6.87) and H-6' (δ_H 7.59) composed an ABD spin system, with H-2' and H-6' exhibiting a long range coupling (J = 2.0 Hz). Both protons also gave a ^{3}J correlation to C-4' (δ_C 150.0), whilst H-2' and H-5' gave an HMBC signal to C-3' (δ_C 145.9). Due to the downfield resonance of these carbons hydroxyls were placed here. This was corroborated by the mass spectrum for this compound. The hexose sugar was deduced as being glucose based on the large couplings measured. The coupling between H-1'' and H-2'' (7.5 Hz) was large and H-2'' appeared as a double doublet with two large couplings (9.5, 8.0 Hz) indicating an axial configuration for H-1'', H-

2'' and H-3''. H-5'' appeared as a triplet (δ_H 3.47 t, J = 6.5 Hz) in the ^1H spectrum which also indicated an axial configuration for H-4'' and H-5''. This confirmed the isolation of the flavonol quercetin-3-*O*-β-D-glucopyranoside. The carbon resonances were in close agreement with data published by Harborne and Mabry (1982). This showed that C-1' and C-2' are almost superimposed. The ^{13}C spectrum acquired for **MS-34** appears to show only 20 carbons, however with the information obtained from previously published data and the mass spectrum for this compound, it can be stated that there are in fact 21 carbons. The two carbons which were superimposed appeared at δ_C 123.0. Quercetin 3-*O*-glucoside is a well known flavonol glycoside and has previously been isolated from grape pomace (Lu and Foo 1999).

Table 31 ^1H and ^{13}C NMR data and ^1H-^{13}C long-range correlations of **MS-34** recorded on CD_3OD

Position	^1H	^{13}C	^2J	^3J
1	-	-		
2	-	158.8		
3	-	135.8		
4	-	179.5		
5	-	163.0		
6	6.19 d (2.0)	100.3		C-10
7	-	167.1		
8	6.38 d (2.0)	95.0	C-7, C-9	C-6, C-10
9	-	158.6		
10	-	105.4		
1'	-	123.0		
2'	7.82 d (2.0)	117.8	C-3', C-1'	C-4', C-6', C-2
3'	-	145.9		
4'	-	150.0		
5'	6.87 d (8.5)	116.1	C-4', C-6'	C-1', C-3'
6'	7.59 dd (8.5, 2.5)	123.0		C-2', C-4', C-2
1"	5.12 d (7.5)	105.6		C-3
2"	3.82 dd (9.5, 8.0)	73.1	C-1", C-3"	
3"	3.57 m	75.2	C-2", C-4"	C-5"
4"	3.85 m	70.1		C-2"
5"	3.47 t (6.5)	77.2	C-4", C-6"	C-1"
6"	3.56 d (11.0)	62.0		
	3.65 dd (11.5, 6.0)	-		

3.8.4 Characterisation of MS-35 as eriodictyol-7-methyl ether (keto-enol tautomer; racemate)

MS-35 was isolated as a pale yellow amorphous powder and a molecular formula of $C_{16}H_{14}O_6$ $[M-H]^+$ (301.1) was established by ESI-MS. Signals in the ^1H and ^{13}C NMR spectra for a methoxyl group (δ_H 3.79, δ_C 56.1, 7-OCH_3), a downfield methylene group (δ_H 2.74, 3.08 dd, δ_C 43.9), 5 aromatic protons arranged in identical fashion as the previously discussed flavonoids and a carbonyl group (δ_C 197.7, C-4) indicated the presence of a flavanone. Two further signals, an olefinic proton (δ_H 6.62 s, δ_C 116.6, C-3) and an oxygen bearing quaternary carbon (δ_C 151.2, C-4), indicated that **MS-35** was in fact a mixture of the keto-enol tautomer. This was confirmed by the mass spectrum obtained.

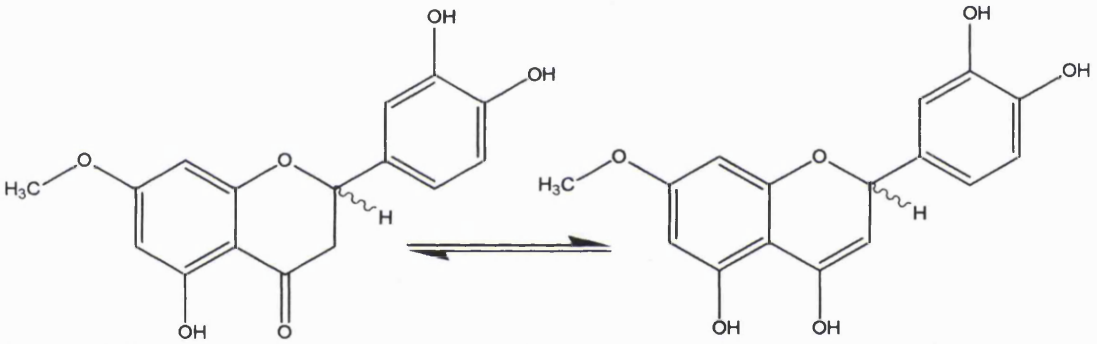

Figure 3.8.4A Structure of the keto-enol tautomers of **MS-35**

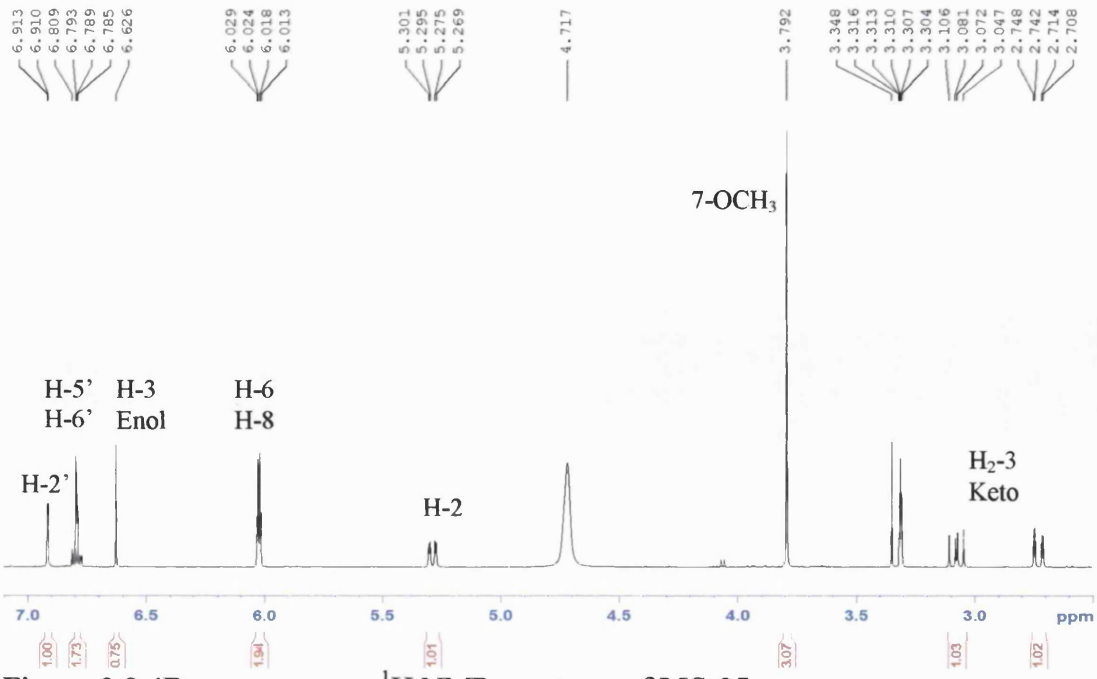

Figure 3.8.4B ^1H NMR spectrum of **MS-35**

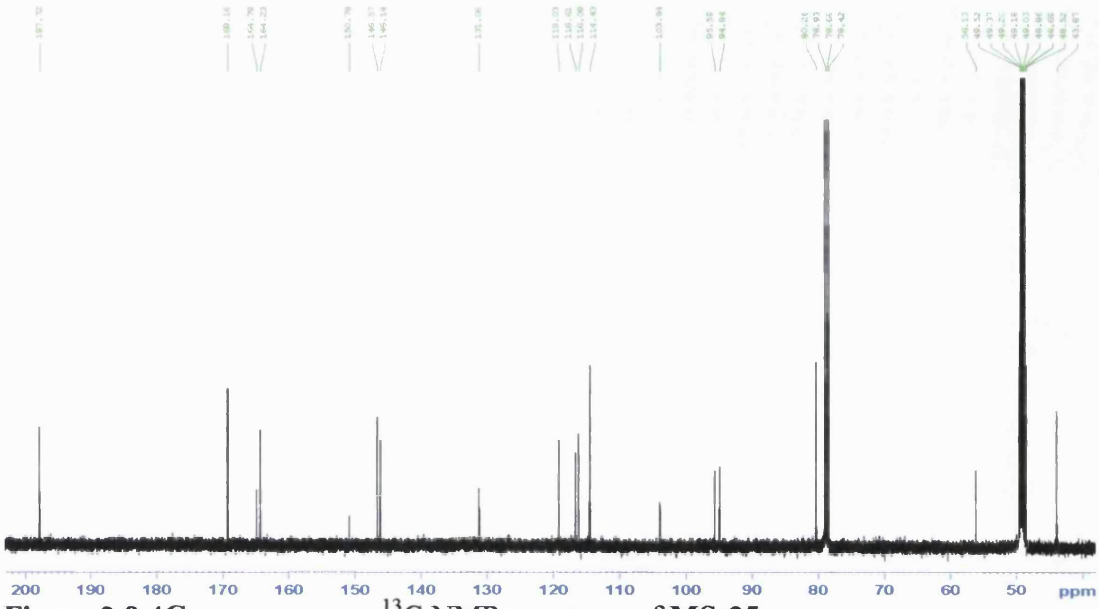

Figure 3.8.4C ^{13}C NMR spectrum of **MS-35**

The aromatic proton H-8 showed HMBC signals to C-10, C-6, C-7 and C-9 to place them in ring A of the flavonoid molecule. H-6 gave an additional HMBC signal to C-5, thus completing the aromatic ring. The quaternary carbons C-5 and C-7 appeared downfield in the ^{13}C spectrum and so an hydroxyl was placed at C-5. A methoxyl was attached at C-7 due to a ^{3}J correlation from the methyl protons to this carbon. Ring B was attached to ring C of the flavonoid *via* an oxymethine carbon, C-2 (δ_C 80.3). This was verified by ^{3}J signals from H-2' and H-6' to C-2. A COSY correlation between the oxymethine proton H-2 (δ_H 5.29 dd, J = 12.5, 2.5 Hz) and a pair of deshielded methylene protons placed them at H_2-3 (δ_H 2.74 dd, J = 17.0, 3.0 and δ_H 3.08 dd, J = 17.0, 12.5 Hz). The B ring was again composed of an ABD spin system, with carbons 3' and 4' both having hydroxyls directly attached. This completed the keto tautomeric form.

An olefinic proton at δ_H 6.62 ppm gave a ^{2}J correlation to an oxyquaternary carbon at δ_C 151.2 ppm. This olefinic proton also gave a weak ^{4}J signal to H-6' indicating these groups were real and part of the enol tautomer. The tautomers were isolated in a 1.00:0.75 keto:enol form, based on the integration of the peaks in ^{1}H spectrum (**Figure 3.8.4B**). **MS-35** was optically inactive indicating that it was isolated as a racemic mixture. This is the first report of eriodictyol-7-methyl ether being isolated as the keto-enol tautomer. The flavanone eriodictyol-7-methyl ether (keto form) has previously been isolated from *Notholaena fendleri*, a rare American fern (Wollenweber 1981) as well as from *A. monosperma* where this compound has been shown to have antispasmodic activity (Abu-Niaaj *et al.*, 1993).

Figure 3.8.4D HMBC and COSY spectra of **MS-35**

Table 32 ^{1}H and ^{13}C NMR data of the keto and enol tautomers of **MS-35** recorded in CD_3OD

	Keto form		Enol form	
Position	^{1}H	^{13}C	^{1}H	^{13}C
1	-	-	-	-
2	5.29 dd (12.5, 2.5)	80.3	5.29 dd (12.5, 2.5)	80.3
3	2.74 dd (17.0, 3.0) 3.08 dd (17.0, 12.5)	43.9	6.62 s	116.6
4	-	197.7	-	151.2
5	-	164.2	-	164.2
6	6.02 (2.5)	94.8	6.02 (2.5)	94.8
7	-	169.2	-	169.2
8	6.02 (2.5)	95.6	6.02 (2.5)	95.6
9	-	164.8	-	164.8
10	-	103.8	-	103.8
1'	-	131.1	-	131.1
2'	6.91 d (1.5)	114.4	6.91 d (1.5)	114.4
3'	-	146.6	-	146.6
4'	-	146.1	-	146.1
5'	6.79 m	119.0	6.79 m	119.0
6'	6.79 m	116.1	6.79 m	116.1
7-OCH_3	3.79 s	56.1	3.79 s	56.1

Table 33 ^{1}H-^{13}C long-range correlations detected in HMBC spectrum of the keto and enol tautomers of **MS-35**

	Keto form		Enol form	
Position	^{2}J	^{3}J	^{2}J	^{3}J
1				
2		C-4, C-1', C-2', C-6'		C-4, C-1', C-2', C-6'
3	C-2, C-4	C-10, C-1'	C-4	
4				
5				
6	C-5, C-7	C-8, C-10	C-5, C-7	C-8, C-10
7				
8	C-7, C-9	C-6, C-10	C-7, C-9	C-6, C-10
9				
10				
1'				
2'	C-3'	C-6', C-2	C-3'	C-6', C-2
3'				
4'				
5'	C-4'		C-4'	
6'		C-2', C-4', C-2		C-2', C-4', C-2
7-OCH_3		C-7		C-7

3.8.5 Biosynthesis of flavonoids

Flavonoids are heterocyclic compounds that are responsible for the colouring of flowers and flavours in food and drink. They are mixed pathway metabolites, being derived from the acetate and shikimate pathways. Phenylalanine undergoes a series of oxidation reactions to yield *p*-coumaroyl-CoA. Condensation of three C_2 units followed by cyclisation produces the chalcone flavonoids. These can then undergo an enzymatic reaction catalysed by chalcone isomerase to yield the flavanone, naringenin. From here, a series of enzymatic reactions leads to the biosynthesis of **MS-32 - MS-35**.

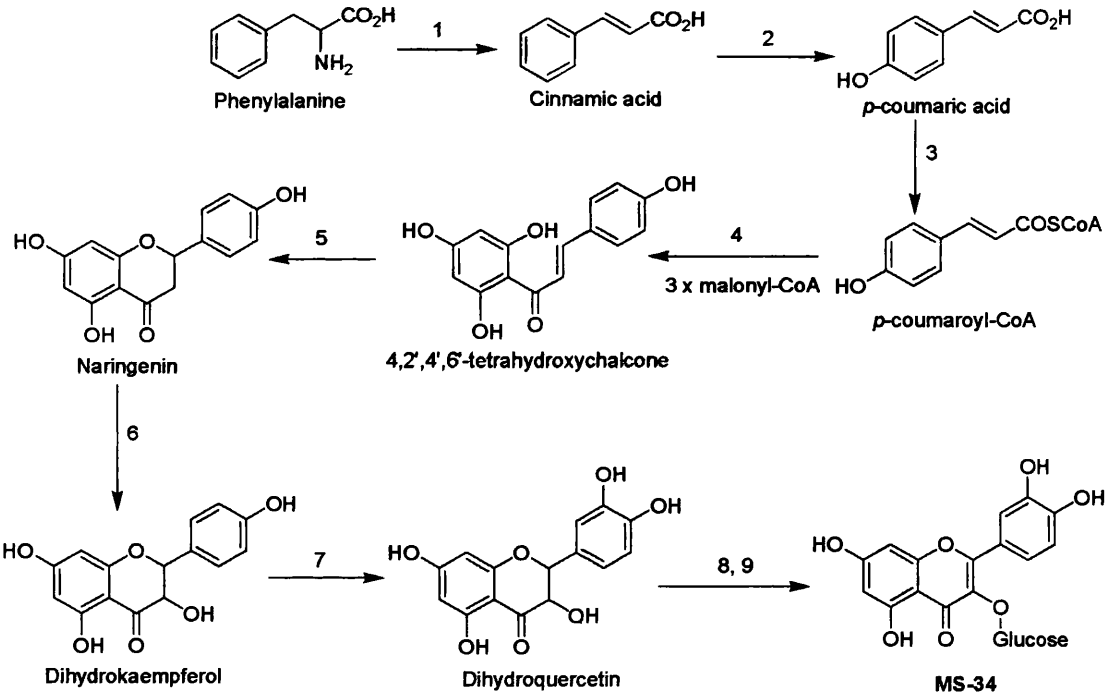

Scheme 7A **Enzyme-mediated biosynthesis of quercetin 3-*O*-β-D-glucoside (MS-34). Adapted from Gibbons (1994).**

List of enzymes mentioned in flavonoid biosynthesis schemes

1 = Phenylalanine ammonia lyase
2 = Cinnamate 4-hydroxylase
3 = 4-coumarate:CoA ligase
4 = Chalcone synthase
5 = Chalcone isomerase
6 = Flavonoid 3-hydroxylase
7 = Flavonoid 3'-hydroxylase
8 = Flavonoid 2,3-dehydrogenase
9 = Flavonol 3-O-glucosyltransferase
10 = SAM:flavonoid methyltransferase
11 = Flavonoid 6-hydroxylase

SAM = S-adenosyl-L-methionine

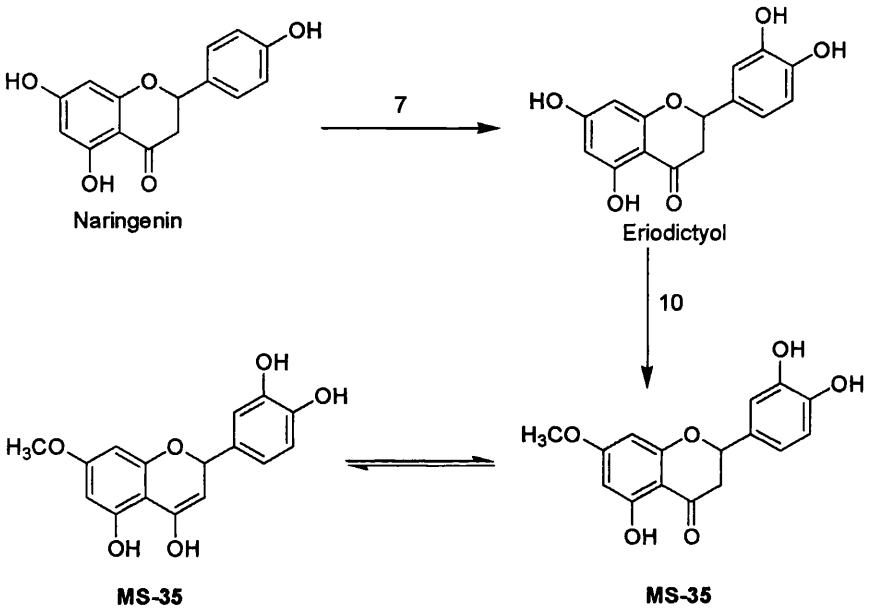

Scheme 7B **Proposed biosynthetic pathway of MS-35 from naringenin**

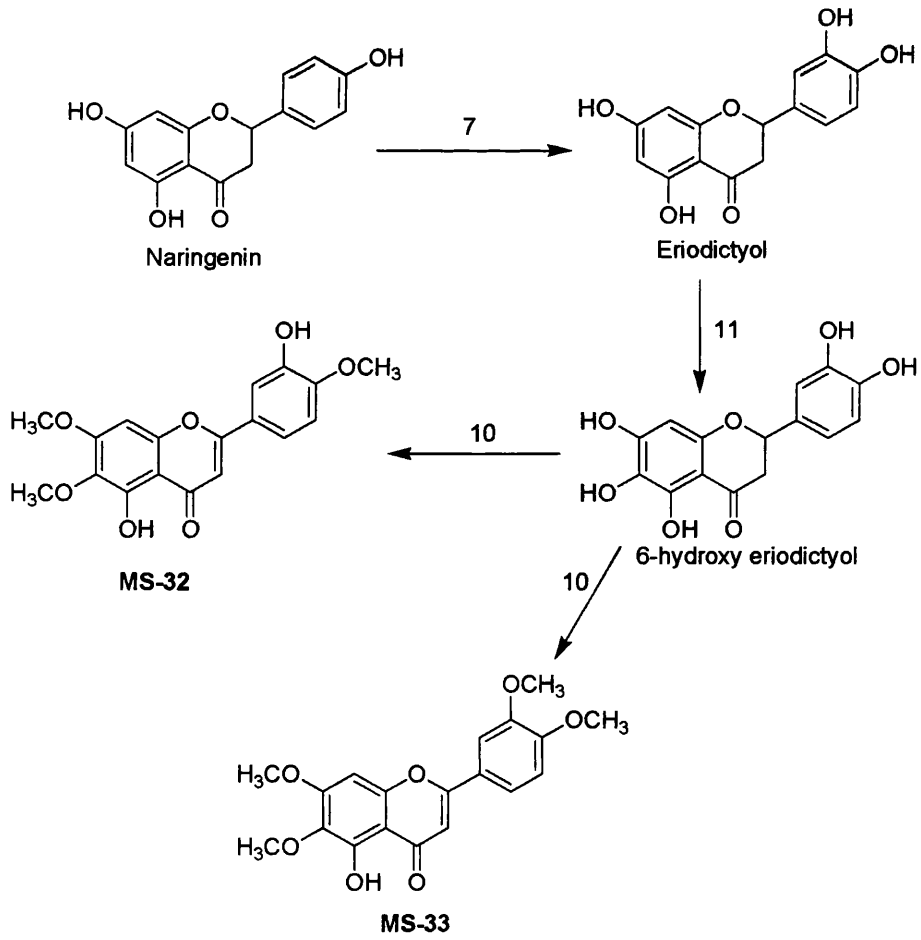

Scheme 7C **Proposed biosynthetic pathway of MS-32 and MS-33 from naringenin.**

3.9 Aromatics/Phenolics

3.9.1 Characterisation of MS-36 as 3-[3'-methyl-2'-butenyl]-5-[4''-hydroxy-3''-methyl-2''-butenyl]-6-hydroxy-*p*-coumaric acid

HREIMS of **MS-36** suggested a molecular formula of $C_{19}H_{24}O_5$ $[M]^+$ (332.1623). This compound was isolated as a colourless oil from the chloroform extract of *A. monosperma*. The ^1H NMR provided signals for four olefinic protons and one aromatic proton (δ_H 7.20). Two of the olefins were coupled to each other (δ_H 7.70 d, J = 16.0 Hz, H-7, δ_H 6.30 d, J = 16.0 Hz, H-8). The remaining two olefins appeared as triplets with fine splitting (δ_H 5.61, H-2'', δ_H 5.31, H-2'). Three methyl singlets and two protons of an oxymethylene group also appearing as a singlet were detected in the ^1H NMR spectrum, suggesting the presence of two prenyl groups. The ^{13}C NMR provided signals for 19 carbons, including 7 quaternary carbons two of which are oxygen bearing, 4 olefinic methine carbons, an aromatic methine carbon and a carbonyl group (δ_C 172.1, C-9). The NMR data acquired indicated the presence of a prenylated dihydroxy *trans*-cinnamate structure.

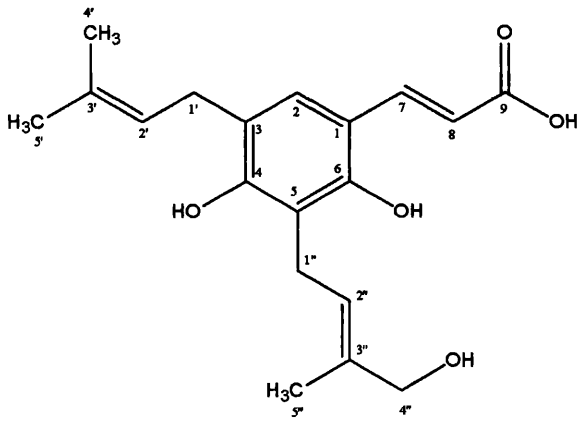

Figure 3.9.1A Structure of **MS-36**

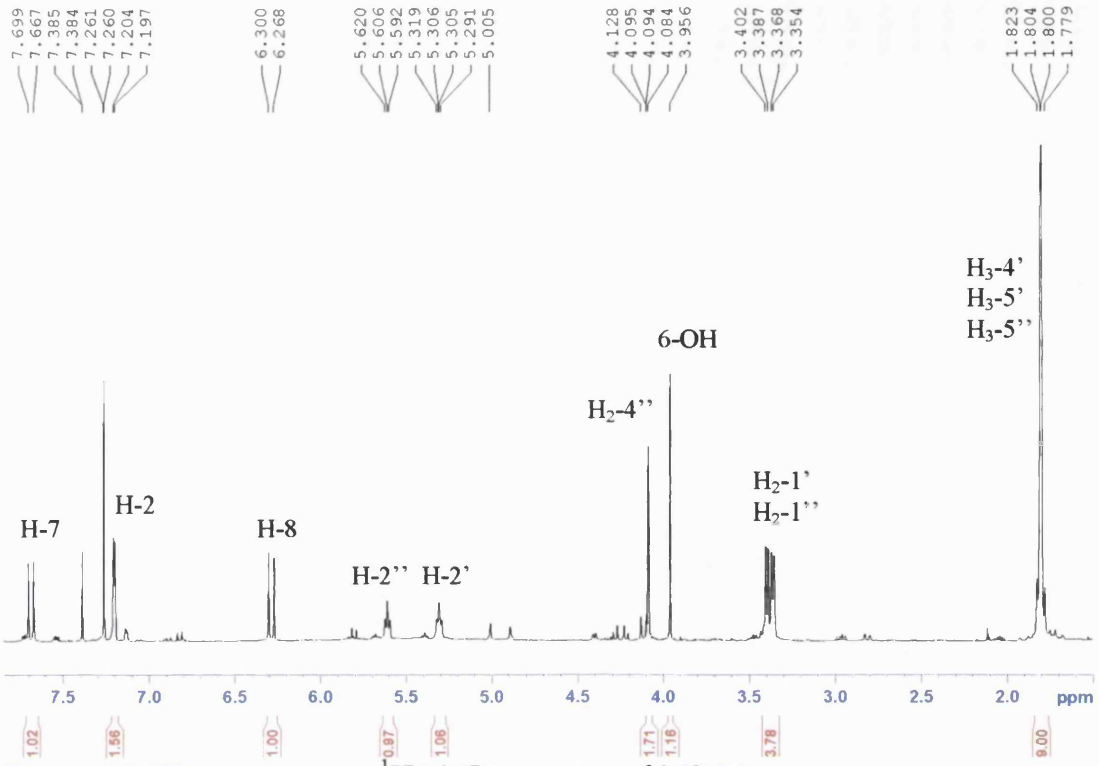

Figure 3.9.2B ^{1}H NMR spectrum of **MS-36**

Assuming a cinnamoyl moiety, a prenyl group was attached to C-3 and C-5 of the aromatic ring based on the HMBC data acquired. Hydroxyl groups were placed at C-4 and C-6 of the aromatic ring. The *trans* olefin, H-8, coupled to its olefinic partner H-7 and also gave a ^{2}J correlation to the carbonyl at C-9. The placement of this group to the aromatic ring was achieved by a ^{3}J correlation between H-8 and C-1 (δ_C 126.5). Another ^{3}J signal between H-7 and C-2 placed the aromatic methine group here. This proton then provided ^{3}J signals to two oxyquaternary carbons positioned at C-4 and C-6. The mass spectrum and NMR data confirmed that hydroxyl groups should be placed on these carbons. H-2 also gave a ^{3}J signal to a methylene group of a prenyl moiety at C-1'. This confirmed that one of the prenyl groups should be attached at C-3 of the aromatic ring. From the ^{1}H NMR spectrum, H-2 appears as a small doublet (J = 3.5 Hz) that couples to H_2-1' in the COSY spectrum. Therefore the coupling constant of 3.5 Hz can be attributed to allylic coupling between H-2 and H_2-1'. The methylene protons H_2-1' coupled to an olefinic proton H-2' and also gave a ^{3}J correlation to an olefinic quaternary carbon (δ_C 135.9) placing it at C-3'. Two methyl groups (both δ_H 1.80 s) both gave ^{2}J signals to C-3' placing these groups on this quaternary carbon. H_2-1' also gave a ^{2}J signal to C-3, the aromatic carbon to which it is attached along with a ^{3}J signal to the oxyquaternary carbon, C-4. The second prenyl

group was placed at C-5 based on a ^{2}J correlation to this carbon. From the H_2-1'' protons, these methylene protons coupled to an olefinic proton and again provided a ^{3}J correlation to the olefinic quaternary carbon placing these groups at C-2'' and C-3'', respectively. A methyl singlet (δ_H 1.80, H_3-5'') and a downfield methylene singlet (δ_H 4.08, H_2-4'') both gave ^{2}J correlations to C-3'', therefore these groups must be directly attached to this carbon. An hydroxyl was placed on the methylene carbon, which would account for the downfield shift of both the ^{1}H and ^{13}C signals. A sharp singlet at δ_H 3.96, corresponding to the hydroxyl at C-6, provided a ^{2}J signal to the quaternary carbon. The prenyl groups must be *ortho* with respect to C-4 as both the methylene protons at H_2-1' and H_2-1'' both gave ^{3}J correlations to this carbon.

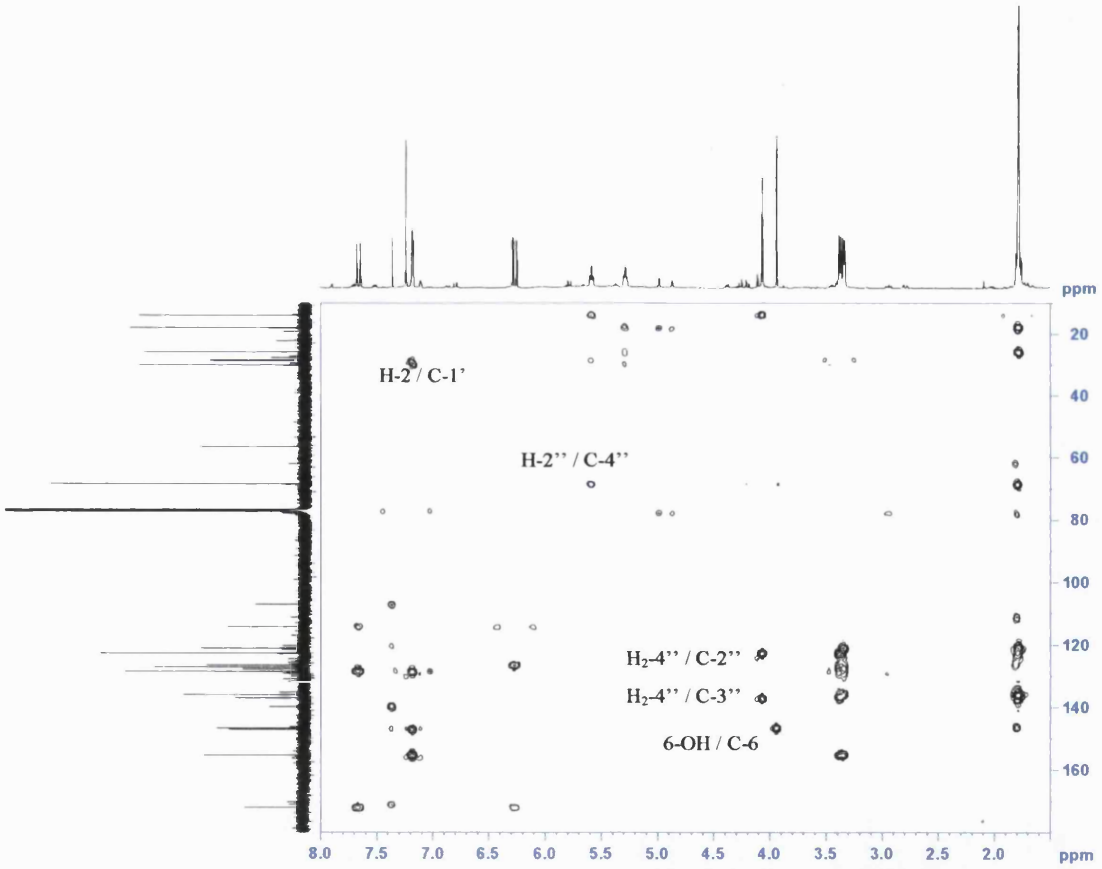

Figure 3.9.2C HMBC spectrum of **MS-36**

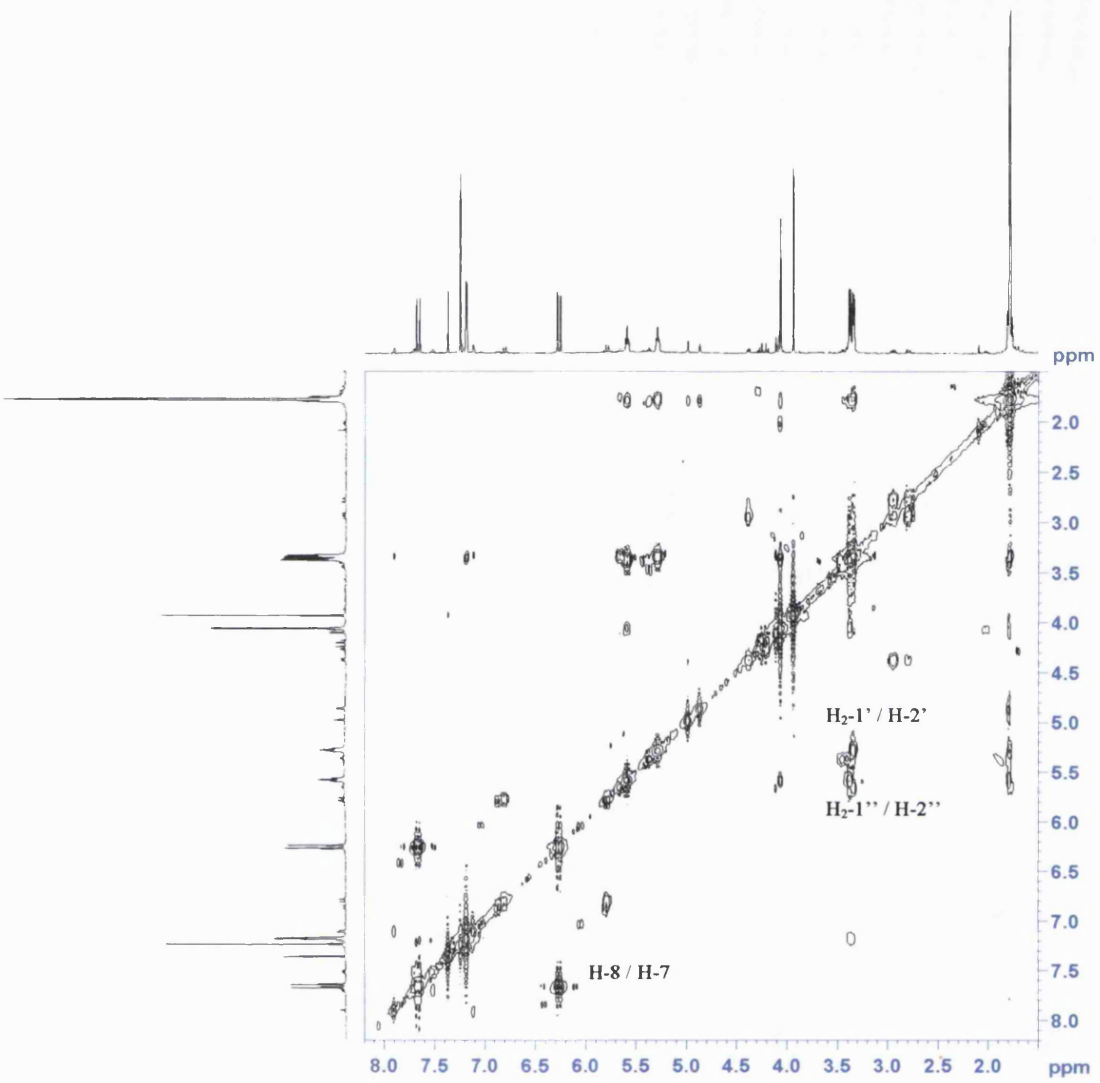

Figure 3.9.2C COSY spectrum of **MS-36**

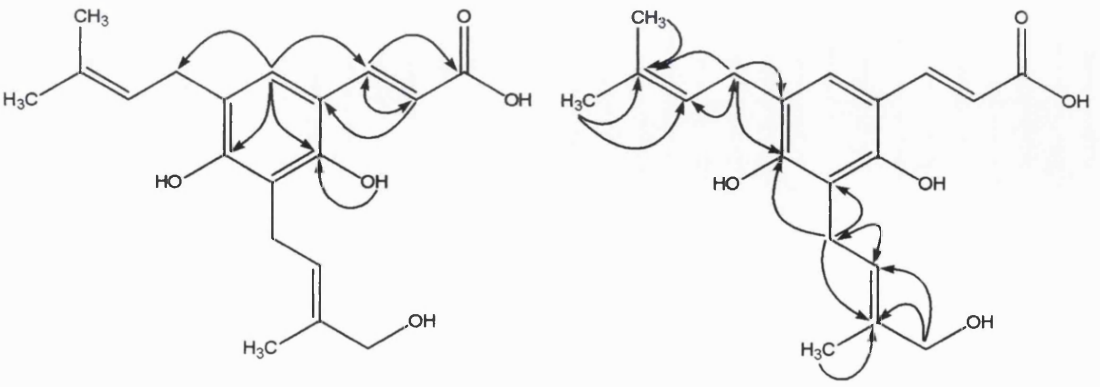

Figure 3.9.2D HMBC and COSY correlations for **MS-36**

The stereochemistry of **MS-36** was determined by NOE's detected in the NOESY spectrum. An 1,3 interaction between H-2 and H_2-1' placed these protons in close spatial proximity. A second NOE between H-2 and H-7 also meant these protons were in close association. Two key NOE's determined the stereochemistry of the second prenyl group. Firstly, a 1,4 interaction between H_2-1'' and H_3-5'' placed these protons on the same face of this group. A second NOE between the olefinic proton H-2'' and the oxymethylene protons H_2-4'' further confirmed the proposed stereochemistry of this prenyl group. **MS-36** is therefore assigned as 3-[3'-methyl-2'-butenyl]-5-[4''-hydroxy-3''-methyl-2''-butenyl]-6-hydroxy-*p*-coumaric acid and is reported here for the first time. This compound is likely to be a precursor for a coumarin. Isomerisation at positions 7,8 needs to occur prior to lactone formation.

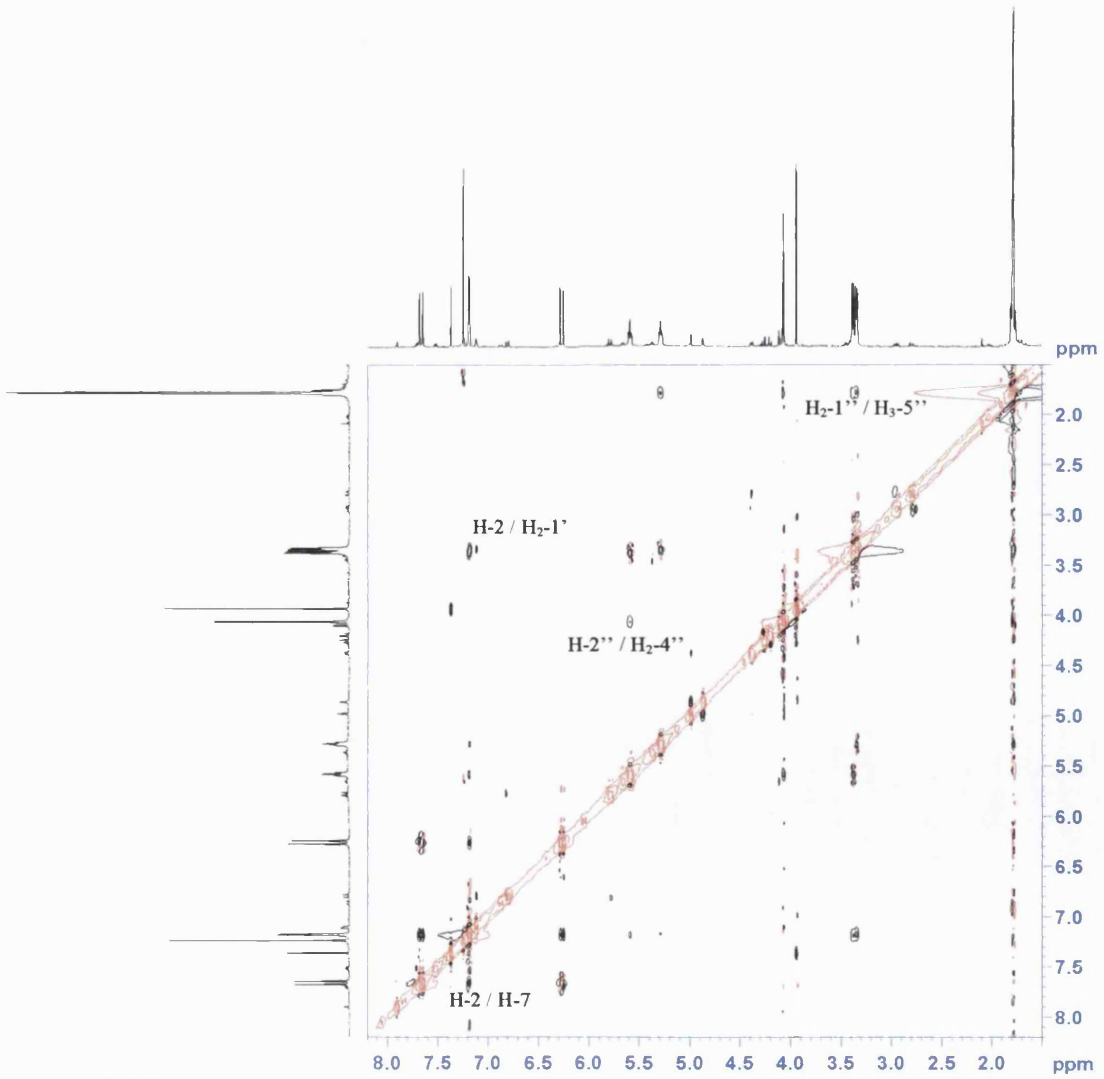

Figure 3.9.2E NOESY spectrum of **MS-36**

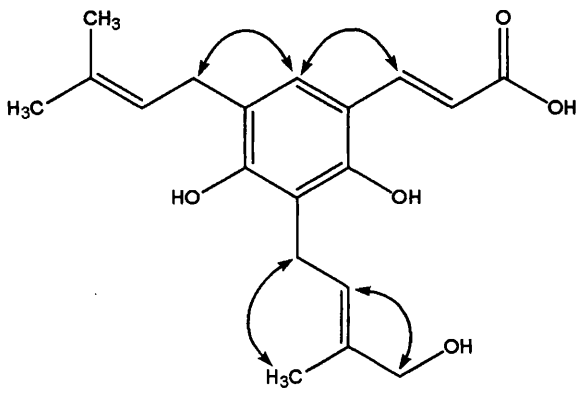

Figure 3.9.2F Key NOE correlations of **MS-36**

Table 34 ^{1}H and ^{13}C NMR data and ^{1}H-^{13}C long-range correlations of **MS-36** recorded in $CDCl_3$

Position	^{1}H	^{13}C	^{2}J	^{3}J
1	-	126.5		
2	7.20 d (3.5)	128.5		C-4, C-6, C-7, C-1'
3	-	127.7		
4	-	155.3		
5	-	127.2		
6	-	146.7		
7	7.70 d (16.0)	147.1	C-8	C-2, C-9
8	6.30 d (16.0)	114.2	C-9	C-1
9	-	172.1		
1'	3.37 d (7.0)	30.0	C-2', C-3	C-3', C-4
2'	5.31 t (7.0)	121.0	C-1'	C-4', C-5'
3'	-	135.9		
4'	1.80 s	17.9	C-3'	C-2', C-5'
5'	1.80 s	25.8	C-3'	C-2', C-4'
1"	3.40 d (7.5)	28.5	C-2", C-5	C-3", C-4
2"	5.61 t (7.0)	122.8	C-1"	C-4", C-5"
3"	-	137.1		
4"	4.08 s	68.5	C-3"	C-2", C-5"
5"	1.80 s	13.8	C-3"	C-2", C-4"
6 - OH	3.96 s	-	C-6	

3.9.2 Characterisation of MS-37 as 5-*O*-caffeoylquinic acid (chlorogenic acid)

MS-37 was isolated as a yellow resin from the methanol extract of *A. monosperma*. A molecular formula of $C_{16}H_{18}O_9$ was assigned by ESI-MS with a base ion of 377 $[M+Na]^+$. The ^1H and ^{13}C NMR spectra showed signals suggesting the presence of a caffeoyl and quinic acid moieties. This included three aromatic protons arranged in an ABD spin system, two *trans*-olefinic protons, three oxymethine groups, two methylene groups and two carbonyl carbons.

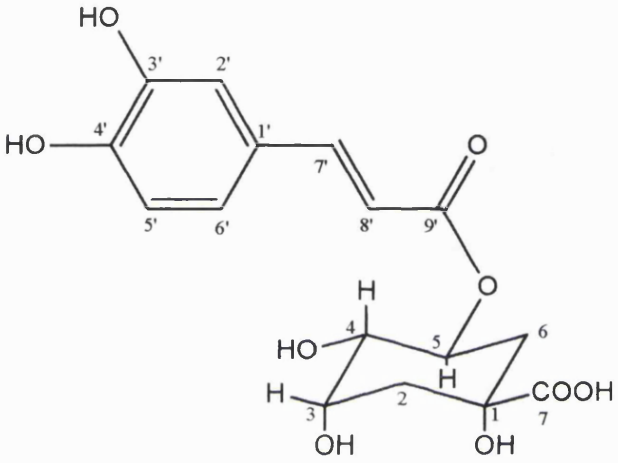

Figure 3.9.2A Structure of **MS-37**

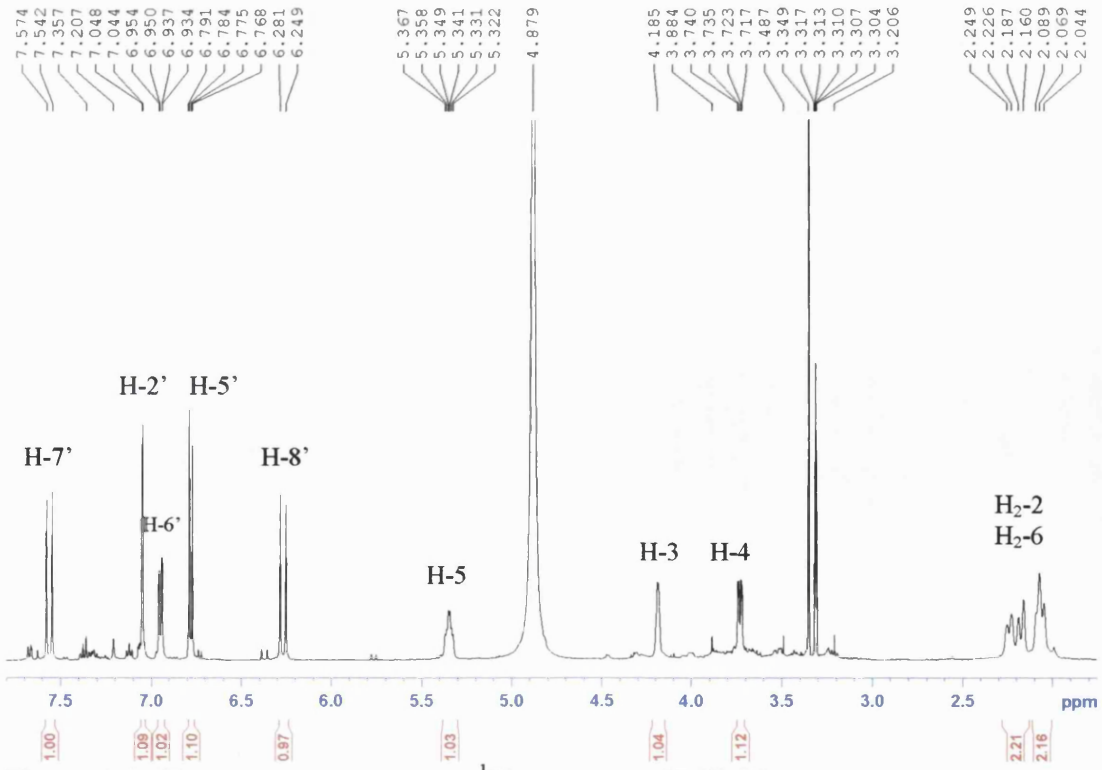

Figure 3.9.2B ^1H spectrum of **MS-37**

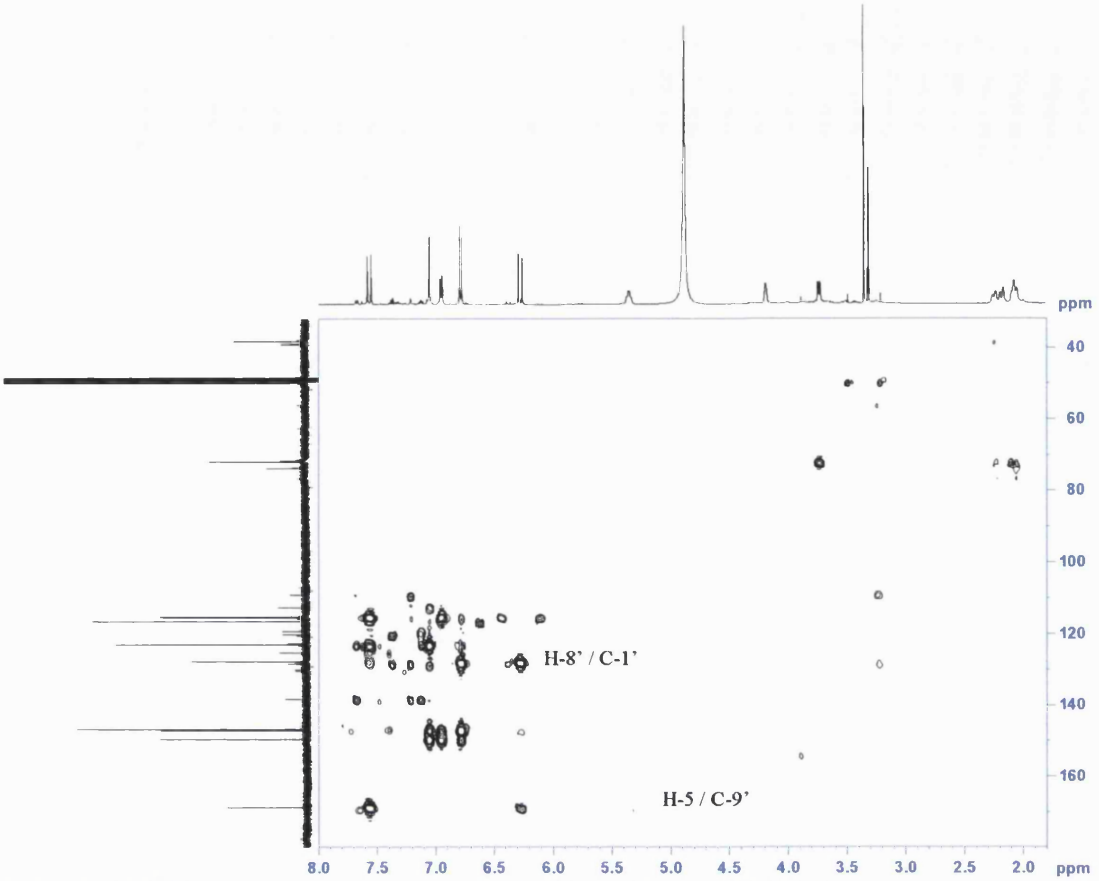

Figure 3.9.2C HMBC spectrum of **MS-37**

The methylene protons, H_2-2, (δ_H 2.04 and δ_H 2.19) gave a weak ^2J correlation to an oxyquaternary carbon (δ_C 76.9, C-1) and a COSY correlation to H-3 of the oxymethine group (δ_H 4.18 bs). This proton showed a COSY correlation to an oxymethine proton which was positioned at H-4 (δ_H 3.74 dd, J = 8.5, 2.5 Hz). Hydroxyl groups were placed at C-3 and C-4 of the quinyl moiety. This oxymethine group exhibited both a ^2J HMBC and COSY correlations to a third oxymethine group, which was positioned at C-5 (δ_H 5.35 dt, J = 9.0, 4.5 Hz, δ_C 72.2). H-5 then showed a COSY correlation to a second methylene group (δ_H 2.07 and δ_H 2.25, H_2-6). The quinic acid moiety was completed by placing a carboxyl (δ_C 178.9) and hydroxyl groups at C-1, which both appeared in the ^{13}C spectrum as broad signals indicative of rotamers. Whilst no signal was detected in the HMBC from either methylene group to confirm the positioning of the carboxyl group, there was no other free site where it could be placed. The presence of the carboxyl was confirmed by the mass spectrometry of this compound. Lack of any discernable coupling by H-3 indicated this proton is in an equatorial configuration. However, H-5 appeared as a doublet of triplets with two coupling constants measured as 9.0 and 4.5 Hz, indicating an axial configuration. The small coupling (4.5 Hz) is an axial-equatorial coupling between H-

5 (axial) and H-6 (equatorial). The large coupling constant is a diaxial coupling between H-5 and H-4 and also H-5 and H-6. This completed the configuration of quinic acid. The caffeoyl moiety was attached at C-5 of quinic acid *via* an ester linkage, due to a ^3J correlation between H-5 and C-9'. This was also confirmed by the downfield appearance of the highly deshielded proton at C-5 whereas the signals for H-4 and H-3 were 1.61 and 1.17 ppm further upfield respectively. This downfield shift is characteristic for an oxymethine proton directly attached to a caffeoyl moiety (Morishita *et al.*, 1984). The caffeoyl moiety provided characteristic signals for its assignment. This included two *trans*-oriented olefins (δ_H 7.57 d, J = 16.0 Hz, H-7', δ_H 6.28 d, J = 16.0 Hz, H-8'), as well as three aromatic protons arranged in an ABD spin system (δ_H 7.05 d, J = 2.0 Hz, H-2'; δ_H 6.78 d, J = 8.0 Hz, H-5'; δ_H 6.95 dd, J = 8.5, 1.5 Hz, H-6'). Hydroxyl groups were placed at C3' (δ_C 146.9) and C-4' (δ_C 149.7), completing the structure of 5-*O*-caffeoylquinic acid.

This compound was previously isolated from green coffee beans (*Coffea canephora* var. Robusta) along with other naturally occurring chlorogenic acids (Morishita *et al.*, 1984). The ^1H and ^{13}C NMR data was found to be in close agreement with that of the literature for 5-*O*-caffeoylquinic acid (Cheminat *et al.*, 1988; Tamura *et al.*, 2004).

Table 35 ^1H and ^{13}C NMR data and ^1H-^{13}C long-range correlations of **MS-37** recorded in CD_3OD

Position	^1H	^{13}C	^2J	^3J
1	-	76.9		
2	2.04 m	38.4	C-1, C-3	
	2.19 d (13.5)			
3	4.18 bs	71.8		
4	3.74 dd (8.5, 2.5)	73.9	C-3, C-5	C-2
5	5.35 dt (9.0, 4.5)	72.2		C-9'
6	2.07 m	39.3	C-5	
	2.25 d (11.5)			
7	-	178.9		
1'	-	128.0		
2'	7.05 d (2.0)	115.5	C-1', C-3'	C-4', C-6', C-7'
3'	-	146.9		
4'	-	149.7		
5'	6.78 d (8.0)	116.7	C-4', C-6'	C-1', C-3'
6'	6.95 dd (8.5, 1.5)	123.1		C-4', C-7'
7'	7.57 d (16.0)	147.2	C-1', C-8'	C-2', C-6', C-9'
8'	6.28 d (16.0)	115.4	C-9'	C-1'
9'	-	168.9		

3.9.3 Characterisation of MS-38 as 7*S*-(4-hydroxyphenyl) ethane-7,8-diol

MS-38 was isolated as a pale yellow oil and a molecular formula of $C_8H_{10}O_3$ was assigned by ESI-MS, giving a base ion of 176.1 $[M+Na-H]^+$. The ^1H and ^{13}C spectra provided signals for four aromatic protons in an AA'BB' spin system (δ_H 7.19 d, J = 8.5 Hz, H-2 and H-6; δ_H 6.76 d, J = 9.0 Hz, H-3 and H-5). An oxyquaternary carbon (δ_C 158.0, C-4), oxymethine (δ_H 4.59 t, J = 6.5 Hz, H-7) and oxymethylene (δ_H 3.58 d, J = 6.5 Hz, H_2-8) groups were also present.

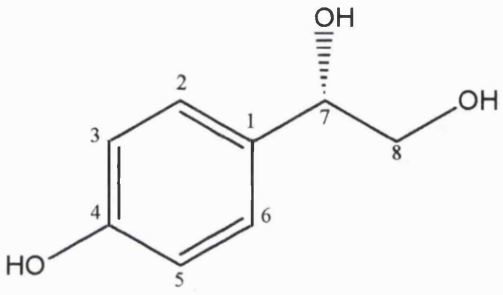

Figure 3.9.3A Structure of **MS-38**

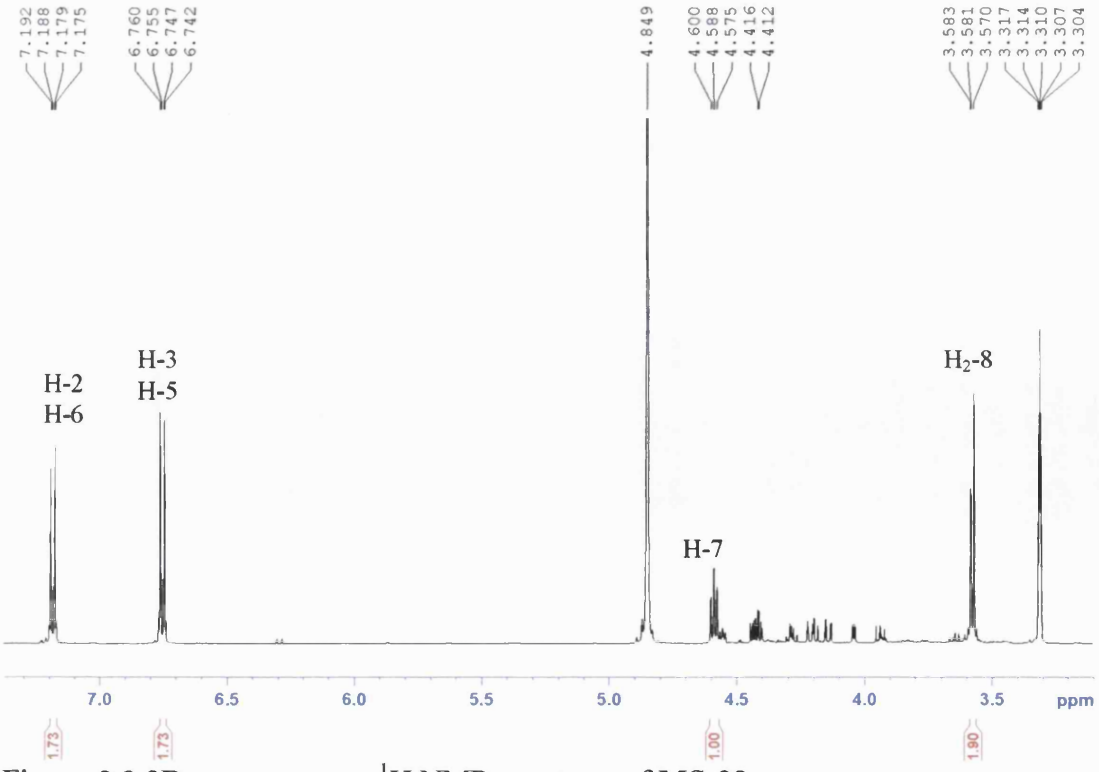

Figure 3.9.3B ^1H NMR spectrum of **MS-38**

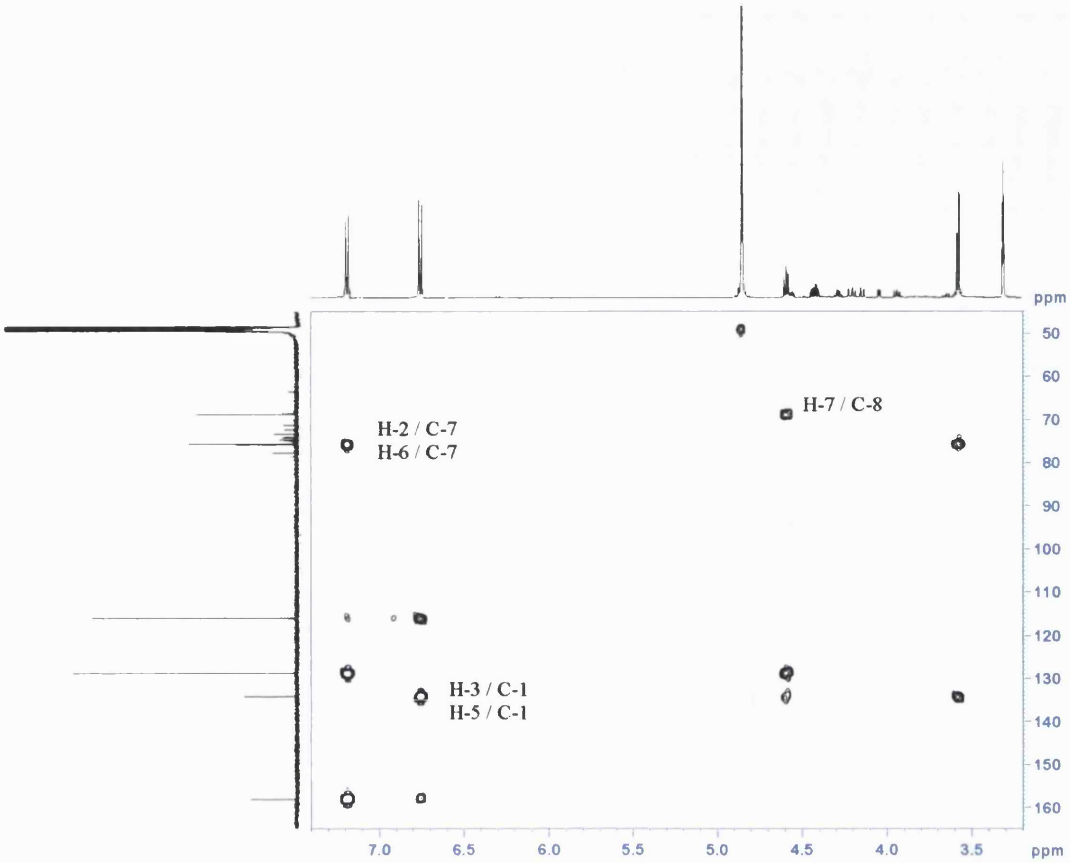

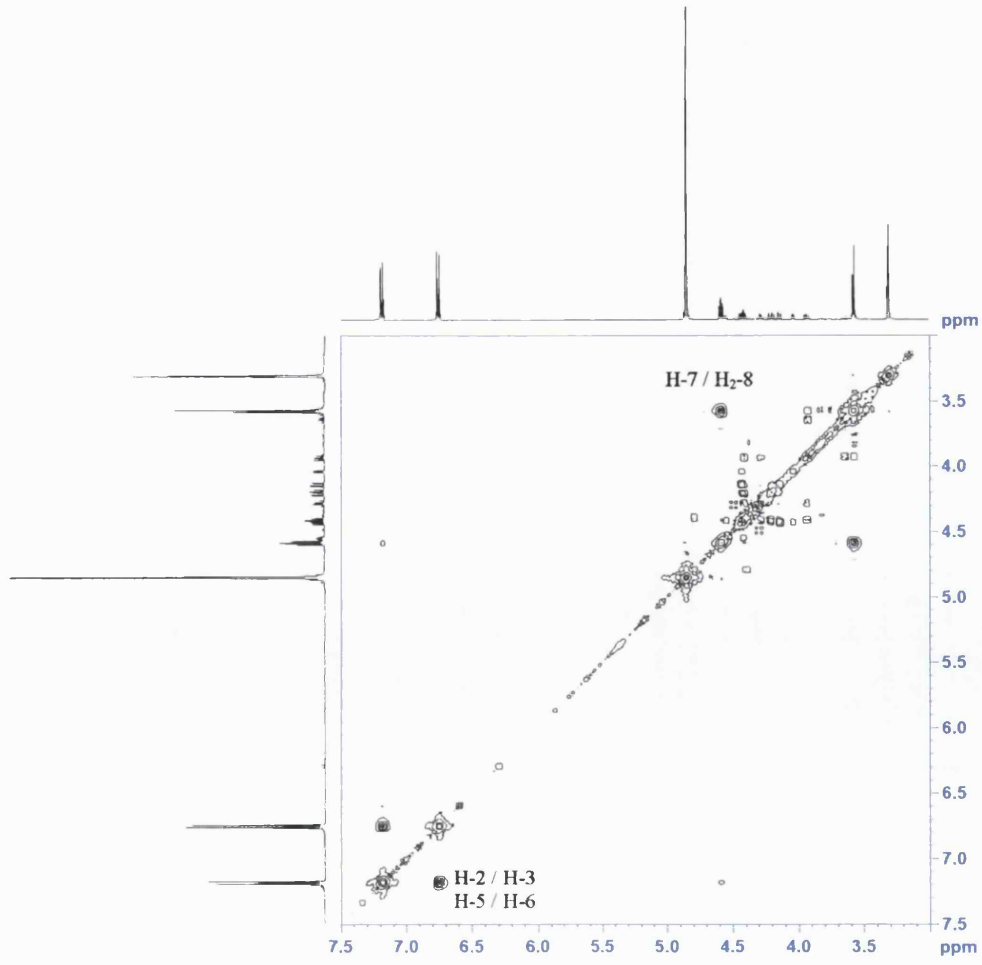

Figure 3.9.3C HMBC and COSY spectra of **MS-38**

The equivalent pair of aromatic protons at δ_H 7.19 coupled to the aromatic protons at δ_H 6.76 and so were placed at H-2, H-6, H-3 and H-5 with respect to the aromatic ring. A ^3J correlation between H-2/H-6 placed the oxygen bearing aromatic carbon at C-4. A further ^3J correlation between H-3/H-5 placed the aromatic carbon at C-1, completing the aromatic ring. H-2/H-6 also gave a ^3J signal to the oxymethine carbon (C-7), placing it next to C-1. The oxymethine proton coupled to the protons of the oxymethylene group, confirming the position of this group at C-8. The downfield shift of C-4, C-7 and C-8 along with the molecular weight determination suggested that hydroxyl groups should be placed here. **MS-38** has previously been isolated from the methanolic extract of coriander (Ishikawa *et al.*, 2003). The stereochemistry of 7-(4-hydroxyphenyl) ethane-7,8-diol was assigned as the *S* stereoisomer as a positive optical rotation value was calculated, $[\alpha]^{25}_D$ +40.5° (*c* 0.20, CH_3OH). This value compared favourably with that of synthetic (7*S*)-7-phenylethane-7,8-diol, commercial (*R*)-7-phenylethane-7,8-diol (purchased from Aldrich Chemical Co.) showed positive optical rotation $[\alpha]^{22}_D$ +45° (CH_3OH) for the *S*-form; $[\alpha]^{22}_D$ -45° (CH_3OH) for the *R*-form (Ishikawa *et al.*, 2003). The absolute stereochemistry at C-7 can therefore be assigned as the *S*-form.

Table 36 ^1H and ^{13}C NMR data and ^1H-^{13}C long-range correlations of **MS-38** recorded in CD_3OD

Position	^1H	^{13}C	^2J	^3J
1	-	134.1		
2	7.19 d (8.5)	128.7	C-3	C-4, C-6, C-7
3	6.76 d (9.0)	116.0	C-4	C-1, C-5
4	-	158.0		
5	6.76 d (9.0)	116.0	C-4	C-1, C-3
6	7.19 d (8.5)	128.7	C-5	C-2, C-4, C-7
7	4.59 t (6.5)	75.7	C-1, C-8	C-2, C-6
8	3.58 dd (6.5, 1.0)	68.7	C-7	C-1

3.9.4 Characterisation of MS-39 as *p*-hydroxybenzoic acid

MS-39 was isolated as a yellow amorphous solid from the chloroform extract of *P. crispa*. The ^{1}H NMR spectrum gave signals for two pairs of equivalent aromatic protons (2H, δ_H 8.10 d, J = 8.5 Hz, H-3/H-5 and 2H, δ_H 6.91 d, J = 8.5 Hz, H-2/H-6) arranged in an AA'BB' spin system. A carbonyl group was also present in the ^{13}C NMR spectrum (δ_C 172.2, C-7). This suggested a 1,4 disubstituted aromatic ring system. ESI-MS in the negative mode showed the M-H$^-$ ion at *m/z* 137.1 indicating a molecular formula of $C_7H_6O_3$. The MS and NMR data showed that a carboxyl group should be attached at C-1 of the aromatic ring whilst the hydroxyl group should be assigned at the *para* position. The NMR data of **MS-39** was in close agreement with that of the literature enabling the assignment of this compound as *p*-hydroxybenzoic acid (Pouchert and Behnke 1992b).

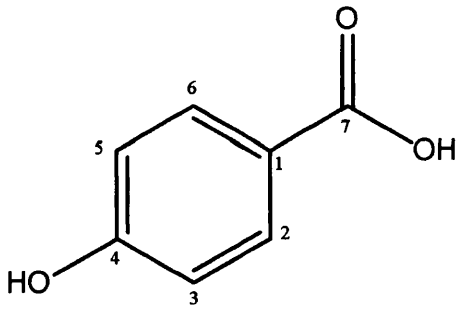

Figure 3.9.4A Structure of **MS-39**

Table 37 ^{1}H and ^{13}C NMR data of **MS-39** recorded in CD_3OD

Position	^{1}H	^{13}C
1	-	100.9
2	6.91 d (8.5)	116.3
3	8.10 d (8.5)	130.7
4	-	160.6
5	8.10 d (8.5)	130.7
6	6.91 d (8.5)	116.3
7	-	172.2

3.9.5 Characterisation of MS-40 as *p*-coumaric acid eicosyl ester

MS-40 was isolated as a white amorphous powder and a molecular formula of $C_{29}H_{48}O_3$ was established by ESI-MS. This showed the $[M-H]^-$ ion at m/z 443.2. The ^1H and ^{13}C NMR spectra provided signals for four aromatic protons arranged in an AA'BB' spin system (2H, δ_H 7.63 d, J = 8.5 Hz, H-3/H-5 and 2H, δ_H 7.16 d, J = 8.5 Hz, H-2/H-6), two *trans*-oriented olefins (δ_H 8.01 d, J = 16.0 Hz, H-7 and δ_H 6.67 d, J = 16.0 Hz, H-8), a carbonyl group (δ_C 167.9, C-9), an oxyquaternary carbon (δ_C 162.0, C-4), a deshielded methylene group (δ_H 4.32 t, J = 7.0 Hz, H_2-1'), a methylene envelope (δ_H 1.32-1.35 m, H_2-4'-H_2-19') and a methyl group.

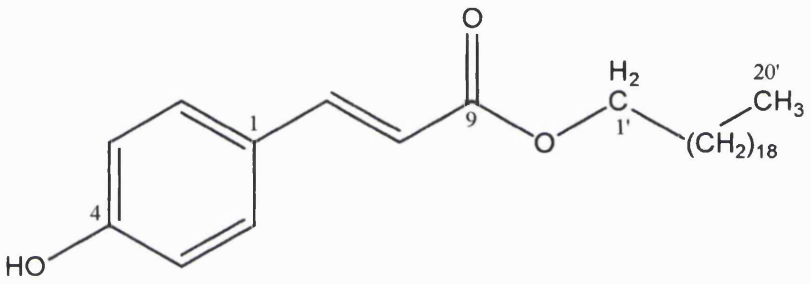

Figure 3.9.5A Structure of **MS-40**

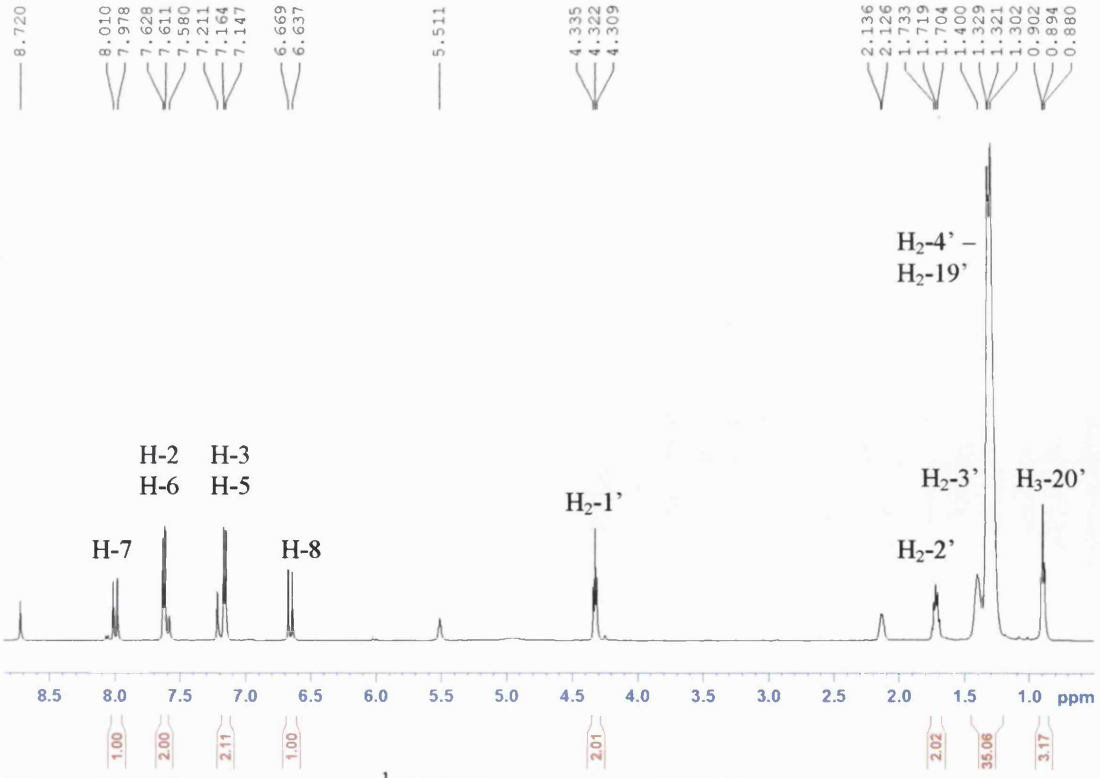

Figure 3.9.5B ^1H NMR spectrum of **MS-40**

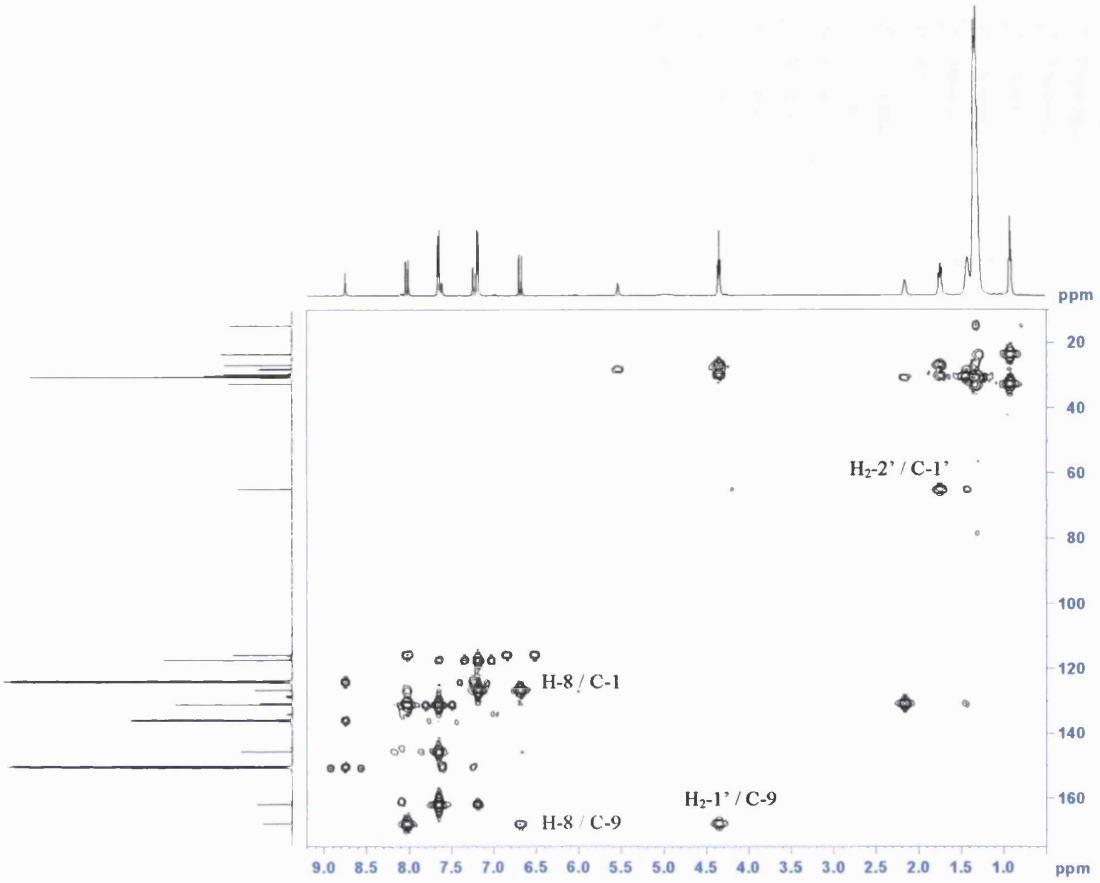

Figure 3.9.5C HMBC spectrum of **MS-40**

The NMR data suggested the presence of a *trans*-oriented *p*-coumaroyl moiety. The number of methylenes in the alkyl chain could not be conclusively ascertained from the NMR data, however, it was possible from the result of the ESI-MS. This indicated the presence of 19 methylene groups and a methyl, providing an eicosanyl moiety attached to the oxygen atom of the carboxylate. This confirmed the isolation of *p*-coumaric acid eicosyl ester, which has previously been isolated from the asteraceous plants *Crepis taraxacifolia* (Kisiel and Jakupowic 1995), *Psiadia punctulata* (Keriko *et al.*, 1997), with ^{1}H and ^{13}C data recorded in $CDCl_3$.

Table 38 ^{1}H and ^{13}C NMR data and ^{1}H-^{13}C long-range correlations of **MS-40** recorded in C_5D_5N

Position	^{1}H	^{13}C	^{2}J	^{3}J
1	-	126.6		
2	7.63 d (8.5)	131.1	C-3	C-4, C-6, C-7
3	7.16 d (8.5)	117.3	C-4	C-1, C-5
4	-	162.0		
5	7.16 d (8.5)	117.3	C-4	C-1, C-3
6	7.63 d (8.5)	131.1	C-5	C-2, C-4, C-7
7	8.01 d (16.0)	145.6	C-1, C-8	C-2, C-6, C-9
8	6.67 d (16.0)	115.8	C-9	C-1
9	-	167.9		
1'	4.32 t (7.0)	65.0	C-2'	C-3', C-9
2'	1.72 m	29.7	C-1', C-3'	C-4'
3'	1.40 m	26.8		
4'-19'	1.32 - 1.35 m	23.5-32.7		
20'	0.89 t (7.0)	14.8	C-19'	C-18'

3.9.6 Characterisation of MS-41 as *R*-tryptophan

The aromatic amino acid, *R*-tryptophan, was isolated as a pale yellow amorphous solid. The ^{1}H and ^{13}C NMR data indicated a molecular formula of $C_{11}H_{12}O_2N_2$. The ^{1}H NMR showed signals for four aromatic protons arranged in a 1,2 disubstituted ring system, with two of the protons (δ_H 7.71, J = 8.0 Hz, H-4 and δ_H 7.37, J = 8.0 Hz, H-7) appearing as doublets and two as triplets (δ_H 7.05, J = 7.5 Hz, H-5 and δ_H 7.12, J = 7.5 Hz, H-6). An olefin belonging to the pyrrole ring was also detected (δ_H 7.19 s, H-2) as well as protons for a methylene and methine groups, which form the branched side-chain of this amino acid. A carbonyl group was detected at δ_C 168.3 ppm. The connectivity is shown in **Table 39**.

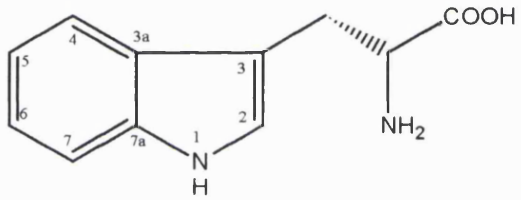

Figure 3.9.6A Structure of **MS-41**

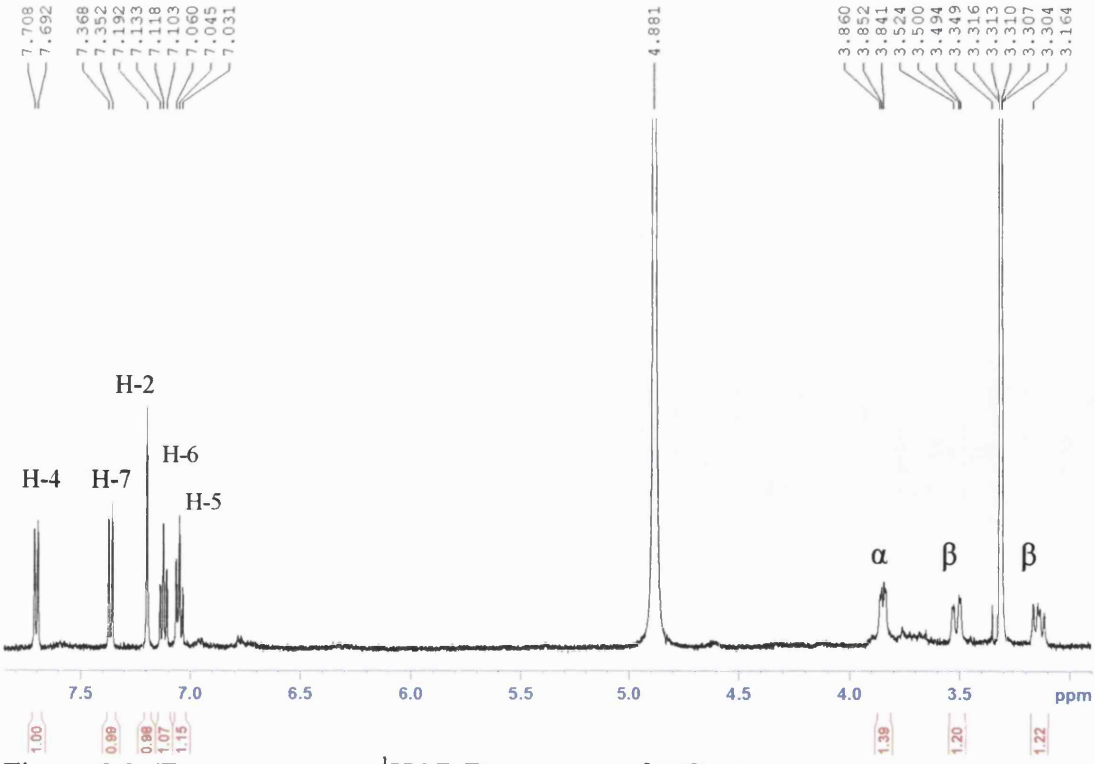

Figure 3.9.6B ^{1}H NMR spectrum of **MS-41**

The NMR data were in close agreement with that of the literature for tryptophan (Pouchert and Behnke 1992a). Measurement of a positive specific rotation enabled the stereochemistry to be confirmed as being the *R*-stereoisomer (Buckingham 2004).

Table 39 ^{1}H and ^{13}C NMR data and ^{1}H-^{13}C long-range correlations of **MS-41** recorded in CD_3OD

Position	^{1}H	^{13}C	^{2}J	^{3}J
1	-	-		
2	7.19 s	125.1	C-3	C-3a, C-7a
3	-	109.9		
3a	-	128.6		
4	7.71 d (8.0)	119.4		C-3, C-6, C-7a
5	7.05 t (7.5)	120.1		C-3a, C-7
6	7.12 t (7.5)	122.7		C-4, C-7a
7	7.37 d (8.0)	112.4		C-3a, C-5
7a	-	138.4		
β	3.14 dd (14.5, 9.0)	28.7	C-3	C-2, C-3a
	3.52 dd (15.0, 3.0)			
α	3.85 dd (8.5, 3.0)	56.8		
COOH	-	168.3		
NH2	-	-		

3.10 Fats/Fatty Acids

3.10.1 Characterisation of MS-42 as 3*R*-1-octan-3-yl-3-*O*-β-D-glucopyranoside

MS-42 was isolated as a colourless oil from the hexane extract of *S. deserti*. A molecular formula $C_{14}H_{26}O_6$ was assigned by ESI-MS, which gave a base ion of 313 $[M+Na]^+$. The ^1H and ^{13}C spectra provided signals for an *exo*-methylene group (δ_H 5.09 d, J = 10.5 Hz and δ_H 5.19 d, J = 17.5 Hz, H_2-1), a highly split olefinic proton (δ_H 5.84 ddd, J = 17.5, 10.5, 7.5 Hz, H-2), an oxymethine group (δ_H 4.08 q, J = 14.5, 7.0 Hz, δ_C 82.8, C-3), a methylene envelope (three methylene groups) and a methyl. This formed the aglycone portion of the molecule. A hexose sugar was also detected, with the presence of an anomeric proton (δ_H 4.32 d, J = 7.5, H-1'), four oxymethines and an oxymethylene group.

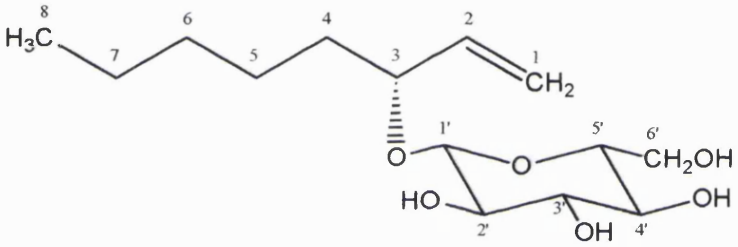

Figure 3.10.1A Structure of **MS-42**

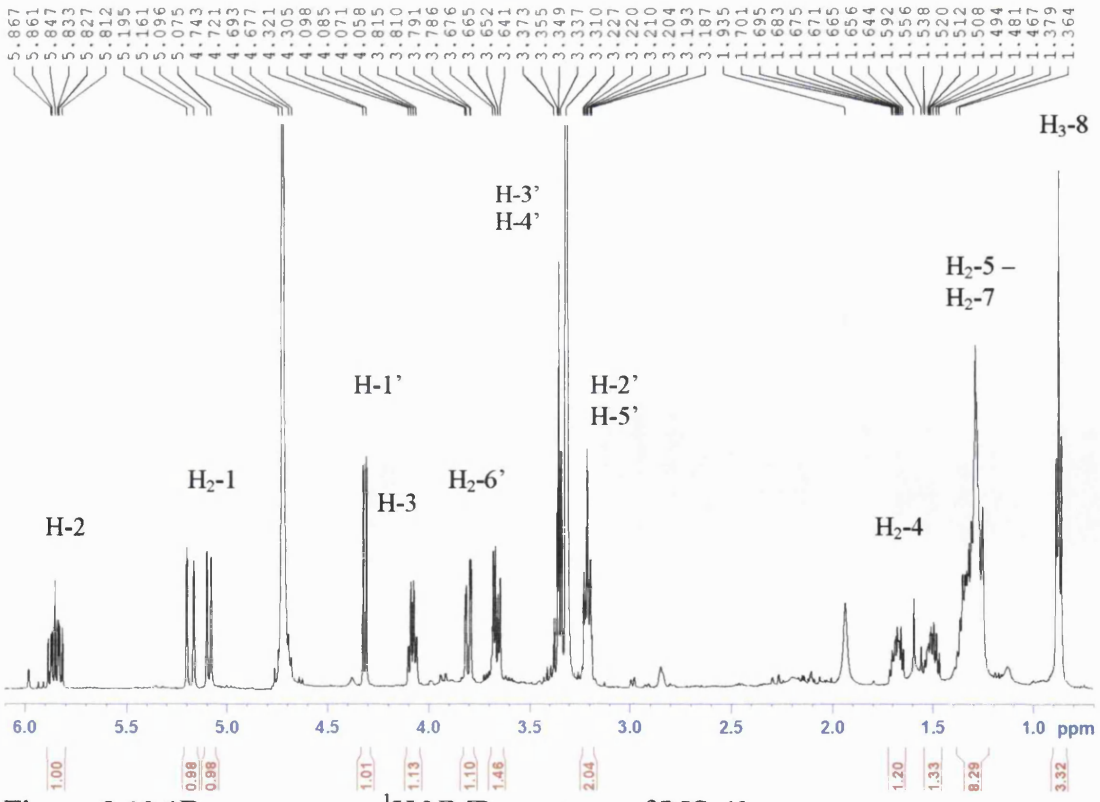

Figure 3.10.1B ^1H NMR spectrum of **MS-42**

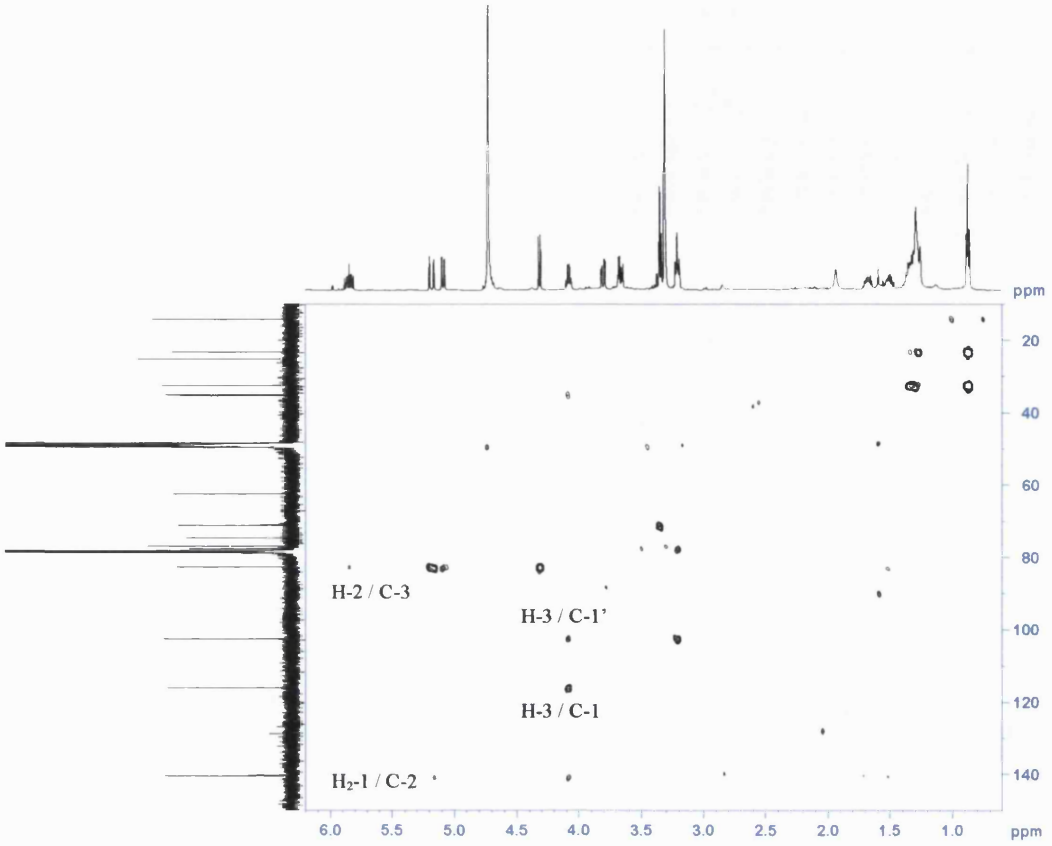

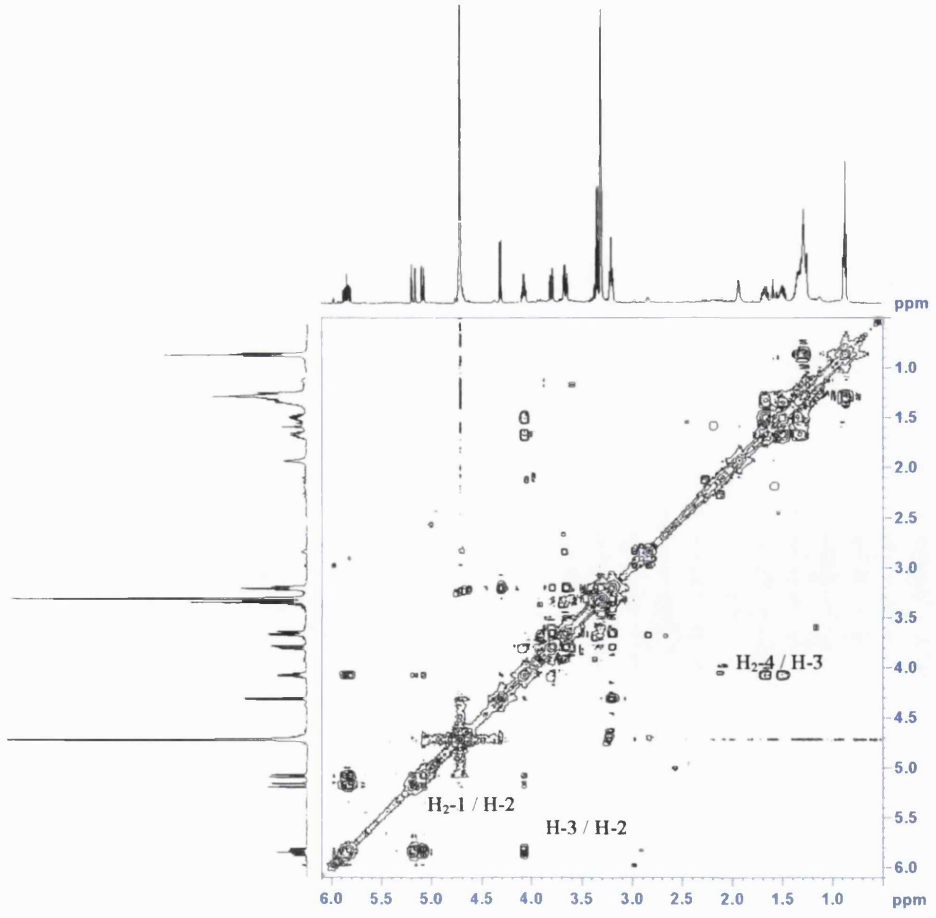

Figure 3.10.1C HMBC and COSY spectra of **MS-42**

The protons of the *exo*-methylene, H_2-1, gave a COSY correlation with the olefinic proton H-2, which in turn coupled to an oxymethine proton, H-3. This proton also showed a coupling with both protons of a highly split methylene (δ_H 1.51 m and δ_H 1.67 m, H_2-4), which in turn coupled to one of the methylenes in the methylene envelope. The methylene protons at δ_H 1.29 showed only one more signal towards a methyl appearing as a triplet (δ_H 0.87, H_3-8). This was confirmed by a ^2J and ^3J correlation from H_3-8 to C-7 and C-6, respectively. The hexose was placed at C-3 of the aglycone due to a ^3J correlation from the anomeric proton of the sugar towards this carbon. H-1' coupled to H-2' (J = 7.5 Hz), which in turn coupled to H-3' as well as C-3' in the HMBC. As H-2' appeared as a triplet in the ^{1}H spectrum with a large coupling constant (J = 8.5 Hz), this indicated that H-1', H-2' and H-3' should be axial. H-3' coupled to H-4', which in turn coupled to H-5'. This proton then exhibited a coupling to the protons of the oxymethylene group. H-5' appeared as a triplet also with a large coupling constant (J = 8.5 Hz), which suggested that H-4' and H-5' are also in an axial configuration. This enabled the assignment of the hexose as being β-glucopyranose.

The optical rotation of this compound was positive, $[\alpha]^{25}_D$ +31.8° (*c* 0.31, $CHCl_3$) indicating an *R* configuration at C-3. Due to a paucity of material, the absolute stereochemistry of **MS-42** could not be determined by chemical means. However, two previous reports of this compound also indicate an *R* configuration at C-3 of the aglycone, with positive optical rotation values measured in both instances (Hou *et al.*, 2002; Yamamura *et al.*, 1998). **MS-42** was therefore assigned as 3*R*-1-octan-3-yl-3-*O*-β-D-glucopyranoside. This compound has previously been isolated from the leaves of *Mentha spicata* (Yamamura *et al.*, 1998), a member of the Lamiaceae family and from *Bacopa monniera* (Hou *et al.*, 2002), a member of the Scrophulariaceae family. The spectroscopic data compared favourably with that of the literature (Yamamura *et al.*, 1998).

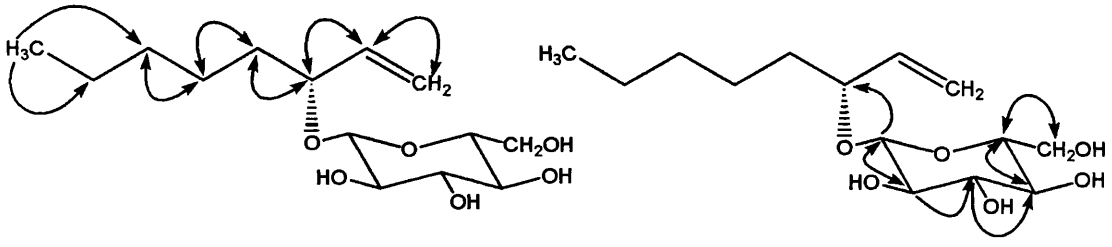

Figure 3.10.1D HMBC and COSY correlations for **MS-42**

Table 40 ^{1}H and ^{13}C NMR data and ^{1}H-^{13}C long-range correlations of **MS-42** recorded in CD_3OD

Position	^{1}H	^{13}C	^{2}J	^{3}J
1	5.09 d (10.5)	116.1	C-2	C-3
	5.19 d (17.5)			
2	5.84 ddd (17.5, 10.5, 7.5)	140.4	C-3	
3	4.08 q (13.5, 7.0)	82.8	C-2, C-4	C-1, C-1'
4	1.51 m	35.2		
	1.67 m			
5	1.29 m	25.3	C-6	C-7
6	1.29 m	32.6		
7	1.29 m	23.2	C-6	C-5
8	0.87 t (7.0)	14.3	C-7	C-6
1'	4.32 d (7.5)	102.7		C-3
2'	3.21 t (8.5)	74.7	C-3'	
3'	3.36 m	77.6	C-4'	
4'	3.34 m	71.2		
5'	3.20 t (8.5)	77.0		
6'	3.66 dd (11.5, 5.5)	62.5		
	3.80 dd (11.5, 2.5)			

3.10.2 Characterisation of MS-43 as 3(ζ)-hydroxy-octadeca-4(*E*),6(*Z*)-dienoic acid

MS-43 was isolated as a colourless oil from the hexane extract of *S. deserti*. HRCIMS confirmed a molecular formula of $C_{18}H_{32}O_3$ with signals for $[M]^+$ (296.2324) and $[M+NH_4]^+$ (314.3). The ^1H and ^{13}C NMR data indicated the presence of four olefinic protons, an oxymethine group, a carbonyl carbon, a methylene envelope, two downfield methylene groups and finally a methyl group.

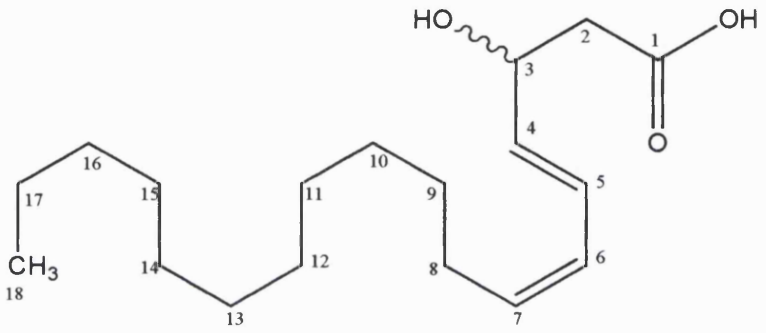

Figure 3.10.2A Structure of **MS-43**

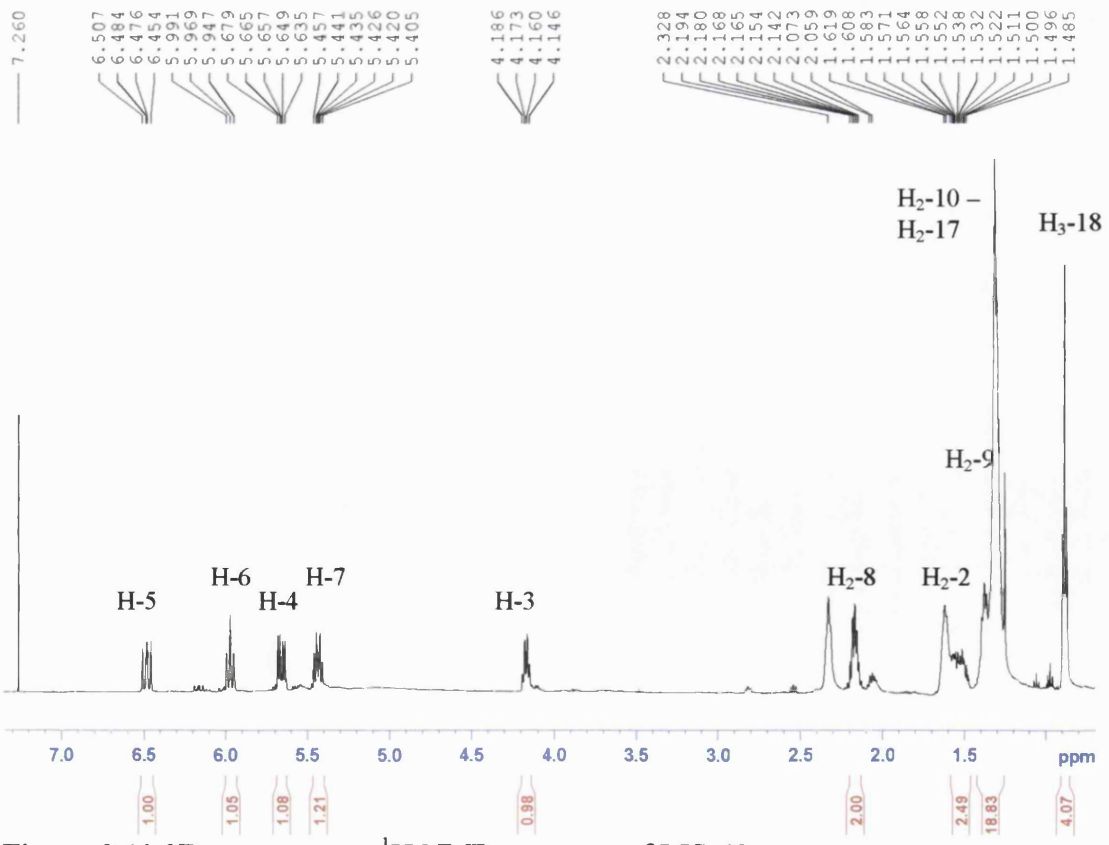

Figure 3.10.2B ^1H NMR spectrum of **MS-43**

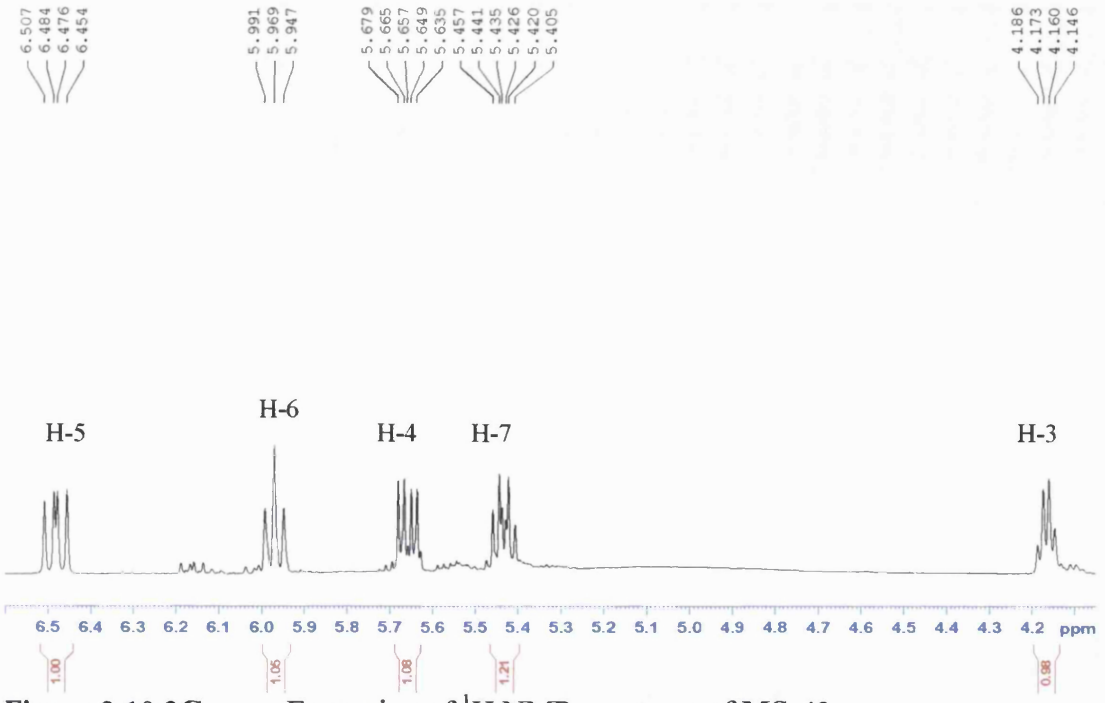

Figure 3.10.2C Expansion of ^{1}H NMR spectrum of **MS-43**

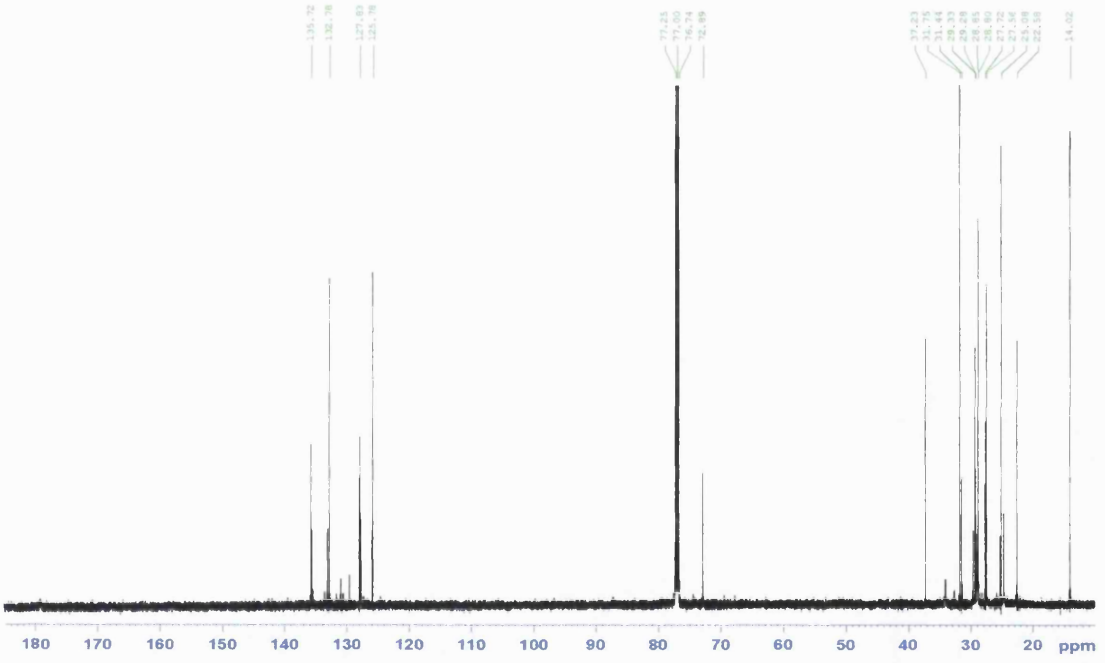

Figure 3.10.2D ^{13}C NMR spectrum of **MS-43**

The HMBC showed a ^{2}J correlation between a downfield methylene (δ_H 1.52 m, H_2-2) towards the carbonyl carbon (δ_C 179.1, C-1) of the carboxyl group. The methylene protons also showed a COSY correlation to the oxymethine proton, placing this group at C-3 (δ_H 4.17 dd, J = 13.0, 6.5 Hz, δ_C 72.9). This oxymethine proton in turn showed a COSY signal to an olefinic proton (δ_H 5.67 dd, J = 15.5, 7.0 Hz, H-4). H-4 coupled to the olefinic proton, H-5 (δ_H 6.49 dd, J = 15.5, 11.0 Hz), in the COSY.

The large coupling constant shown between H-4 and H-5 (J = 15.5 Hz) indicated these protons are *trans*-orientated. The olefin H-5 also coupled to a third olefinic proton H-6 (δ_H 5.97 t, J = 11.0 Hz) which in turn coupled to a fourth olefin, H-7 (δ_H 5.44 dt, J = 11.0, 8.0 Hz). As H-6 appeared as a triplet in the ^{1}H spectrum, with a smaller coupling constant (J = 11.0 Hz), this suggested that H-5 and H-7 are *cis*-orientated with respect to this proton. The olefin, H-7, gave a COSY and HMBC correlation to a methylene group (δ_H 2.18 m, H_2-8). This then went into the methylene envelope at δ_H 1.31 ppm, indicating the beginning of the alkyl chain. The alkyl chain was found to consist of ten methylene groups and a terminal methyl group based on the result of mass spectrometry for this compound.

The absolute stereochemistry at the C-3 position was unable to be determined due to the unstable nature of the compound. However, 3(ζ)-hydroxy-octadeca-4(*E*),6(*Z*)-dienoic acid is new and the full NMR data are reported here for the first time.

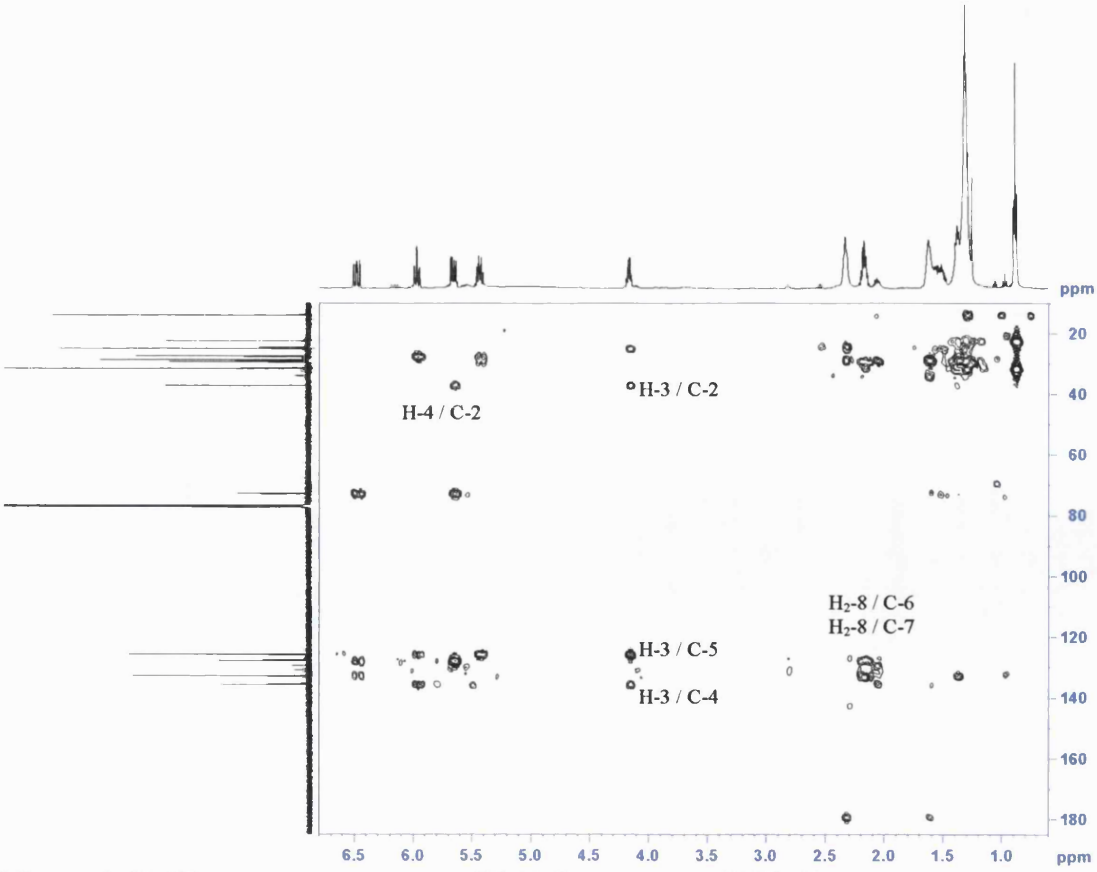

Figure 3.10.2E HMBC spectrum of **MS-43**

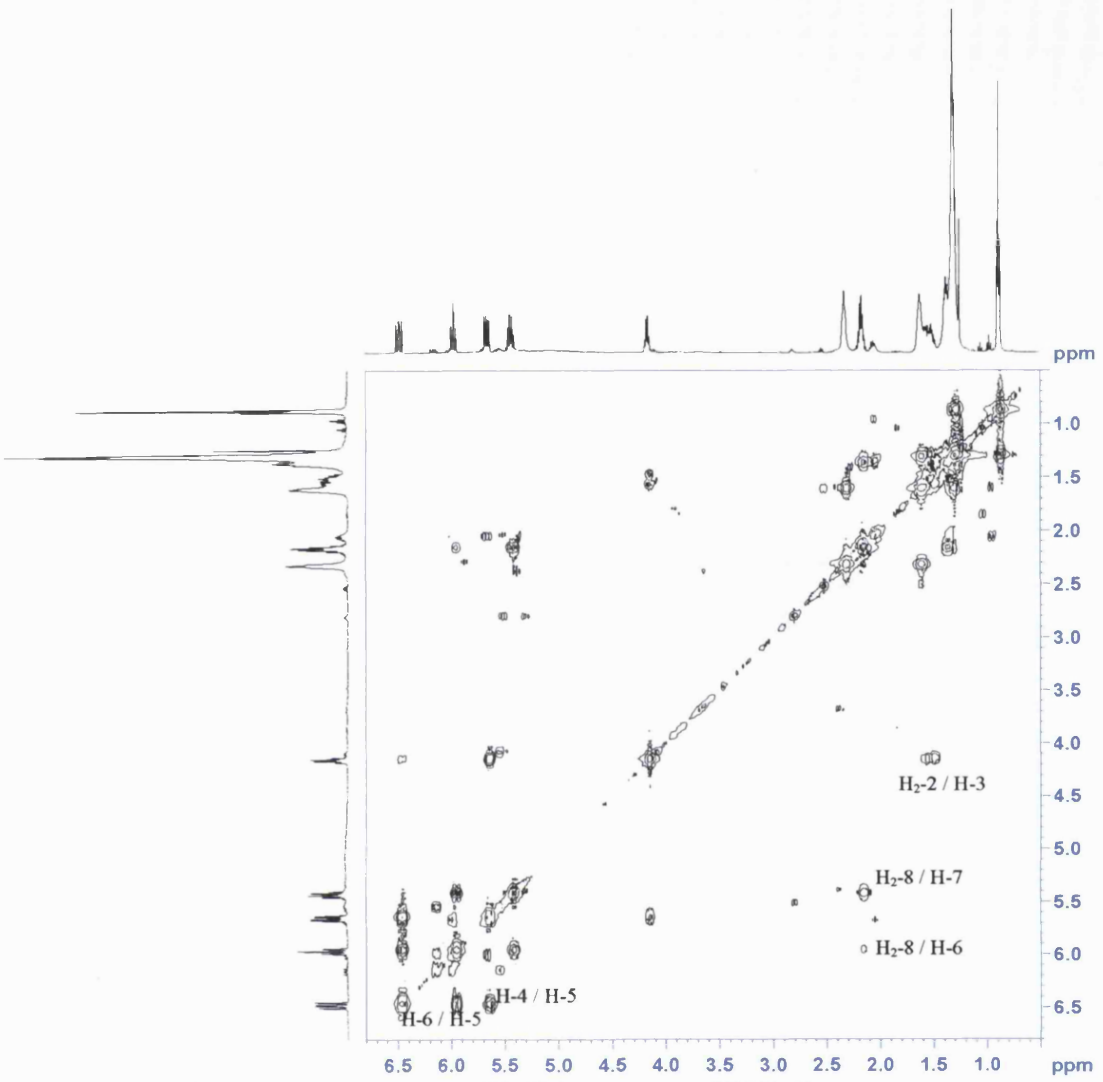

Figure 3.10.2F COSY spectrum of **MS-43**

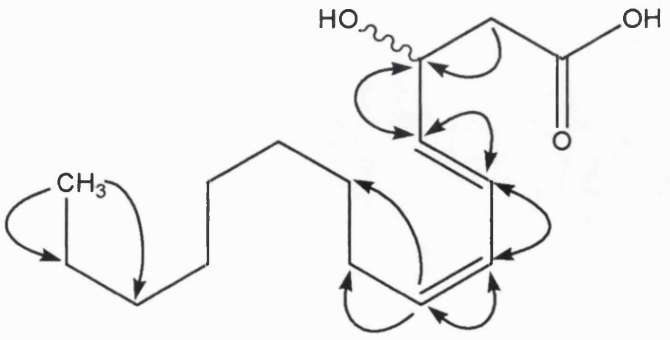

Figure 3.10.2G HMBC and COSY correlations for **MS-43**

Table 41 ^{1}H and ^{13}C NMR data and ^{1}H-^{13}C long-range correlations of **MS-43** recorded in $CDCl_3$

Position	^{1}H	^{13}C	^{2}J	^{3}J
1	-	179.1		
2	1.52 m	37.2	C-3	
3	4.17 dd (13.0, 6.5)	72.9	C-2, C-4	C-5
4	5.67 dd (15.5, 7.0)	135.7	C-3	C-2, C-6
5	6.49 dd (15.5, 11.0)	125.8	C-6	C-3, C-7
6	5.97 t (11.0)	127.8	C-5	C-4, C-8
7	5.44 dt (11.0, 8.0)	132.8	C-8	C-5, C-9
8	2.18 m	27.6	C-7	C-6
9	1.39 m	25.1		C-7
10	1.31 m	28.9		
11	1.31 m	28.9		
12	1.31 m	28.9		
13	1.31 m	28.9		
14	1.31 m	28.8		
15	1.31 m	29.3		
16	1.31 m	31.8		
17	1.31 m	22.6		
18	0.88 t (7.0)	14.0	C-17	C-16

3.10.3 MS-44 tentatively assigned as 3(ζ)-hydroxy-octadeca-4,6,8-trienoic acid

MS-44 was also isolated as a colourless oil from the hexane extract of *S. deserti*. The 1D and 2D NMR data acquired showed that **MS-44** was closely related to **MS-43**. However, **MS-44** was found to be even more unstable than **MS-43**, meaning that the proposed structure is based solely on the NMR data acquired. **MS-44** also suffered from the presence of **MS-43** as an impurity.

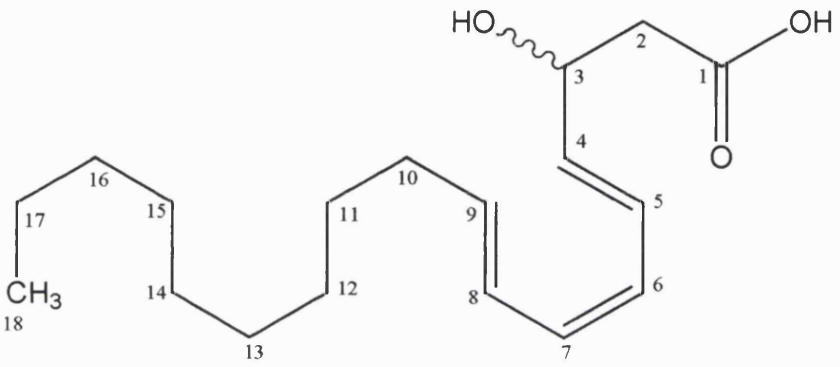

Figure 3.10.3A Proposed structure of **MS-44**

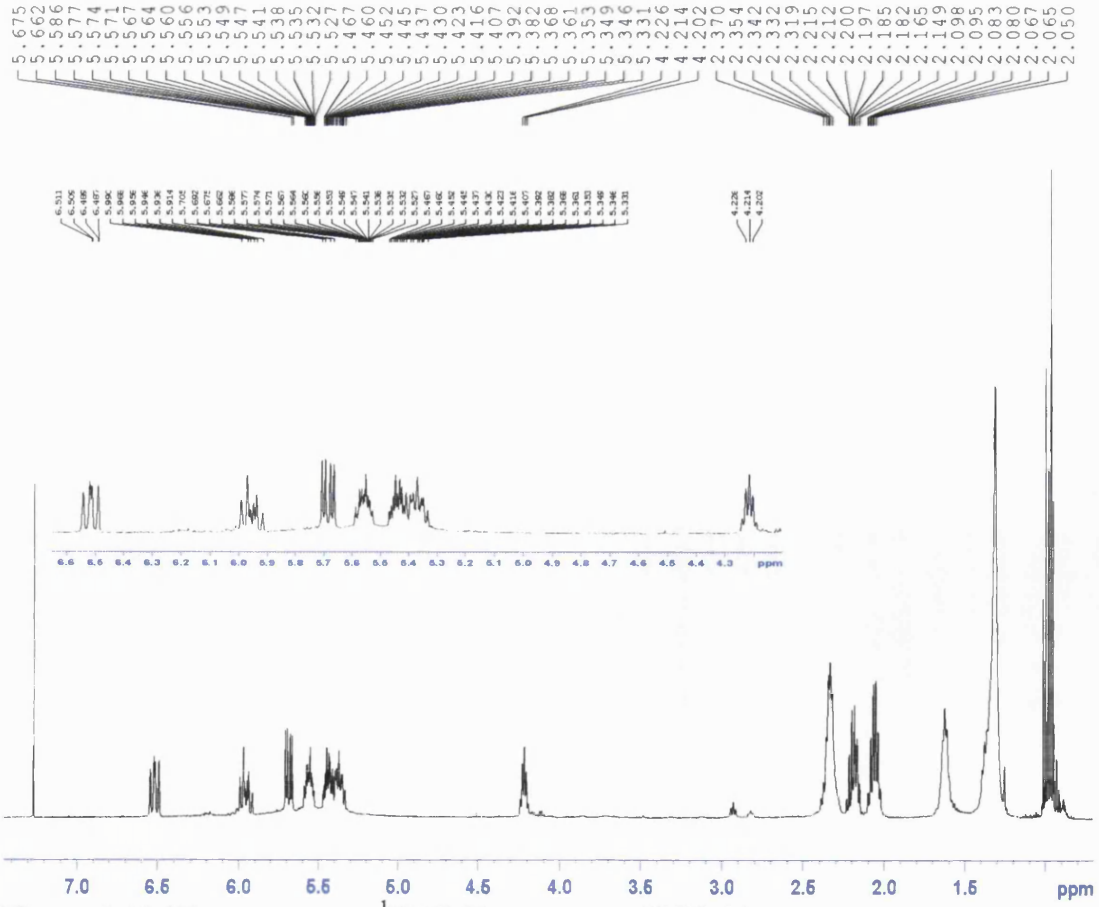

Figure 3.10.3B ^{1}H NMR spectrum of **MS-44**

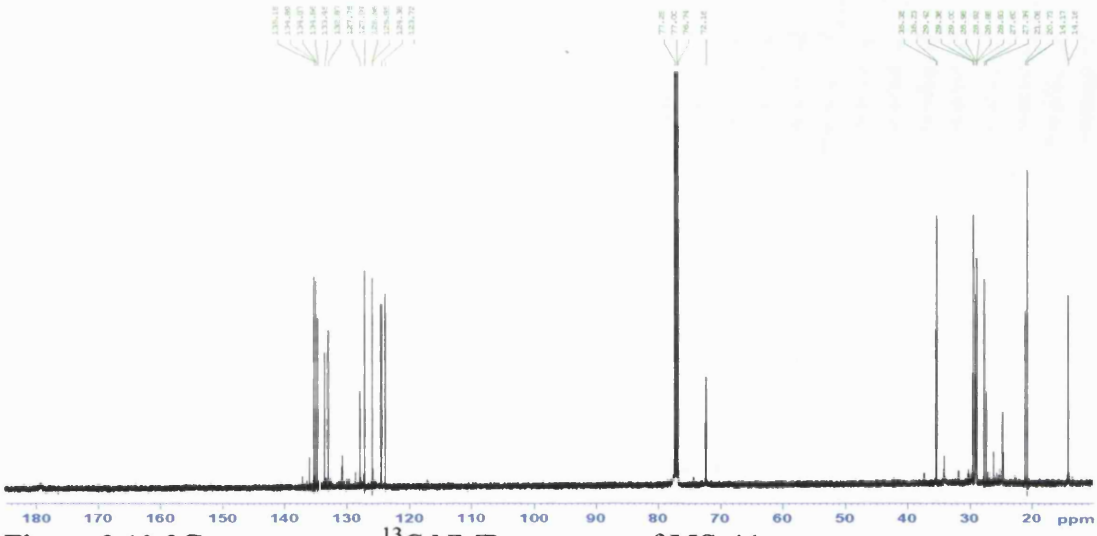

Figure 3.10.3C ^{13}C NMR spectrum of **MS-44**

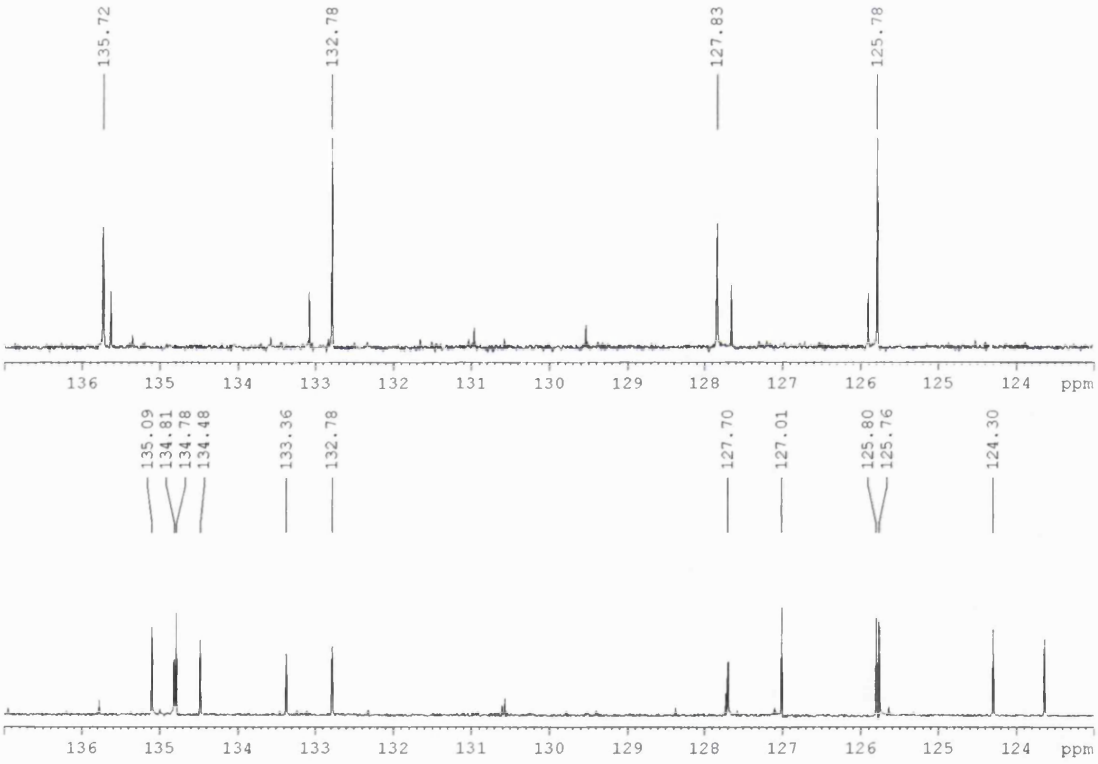

Figure 3.10.3D Comparison of ^{13}C NMR olefinic region of **MS-43** (upper spectrum) and **MS-44** (lower spectrum)

From **figure 3.10.3D**, the olefinic carbons for **MS-43** (upper spectrum) can be detected in **MS-44** (lower spectrum). Subtraction of these carbons leaves six olefinic carbons which from the HMBC and COSY spectra are proposed to be arranged in a conjugated triene-ol system (**Figure 3.10.3A**). **MS-44** is therefore tentatively assigned as 3(ζ)-hydroxy-octadeca-4,6,8-trienoic acid.

3.10.4 Characterisation of MS-45 as a mixture of linoleic, linolenic and palmitic acids

MS-45 was isolated from the methanol extract of *P. crispa* as a colourless oil and gave a yellow colouration on an analytical normal phase silica plate after spraying with vanillin-sulphuric acid followed by heating. GC-MS of this sample showed that **MS-45** was in fact a mixture of three fatty acids. The major component was identified as linoleic acid along with palmitic acid and linolenic acid which were present in smaller quantities. The GC spectrum shows the methyl ester derivatives of these three fatty acids.

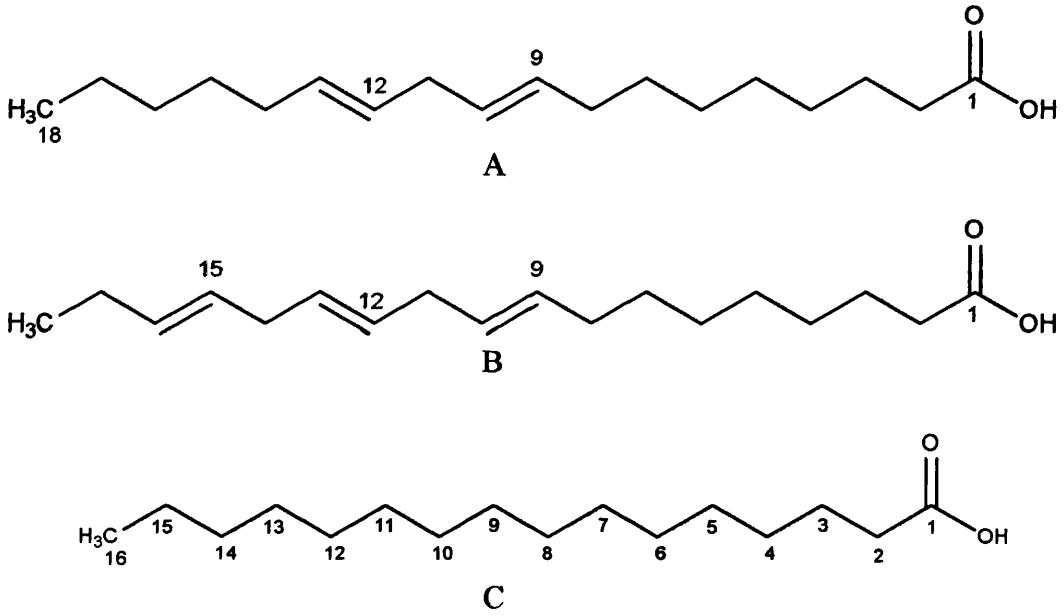

Figure 3.10.4A Structures of linoleic (A), linolenic (B) and palmitic (C) acid

3.10.5 Characterisation of MS-46 as a mixture of myristic acid and an unidentified C_{15} fatty acid

MS-46 was isolated from the hexane extract of *A. graveolens* as a colourless oil. **MS-46** appeared as a single red band on a reverse phase analytical plate after spraying with vanillin-sulphuric acid followed by heating. However, GC-MS revealed that **MS-46** was in fact a mixture of two fatty acids. The first being myristic acid as the methyl ester derivative, whilst the second fatty acid was unable to be identified by this technique. These compounds were isolated in approximately a 1:1 ratio based on the GC-MS spectrum.

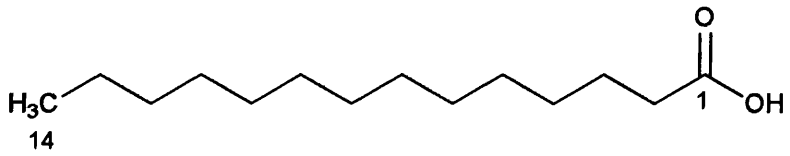

Figure 3.10.5A Structure of myristic acid

3.11 Biological Activity

Table 3.11A Antimycobacterial and anti-staphylococcal activity of compounds isolated in this thesis

Compound	*M. fortuitum* ATCC 6841	*M. phlei* ATCC 11758	*M. aurum* Pasteur Institute 104482	*M. smegmatis* ATCC 14468	*M. abscessus* ATCC 19977	*S. aureus* 1199B (NorA)	*S. aureus* EMRSA-15	*S. aureus* ATCC 25923
MS-5	[a]	[a]	[a]	[a]	ξ	32	[a]	128
MS-10	[a]	[a]	[a]	[a]	ξ	[a]	[a]	128
MS-18	[a]	128	[RG] 128	[RG] 128	ξ	[a]	[a]	[a]
MS-23	4	2	4	4	2	8	32	32
MS-28	128	64	64	64	[a]	[a]	[a]	[a]
MS-29	128	64	32	64	ξ	[a]	[a]	[a]
MS-30	128	64	32	32	ξ	[a]	[a]	[a]
MS-34	[a]	[a]	[a]	[a]	ξ	16	[a]	[a]
MS-35	128	[a]	64	128	ξ	[a]	[a]	128
MS-39	64	64	64	32	ξ	32	128	64
MS-43	32	32	32	32	ξ	64	128	128
MS-46	32	8	16	16	ξ	32	64	64

ξ = Not tested [a] = Not active [RG] = Reduced growth

MS-23 was also active against *S. aureus* XU-212 (16 μg/ml) and *S. aureus* RN-4220 (16 μg/ml)

The bioassay-guided fractionation of the hexane extract of *A. graveolens* led to the isolation of the active component, identified as the C_{17} polyacetylene falcarindiol (**MS-23**). This metabolite was strongly active against a panel of rapidly growing mycobacteria, with MIC's ranging between 2 – 4 μg/ml. All strains of mycobacteria tested were of the non-resistant ATCC type. Falcarindiol showed remarkable activity against *M. abscessus* ATCC 19977 with an MIC of 2 μg/ml. This was 64-fold lower than the MIC's recorded for ethambutol and isoniazid, which were the standard antimycobacterial drugs used in the assay. Falcarindiol also showed comparable activity to that of ethambutol (data not shown) against the remaining mycobacteria strains with the exception of *M. smegmatis*, which was far more susceptible to the control drug ethambutol.

Falcarindiol was also active against a panel of methicillin-resistant and MDR strains of *S. aureus*, although the MIC's were slightly higher than for the mycobacteria, ranging from 8 – 32 μg/ml. An interesting observation from these results was that falcarindiol exerted a greater antibacterial effect on the MDR *S. aureus* strains. For example, the two *S. aureus* strains, XU-212 and RN-4220, possessing the TetK and MsrA transporters that efflux tetracycline and macrolide antibiotics respectively, yielded MIC's of 16 μg/ml. Whilst SA-1199B, possessing the NorA MDR efflux mechanism, which is the major efflux pump in this organism showed even greater activity with a recorded MIC of 8 μg/ml. Falcarindiol was also active against an epidemic MRSA strain, EMRSA-15 which was a clinical isolate from hospitals in the Midlands and the south-east of England (Richardson and Reith 1993), as well as a non-resistant ATCC strain of *S. aureus* but to a lesser extent with an MIC of 32 μg/ml for each. This polyacetylene natural product has previously been reported to be active against both Gram-positive and Gram-negative bacteria as well as the yeast *Candida albicans* (Kobaisy *et al.*, 1997; Lechner *et al.*, 2004; Matsuura *et al.*, 1996). However, the toxicity and instability of falcarindiol, like many C_{17} polyacetylenes, has meant that further research in to this natural product class for its therapeutic potential has not been pursued.

Whilst falcarindiol exhibited strong antibacterial and antimycobacterial activity, this was not found to be true of 16,17-dehydrofalcarindiol (**MS-24**) which was not active against any of the strains of *S. aureus* or mycobacteria. Falcarindiol differs from 16,17-dehydrofalcarindiol by only two protons at positions 16 and 17, which are saturated. The saturation at C-16 and C-17 of falcarindiol appears to play a

crucial role in its activity. The polyacetylene falcarinol, which was not isolated during this research, has been reported to possess greater antibacterial activity than falcarindiol against both Gram-positive and Gram-negative bacteria, including *S. aureus* (Kobaisy *et al.*, 1997). Due to the instability of 16,17-dehydrofalcarinol (**MS-25**) no antibacterial assays could be carried out on this sample. However, there have been no reports describing antibacterial activity associated with this particular polyacetylene. From the results obtained during this research and those of the literature reports this would strongly indicate that the antibacterial activity recorded for falcarindiol is closely associated with saturation at positions 16 and 17. The specificity at C-16 and C-17, required for falcarindiol's activity indicates a specific rather than non-specific mechanism of action. A possible mechanism of action of falcarindiol is the inhibition of an enzyme involved in the biosynthesis of fatty acids. It has been proposed that polyacetylenes are derived from the step-wise desaturation of the fatty acid oleic acid (**Scheme 5A**). Since polyacetylenes share structural similarity with unsaturated fatty acids it is proposed that falcarindiol's activity is achieved by competitive inhibition of a fatty acid synthase enzyme. The elucidation of the structure-activity-relationship (SAR) was beyond the scope of this thesis.

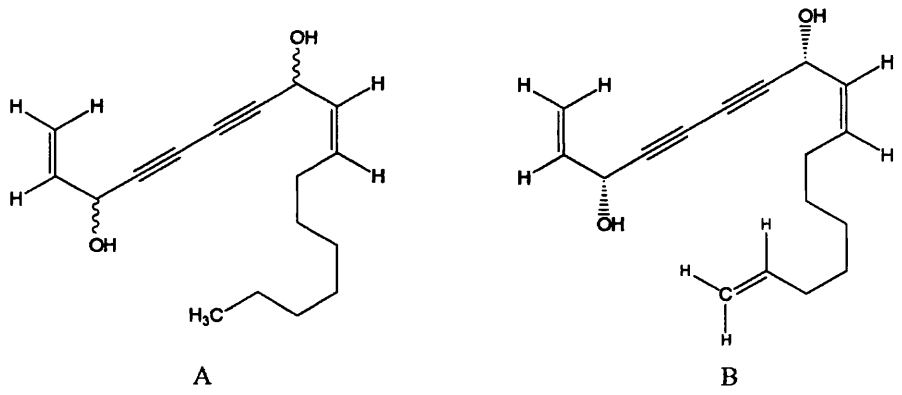

Figure 3.11A Structure of falcarindiol (A) and 3*R*,8*R*-16,17-dehydrofalcarindiol (B)

Falcarindiol has also been reported to be a strong inhibitor of the enzyme 5-lipoxygenase (5-LOX) with an IC_{50} value of 9.4 μM but only a weak inhibitor of cyclooxygenase (COX-1) with an IC_{50} value of 66 μM.(Liu *et al.*, 1998; Zschocke *et al.*, 1997). These enzymes are important in the metabolism of arachidonic acid for the formation of leukotrienes and prostaglandins respectively, which act as mediators in many inflammatory processes (Zschocke *et al.*, 1997).

Falcarindiol and the polyacetylene natural product class as a whole deserve further investigation as a source of antibiotic leads. This must also include identifying solutions to reduce the toxicity problems encountered with these natural products as well as increasing their stability. The antimycobacterial activity of falcarindiol against a panel of rapidly growing mycobacteria is reported here for the first time.

The prenylated linear furocoumarins pangelin **(MS-28)**, oxypeucedanin hydrate **(MS-29)** and oxypeucedanin **(MS-30)** all exhibited moderate antimycobacterial activity ranging from 32 – 128 μg/ml, but none of the coumarins were active against any of the *S. aureus* strains. Coumarin natural products are known to exert their effects by inhibition of DNA gyrase. Novobiocin and coumermycin A_1 have been known to inhibit bacterial nucleic acid synthesis since the 1950's (Maxwell 1997). Studies to elucidate the mechanism of action of coumarin antibiotics have revealed that they inhibit the ATP-dependent catalytic functions of DNA gyrase, such as DNA supercoiling and decatenation (Periers *et al.*, 2000). This is achieved by competitive inhibition of ATP binding (Periers *et al.*, 2000).

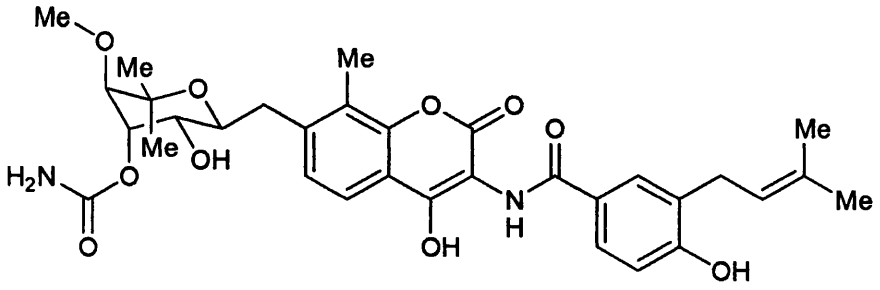

Figure 3.11B Structure of novobiocin

The prenylation of the isolated furocoumarins appears to play a significant role in the activity of these compounds by increasing the lipophilicity of these molecules. This would enable the furocoumarins to diffuse through the thick hydrophobic outer membrane of the mycobacteria to their site of action, DNA gyrase. There is evidence to indicate that increasing the lipophilicity of coumarin natural products further still would result in even greater antimycobacterial activity being achieved. For example, ostruthin has a geranyl side-chain attached at position 6 of the coumarin molecule and this has resulted in an increase in the antimycobacterial activity against *M. fortuitum*, *M. phlei*, *M. aurum* and *M. smegmatis* with MIC's ranging from 1 - 2 μg/ml (Schinkovitz *et al.*, 2003). These results were comparable to that of ethambutol with the exception of *M. smegmatis* which was more susceptible to the positive control.

Ferulenol, a coumarin with a farnesyl side-chain located at position 3 of the molecule also showed strong antimycobacterial activity against the same panel of mycobacteria as for ostruthin with MIC's ranging from 0.5 - 4 μg/ml (Appendino *et al.*, 2004).

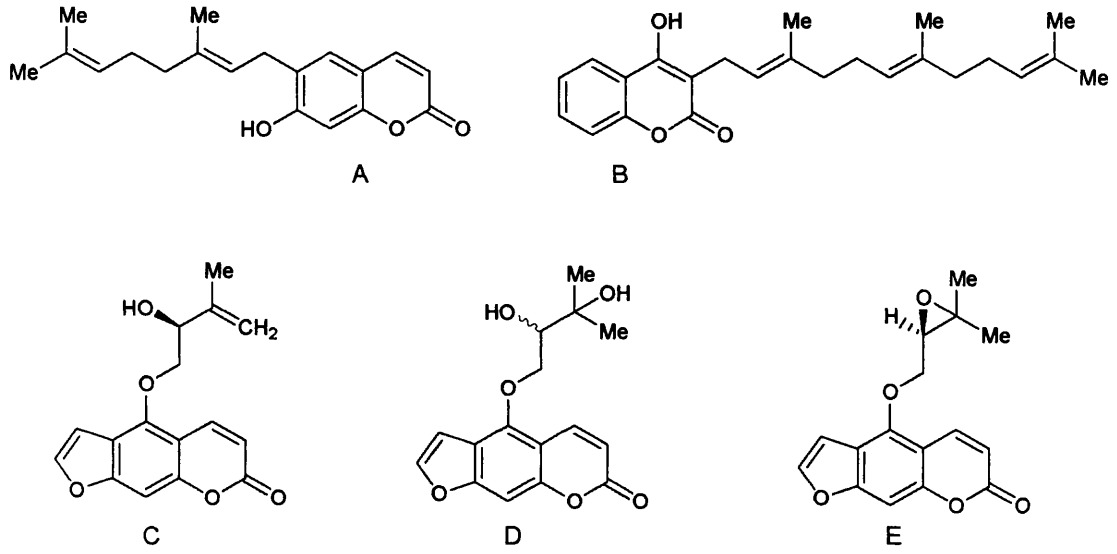

Figure 3.11C Structure of ostruthin (A), ferulenol (B), pangelin (C), oxypeucedanin hydrate (D) and (*R*)-(+)-oxypeucedanin (E)

A possible explanation why none of the coumarins were active against MDR strains of *S. aureus* could be due to the structural similarity of these compounds to that of the synthetic fluoroquinolones. Therefore coumarins may also be substrates for the NorA efflux pump, reducing the cytosol concentration of these natural products. There may also be other as yet unidentified efflux mechanisms to which coumarins are substrates. Another possible reason for the coumarins not being active against the strains of *S. aureus* could be due to conformational differences of the active site of GyrB of DNA gyrase as compared to the mycobacteria.

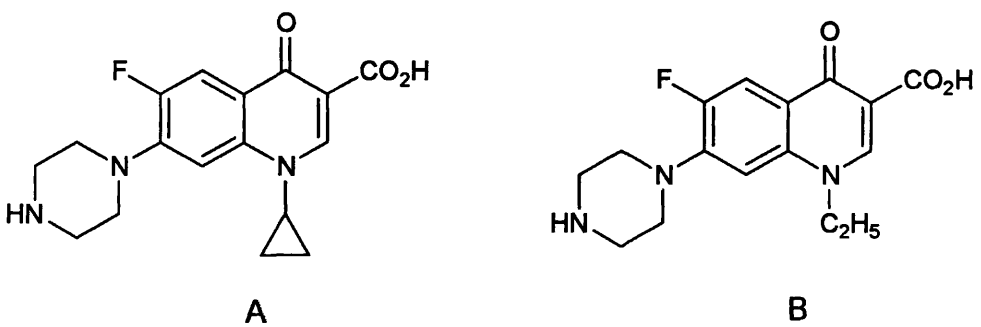

Figure 3.11D Structure of ciprofloxacin (A) and norfloxacin (B)

Further investigation of coumarin natural products as possible antimycobacterial agents would be worthwhile. The *in vitro* activity of coumarins, such as ostruthin and ferulenol, that show comparable if not greater activity to drugs currently used in the clinical setting have already been reported.

The phenolic compound *p*-hydroxybenzoic acid (**MS-39**) displayed moderate activity against a panel of rapidly growing mycobacteria and *S. aureus*, including MDR and MRSA strains. MIC values ranged from 32 – 128 μg/ml. *S. aureus* 1199B (NorA) was found to be more susceptible to this compound than the EMRSA or ATCC strains. It is highly probable that *p*-hydroxybenzoic acid acts as a competitive inhibitor to *p*-aminobenzoic acid (*p*-ABA) to prevent the formation of dihydrofolic acid. A similar molecule, *p*-aminosalicylic acid, was shown to act as a competitive inhibitor of *p*-ABA oxidation as far back as 1960 (Durham and Hubbard 1960) and so it is unsurprising that *p*-hydroxybenzoic acid should also possess moderate antimicrobial activity.

The flavonol quercetin-3-*O*-β-D-glucopyranoside (**MS-34**) displayed anti-staphylococcal activity against the MDR strain *S. aureus* 1199B with an MIC of 16 μg/ml. However this flavonol was not active against either *S. aureus* EMRSA-15 or the ATCC strain. Recent work has revealed the molecular basis for quercetin's antimicrobial activity (Plaper *et al.*, 2003). Quercetin's activity is achieved by binding to the 24 kDa fragment of gyrase B and causes the inhibition of the ATPase activity of gyrase B (Plaper *et al.*, 2003). The binding sites of quercetin and ATP overlap and so this is the likely cause of inhibition of DNA supercoiling activity (Plaper *et al.*, 2003). It is therefore likely that once quercetin-3-*O*-β-D-glucopyranoside enters the bacterial cell, the sugar moiety is cleaved leaving the aglycone to exert its antibacterial activity.

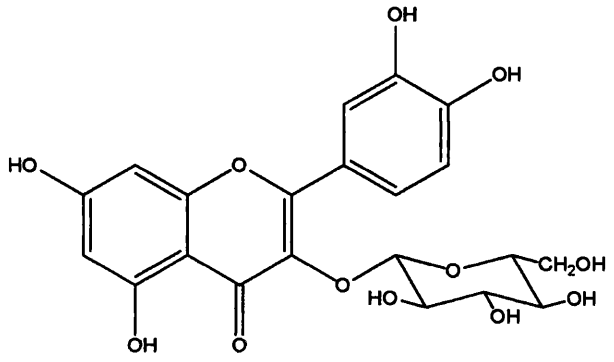

Figure 3.11E Structure of quercetin-3-*O*-β-D-glucopyranoside

The keto-enol tautomer, eriodictyol-7-methyl ether (**MS-35**), also possessed antimicrobial activity. The anti-staphylococcal activity was confined to *S. aureus* ATCC 25923 with a weak MIC of 128 μg/ml. This was also the case against the strains of mycobacteria with an MIC range of 64 – 128 μg/ml, with *M. phlei* not being susceptible to this racemic mixture even at 128 μg/ml. As **MS-35** was isolated as the keto-enol tautomers it was not possible to identify which of the tautomers possessed the antimicrobial activity or whether both forms were equally active as each other.

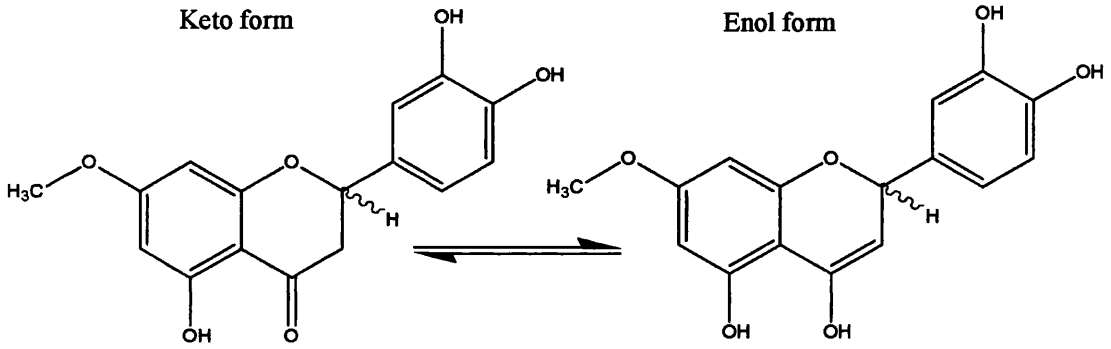

Figure 3.11F Keto-enol tautomers of eriodictyol-7-methyl ether

Two of the iridoid glycosides, 6-*epi*-ajugoside (**MS-5**) and scropolioside B (**MS-10**), displayed weak anti-staphylococcal activity versus the ATCC strain with MIC's of 128 μg/ml. 6-*epi*-ajugoside exerted a four-fold greater anti-staphylococcal effect on the MDR strain *S. aureus* 1199B (MIC = 32 μg/ml). None of the iridoids exhibited any antimycobacterial activity.

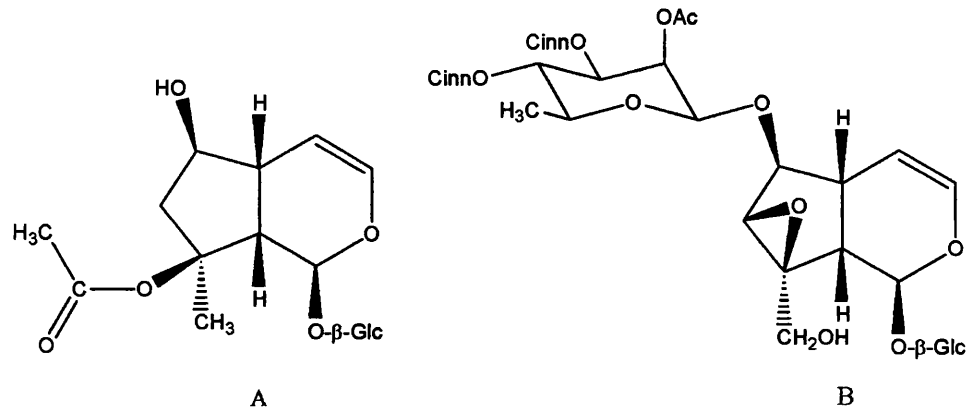

A B

Figure 3.11G Structure of 6-*epi*-ajugoside (A) and scropolioside B (B)

The new guaianolide epimer 5,10-*epi*-2,3-dihydroaromatin (**MS-18**) was the only compound of this sesquiterpene class to exert any antimicrobial activity. Activity was confined to the mycobacteria and was weakly active against *M. phlei* with an

MIC of 128 μg/ml. This compound also showed reduced growth against *M. aurum* and *M. smegmatis* at the same concentration.

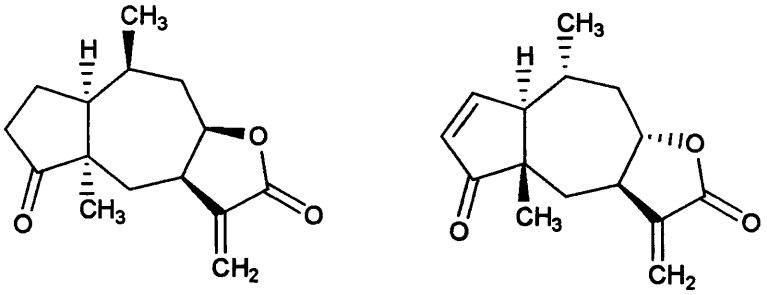

MS-18 Aromaticin

Figure 3.11H Structure of 5,10-*epi*-2,3-dihydroaromatin (**MS-18**) and aromaticin

Figure 3.11H shows the similarity between 5,10-*epi*-2,3-dihydroaromatin and the known guaianolide aromaticin. However the slight differences that exist between these two molecules are highlighted by their respective antimycobacterial activity that they possess. Aromaticin has been reported to exert an antimycobacterial effect with an MIC of 16 μg/ml (Cantrell *et al.*, 2001; Copp 2003), this is eight-fold lower than the MIC recorded for **MS-18**. This highlights the point that small alterations of a molecule can result in an exponential increase in activity. So whilst the activity of **MS-18** reported is weak it can represent a starting point from which synthetic analogues can be produced with greater antimicrobial activity.

The unsaturated fatty acids isolated in this thesis were shown to display antimicrobial activity. The difficulty in isolating these fatty acids in a pure form by standard chromatography techniques meant that in some cases these compounds were isolated as mixtures. The MIC values of the compounds isolated are shown in **Table 3.11A**. The new, unsaturated C_{18} fatty acid 3(ζ)-hydroxy-octadeca-4(*E*),6(*Z*)-dienoic acid (**MS-43**) exhibited moderate activity against the panel of rapidly growing mycobacteria used in the assay with an MIC value of 32 μg/ml recorded against all the species except for *M. abscessus*, which was not tested. This compound also exhibited moderate to weak anti-staphylococcal activity against all three strains tested with MIC's ranging from 64 – 128 μg/ml. Again like other compounds reported in this thesis, **MS-43** exerted a greater anti-staphylococcal effect on the MDR strain (two-fold lower MIC value) than against the EMRSA and ATCC strains.

A definitive reason for the increased activity of some anti-staphylococcal compounds against MDR strains as compared to wild-type strains has not been

conclusively proven. However there are theories that attempt to answer this phenomenon. They include:

- direct binding of the inhibitor to one or more of the binding sites on the protein, therefore preventing transport either by competitive or non-competitive inhibition (Bradley and Ling 1994).
- depletion of pump energy by inhibiting binding of ATP (Ambudkar *et al.*, 1999).
- modifying protein conformation by an inhibitor interaction with the cell membrane (Ambudkar *et al.*, 1999).

A theory proposed by Zloh *et al.*, (2004) suggests that MDR inhibitors may have an affinity for substrates to form a complex, allowing the drug to enter the cell. By forming a complex, this masks the substrate from the MDR transporter. Once the complex enters the cell it may dissociate leaving the drug to exert its effect. Another possible explanation of this phenomenon could be that certain natural products possess dual activity as MDR inhibitors as well as antibacterial activity therefore enabling these compounds to exert a greater antibacterial effect on MDR strains as opposed to wild-type strains.

MS-45 was a mixture of fatty acids, the major component being linoleic acid along with the minor components linolenic and palmitic acids. Due to a paucity of material isolated, antimicrobial testing was not able to be performed. However, pure fatty acid standards of linoleic and palmitic acids were obtained from the Sigma Chemical Company and tested to determine the actual activity of these compounds (**Table 3.11B**).

Table 3.11B Minimum inhibitory concentrations of fatty acids and standard antibiotics against rapidly growing species of mycobacteria

Compound	*M. fortuitum*	*M. phlei*	*M. aurum*	*M. smegmatis*
Linoleic acid	4	8	8	8
Palmitic acid	512	ξ	ξ	ξ
Ethambutol	4	2	1	0.5
Isoniazid	0.5	2	2	2

ξ = Not tested (Stavri *et al.*, 2004b)

Palmitic acid was found to be only very weakly active against *M. fortuitum*, conversely linoleic acid displayed strong activity against the panel of rapidly growing mycobacteria tested with MIC's ranging between 4 – 8 μg/ml. Linolenic acid was not tested. The activity of linoleic acid has been shown to be associated with cell membrane disruption (Khulusi *et al.*, 1995).

Finally, **MS-46** was also isolated as mixture of myristic acid and an unidentified C_{15} fatty acid. **MS-46** showed good antimycobacterial activity (MIC range of 8 – 32 μg/ml) and also moderate anti-staphylococcal activity (MIC range of 32 - 64 μg/ml). The activity observed with **MS-46** was found to be solely due to the unidentified C_{15} fatty acid as myristic acid was inactive at a concentration of 256 μg/ml (Stavri *et al.*, 2004b).

The polyacetylene dehydrofalcarindiol (**MS-24**) displayed cytotoxic activity when tested against six cancer cell lines (four colorectal and two breast cancer cell lines). This was conducted by Professor Christopher Ford, Department of Surgery, Kuwait University. Dehydrofalcarindiol showed greatest activity against the breast cancer cell line MCF7 with an IC_{50} concentration of 5.85 μg/ml (**Table 3.11C**). This activity can only be regarded as moderate but represents a good starting point from which analogues can be synthesised to achieve lower IC_{50} values. Antitumour agents such as vincristine, 5-fluorouracil, camptothecin and mitomycin all display activity at nanomolar concentrations (Yoshimatsu *et al.*, 1997). The activities against the colorectal cancer cell lines COLO320DM and WIDR were almost two-fold higher than for MCF7 with IC_{50} values of 9.64 and 10.97 μg/ml respectively but still represent moderate activity towards these cancer cell lines. The remaining cell lines tested gave only weak cytotoxic activity.

Table 3.11C Summary of the Preliminary Screening of **MS-24** with Cancer Cell Lines in MTT assays

Cell line	Type of cancer	Number of repeat assays	IC_{50} with **MS-24** (μg/ml)*	Dilutions of DMSO causing toxicity
LS174T	Colorectal	3	14.815 (7.2)	1/20 – 1/40
SKCO1	Colorectal	3	13.335 (5.4)	1/20 – 1/40
COLO320DM	Colorectal	2	9.643	1/20 – 1/40
WIDR	Colorectal	2	10.97	1/20 – 1/80
MDA231	Breast	1	37.65	1/20 – 1/40
MCF7	Breast	2	5.85	1/20 – 1/40

* **MS-24** was tested from 500 – 1.95 μg/ml and the DMSO control from 1/10 – 1/2560 dilutions to equate with the amount that would be present in the drug dilutions. Initially the concentration of **MS-24** used was from 1000 μg/ml but this was lowered to 500 μg/ml to conserve the compound.

3.12 Physical Properties of Compounds MS-1 – MS-43

Properties of MS-1 (2*RS*,3*RS*-2-methyl-1,2,3,4-butanetetrol)

Pale yellow oil. $[\alpha]_D^{25}$ 0° (CH_3OH). IR (film) ν_{max}: 3317, 2933, 1653, 1541, 1507, 1041 cm^{-1}. ^1H NMR (500 MHz, CD_3OD) and ^{13}C NMR (125 MHz, CD_3OD) **Table 1**. Positive ESI-MS: *m/z* = 136.8 $[M+H]^+$.

Properties of MS-2 (8-debenzoylpaeoniflorin)

Colourless amorphous solid. $[\alpha]_D^{23}$ -12.8° (*c* 0.195, CH_3OH). IR (film) ν_{max}: 3344, 2925, 1386, 1075, 1049, 1011 cm^{-1}. ^1H NMR (500 MHz, CD_3OD) and ^{13}C NMR (125 MHz, CD_3OD) **Table 2**. Positive FABMS: *m/z* (rel. int) = 399 $[M+Na]^+$ (100), 329 (30), 286 (35), 199 (47), 191 (30).

Properties of MS-3 (methyl-1'-(2',3'α-epoxy-3'-methyl-5'-oxo-cyclopentyl)-propen-2-oate)

Yellow amorphous solid. $[\alpha]_D^{25}$ -100° (*c* 0.62, CH_3OH). UV (CH_3OH): λ_{max}: (log ε) 209 (8.65) nm. IR (film) ν_{max}: 2958, 2953, 2860, 1715, 1437, 1244, 1152, 1110 cm^{-1}. ^1H NMR (500 MHz, CD_3OD) and ^{13}C NMR (125 MHz, CD_3OD) **Table 3**. Positive CI-MS: *m/z* = 261.1 $[M+H-H_2O]^+$, 279.1 $[M+H]^+$, 296.2 $[M+NH_4]^+$. HREIMS *m/z* 278.1526 (calc. for $C_{16}H_{22}O_4$, 278.1518).

Properties of MS-4 (9-hydroxylinaloyl-3-*O*-β-D-glucopyranoside) (racemate)

Yellow oil. $[\alpha]_D^{25}$ 0° (CH_3OH). IR (film) ν_{max}: 3566, 3329, 2933, 1075, 1035 cm^{-1}. ^1H NMR (500 MHz, CD_3OD) and ^{13}C NMR (125 MHz, CD_3OD) **Table 4**. Positive ESI-MS: *m/z* = 355.2 $[M+Na]^+$, 687.2 $[M+2Na]^+$.

Properties of MS-5 (6-*epi*-ajugoside)

Colourless oil. $[\alpha]_D^{25}$ -117.5° (*c* 2.757, CH_3OH). IR (film) ν_{max}: 3383, 2910, 1707, 1653, 1089, 1005, 754 cm^{-1}. ^1H NMR (500 MHz, CD_3OD) and ^{13}C NMR (125 MHz, CD_3OD) **Table 5**. HRCIMS *m/z* 391.1613 (calc. for $C_{17}H_{27}O_{10}$, 391.1604), 408.1865 (calc. for $C_{17}H_{30}O_{10}N$, 408.1870).

Properties of MS-6 (6-*epi*-laterioside)

White amorphous powder. $[\alpha]_D^{25}$ -51.1° (*c* 0.587, CH_3OH). UV (CH_3OH): λ_{max}: (log ε) 275 (8.95), 214 (8.61), 204 (8.62) nm. IR (film) ν_{max}: 3648, 1708, 1684, 1652, 1558, 1507. ^1H NMR (500 MHz, CD_3OD) and ^{13}C NMR (125 MHz, CD_3OD) **Table 6**. HRCIMS *m/z* 496.2173 (calc. for $C_{24}H_{34}O_{10}N$, 496.2183).

Properties of MS-7 (6-*O*-*α*-L-rhamnopyranosylcatalpol)

Colourless oil. $[\alpha]_D^{25}$ -109.3° (*c* 0.677, CH_3OH). IR (film) ν_{max}: 3265, 3163, 1717, 1652, 1113, 1018 cm^{-1}. ^1H NMR (500 MHz, CD_3OD) and ^{13}C NMR (125 MHz, CD_3OD) **Table 7**. Positive ESI-MS: *m/z* = 531.2 $[M+Na]^+$, 553.1 $[M-H+2Na]^+$.

Properties of MS-8 (buddlejoside A_8)

Colourless oil. $[\alpha]_D^{25}$ -78.7° (*c* 0.483, CH_3OH). UV (CH_3OH): λ_{max}: 309, 296, 231, 217 nm. IR (film) ν_{max}: 3355, 2931, 1653, 1558, 1260, 1072 cm^{-1}. ^1H NMR (500 MHz, CD_3OD) and ^{13}C NMR (125 MHz, CD_3OD) **Table 8**. Positive ESI-MS: *m/z* = 721.0 $[M+Na]^+$, 743.0 $[M-H+2Na]^+$.

Properties of MS-9 (scrospioside A)

White amorphous powder. $[\alpha]_D^{25}$ -84.5° (*c* 1.492, CH_3OH). UV (CH_3OH): λ_{max}: 257, 253, 222 nm. IR (film) ν_{max}: 3392, 1717, 1653, 1558, 1226, 1075 cm^{-1}. ^1H NMR (500 MHz, CD_3OD) and ^{13}C NMR (125 MHz, CD_3OD) **Table 9**. Negative ESI-MS: *m/z* = 721.1 $[M-H]^-$, 745.1 $[M+Na]^-$, 767.1 $[M-H+2Na]^-$.

Properties of MS-10 (scropolioside B)

White amorphous solid. $[\alpha]_D^{25}$ -9.6° (*c* 1.041, CH_3OH). UV (CH_3OH): λ_{max}: 266, 221 nm. IR (film) ν_{max}: 3385, 2929, 1717, 1636, 1153, 1075 cm^{-1}. ^1H NMR (500 MHz, CD_3OD) and ^{13}C NMR (125 MHz, CD_3OD) **Table 10**. HRCIMS *m/z* 833.2628 (calc. for $C_{41}H_{46}O_{17}Na$, 833.2633).

Properties of MS-11 (scorodioside)

Colourless oil. $[\alpha]_D^{25}$ -46.8° (*c* 0.470, CH_3OH). UV (CH_3OH): λ_{max}: 276, 214, 205 nm. IR (film) ν_{max}: 3421, 1717, 1653, 1558, 1229, 1072 cm^{-1}. ^1H NMR (500 MHz, CD_3OD) and ^{13}C NMR (125 MHz, CD_3OD) **Table 11**. Positive ESI-MS: *m/z* = 703.0 $[M+Na]^+$.

Properties of MS-12 (pulicrispiolide)

Pale yellow oil. $[\alpha]_D^{25}$ +22.9° (*c* 0.350, $CHCl_3$). IR (film) ν_{max}: 3649, 2968, 2931, 1770, 1507, 1015 cm^{-1}. ^1H NMR (500 MHz, C_6D_6) and ^{13}C NMR (125 MHz, C_6D_6) **Table 12**. HREIMS *m/z* 246.1264 (calc. for $C_{15}H_{18}O_3$, 246.1256).

Properties of MS-13 (spathulenol)

Colourless oil. $[\alpha]_D^{24}$ +10.5° (*c* 0.762, $CHCl_3$). IR (film) ν_{max}: 3383, 2922, 2863, 1635, 1456, 1375, 889 cm^{-1}. ^1H NMR (500 MHz, $CDCl_3$) and ^{13}C NMR (125 MHz, $CDCl_3$) **Table 13**.

Properties of MS-14 (*rel*-1β,3α,6β-trihydroxyeudesm-4-ene)

Colourless oil. $[\alpha]_D^{25}$ +314° (*c* 0.05, $CHCl_3$). IR (film) ν_{max}: 3362, 2939, 2868, 1738, 1217, 781 cm^{-1}. ^1H NMR (500 MHz, $CDCl_3$) and ^{13}C NMR (125 MHz, $CDCl_3$) **Table 14**. HREIMS *m/z* 254.1864 (calc. for $C_{15}H_{26}O_3$, 254.1882).

Properties of MS-15 (1,2-dehydro-1,10α-dihydropseudoivalin)

Colourless oil. $[\alpha]_D^{24}$ +23.9° (*c* 0.418, $CHCl_3$). UV (CH_3OH): λ_{max}: 218 nm. IR (film) ν_{max}: 3420, 2963, 1759, 1270, 1128, 969 cm^{-1}. ^1H NMR (500 MHz, CD_3OD) and ^{13}C NMR (125 MHz, CD_3OD) **Table 15**. Negative ESI-MS: *m/z* = 293.1 $[M-H+2Na]^-$.

Properties of MS-16 (2α,4α-dihydroxy-10β-methyl-guaia-1(5),11(13)-dien-8β,12-olide)

Colourless oil. $[\alpha]_D^{23}$ +37.0° (*c* 0.378, $CHCl_3$). UV (CH_3OH): λ_{max}: (log ε) 218 (8.56) nm. IR (film) ν_{max}: 3352, 2963, 1748, 1653, 1276, 986 cm^{-1}. ^1H NMR (500 MHz, CD_3OD) and ^{13}C NMR (125 MHz, CD_3OD) **Table 16**. HREIMS *m/z* 264.1355 (calc. for $C_{15}H_{20}O_4$, 264.1362).

Properties of MS-17 (4-*epi*-1α,2α-epoxy-1,10α-dihydropseudoivalin)

Pale yellow oil. $[\alpha]_D^{23}$ +33.7° (*c* 0.475, $CHCl_3$). UV (CH_3OH): λ_{max}: (log ε) 214 (8.52) nm. IR (film) ν_{max}: 3566, 2933, 1761, 1653, 1271, 1128 cm^{-1}. ^1H NMR (500 MHz, $CDCl_3$) and ^{13}C NMR (125 MHz, $CDCl_3$) **Table 17**. HREIMS *m/z* 264.1363 (calc. for $C_{15}H_{20}O_4$, 264.1362).

Properties of MS-18 (5,10-*epi*-2,3-dihydroaromatin)

White amorphous powder. $[\alpha]_D^{25}$ +104.8° (*c* 4.75, $CHCl_3$). UV (ACN): λ_{max}: (log ε) 222 (7.20) nm. IR (film) ν_{max}: 2968, 2931, 1763, 1736, 1125, 996 cm^{-1}. ^1H NMR (500 MHz, C_6D_6) and ^{13}C NMR (125 MHz, C_6D_6) **Table 18**. HREIMS *m/z* 248.1412 (calc. for $C_{15}H_{20}O_3$, 248.1413).

Properties of MS-19 (paniculoside V)

Colourless solid. $[\alpha]_D^{25}$ -27.0° (*c* 1.186, CH_3OH). IR (film) ν_{max}: 3384, 2933, 2360, 1717, 1075, 1028 cm^{-1}. ^1H NMR (500 MHz, CD_3OD) and ^{13}C NMR (125 MHz, CD_3OD) **Table 19**. Positive ESI-MS: *m/z* = 665.3 $[M+Na]^+$.

Properties of MS-20 (β-sitosterol)

Colourless oil. $[\alpha]_D^{26}$ -31.6° (*c* 1.267, $CHCl_3$). IR (film) ν_{max}: 2957, 2931, 2868, 1645, 1379, 1050 cm^{-1}.

Properties of MS-21 (lupeol)

Colourless oil. $[\alpha]_D^{26}$ +13.9° (*c* 0.574, $CHCl_3$). IR (film) ν_{max}: 3562, 2932, 2851, 1733, 1362, 1216 cm^{-1}.

Properties of MS-22 (α-amyrin)

Colourless oil. $[\alpha]_D^{26}$ +55.5° (*c* 2.377, $CHCl_3$). IR (film) ν_{max}: 3446, 2925, 1653, 1457, 1216, 994 cm^{-1}.

Properties of MS-23 (falcarindiol)

Pale yellow oil. $[\alpha]_D^{23}$ +72.6° (*c* 0.441, $CHCl_3$). IR (film) ν_{max}: 3329, 2925, 2855, 1701, 1464, 1020 cm^{-1}. ^1H NMR (500 MHz, $CDCl_3$) and ^{13}C NMR (125 MHz, $CDCl_3$) **Table 20**.

Properties of MS-24 (3*R*,8*R*-16,17-dehydrofalcarindiol)

Pale yellow oil. $[\alpha]_D^{25}$ +39.8° (*c* 2.661, $CHCl_3$). UV ($CHCl_3$): λ_{max}: (log ε) 284 (8.27), 268 (8.52), 254 (8.36), 244 (8.25) nm. IR (film) ν_{max}: 3351, 2929, 2856, 2232, 2146, 1641, 1457, 1285, 993 cm^{-1}. ^1H NMR (500 MHz, $CDCl_3$) and ^{13}C NMR (125 MHz, $CDCl_3$) **Table 21**. Positive ESI-MS: *m/z* = 259.0 $[M+H]^+$, 279.0 $[M+K-H_2O]^+$.

Properties of MS-25 (16,17-dehydrofalcarinol)

Yellow oil. IR (film) ν_{max}: 3171, 2918, 2850, 1725, 1272, 1051, 1018 cm^{-1}. ^1H NMR (500 MHz, $CDCl_3$) and ^{13}C NMR (125 MHz, $CDCl_3$) **Table 22**.

Properties of MS-26 (1,3*R*,8*R*-trihydroxydec-9-en-4,6-yne)

Colourless oil. $[\alpha]_D^{25}$ +127° (*c* 0.24, CH_3OH). UV (CH_3OH): λ_{max}: (log ε) 234 (7.32), 255 (7.03), 282 (7.03) nm. IR (film) ν_{max}: 3259, 2357, 1635, 1507, 792 cm^{-1}. ^1H NMR (500 MHz, CD_3OD) and ^{13}C NMR (125 MHz, CD_3OD) **Table 23**. HREIMS *m/z* 180.0788 (calc. for $C_{10}H_{12}O_3$, 180.0786).

Properties of MS-27 (3(ζ),8(ζ)-dihydroxydec-9-en-4,6-yne-1-*O*-β-D-glucopyranoside)

Pale yellow oil. $[\alpha]_D^{25}$ -45.3° (*c* 0.750, CH_3OH). UV (CH_3OH): λ_{max}: (log ε) 265 (7.97), 212 (8.06) nm. IR (film) ν_{max}: 3376, 2889, 1654, 1244, 1077, 1035 cm^{-1}. ^1H NMR (500 MHz, CD_3OD) and ^{13}C NMR (125 MHz, CD_3OD) **Table 24**. HRESI-MS *m/z* 365.1190 (calc. for $C_{16}H_{22}O_8Na$, 365.1212).

Properties of MS-28 (Pangelin)

Colourless amorphous solid. $[\alpha]_D^{20}$ +11° (*c* 0.300, $CHCl_3$). UV (CH_3OH): λ_{max}: 311, 251 nm. IR (film) ν_{max}: 3649, 2916, 1717, 1624, 1134 cm^{-1}. ^1H NMR (400 MHz, $CDCl_3$) and ^{13}C NMR (100 MHz, $CDCl_3$) **Table 25**. Positive FABMS: *m/z* (rel. int) = 287 $[M+H]^+$ (100), 202 (73), 187 (14), 174 (16).

Properties of MS-29 (oxypeucedanin hydrate) (racemate)

Colourless amorphous solid. $[\alpha]_D^{23}$ 0° ($CHCl_3$). UV ($CHCl_3$): λ_{max}: 306, 253 nm. IR (film) ν_{max}: 3447, 2979, 2918, 1731, 1624, 1457, 1133 cm^{-1}. ^1H NMR (500 MHz, $CDCl_3$) and ^{13}C NMR (125 MHz, $CDCl_3$) **Table 26**. Positive ESI-MS: *m/z* = 287.0 $[M+H-H_2O]^+$.

Properties of MS-30 ((*R*)-(+)-oxypeucedanin)

Colourless amorphous solid. $[\alpha]_D^{23}$ +9.1° (*c* 1.755, $CHCl_3$). UV ($CHCl_3$): λ_{max}: 303, 253, 251 nm. IR (film) ν_{max}: 3128, 2967, 1728, 1625, 1458, 1345, 1128 cm^{-1}. ^1H NMR (500 MHz, $CDCl_3$) and ^{13}C NMR (125 MHz, $CDCl_3$) **Table 27**. Positive ESI-MS: *m/z* = 287.1 $[M+H]^+$.

Properties of MS-31 (5-[4''-hydroxy-3''-methyl-2''-butenyloxy]-6,7-furocoumarin)

White amorphous solid. UV ($CHCl_3$): λ_{max}: (log ε) 305 (8.94), 266 (9.01), 258 (9.04), 255 (9.04) nm. IR (film) ν_{max}: 3631, 2936, 1541, 1507 cm^{-1}. ^1H NMR (500 MHz, $CDCl_3$) and ^{13}C NMR (125 MHz, $CDCl_3$) **Table 28**. HREIMS *m/z* 286.0840 (calc. for $C_{16}H_{14}O_5$, 286.0841).

Properties of MS-32 (3',5-dihydroxy-4',6,7-trimethoxyflavone)

Yellow amorphous powder. UV (ACN): λ_{max}: 234, 272, 344 nm. IR (film) ν_{max}: 3273, 3170, 1733, 1457, 1271, 1046, 1020 cm^{-1}. ^1H NMR (500 MHz, $CDCl_3$) and ^{13}C NMR (125 MHz, $CDCl_3$) **Table 29**. Negative ESI-MS: *m/z* = 343.3 $[M-H]^-$.

Properties of MS-33 (5-hydroxy-3',4',6,7-tetramethoxyflavone)

Yellow amorphous powder. UV (ACN): λ_{max}: 234, 274, 342 nm. IR (film) ν_{max}: 3245, 3162, 1733, 1652, 1507,1269, 1020 cm^{-1}. ^1H NMR (500 MHz, $CDCl_3$) and ^{13}C NMR (125 MHz, $CDCl_3$) **Table 30**. Positive ESI-MS: *m/z* = 359.1 $[M+H]^+$.

Properties of MS-34 (quercetin-3-*O*-β-D-glucopyranoside)

Yellow amorphous powder. UV (CH_3OH): λ_{max}: 355, 254, 207 nm. IR (film) ν_{max}: 3249, 2917, 1733, 1647, 1457, 1303, 1055, 1019 cm^{-1}. ^1H NMR (500 MHz, $CDCl_3$) and ^{13}C NMR (125 MHz, $CDCl_3$) **Table 31**. Negative ESI-MS: *m/z* = 463.3 $[M-H]^-$.

Properties of MS-35 (eriodictyol-7-methyl ether) (keto-enol tautomer; racemate)

Yellow amorphous powder. UV (CH_3OH): λ_{max}: (log ε) 284 (9.70), 280 (9.70), 226 (9.66) nm. IR (film) ν_{max}: 3552, 1648, 1271, 1225, 1156, 1090 cm^{-1}. ^1H NMR (500 MHz, $CDCl_3$) and ^{13}C NMR (125 MHz, $CDCl_3$) **Table 32**. Positive ESI-MS: *m/z* = 301.1 $[M-H]^+$.

Properties of MS-36 (3-[3'-methyl-2'-butenyl]-5-[4''-hydroxy-3''-methyl-2''-butenyl]-6-hydroxy-*p*-coumaric acid)

Colourless oil. UV ($CHCl_3$): λ_{max}: (log ε) 314 (8.15), 241 (7.86) nm. IR (film) ν_{max}: 3388, 2915, 1684, 1635, 1473, 1270, 1199, 982 cm^{-1}. ^1H NMR (500 MHz, $CDCl_3$) and ^{13}C NMR (125 MHz, $CDCl_3$) **Table 34**. HREIMS *m/z* 332.1623 (calc. for $C_{19}H_{24}O_5$, 332.1624).

Properties of MS-37 (5-*O*-caffeoylquinic acid)

Yellow resin. $[\alpha]_D^{25}$ -19.0° (*c* 1.050, CH_3OH). UV (CH_3OH): λ_{max}: 341, 294, 243, 224 nm. IR (film) ν_{max}: 3390, 2960, 1684, 1635, 1521, 1277, 1182, 1120 cm^{-1}. ^1H NMR (500 MHz, CD_3OD) and ^{13}C NMR (125 MHz, CD_3OD) **Table 35**. Positive ESI-MS: *m/z* = 355.1 $[M+H]^+$, 377.1 $[M+Na]^+$.

Properties of MS-38 (7*S*-(4-hydroxyphenyl) ethane-7,8-diol)

Pale yellow oil. $[\alpha]_D^{25}$ +40.5° (*c* 0.198, CH_3OH). UV (CH_3OH): λ_{max}: 274, 224 nm. IR (film) ν_{max}: 3400, 2927, 1734, 1511, 1230, 1081 cm^{-1}. ^1H NMR (500 MHz, CD_3OD) and ^{13}C NMR (125 MHz, CD_3OD) **Table 36**. Positive ESI-MS: *m/z* = 176.1 $[M-H+Na]^+$.

Properties of MS-39 (*p*-hydroxy benzoic acid)

Yellow amorphous solid. UV (CH_3OH): λ_{max}: 355, 267, 206 nm. IR (film) ν_{max}: 3649, 1653, 1558, 1507, 1272 cm^{-1}. ^1H NMR (500 MHz, CD_3OD) and ^{13}C NMR (125 MHz, CD_3OD) **Table 37**. Negative ESI-MS: *m/z* = 137.1 $[M-H]^-$.

Properties of MS-40 (*p*-coumaric acid eicosyl ester)

White amorphous powder. UV ($CHCl_3$): λ_{max}: 282, 274, 238 nm. IR (film) ν_{max}: 3381, 2916, 2849, 1675, 1604, 1467, 1168, 981 cm^{-1}. ^1H NMR (500 MHz, C_5D_5N) and ^{13}C NMR (125 MHz, C_5D_5N) **Table 38**. Negative ESI-MS: *m/z* = 443.2 $[M-H]^-$.

Properties of MS-41 (*R*-tryptophan)

Pale yellow amorphous solid. $[\alpha]_D^{25}$ +47.1° (*c* 0.17, CH_3OH). UV (CH_3OH): λ_{max}: 324, 287, 280, 224 nm. IR (film) ν_{max}: 3649, 1684, 1653, 1558, 1507, 1457 cm^{-1}. ^1H NMR (500 MHz, CD_3OD) and ^{13}C NMR (125 MHz, CD_3OD) **Table 39**.

Properties of MS-42 (3*R*-1-octan-3-yl-3-*O*-β-D-glucopyranoside)

Colourless oil. $[\alpha]_D^{25}$ +31.8° (*c* 0.314, $CHCl_3$). IR (film) ν_{max}: 3354, 2929, 2861, 1558, 1457, 1077, 1021 cm^{-1}. ^1H NMR (500 MHz, CD_3OD) and ^{13}C NMR (125 MHz, CD_3OD) **Table 40**. Positive ESI-MS: *m/z* = 313.2 $[M+Na]^+$.

Properties of MS-43 (3(ζ)-hydroxy-octadeca-4(*E*),6(*Z*)-dienoic acid)

Colourless oil. $[\alpha]_D^{24}$ 0° ($CHCl_3$). UV ($CHCl_3$): λ_{max}: (log ε) 275 (6.68), 243 (8.19) nm. IR (film) ν_{max}: 3359, 2928, 2855, 1709, 1412, 1248, 985 cm^{-1}. ^1H NMR (500 MHz, $CDCl_3$) and ^{13}C NMR (125 MHz, $CDCl_3$) **Table 41**. HRCIMS *m/z* 296.2324 (calc. for $C_{18}H_{32}O_3$, 296.2352).

4.0 Conclusion

There is an urgent need to identify new antimycobacterial agents to fight the worldwide resurgence of tuberculosis as well as non-tuberculosis infections. Currently there are no plant-derived antimicrobials used as systemic antibiotics (Tegos *et al.*, 2002). This is somewhat surprising considering the rich diversity of natural products produced by plants. Recent reviews indicate that plants have potential for producing antimycobacterial and anti-staphylococcal agents that can serve as antibiotic leads for the development of more potent drugs (Cantrell *et al.*, 2001; Gibbons 2004; Newton *et al.*, 2000; Newton *et al.*, 2002).

The isolation of the antimicrobial active C_{17} polyacetylene falcarindiol is an example of the potential for finding not just antimycobacterial agents but compounds which have a broader spectrum of activity. This polyacetylenic natural product exhibited an MIC range of 2 – 4 μg/ml against the panel of rapidly growing mycobacteria assayed. These values were comparable to ethambutol, a standard drug used for the treatment of tuberculosis. Against *M. abscessus* falcarindiol demonstrated a 64-fold lower MIC compared to both ethambutol and isoniazid. Falcarindiol also exhibited moderate anti-staphylococcal activity against the MDR strain *S. aureus* 1199B (NorA), the major drug pump in this pathogenic organism. The MIC reported was comparable to some of the newest drugs in development to treat MRSA infections (Lechner *et al.*, 2004). The relative instability of falcarindiol and similar C_{17} enynols has been a reason for not pursuing further *in vivo* investigations of these compounds as cytotoxic agents (Bernart *et al.*, 1996). Further evaluation of the antibiotic activity of falcarindiol and of acetylenes is therefore warranted especially due to the specific mechanism of action that appears to be responsible for the antimicrobial activity. Further development would have to focus on increasing the stability and also decreasing the toxicity associated with this natural product class.

The prenylated furocoumarins are also another natural product class worthy of further investigation. **MS-28** – **MS-30** demonstrated moderate antimycobacterial activity (MIC range 32 – 128 μg/ml). The lipophilicity of these furocoumarins as well as the polyacetylene falcarindiol, is likely to facilitate the passage of these compounds through the thick hydrophobic outer membrane into the cytosol where they can exert their effect. Coumarins have long been known to inhibit bacterial DNA gyrase and so must be able to penetrate the outer membrane to exert their effect. Increasing the lipophilicity of these compounds further by replacing the prenyl group with a geranyl

or even farnesyl moiety has increased activity greatly with MIC's ranging from 0.5 – 4 μg/ml. Given the need to find compounds with activity against rapidly growing strains, which are naturally resistant and difficult to treat, and given the burden of drug-resistant tuberculosis, further investigation of the antimycobacterial properties of coumarin natural products is worthwhile (Stavri *et al.*, 2003).

The new guaianolide, 5,10-*epi*-2,3-dihydroaromatin (**MS-18**), whilst exhibiting only weak antimycobacterial activity is yet another class of natural product that deserves further investigation. Guaianolides have been isolated such as aromaticin (MIC = 16 μg/ml), similar to **MS-18**, that possess strong antimycobacterial activity. The lipophilic guaianolide dehydrocostuslactone has shown even greater activity with an MIC of 2 μg/ml versus *Mycobacterium tuberculosis*.

This thesis highlights some of the diverse natural products synthesised by plants. It represents a largely untapped source of antimicrobial agents which could provide leads for future development to fight against the ever increasing rise of multidrug resistant infectious diseases such as those caused by *M. tuberculosis* and *S. aureus*.

From a phytochemical standpoint the isolation and structure elucidation of 2α,6α-dimethyltetracyclo-decal-3-en-2,12-diol-8α,13-olide (pulicrispiolide), with a novel sesquiterpene skeleton, can be used as a chemotaxonomic marker for the species *P. crispa*.

5.0 References

Abdel-Mogib,M., Jakupovic,J., Dawidar,A.M., Metwally,M.A. and Abou-Elzahab,M. (1990) Sesquiterpene Lactones and Kaurane Glycosides from *Francoeuria crispa*. *Phytochemistry* **29**, 8, 2581-2584.

Abu-Niaaj,L., Abu-Zarga,M. and Abdalla,S. (1996) Isolation and Inhibitory Effects of Eupatilin, a Flavone Isolated from *Artemisia monosperma* Del., on Rat Isolated Smooth Muscle. *Pharmaceutical Biology* **34**, 2, 134-140.

Abu-Niaaj,L., Abu-Zarga,M., Sabri,S. and Abdalla,S. (1993) Isolation and Biological Effects of 7-*O*-Methyleriodictyol, a Flavanone Isolated from *Artemisia monosperma*, on rat Isolated Smooth Muscle. *Planta Medica* **59**, 42-45.

Ahmed,B., Al-Rehaily,A.J., Al-Howiriny,T.A., El-Sayed,K.A. and Ahmad,M.S. (2003) Scropolioside-D_2 and Harpagoside-B: Two New Iridoid Glycosides from *Scrophularia deserti* and Their Antidiabetic and Antiinflammatory Activity. *Biological and Pharmaceutical Bulletin* **26**, 4, 462-467.

Ainsa,J.A., Blokpoel,M.C.J., Otal,I., Young,D.B., Smet,A.L.D. and Martin,C. (1998) Molecular Cloning and Characterization of Tap, a Putative Multidrug Efflux Pump Present in *Mycobacterium fortuitum* and *Mycobacterium tuberculosis*. *Journal of Bacteriology* **180**, 22, 5836-5843.

Ainsworth,C. and Mackenzie,D. (2001) Coming Home. *New Scientist* **July 7**, 28-33.

Albach,D.C., Grayer,R.J., Jensen,S.R., Ozgokce,F. and Veitch,N.C. (2003) Acylated flavone glycosides from *Veronica*. *Phytochemistry* **64**, 1295-1301.

Ambudkar,S.V., Dey,S., Hrycyna,C.A., Ramachandra,M., Pastan,I. and Gottesman,M.M. (1999) Biochemical, cellular, and pharmacological aspects of the multidrug transporter. *Annual Review of Pharmacology and Toxicology* **39**, 361-398.

Ang,J.Y., Ezike,E. and Asmar,B.I. (2004) Antibacterial resistance. *The Indian Journal of Pediatrics* **71**, 3, 229-239.

Anthonsen,T., Hagen,S., Kazi,M.A., Shah,S.W. and Tagar,S. (1976) 2-C-Methyl-erythritol, a New Branched Alditol from *Convolvulus glomeratus*. *Acta Chemica Scandinavia Series B* **30**, 1, 91-93.

Appendino,G., Arnoldi,L., Stavri,M., Gibbons,S. and Ballero,M. (2004) An Antitubercular Coumarin from Sardinian Giant Fennel (*Ferula communis*). *Journal of Natural Products* (Submitted).

Ashraf,M., Karim,A., Asghar,B. and Bhatty,M.K. (1979) Studies on the Essential Oils of the Pakistani Species of the Family Umbelliferae. *Pakistan Journal of Scientific and Industrial Research* **22**, 5, 252-254.

Ball,P.R., Shales,S.W. and Chopra,I. (1980) Plasmid-mediated tetracycline resistance in *Escherichia coli* involves increased efflux of the antibiotic. *Biochemical and Biophysical Research Communications* **93**, 74-81.

Baysallar,M., Kilic,A., Aydogan,H., Cilli,F. and Doganci,L. (2004) Linezolid and quinupristin/dalfopristin resistance in vancomycin-resistant enterococci and methicillin-resistant *Staphylococcus aureus* prior to clinical use in Turkey. *International Journal of Antimicrobial Agents* **23**, 510-512.

Bernart,M.W., Cardellina,I.J.H., Balaschak,M.S., Alexander,M.R., Shoemaker,R.H. and Boyd,M.R. (1996) Cytotoxic Falcarinol Oxylipins from *Dendropanax arboreus*. *Journal of Natural Products* **59**, 748-753.

Bhandari,S.P.S., Mishra,A., Roy,R. and Garg,H.S. (1992) Koelzioside, an Iridoid Diglycoside from *Scrophularia koelzii*. *Phytochemistry* **31**, 2, 689-691.

Blank,I. and Grosch,W. (1991) Evaluation of potent odorants in dill seed and dill herb (*Anethum graveolens* L.) by aroma extract dilution analysis. *Journal of Food Science* **56**, 63-67.

Blank,I., Sen,A. and Grosch,W. (1992) Sensory study on the character-impact flavour compounds of dill herb (*Anethum graveolens* L.). *Food Chemistry* **43**, 337-343.

Bohlmann,F. and Mahanta,P.K. (1979) Zwei neue pseudoguajanolide aus *Telekia speciosa*. *Phytochemistry* **18**, 5, 887-888.

Bozdogan,B. and Appelbaum,P.C. (2004) Oxazolidinones: activity, mode of action, and mechanism of resistance. *International Journal of Antimicrobial Agents* **23**, 113-119.

Bradley,G. and Ling,V. (1994) P-glycoprotein, multidrug resistance and tumor progression. *Cancer Metastasis Reviews* **13**, 2, 223-233.

Breitmaier, E. (1999) *Structure Elucidation by NMR in Organic Chemistry*. NewYork: John Wiley & Sons Ltd.

Buckingham, J. (2004) *Dictionary of Natural Products on CD-ROM*. Chapman and Hall.

Calis,I., Gross,G.A., Winkler,T. and Sticher,O. (1988) Isolation and Structure Elucidation of Two Highly Acylated Iridoid Diglycosides from *Scrophularia scopolii*. *Planta Medica* **54**, 168-170.

Calis,I. and Yuruker,A. (1993) Anatolioside E: A New Acyclic Monoterpene Glycoside from *Viburnum orientale*. *Helvetica Chimica Acta* **76**, 2563-2569.

Cantrell,C.L., Franzblau,S.G. and Fischer,N.H. (2001) Antimycobacterial Plant Terpenoids. *Planta Medica* **67**, 685-694.

Catalan,C.A.N., Vega,M.I., Lopez,M.E., del R.Cuenca,M., Gedris,T.E. and Herz,W. (2003) Coumarins and a kaurane from *Gochnatia polymorpha* ssp. *polymorpha* from Paraguay. *Biochemical Systematics and Ecology* **31**, 417-422.

Cha,R., Brown,W.J. and Rybak,M.J. (2003) Bactericidal Activities of Daptomycin, Quinupristin/Dalfopristin, and Linezolid against Vancomycin-Resistant *Staphylococcus aureus* in an In Vitro Pharmacodynamic Model with Simulated Endocardial Vegetations. *Antimicrobial Agents and Chemotherapy* **47**, 12, 3960-3963.

Charles,D.J., Simon,J.E. and Widrlechner,M.P. (1995) Characterization of essential oil of dill (*Anethum graveolens* L.). *Journal of Essential Oil Research* **7**, 11-20.

Chaudhary, S. A. and Al-Jowaid, A. A. A. (1999) *Vegetation of the Kingdon of Saudi Arabia.* Kingdom of Saudi Arabia: Ministry of Agriculture and Water.

Cheminat,A., Zawatzky,R., Becker,H. and Brouillard,R. (1988) Caffeoyl Conjugates From *Echinacea* Species: Structures And Biological Activity. *Phytochemistry* **27**, 9, 2787-2794.

Christensen,L.P. and Lam,J. (1991) Acetylenes and Related Compounds in Heliantheae. *Phytochemistry* **30**, 1, 11-49.

Contin,A., Heijden,R.V.D., Lefeber,A.W.M. and Verpoorte,R. (1998) The iridoid glucoside secologanin is derived from the novel triose phosphate/pyruvate pathway in a *Catharanthus roseus* cell culture. *Federation of European Biochemical Societies Letters* **434**, 413-416.

Copp,B.R. (2003) Antimycobacterial natural products. *Natural Product Reports* **20**, 535-557.

Daoud, H. S. (1985b) *Flora of Kuwait.* **1**. London: KPI Limited.

Daoud, H. S. (1985a) *Flora of Kuwait.* **2**. London: KPI Limited.

Dewick,P.M. (2002) The biosynthesis of C_5-C_{25} terpenoid compounds. *Natural Product Reports* **19**, 181-222.

Dobberstein,R.H., Tin-Wa,M., Fong,H.H.S., Crane,F.A. and Farnsworth,N.R. (1977) Flavonoid Constituents from *Eupatorium altissimum* L. (Compositae). *Journal of Pharmaceutical Sciences* **66**, 4, 600-602.

Durham,N.N. and Hubbard,J.S. (1960) Mechanism of competitive inhibition of *p*-aminobenzoic acid oxidation by *p*-aminosalicylic acid. *Journal of Bacteriology* **80**, 2, 225-231.

Elgamal,M.H.A., Ouf,S.A., Hanna,A.G. and Yassin,F.Y. (1997) Phytochemical and Mycological Investigation of *Artemisia monosperma. Folia Microbiologica* **42**, 3, 203-210.

Fernandez,L., Diaz,A.M., Ollivier,E., Faure,R. and Balansard,G. (1995) An Iridoid Diglycoside Isolated from *Scrophularia scorodonia. Phytochemistry* **40**, 5, 1569-1571.

Flores-Sanchez,I.J., Ortega-Lopez,J., Montes-Horcasitas,M.D.C. and Ramos-Valdivia,A.C. (2002) Biosynthesis of Sterols and Triterpenes in Cell Suspension Cultures of *Uncaria tomentosa. Plant Cell Physiology* **43**, 12, 1502-1509.

Ford,C.H.J., Richardson,V.J. and Tsaltas,G. (1989) Comparison of tetrazolium colorimetric and [^{3}H]-uridine assays for *in vitro* chemosensitivity testing. *Cancer Chemotherapy and Pharmacology* **24**, 295-301.

Furumi,K., Fujioka,T., Fujii,H., Okabe,H., Mihashi,K., Nakano,Y., Matsunaga,H., Katano,M. and Mori,M. (1998) Novel antiproliferative falcarindiol furanocoumarin ethers from the root of *Angelica japonica*. *Bioorganic Medicinal Chemistry Letters* **8**, 93-96.

Garcia-Granados,A., Molina,A., Saenz de Buruaga,A. and Saenz de Buruaga,J.M. (1985) Sesquiterpenes from two subspecies of *Sideritis varoi*. *Phytochemistry* **24**, 97-101.

Gemmell,C.G. (2004) Glycopeptide resistance in Staphylococcus aureus: is it a real threat? *Journal of Infection and Chemotherapy* **10**, 2, 69-75.

Ghafoor, A. (2002) *Flora of Pakistan: No. 27; Asteraceae (I) - Anthemidae*. Karachi: University of Karachi.

Gibbons, S. Phytochemical Studies on the *Flacourtiaceae* and *Simaroubaceae*. 1994. University of Strathclyde.
Ref Type: Thesis/Dissertation

Gibbons,S. (2004) Anti-staphylococcal plant natural products. *Natural Product Reports* **21**, 263-277.

Goad, L. J. and Akihisa, T. (1997) *Analysis of Sterols*. London: Blackie Academic and Professional.

Guiso,M., Marini-Bettolo,R. and Agostini,A. (1974) Iridoids - XIII: Ajugoside and Ajugol: Structure and Configuration. *Gazzetta Chimica Italiana* **104**, 25-33.

Hansen,L. and Boll,P.M. (1986) Polyacetylenes in Araliaceae: Their Chemistry, Biosynthesis and Biological Significance. *Phytochemistry* **25**, 2, 285-293.

Haralampidis,K., Trojanowska,M. and Osbourn,A.E. (2002) Biosynthesis of Triterpenoid Saponins in Plants. *Advances in Biochemical Engineering/Biotechnology* **75**, 31-49.

Harborne, J. B. and Mabry, T. J. (1982) *The Flavonoids: Advances in Research*. London: Chapman and Hall.

Harkar,S., Razdan,T.K. and Waight,E.S. (1984) Steroids, Chromone and Coumarins from *Angelica officinalis*. *Phytochemistry* **23**, 2, 419-426.

Heinrich, M., Barnes, J., Gibbons, S. and Williamson, E. M. (2004) *Fundamentals of Pharmacognosy and Phytotherapy*. London: Churchill Livingstone.

Helfrich,E. and Rimpler,H. (2000) Iridoid glycosides from *Gmelina philippensis*. *Phytochemistry* **54**, 191-199.

Horibe,I., Nakai,H., Sato,T., Seo,S. and Takeda,K. (1989) Stereoselective Synthesis of the C-24 and C-25 Stereoisomeric Pairs of 24-Ethyl-26-hydroxy- and 24-Ethyl-[26-^{2}H]sterols and their Ä^{22}-Derivatives: Reassignment of ^{13}C N.m.r. Signals of the *pro-R* and the *pro-S* Methyl Groups at C-25 of 24-Ethylsterols. *Journal of the Chemical Society Perkin Transactions 1* 1957-1967.

Hosny,M. and Rosazza,J.P.N. (1998) Gmelinosides A-L, Twelve Acylated Iridoid Glycosides from *Gmelina arborea*. *Journal of Natural Products* **61**, 734-742.

Hou,C.C., Lin,S.J., Cheng,J.T. and Hsu,F.L. (2002) Bacopaside III, Bacopasaponin G, and Bacopasides A, B, and C from *Bacopa monniera*. *Journal of Natural Products* **65**, 1759-1763.

Hsu,F., Lai,C. and Cheng,J. (1997) Antihyperglycaemic effects of paeoniflorin and 8-debenzoylpaeoniflorin, glucosides from the root of *Paeonia lactiflora*. *Planta Medica* **63**, 323-325.

Inagaki,F. and Abe,A. (1985) Analysis of ^{1}H and ^{13}C Nuclear Magnetic Resonance Spectra of Spathulenol by Two-dimensional Methods. *Journal of Chemical Society Perkin Transactions II* 1773-1778.

Ishihara,K., Fukutake,M., Asano,T., Mizuhara,Y., Wakui,Y., Yanagisawa,T., Kamei,H., Ohmori,S. and Kitada,M. (2001) Simultaneous determination of byak-angelicin and oxypeucedanin hydrate in rat plasma by column-switching high-performance liquid chromatography with ultraviolet detection. *Journal of Chromatography B* **753**, 2, 309-314.

Ishikawa,T., Kondo,K. and Kitajima,J. (2003) Water-Soluble Constituents of Coriander. *Chemical and Pharmaceutical Bulletin* **51**, 1, 32-39.

Ishikawa,T., Kudo,M. and Kitajima,J. (2002) Water-Soluble Constituents of Dill. *Chemical and Pharmaceutical Bulletin* **50**, 4, 501-507.

Iwabuchi,H., Yoshikura,M. and Kamisako,W. (1989) Studies on the Sesquiterpenoids of *Panax ginseng* C. A. Meyer. III. *Chemical and Pharmaceutical Bulletin* **37**, 2, 509-510.

Janssen,A.M., Scheffer,J.J.C., Svendsen,A.B. and Aynehchi,Y. (1984) The essential oil of *Ducrosia anethifolia* (DC.) Boiss. *Pharmaceutisch Weekblad Scientific Edition* **6**, 157-160.

Jirovetz,L., Buchbauer,G., Stoyanova,A.S., Georgiev,E.V. and Damianova,S.T. (2003) Composition, Quality Control, and Antimicrobial Activity of the essential Oil of Long-Time Stored Dill (*Anethum graveolens* L.) Seeds from Bulgaria. *Journal of Agricultural and Food Chemistry* **51**, 3854-3857.

Kaatz,G.W. (2002) Inhibition of bacterial efflux pumps: a new strategy to combat increasing antimicrobial agent resistance. *Expert Opinion* **7**, 2, 1-11.

Kaneda,M., Itaka,Y. and Shibata,S. (1972) Chemical studies on the oriental plant drugs - XXXII The absolute structures of paeoniflorin, albiflorin, oxypaeoniflorin and benzoylpaeoniflorin isolated from Chinese paeony root. *Tetrahedron* **28**, 4309, 4317.

Keriko,J.M., Nakajima,S., Baba,N. and Iwasa,J. (1997) Eicosanyl *p*-Coumarates from a Kenyan Plant, *Psiadia punctulata*: Plant Growth Inhibitors. *Bioscience, Biotechnology and Biochemistry* **61**, 12, 2127-2128.

Khulusi,S., Ahmed,H.A., Patel,P., Mendall,M.A. and Northfield,T.C. (1995) The effects of unsaturated fatty acids on *Helicobacter pylori in vitro*. *Journal of Medical Microbiology* **42**, 276-282.

Kisiel,W. and Jakupowic,J. (1995) Long-Chain Alkyl Hydroxycinnamates from *Crepis taraxacifolia*. *Planta Medica* **61**, 87-88.

Kobaisy,M., Abramowski,Z., Lermer,L., Saxena,G., Hancock,R.E., Towers,G.H.N., Doxsee,D. and Stokes,R.W. (1997) Antimycobacterial polyynes of Devil's Club (*Oplopanax horridus*), a North American native medicinal plant. *Journal of Natural Products* **60**, 11, 1210-1213.

Kraker,J.W.D., Franssen,M.C.R., Joerink,M., Groot,A.D. and Bouwmeester,H.J. (2002) Biosynthesis of Costunolide, Dihydrocostunolide, and Leucodin. Demonstration of Cytochrome P450-Catalyzed Formation of the Lactone Ring Present in Sesquiterpene Lactones of Chicory. *Plant Physiology* **129**, 257-268.

Lambert,P.A. (2002) Cellular impermeability and uptake of biocides and antibiotics in Gram-positive bacteria and mycobacteria. *Journal of Applied Microbiology Symposium Symposium Supplement* **92**, 46S-54S.

Lechner,D., Stavri,M., Oluwatuyi,M., Pereda-Miranda,R. and Gibbons,S. (2004) The anti-staphylococcal activity of *Angelica dahurica* (Bai Zhi). *Phytochemistry* **65**, 331-335.

Lemmich,J., Pedersen,P.A. and Nielsen,B.E. (1971) Coumarins and Terpenoids of the Fruits of *Ligusticum seguieri*. *Phytochemistry* **10**, 3333-3334.

Li,X.Z., Poole,K. and Nikaido,H. (2003) Contributions of MexAB-OprM and an EmrE Homolog to Intrinsic Resistance of *Pseudomonas aeruginosa* to Aminoglycosides and Dyes. *Antimicrobial Agents and Chemotherapy* **47**, 1, 27-33.

Li,X.Z., Zhang,L. and Nikaido,H. (2004) Efflux Pump-Mediated Intrinsic Drug Resistance in *Mycobacterium smegmatis*. *Antimicrobial Agents and Chemotherapy* **48**, 7, 2415-2423.

Liu,J.H., Zschocke,S., Reininger,E. and Bauer,R. (1998) Inhibitory Effects of *Angelica pubescens* f. *biserrata* on 5-Lipoxygenase and Cyclooxygenase. *Planta Medica* **64**, 525-529.

Liva,R.R.H., Kasai,R., Rakotovao,M. and Yamasaki,K. (2001) New iridoid and phenethyl glycosides from Malagasy medicinal plant, *Phyllarthron madagascariense*. *Natural Medicines* **55**, 4, 187-192.

Lomovskaya,O., Lee,A., Hoshino,K., Ishida,H., Mistry,A., Warren,M.S., Boyer,E., Chamberland,S. and Lee,V.J. (1999) Use of a Genetic Approach to Evaluate the Consequences of Inhibition of Efflux Pumps in *Pseudomonas aeruginosa*. *Antimicrobial Agents and Chemotherapy* **43**, 1340-1346.

Lu,Y. and Foo,L.Y. (1999) The polyphenol constituents of grape pomace. *Food Chemistry* **65**, 1-8.

Mann, J. (1996) *Secondary Metabolism*. New York: Oxford University Press.

Mann, J. and Crabbe, M. J. C. (1996) *Bacteria and Antibacterial Agents*. Oxford: Spektrum Academic Publishers.

Manns,D. (1995) Linalool And Cineole Type Glucosides From *Cunila spicata*. *Phytochemistry* **39**, 5, 1115-1118.

Marshall,N.J. and Piddock,L.J.V. (1997) Antibacterial efflux systems. *Microbiologia* **13**, 285-300.

Matsumoto,T., Shigemoto,T. and Itoh,T. (1983) Occurrence of 24-Ethyl-Δ^5- and 24-Ethyl-Δ^7-Sterols as C-24 Epimeric Mixtures in Seeds of *Cucumis sativus*. *Phytochemistry* **22**, 11, 2622-2624.

Matsuura,H., Saxena,G., Farmer,S.W., Hancock,R.E.W. and Towers,G.H.N. (1996) Antibacterial and Antifungal Polyine Compounds from *Glehnia littoralis* ssp. *leiocarpa*. *Planta Medica* **62**, 256-259.

Maurer,B. and Hauser,A. (1983) New Sesquiterpenoids from Clary Sage Oil (*Salvia sclarea* L.). *Helvetica Chimica Acta* **66**, 2223-2235.

Maxwell,A. (1997) DNA gyrase as a drug target. *Trends in Microbiology* **5**, 3, 102-109.

McMurry,L.M., Petrucci Jr,R.E. and Levy,S.B. (1980) Active efflux of tetracycline encoded by four genetically different tetracycline resistance determinants in *Escherichia coli*. *Proceedings of the National Academy of Sciences of the United States of America* 77, 3974-3977.

Merfort,I. and Wendisch,D. (1993) Sesquiterpene lactones of *Arnica cordifolia*, subgenus *Austromontana*. *Phytochemistry* **34**, 5, 1436-1437.

Miyase,T., Akahori,C., Kohsaka,H. and Ueno,A. (1991) Acylated Iridoid Glycosides from *Buddleja japonica* HEMSL. *Chemical and Pharmaceutical Bulletin* **39**, 11, 2944-1951.

Morishita,H., Iwahashi,H., Osaka,N. and Kido,R. (1984) Chromatographic Separation And Identification Of Naturally Occurring Chlorogenic Acids By ^{1}H Nuclear Magnetic Resonance Spectroscopy And Mass Spectrometry. *Journal of Chromatography* **315**, 253-260.

Newton,S.M., Lau,C., Gurcha,S.S., Besra,G.S. and Wright,C.W. (2002) The evaluation of forty-three plant species for *in vitro* antimycobacterial activities;isolation of active constituents from *Psoralea corylifolia* and *Sanguinaria canadensis*. *Journal of Ethnopharmacology* **79**, 57-67.

Newton,S.M., Lau,C. and Wright,C.W. (2000) A review of Antimycobacterial Natural Products. *Phytotherapy Research* **14**, 303-322.

Nikaido,H. (1994) Prevention of Drug Access to Bacterial Targets: Permeability Barriers and Active Efflux. *Science* **264**, 382-388.

Nikaido,H. (2001) Preventing drug access to targets: cell surface permeability barriers and active efflux in bacteria. *Cell and Development Biology* **12**, 215-223.

Ognyanov,I. and Botcheva,D. (1971) Pangeline and angeloylpangeline - two new furocoumarins in the roots of *Angelica pancici* Vandas. *Comptes Rendus de l'Academie Bulgare des Sciences* **24**, 315-318.

Ohtani,I., Kusumi,T., Kashman,Y. and Kakisawa,H. (1991) High-field FT NMR application of Mosher's method. The absolute configurations of marine terpenoids. *Journal of the American Chemical Society* **113**, 4092-4096.

Pachaly,P., Barion,J. and Sin,K.S. (1994) Isolation and analysis of new iridoids from roots of *Scrophylaria korainensis*. *Pharmazie* **49**, 150-155.

Pardo,F., Perich,F., Torres,R. and Delle Monache,F. (1998) Phytotoxic iridoid glucosides from the roots of *Verbascum thapsus*. *Journal of Chemical Ecology* **24**, 4, 645-653.

Periers,A.M., Laurin,P., Ferroud,D., Haesslein,J.L., Klich,M., Dupuis-Hamelin,C., Mauvais,P., Lassaigne,P., Bonnefoy,A. and Musicki,B. (2000) Coumarin Inhibitors of Gyrase B with *N*-propargyloxy-carbamate as an Effective Pyrrole Bioisostere. *Bioorganic and Medicinal Chemistry Letters* **10**, 161-165.

Plaper,A., Golob,M., Hafner,I., Oblak,I., Solmajer,T. and Jerala,R. (2003) Characterization of quercetin binding site on DNA gyrase. *Biochemical and Biophysical Research Communications* **306**, 530-536.

Pongprayoon,U., Baeckstrom,P., Jacobsson,U., Lindstrom,M. and Bohlin,L. (1991) Compounds Inhibiting Prostaglandin Synthesis Isolated from *Ipomoea pes-caprae*. *Planta Medica* **57**, 515-518.

Pongprayoon,U., Baeckstrom,P., Jacobsson,U., Lindstrom,M. and Bohlin,L. (1992) Antispasmodic Activity of *β*-Damascenone and *E*-Phytol Isolated from *Ipomoea pes-caprae*. *Planta Medica* **58**, 19-21.

Poole,K. (2001) Overcoming antimicrobial resistance by targeting resistance mechanisms. *Journal of Pharmacy and Pharmacology* **53**, 283-294.

Poole,K. (2002) Mechanisms of bacterial biocide and antibiotic resistance. *Journal of Applied Microbiology Symposium Symposium Supplement* **92**, 55S-64S.

Pouchert, C. J. and Behnke, J. (1992a) *Aldrich Library of ^{13}C and ^{1}H FT NMR Spectra*. **3**. Milwaukee: Aldrich Chemical Company.

Pouchert, C. J. and Behnke, J. (1992b) *Aldrich Library of ^{13}C and ^{1}H FT NMR Spectra*. **2**. Milwaukee: Aldrich Chemical Company.

Price,C.T.D., Kaatz,G.W. and Gustafson,J.E. (2002) The multidrug efflux pump NorA is not required for salicylate-induced reduction in drug accumulation by *Staphylococcus aureus*. *International Journal of Antimicrobial Agents* **20**, 206-213.

Richardson,J.F. and Reith,S. (1993) Characterization of a strain of methicillin-resistant *Staphylococcus aureus* (EMRSA-15) by conventional and molecular methods. *Journal of Hospital Infection* **25**, 45-52.

Rizk, A. M. (1986) *The Phytochemistry of the Flora of Qatar*. London: Kingprint.

Ross,S.A., El-Sayed,K.A., El-Sohly,M.A., Hamann,M.T., Abdel-Halim,O.B., Ahmed,A.F. and Ahmed,M.M. (1997) Phytochemical Analysis of *Geigeria alata* and *Francoeuria crispa* Essential Oils. *Planta Medica* **63**, 479-482.

Rustaiyan,A., Jakupovic,J., Chau-Thi,T.V., Bohlmann,F. and Sadjadi,A. (1987) Further sesquiterpene lactones from the genus *Dittrichia*. *Phytochemistry* **26**, 9, 2603-2606.

Saleh,M.A. (1984) An Insecticidal Diacetylene from *Artemisia monosperma*. *Phytochemistry* **23**, 11, 2497-2498.

Saleh,M.A. (1985) Volatile Components of *Artemisia monosperma* and *Artemisia judaica* Growing in the Egyptian Deserts. *Biochemical Systematics and Ecology* **13**, 3, 265-269.

Saracoglu,I., Inoue,M., Calis,I. and Ogihara,Y. (1995) Studies on Constituents with Cytotoxic and Cytostatic Activity of Two Turkish Medicinal Plants *Phlomis armeniaca* and *Scutellaria salviifolia*. *Biological and Pharmaceutical Bulletin* **18**, 10, 1396-1400.

Schinkovitz,A., Gibbons,S., Stavri,M., Cocksedge,M.J. and Bucar,F. (2003) Ostruthin: An Antimycobacterial Coumarin from the Roots of *Peucedanum ostruthium*. *Planta Medica* **69**, 369-371.

Seifert,K., Lien,N.T., Schmidt,J., Johne,S., Popov,S.S. and Porzel,A. (1989) Iridoids from *Verbascum pulverulentum*. *Planta Medica* **55**, 470-473.

Seo,S., Tomita,Y. and Tori,K. (1981) Biosynthesis of Oleanene- and Ursene-Type Triterpenes from [4-^{13}C]Mevalonolactone and [1,2-$^{13}C_2$] Acetate in Tissue Cultures of *Isodon japonicus* Hara. *Journal of American Chemical Society* **103**, 2075-2080.

Shah,S.W., Brandange,S., Behr,D., Dahmen,J., Hagen,S. and Anthonsen,T. (1976) Absolute Configuration of 2-C-Methylerythritol from *Convolvulus glomeratus*. *Acta Chemica Scandinavia Series B* **30**, 9, 903.

Sholichin,M., Yamasaki,K., Kasai,R. and Tanaka,O. (1980) ^{13}C Nuclear Magnetic Resonance of Lupane-Type Triterpenes, Lupeol, Betulin, and Betulinic Acid. *Chemical and Pharmaceutical Bulletin* **28**, 1006-1008.

Shuaib, L. (1995) *Wildflowers of Kuwait*. London: Stacey International.

Silva,P.E.A., Bigi,F., Santangelo,M.P., Romano,M.I., Martin,C., Cataldi,A. and Ainsa,J.A. (2001) Characterization of P55, a Multidrug Efflux Pump in *Mycobacterium bovis* and *Mycobacterium tuberculosis*. *Antimicrobial Agents and Chemotherapy* **45**, 3, 800-804.

Souza,M.M.D., Madeira,A., Berti,C., Krogh,R., Yunes,R.A. and Cechinel-Filho,V. (2000) Antinociceptive properties of the methanolic extract obtained from *Ipomoea pes-caprae* (L.) R. Br. *Journal of Ethnopharmacology* **69**, 85-90.

Stanjek,V., Piel,J. and Boland,W. (1999) Biosynthesis of furanocoumarins: mevalonate-independent prenylation of umbelliferone in *Apium graveolens* (Apiaceae). *Phytochemistry* **50**, 1141-1145.

Stavri,M., Mathew,K.T., Bucar,F. and Gibbons,S. (2003) Pangelin, an Antimycobacterial Coumarin from *Ducrosia anethifolia*. *Planta Medica* **69**, 953-956.

Stavri,M., Mathew,K.T., Gibson,T., Williamson,R.T. and Gibbons,S. (2004a) New Constituents of *Artemisia monosperma*. *Journal of Natural Products* **67**, 5, 892-894.

Stavri,M., Schneider,R., O'Donnell,G., Lechner,D., Bucar,F. and Gibbons,S. (2004b) The antimycobacterial components of Hops (*Humulus lupulus*) and their dereplication. *Phytotherapy Research* (Accepted).

Sumaryono,W., Proksch,P., Wray,V., Witte,L. and Hartmann,T. (1991) Qualitative and Quantitative Analysis of the Phenolic Constituents from *Orthosiphon aristatus*. *Planta Medica* **57**, 176-180.

Swiatek,L., Lehmann,D. and Sticher,O. (1981) Iridoid Glucoside from *Scrophularia lateriflora* Trautv. (Scrophulariaceae). *Pharmaceutica Acta Helvetiae* **56**, 2, 37-44.

Takiff,H.E., Cimino,M., Musso,M.C., Weisbrod,T., Martinez,R., Delgado,M.B., Salazar,L., Bloom,B.R. and Jacobs Jr,W.R. (1996) Efflux pump of the proton antiporter family confers low-level fluoroquinolone resistance in *Mycobacterium smegmatis*. *Proceedings of the National Academy of Sciences of the United States of America* **93**, 362-366.

Tamura,Y., Hattori,M., Konno,K., Kono,Y., Honda,H., Ono,H. and Yoshida,M. (2004) Triterpenoid and caffeic acid derivatives in the leaves of ragweed, *Ambrosia artemisiifolia* L. (Asterales: Asteraceae), as feeding stimulants of *Ophraella communa* LeSage (Coleoptera: Chrysomelidae). *Chemoecology* **14**, 113-118.

Tan,R.X., Zheng,W.F. and Tang,H.Q. (1998) Biologically Active Substances from the Genus *Artemisia*. *Planta Medica* **64**, 295-302.

Tegos,G., Stermitz,F.R., Lomovskaya,O. and Lewis,K. (2002) Multidrug Pump Inhibitors Uncover Remarkable Activity of Plant Antimicrobials. *Antimicrobial Agents and Chemotherapy* **46**, 10, 3133-3141.

Towner, K. J. (2001) Mechanisms of acquired resistance. In *Antimicrobial Chemotherapy* ed. Greenwood,D. pp. 145-155. Oxford: Oxford University Press.

Uchiyama,T., Miyase,T., Ueno,A. and Usmanghani,K. (1989) Terpenic Glycosides From *Pluchea indica*. *Phytochemistry* **28**, 12, 3369-3372.

Viveiros,M., Leandro,C. and Amaral,L. (2003) Mycobacterial efflux pumps and chemotherapeutic implications. *International Journal of Antimicrobial Agents* **22**, 274-278.

WHO. WHO Tuberculosis Fact Sheet No. 104. 104. 2000.
Ref Type: Report

Williams, D. H. and Fleming, I. (1995) *Spectroscopic Methods in Organic Chemistry*. London: McGraw Hill Publishers.

Williams, R. A. D., Lambert, P. A. and Singleton, P. (1996) *Antimicrobial Drug Action*. Oxford: BIOS Scientific Publishers Ltd.

Wolinsky,E. (1992) Mycobacterial Diseases Other Than Tuberculosis. *Clinical Infectious Diseases* **15**, 1-12.

Wollenweber,E. (1981) Unusual Flavanones from a Rare American Fern. *Zeitschrift für Naturforschung* **36**, 604-606.

Wright, C. W. (2002) *Artemisia*. London: Taylor and Francis.

Wu,C.M. (1985) The chemical constituents of *Artemisia* species (III). Isolation and identification of the lipophilic constituents from *Artemisia argyi*. *Zhong Yao Tong Bao* **10**, 1, 31-32.

Xu,Z.Q., Barrow,W.W., Suling,W.J., Westbrook,L., Barrow,E., Lin,Y.M. and Flavin,M.T. (2004) Anti-HIV natural product (+)-calanolide A is active against both drug-susceptible and drug-resistant strains of *Mycobacterium tuberculosis*. *Bioorganic and Medicinal Chemistry* **12**, 1199-1207.

Yamamura,S., Ozawa,K., Ohtani,K., Kasai,R. and Yamasaki,K. (1998) Antihistaminic Flavones and Aliphatic Glycosides from *Mentha spicata*. *Phytochemistry* **48**, 1, 131-136.

Yamasaki,K., Kaneda,M. and Tanaka,O. (1976) Carbon-13 NMR spectral assignments of paeoniflorin homologues with the aid of spin-lattice relaxation time. *Tetrahedron* **44**, 3965-3968.

Yamasaki,K., Kohda,H., Kobayashi,T., Kaneda,N., Kasai,R., Tanaka,O. and Nishi,K. (1977) Application of ^{13}C Nuclear Magnetic Resonance Spectroscopy to Chemistry of Glycosides: Structures of Paniculosides-I, -II, -III, -IV, and -V, Diterpene Glucosides of *Stevia paniculata* Lag. *Chemical and Pharmaceutical Bulletin* **25**, 11, 2895-2899.

Yoshimatsu,K., Yamaguchi,A., Yoshino,H., Koyanagi,N. and Kitoh,K. (1997) Mechanism of action of E7010, an orally active sulfonamide antitumour agent: inhibition of mitosis by binding to the colchicine site of tubulin. *Cancer Research* **57**, 15, 3208-3213.

Zdero,C., Bohlmann,F., King,R.M. and Robinson,H. (1989) Sesquiterpene lactones and other constituents from Australian *Helipterum* species. *Phytochemistry* **28**, 2, 517-526.

Zdero,C., Bohlmann,F. and Rizk,A.M. (1988) Sesquiterpene Lactones from *Pulicaria sicula*. *Phytochemistry* **27**, 4, 1206-1208.

Zhang,W.J., Yang,H.J., Liu,Y.Q., He,Z.D., Jin,Y.Q. and Yang,C.R. (1992) Iridoidal Glycosides from *Scrophularia spicata*. *Acta Botanica Yunnanica* **14**, 4, 437-441.

Zhao,Y., Yue,J., Lin,Z., Ding,J. and Sun,H. (1997) Eudesmane sesquiterpenes from *Laggera pterodonta*. *Phytochemistry* **44**, 459-464.

Zloh,M., Kaatz,G.W. and Gibbons,S. (2004) Inhibitors of multidrug resistance (MDR) have affinity for MDR substrates. *Bioorganic and Medicinal Chemistry Letters* **14**, 881-885.

Zschocke,S., Lehner,M. and Bauer,R. (1997) 5-Lipoxygenase and Cyclooxygenase Inhibitory Active Constituents from *Qianghuo* (*Notopterygium incisum*). *Planta Medica* **63**, 203-206.

6.0 List of Publications

Schinkovitz, A., Gibbons, S., Stavri, M., Cocksedge, M.J., Bucar, F. Ostruthin: An Antimycobacterial Coumarin from the Roots of *Peucedanum ostruthium*. Planta Medica 2003; 69 (4): 369-371

Stavri, M., Mathew, K.T., Bucar, F., Gibbons, S. The Antimycobacterial Activity of *Ducrosia anethifolia*. Planta Medica 2003; 69 (10): 956-959

Lechner, D., Stavri, M., Oluwatuyi, M., Pereda-Miranda, R., Gibbons, S. The Anti-staphylococcal Activity of *Angelica dahurica* (Bai Zhi). Phytochemistry 2004; 65 (3): 331-335

Stavri, M., Mathew, K.T., Gibbons, S. A Novel Polyacetylene and Sesquiterpene from *Artemisia monosperma*. Journal of Natural Products 2004; 67(5): 892-894

Stavri, M., Schneider, R., O'Donnell, G., Lechner, D., Bucar, F., Gibbons, S. The Antimycobacterial Components of Hops (*Humulus lupulus*) and their Dereplication. Phytotherapy Research (Accepted)

Appendino, G., Arnoldi, L., Stavri, M., Gibbons, S., Ballero, M. An Antitubercular Coumarin from Sardinian Giant Fennel (*Ferula communis*). Journal of Natural Products (Submitted)

Publications in Preparation

Stavri, M., Mathew, K.T., Gibbons, S. New constituents from *Scrophularia deserti*. Phytochemistry (In preparation)

Stavri, M., Mathew, K.T., Bucar, F., Gibbons, S. Antimycobacterial and antitumour activity associated with *Artemisia monosperma*. Phytochemistry (In preparation)

Stavri, M., Mathew, K.T., Gibbons, S. A new furocoumarin from *Anethum graveolens*. Phytochemistry (In preparation)

Stavri, M., Mathew, K.T., Gibbons, S. A novel sesquiterpene skeleton from *Pulicaria crispa*. Pharmazie (In preparation)

Stavri, M., Mathew, K.T., Gibbons, S. Anti-staphylococcal activity of *Ipomoea pes-caprae*. Phytotherapy Research (In preparation)